

# Modal Analysis of Generally Damped Linear Structures Subjected to Seismic Excitations

by  
Jianwei Song, Yi-Lun Chu, Zach Liang and George C. Lee

Technical Report MCEER-08-0005

March 4, 2008

## NOTICE

This report was prepared by the University at Buffalo, State University of New York as a result of research sponsored by MCEER through a contract from the Federal Highway Administration. Neither MCEER, associates of MCEER, its sponsors, the University at Buffalo, State University of New York, nor any person acting on their behalf:

- a. makes any warranty, express or implied, with respect to the use of any information, apparatus, method, or process disclosed in this report or that such use may not infringe upon privately owned rights; or
- b. assumes any liabilities of whatsoever kind with respect to the use of, or the damage resulting from the use of, any information, apparatus, method, or process disclosed in this report.

Any opinions, findings, and conclusions or recommendations expressed in this publication are those of the author(s) and do not necessarily reflect the views of MCEER or the Federal Highway Administration.

## Modal Analysis of Generally Damped Linear Structures Subjected to Seismic Excitations

by

Jianwei Song,<sup>1</sup> Yi-Lun Chu,<sup>2</sup> Zach Liang<sup>3</sup> and George C. Lee<sup>4</sup>

Publication Date: March 4, 2008

Submittal Date: February 1, 2008

Technical Report MCEER-08-0005

Task Number 094-D-1.2

FHWA Contract Number DTFH61-98-C-00094

- 1 Senior Research Scientist, Department of Civil, Structural and Environmental Engineering, University at Buffalo, State University of New York
- 2 Ph.D. Student, Department of Civil, Structural and Environmental Engineering, University at Buffalo, State University of New York
- 3 Research Associate Professor, Department of Civil, Structural and Environmental Engineering, University at Buffalo, State University of New York
- 4 Special Tasks Director, MCEER; Samuel P. Capen Professor of Engineering, Department of Civil, Structural and Environmental Engineering, University at Buffalo, State University of New York

MCEER

University at Buffalo, The State University of New York

Red Jacket Quadrangle, Buffalo, NY 14261

Phone: (716) 645-3391; Fax (716) 645-3399

E-mail: [mceer@buffalo.edu](mailto:mceer@buffalo.edu); WWW Site: <http://mceer.buffalo.edu>

---



## Preface

The Multidisciplinary Center for Earthquake Engineering Research (MCEER) is a national center of excellence in advanced technology applications that is dedicated to the reduction of earthquake losses nationwide. Headquartered at the University at Buffalo, State University of New York, the Center was originally established by the National Science Foundation in 1986, as the National Center for Earthquake Engineering Research (NCEER).

Comprising a consortium of researchers from numerous disciplines and institutions throughout the United States, the Center's mission is to reduce earthquake losses through research and the application of advanced technologies that improve engineering, pre-earthquake planning and post-earthquake recovery strategies. Toward this end, the Center coordinates a nationwide program of multidisciplinary team research, education and outreach activities.

MCEER's research is conducted under the sponsorship of two major federal agencies, the National Science Foundation (NSF) and the Federal Highway Administration (FHWA), and the State of New York. Significant support is also derived from the Federal Emergency Management Agency (FEMA), other state governments, academic institutions, foreign governments and private industry.

The Center's Highway Project develops improved seismic design, evaluation, and retrofit methodologies and strategies for new and existing bridges and other highway structures, and for assessing the seismic performance of highway systems. The FHWA has sponsored three major contracts with MCEER under the Highway Project, two of which were initiated in 1992 and the third in 1998.

Of the two 1992 studies, one performed a series of tasks intended to improve seismic design practices for new highway bridges, tunnels, and retaining structures (MCEER Project 112). The other study focused on methodologies and approaches for assessing and improving the seismic performance of existing "typical" highway bridges and other highway system components including tunnels, retaining structures, slopes, culverts, and pavements (MCEER Project 106). These studies were conducted to:

- assess the seismic vulnerability of highway systems, structures, and components;
- develop concepts for retrofitting vulnerable highway structures and components;
- develop improved design and analysis methodologies for bridges, tunnels, and retaining structures, which include consideration of soil-structure interaction mechanisms and their influence on structural response; and
- develop, update, and recommend improved seismic design and performance criteria for new highway systems and structures.

The 1998 study, “Seismic Vulnerability of the Highway System” (FHWA Contract DTFH61-98-C-00094; known as MCEER Project 094), was initiated with the objective of performing studies to improve the seismic performance of bridge types not covered under Projects 106 or 112, and to provide extensions to system performance assessments for highway systems. Specific subjects covered under Project 094 include:

- development of formal loss estimation technologies and methodologies for highway systems;
- analysis, design, detailing, and retrofitting technologies for special bridges, including those with flexible superstructures (e.g., trusses), those supported by steel tower substructures, and cable-supported bridges (e.g., suspension and cable-stayed bridges);
- seismic response modification device technologies (e.g., hysteretic dampers, isolation bearings); and
- soil behavior, foundation behavior, and ground motion studies for large bridges.

In addition, Project 094 includes a series of special studies, addressing topics that range from non-destructive assessment of retrofitted bridge components to supporting studies intended to assist in educating the bridge engineering profession on the implementation of new seismic design and retrofitting strategies.

*Motivated by the need for a systematic approach for seismic evaluation and design of structures with supplemental damping, a general modal analysis method considering over-damped modes is developed and described in this report. The method deals with a unified formulation used to evaluate most structural response quantities of interest, such as displacements, velocity, inter-story drifts, story shear, damping forces and absolute accelerations, etc. In addition, a novel general real-valued transformation matrix is established, which can be used to decouple the equations of motion of a generally damped structure in terms of real-valued modal coordinates. The properties related to this transformation are discussed in detail to explain the dynamic nature of the generally damped structural system. Also, on the basis of the general modal response history analysis, two general modal combination rules for the response spectrum analysis, GCQC and GSRSS, are formulated. To enable the new rules to be applicable to the practicing earthquake engineering community, a conversion procedure to construct an over-damped mode response spectrum compatible with the given 5% standard design response spectrum is established. The adequacy of this conversion procedure is also validated. Examples are given to demonstrate the application of the modal analysis method, assess the accuracy of the new modal combination rules, and show that over-damped modes may develop in structures with supplemental damping, which can provide significant response contributions to certain response parameters.*

## ABSTRACT

Motivated by the need for a systematic approach for seismic evaluation and design of civil engineering structures with supplemental damping, a general modal analysis method, in which over-damped modes are taken into account, is developed and described in this report.

This general modal analysis method deals with a unified formulation used to evaluate most structural response quantities of interest, such as displacements, velocity, inter-story drifts, story shear, damping forces and absolute accelerations etc. In addition, a novel general real-valued transformation matrix is established, which can be utilized to decouple the equations of motion of a generally damped structure in terms of real-valued modal coordinates. Non-singularity of this matrix and other properties related to this transformation, such as modal responses to initial conditions, modal energy distribution, modal effective masses and modal truncation etc., are discussed in details to explain the dynamic nature of the generally damped structural system.

Furthermore, on the basis of the general modal response history analysis and the white noise input assumption as well as the theory of random vibration, two general modal combination rules for the response spectrum analysis, GCQC and GSRSS are formulated to handle non-classical damping and over-damped modes. To enable the new rules applicable to the practical earthquake engineering, a conversion procedure to construct an over-damped mode response spectrum compatible with the given 5% standard design response spectrum is established. The adequacy of this conversion procedure is also validated.

Examples are given to demonstrate the application of the modal analysis method, to assess the accuracy of the new modal combination rules, and to show that over-damped modes may develop in structures with supplemental damping which can provide significant response contributions to certain response parameters.





## **ACKNOWLEDGEMENT**

This study is originally motivated by the need for a more comprehensive and systematic approach for the design of structure with added earthquake response control devices, especially for large, unusual and complex bridges and buildings. The authors greatly acknowledge the support of the Federal Highway Administration (Contract Number: DTFH61-98-C-00094) and the National Science Foundation through MCEER (CMS 97-01471) for the development of a modal analysis approach for generally damped linear MDOF system reported herein. This fundamental study will be further developed for the design of seismic response modification devices and systems for highway bridges and other structures under the sponsorship of FHWA.



# TABLE OF CONTENTS

Chapter	Title	Page
1	Introduction.....	1
1.1	Overview.....	1
1.2	Research Objectives.....	5
1.3	Scope of Work .....	6
1.4	Organization of the Report.....	7
2	Equation of Motion and Eigen Analysis.....	9
2.1	Introduction.....	9
2.2	Equation of Motion.....	9
2.3	Eigen Analysis .....	10
2.4	Orthogonality .....	13
2.5	Modal Decomposition and Superposition of Modal Responses.....	16
2.6	Expansion of System Matrices in terms of Modal Parameters.....	17
2.6.1	A Special Property of System Modal Shapes .....	17
2.6.2	Expansion of the Mass Matrix $\mathbf{M}$ and Its Inverse .....	18
2.6.3	Expansion of the Damping Matrix $\mathbf{C}$ .....	19
2.6.4	Expansion of the Stiffness Matrix $\mathbf{K}$ and Flexibility Matrix $\mathbf{K}^{-1}$ .....	20
2.6.5	Expansion of the Total Mass of the System $M_{\Sigma}$ .....	21
2.7	Reduction to Classically-Damped System.....	22
3	General Modal Response History Analysis.....	25
3.1	Introduction.....	25
3.2	Analytical Formulation.....	25
3.2.1	Laplace Transform Operation.....	25
3.2.2	Frequency Response Functions.....	31
3.2.3	Response Solutions to Displacement, Velocity and Absolute Acceleration .....	32
3.2.3.1	Displacement Response Vector.....	32
3.2.3.2	Velocity Response Vector.....	33
3.2.3.3	Absolute Response Vector .....	35
3.3	A Unified Form for Structural Responses .....	37
3.3.1	Inter-Story Drift .....	38

## TABLE OF CONTENTS (CONT'D)

Chapter	Title	Page
	3.3.2 Inter-Story Shear .....	38
	3.3.3 General Inter-Story Shear .....	38
	3.3.4 Inter-Story Moment .....	39
	3.3.5 General Inter-Story Moment .....	39
	3.3.6 Damper Forces .....	40
	3.3.7 Generalization .....	40
3.4	Reduction to Classically Damped Systems .....	41
4	General Modal Coordinate Transformation and Modal Energy .....	45
4.1	Introduction .....	45
4.2	General Modal Transformation Matrix .....	45
4.3	Proof of Modal Decoupling .....	47
4.4	Non-Singularity Analysis for General Transformation Matrix .....	56
4.5	Numerical Example for General Modal Responses .....	59
4.6	General Modal Responses to Initial Conditions .....	68
4.7	General Modal Energy .....	77
4.7.1	Energy Integral for Arbitrary Ground Motion Excitation .....	77
4.7.2	Energy Integral for Sinusoidal Ground Motion Excitation .....	81
4.8	Reduction to Classically Damped System .....	86
4.8.1	Reduction of Modal Transformation Matrix .....	86
4.8.2	Reduction of Modal Responses to Initial Conditions .....	90
4.8.3	Reduction of Energy Integral .....	91
4.9	Dual Modal Space Approach and Structural DOFs Reduction .....	93
4.9.1	Formulas Development .....	93
4.9.2	Numerical Example .....	99
5	Truncation of Modes .....	105
5.1	Introduction .....	105
5.2	Effective Modal Mass for Classically Damped Systems w/o Over-Damped Modes .....	105
5.3	Effective Modal Mass for Generally Damped Systems .....	109
5.4	Example .....	117

## TABLE OF CONTENTS (CONT'D)

Chapter	Title	Page
6	Response Spectrum Method .....	119
6.1	Introduction.....	119
6.2	Analytical Formulation.....	119
6.2.1	Definition of Vector Operation Symbols.....	120
6.2.2	Covariance of Responses to Stationary Excitation.....	120
6.2.3	Development of Response Spectrum Method.....	127
6.2.4	Investigation of the Correlation Factors .....	128
6.2.5	Reduction to Classically under-Damped Structures .....	129
6.3	Over-Damped Mode Response Spectrum.....	131
6.3.1	The Concept.....	132
6.3.2	Construction of Over-Damped Mode Response Spectrum Consistent with 5% Displacement Response Spectrum .....	133
6.3.2.1	Response Spectrum Consistent PSD $G_{\ddot{x}_g}(\omega)$ .....	134
6.3.2.2	Procedures.....	134
6.3.2.3	$\eta$ Factor Determination.....	135
6.3.3	Validation of the Over-Damped Mode Response Spectrum .....	136
7	Analysis Application Examples.....	149
7.1	Introduction.....	149
7.2	Example Building Frames .....	149
7.3	Response History Analysis using Modal Superposition Method .....	151
7.3.1	Ground Motions.....	152
7.3.2	Comparison of the Analysis Results.....	152
7.4	Response Spectrum Analysis.....	153
7.4.1	Ground Motions.....	154
7.4.2	Comparison of the Analysis Results.....	154
8	Summary, Conclusions and Future Research .....	165
8.1	Summary.....	165
8.2	Conclusions.....	166
8.3	Future Research .....	168

## TABLE OF CONTENTS (CONT'D)

Chapter	Title	Page
9	REFERENCES .....	171
APPENDIX A	Non-singularity of Matrices $\mathbf{A}$ , $\mathbf{B}$ , $\hat{\mathbf{a}}$ and $\hat{\mathbf{b}}$ .....	175
A.1	Non-Singularity of $\mathbf{A}$ and $\mathbf{B}$ .....	175
A.2	Non-Singularity of $\hat{\mathbf{a}}$ and $\hat{\mathbf{b}}$ .....	175
APPENDIX B	Proof of Caughey Criterion .....	177

## LIST OF FIGURES

Figure	Title	Page
3.1	FRF of modal displacement response (periods equal to 0.2s, 0.4s, 0.6s, 0.8s, 1.0s, 2.0s, 3.0s and 5.0s; damping ratio=5%).....	44
3.2	FRF of modal displacement response (damping ratios equal to 2%, 5%, 10%, 20%, 50% and 80%; period=1 sec) .....	44
3.3	FRF of over-damped modal (periods equal to 0.2s, 0.4s, 0.6s, 0.8s, 1.0s, 2.0s, 3.0s and 5.0s).....	44
4.1	4-DOFs Symmetric Structural Model.....	60
4.2	Modal Shapes.....	63
4.3	EL Centro Earthquake Acceleration Time History.....	64
4.4	General Modal Responses.....	64
4.5	Modal Structural Displacement Responses of the 1st DOF.....	65
4.6	Modal Structural Velocity Responses of the 1st DOF .....	66
4.7	Modal Structural Absolute Acceleration Responses of the 1st DOF .....	66
4.8	Structural Displacement and Velocity Responses of the 1st DOF .....	67
4.9	Four Typical Examples of First Order Subsystem.....	75
4.10	Modal Responses to Modal Initial Conditions.....	76
4.11	Structural Displacement and Velocity Responses of the 1 <sup>st</sup> and 2 <sup>nd</sup> DOF ....	76
4.12	Structural Displacement and Velocity Responses of the 1 <sup>st</sup> and 2 <sup>nd</sup> DOF ....	77
4.13	Physical Interpretation of Effective Modal Mass .....	89
4.14	10-Story Shear Frame Structure Model (10 DOFs).....	100
5.1	A planar N-DOFs multistory frame .....	106
5.2	Illustration of the static structural response subjected to $\mathbf{s}_i$ .....	107
5.3	Conceptual explanation of the expansion of $\mathbf{s} = \mathbf{MJ}$ and the resulting base shear forces .....	112
5.4	Cumulative effective modal mass.....	118
6.1	Correlation coefficient $\rho_{ij}^{DD}$ for responses to white noise excitations.....	141
6.2	Correlation coefficient $\rho_{ij}^{VV}$ for responses to white noise excitations.....	142
6.3	Correlation coefficient $\rho_{ij}^{VD}$ for responses to white noise excitations.....	143
6.4	Correlation coefficient $\rho_{ij}^{DP}$ for responses to white noise excitations.....	144

## LIST OF FIGURES (CONT'D)

Figure	Title	Page
6.5	Correlation coefficient $\rho_{ij}^{pp}$ for responses to white noise excitations .....	144
6.6	Generation of over-damped modal response spectrum.....	145
6.7	Variation of $\eta$ factor for over-damped modal response .....	145
6.8	Over-damped modal response spectrum construction procedures.....	146
6.9	Mean 5% damping displacement response spectrum (a) ensemble A (b) ensemble B.....	147
6.10	Comparisons of exact and estimated over-damped modal response spectrum (a) ensemble A (b) ensemble B.....	147
7.1	Configurations of example building frames A, B and C .....	160
7.2	Estimated errors of forced classical damping assumption and exclusion of over-damped mode in example A.....	161
7.3	Estimated errors of forced classical damping assumption and exclusion of over-damped modes in example B .....	161
7.4	Estimated errors of forced classical damping assumption and exclusion of over-damped modes in example C .....	162
7.5	Estimated errors due to GCQC,CDA and EPM in example A .....	162
7.6	Estimated errors due to GCQC,CDA and EPM in example B .....	163
7.7	Estimated errors due to GCQC,CDA and EPM in example C .....	163



## LIST OF TABLES

<b>Table</b>	<b>Title</b>	<b>Page</b>
4.1	Modal Frequency, Period and Damping Ratio .....	61
4.2	Original Structural Modal Parameters .....	99
4.3	Modal Periods Estimation Results and Error Comparison .....	102
4.4	Damping Ratio Estimation Results and Error Comparison .....	103
5.1	Summary of the expressions of the effective modal mass .....	116
6.1	White-noise-determined $\eta$ factor for over-damped modal response .....	138
6.2	Far-field ground motions used in ATC-58.....	139
6.3	Far-field ground motions used by Vamvatsikos and Cornell 2004 .....	140
7.1	Modal periods of example buildings A, B and C.....	157
7.2	Modal damping ratios of example buildings A, B and C .....	157
7.3	Results of mean peak responses of example A via modal superposition methods .....	158
7.4	Results of mean peak responses of example B via modal superposition methods .....	158
7.5	Results of response –history analysis of example C via modal superposition methods .....	158
7.6	Comparisons of results by GCQC, CDA and EOM to mean results of response history analysis for examples A, B and C .....	159



# CHAPTER 1

## INTRODUCTION

### 1.1 Overview

Modal analysis to a linear structural system may be explained as a method for decoupling the equations of motion by means of modal coordinate transformation matrix as well as evaluating modal responses and further combined modal responses to estimate the structural responses. By the aid of modal analysis, the structural solutions, especially to a complicated structure with large degrees of freedom (DOFs), can be significantly simplified and the computation efforts can be largely reduced. Meanwhile, the resulting analysis accuracy can still be ensured within the range that is reasonable or acceptable in engineering applications. In addition, using this method, certain of the structural inherent properties may be much easier to be exposed.

The decoupling coordinate transformation can be determined by the solution of an algebraic eigenvalue problem of the system. In earthquake engineering, the classical modal analysis method is considered as a powerful approach to analyze the seismic responses of classical damped linear structures. Two approaches of this method are: the modal response history analysis, which gives the complete response history of the structures, and the response spectrum analysis. When the structures satisfy the criterion specified by Caughey and O'Kelly (1965), the modes of the structure are real-valued and are identical to those of the associated undamped systems. This linear vibrating structure is said to be classically damped and possesses normal modes as well as can be decoupled by the same modal transformation that decouples the associated undamped structures. Those structures that do not satisfy the Caughey and O'Kelly criterion are said to be non-classically damped; consequently, their equations of motion cannot be decoupled by the classical modal transformation. In principle, the coupling arises from the damping term. Typical examples include the structures with added damping devices and base-isolated structures as well as primary-secondary systems.

Basically, responses of the non-classically damped systems may be evaluated by using the decoupled method suggested by Foss (1958). However, it is generally believed that, concurrent with the classical damping assumption, the structural responses calculated by the classical modal superposition method are acceptable. For example, current methods for seismic design of structures enhanced with damping devices are developed based on the classical damping assumption (BSSC 2003). This may not always be true due to the uncertainty of the nature and magnitude of the damping in structures. This phenomenon can be further magnified when the structure is irregularly shaped. There are instances that the structures can be highly non-classically damped (Warburton and Soni 1977) and, in some occasions, develop over-damped modes (Inman and Andry 1980), which in turn result in a chance of the inaccuracy of the response estimations. For example, Takewaki (2004) has demonstrated that the structural energy transfer function and displacement transfer function will be underestimated if the over-damped modes are neglected.

To advance the applications of the classical modal analysis to the non-classically damped systems, a number of researchers have conducted extensive studies on developing complex modal superposition methods for systems not satisfying the classical damping condition. Igusa et al. (1984) studied the stationary response of multi-degrees-of-freedom (MDOF) non-classically damped linear systems subjected to stationary input excitations. Veletsos and Ventura (1986) presented a critical review of the modal superposition method of evaluating the dynamic response of non-classically damped structures. Singh and Ghafory-Ashtiany (1986) studied the modal time-history analysis approach for non-classically damped structures subjected to seismic forces. Yang et al. (1987 and 1988) used real-valued canonical transformation approach to decouple non-classically damped system from a set of second order differential equations to a set of first order ones, and then performed the time history analysis as well as response spectrum analysis. Zhou et al. (2004) provided a refined complex mode superposition algorithm to evaluate the seismic responses of non-classically damped systems. All the above are important contributions but none addressed the over-damped modes.

In addition, in earthquake engineering, the response spectrum method is commonly used as an alternative approach to response history analysis for determining the maximum values of the seismic responses of classically damped structures. In this method, the modal peak responses are obtained using the prescribed response spectrum. These modal maxima are then appropriately combined to estimate the peak values of the responses of interest. There are several combination rules proposed by various researchers. Among which, the simplest is the square-root-of-sum-of-squares (SRSS) modal combination rule (Rosenblueth 1951). This rule ignores the correlations between vibration modes and can provide excellent estimates for structures with well-separated modal frequencies. To further consider the correlations between each vibration mode, Der Kiureghian (1980 and 1981) proposed a rational rule, known as complete quadratic combination (CQC) rule, in which the correlations among modes are connected by correlation coefficients. Both rules deal with classically damped structures.

The conventional response spectrum method is ideal to structures satisfying classical damping condition. For structures that are strongly non-classically damped, the accuracy of SRSS or CQC rule becomes questionable (Clough and Mojtahedi 1976, Warburton and Soni 1977 and Veletsos and Ventura 1986). For this reason, several modal combination rules accounting for the effect of the non-classical damping are developed. Singh (1980) formed a modified conventional SRSS approach where nonproportional damping effects can be included properly. Igusa et al. (1984) described the responses in terms of spectral moments and provided the formulations of correlation coefficients among modes using filtered white noise process as inputs. Ventura (1985) stated that the peak modal responses can be obtained by taking square roots of the sum of squares of the individual modal maxima contributing from displacement and velocity responses, assuming harmonic excitations. Gupta and Jaw (1986) developed the response spectrum combination rules for non-classically damped systems by using the displacement and velocity response spectrum. Villaverde (1988) improved Rosenblueth's rule (1951) by including the effect of modal velocity responses. Maldonado and Singh (1991) proposed an improved response spectrum method for non-classically damped systems. It reduces the error associated with the truncation of the high frequency modes without explicitly using them in the analysis. Zhou et al. (2004) generalized the CQC rule for its application

to non-classically damped systems. However, all above-mentioned combination rules did not incorporate the over-damped modes in the formulation and the response quantities considered in these rules are limited to deformation-related response quantities.

In general, when using modal superposition method, the response contributions of all modes should be included to obtain the exact results. At the same time, it is observed that limited amount of modes can usually give sufficiently accurate results. The number of modes required is well-defined in the classical damping cases through the use of the cumulative effective modal mass. The corresponding criteria, however, for the non-classically damped structures with or without over-damped modes are not well addressed. To address this issue, an appropriate expression of the effective modal mass for non-classical damping structures is formulated.

Initially motivated by the need for a systematic approach for the design of structures with added damping devices, a general modal response history analysis method is developed and presented in this report. The method advances the complex modal analysis to be applicable to structure with over-damped modes. In addition, a unified form that is able to express any response quantities of the systems, including the velocities and absolute accelerations, is established. This unified form is made possible by several novel modal properties found in this study. Also, on the basis of the general modal response history analysis and the white noise input assumption as well as the theory of random vibration, a general modal combination rule for response spectrum method is formulated to deal with the non-classical damping and over-damped modes. This general modal combination rule is referred to as “General-Complete-Quadratic-Combination” (GCQC) rule in this report. To enable the new rules applicable to the practical earthquake engineering, an over-damped modal response spectrum, following a similar definition as the conventional response spectrum, is introduced to account for the peak modal responses of the over-damped modes. A conversion procedure to construct an over-damped mode response spectrum compatible with the given 5% standard design response spectrum is established. The adequacy of this conversion procedure is also validated. In addition to the displacement correlation coefficient given in the CQC rule, new correlation coefficients to account for the cross correlations between modal displacement,

modal velocity and over-damped modal responses are also provided. It is shown that this rule is also suitable to estimate the velocity-related and absolute acceleration-related response quantities. For example, the absolute acceleration of a single-degree-of-freedom system can be approximated more accurately by this rule instead of using the corresponding pseudo-acceleration values. The applicability of the general modal response history analysis method is demonstrated by two numerical examples. Also, the errors in structural response estimations arising from the classical damping assumption are identified, and the effect of the over-damped modes on certain response quantities is observed. The accuracy of the GCQC rule is also evaluated through the two examples by comparing it to the mean response history results. For engineering applications, a procedure to convert the given 5% design spectrum to the over-damped mode response spectrum is given. Its accuracy is also verified. In addition, a general real-valued modal coordinate transformation matrix which can decouple the equations of motion of generally damped structures is derived in the process of theoretical formulation. A rigorous proof of the modal decoupling by using this general modal coordinate transformation is given. Further, based on this transformation matrix, the formulation of the general modal responses subjected to structural initial conditions and the formulation of the general modal energy for arbitrary ground motion are established. Finally, a dual modal space approach to reduce the scale of the modeling and computation burden is proposed.

## **1.2 Research Objectives**

The primary objectives of this research are:

- (1) To explore the modal properties of the non-classically damped systems with over-damped modes and to further expand/complement current linear structural modal analysis theory.
- (2) To improve the present modal analysis procedure to accurately evaluate the peak seismic responses of damped linear structures with over-damped modes.

- (3) To extend the present response spectrum method to be applicable to the non-classically damped systems with over-damped modes and to establish a solid foundation for structural damping design.
- (4) To propose an easy and reasonable criterion to determine the number of modes required to be included in the modal analysis of non-classically damped systems with over-damped modes to achieve an acceptable level of accuracy.

### **1.3 Scope of Work**

The work has proceeded as follows:

- (1) Examine the theory presently being used for analyzing the non-classically damped linear systems.
- (2) Formulate the equation of motion of a MDOF system by means of the state space method, as well as perform an eigen analysis and explore the modal properties. All the formulations are presented in the form of matrix.
- (3) Clarify the modal energy distributions of non-classically damped linear MDOF structures.
- (4) Formulate the response history analysis procedure in the manner of modal superposition and offer interpretation of the physical meaning in the formulation. Main effort focuses on the analytical formulation about the over-damped modes.
- (5) Formulation for the response history analysis procedure is extended for the use of response spectrum method. Much of this effort focuses on the treatment of the over-damped modes.
- (6) Review the criterion that is used to determine the number of modes required for the classically damped structures and develop a corresponding criterion for the generally damped linear MDOF structures.



## 1.4 Organization of the Report

Chapter 2 details the eigen-analysis of a generally damped linear system, stressing on the treatment of the over-damped modes. Several fundamental modal properties are explored and presented.

Chapter 3 presents the formulation of the modal analysis procedures for the generally damped linear MDOF systems with highlight on the treatment of the over-damped modes. This chapter also presents a unified form suitable for any response quantities, which is obtained based on the modal properties found in Chapter 2. It should be noted that Laplace transform approach is utilized in this Chapter, which simplifies the process of the formulation with certain level and may make it possible that new attractive formulas can be developed.

Chapter 4 describes a general modal coordinate transformation resulted from the unified formulation obtained in Chapter 3. Based on this transformation matrix, the structural modal responses subjected to structural initial conditions are given. A simplified numerical example model with 4-DOFs is provided to further clarify some properties related to modal transformation matrix, over-damped modes and modal responses. Also, the general modal energy for structural initial conditions, sinusoidal excitations and seismic excitations is derived, leading to a deep physical insight of the formulation work. A dual modal space approach to reduce the scale of the modeling and computation effort is also given.

Chapter 5 proposes a criterion on determining the number of modes that should be included in the modal analysis for the generally damped linear MDOF system.

Chapter 6 shows the rigorous formulation of the response spectrum method for the analysis of the generally damped linear MDOF system with over-damped modes. This chapter focuses on the development of a manner to handle the over-damped when using the prescribed site response spectra.

Chapter 7 demonstrates the use of the proposed modal analysis method and response spectrum method through three example buildings. The results obtained by using the

classical damping assumption and the exact solutions are compared. The effect of the over-damped modes on the peak response estimation is examined and discussed.

Finally, Chapter 8 presents the summary as well as conclusions, and provides some suggestions for future research needs.

## CHAPTER 2

### EQUATION OF MOTION AND EIGEN ANALYSIS

#### 2.1 Introduction

This chapter presents the mathematical modeling of a generally damped planar linear MDOF structure subjected to a dynamic loading. Corresponding eigen analysis of the system is performed and its modal properties are explored, in which the case with real-valued eigenvalues is also addressed. The real-valued eigenvalues correspond to the presence of over-damped modes are usually assumed to be unlikely to occur in the engineering practice. However, this may not be always true for systems with added earthquake protective systems. Also, the orthogonality of the modal vectors is examined and the system mass, damping and stiffness matrices are expanded in terms of modal parameters. The results shown in this chapter are shown to be useful for the analytical formulations in the subsequent chapters.

#### 2.2 Equation of Motion

For a linear, discrete, generally damped planar structure with  $N$  degree-of-freedom (DOF) subjected to a dynamic loading  $\mathbf{f}(t)$ , which has  $N$  dimensional real field vector, i.e.,  $\mathbf{f}(t) \in \mathbb{R}^N$ , the equation of motion can be described as

$$\mathbf{M}\ddot{\mathbf{x}}(t) + \mathbf{C}\dot{\mathbf{x}}(t) + \mathbf{K}\mathbf{x}(t) = \mathbf{f}(t) \quad (2.1)$$

in which  $\mathbf{x}(t) \in \mathbb{R}^N$ ,  $\dot{\mathbf{x}}(t) \in \mathbb{R}^N$  and  $\ddot{\mathbf{x}}(t) \in \mathbb{R}^N$  are the relative structural nodal displacement, velocity and acceleration vectors, respectively.  $\mathbf{M} \in \mathbb{R}^{N \times N}$ ,  $\mathbf{C} \in \mathbb{R}^{N \times N}$  and  $\mathbf{K} \in \mathbb{R}^{N \times N}$  are  $N \times N$  real and symmetric mass, viscous damping and stiffness matrix, respectively.  $\mathbf{M}$  and  $\mathbf{K}$  are positive-definite matrices when the structure is completely constrained, while  $\mathbf{C}$  is a semi-positive definite matrix. It is noted that no further restriction is imposed on the form of the damping matrix.

### 2.3 Eigen Analysis

In general, when the structure is non-classically damped, the formulation in the  $2N$  dimensional state space is essential for solving the equation of motion via the modal analysis approach. In turn, Equation (2.1) can be reduced to a set of first-order  $2N$  dimensional equations as

$$\mathbf{A}\dot{\mathbf{y}}(t) + \mathbf{B}\mathbf{y}(t) = \mathbf{f}_s(t) \quad (2.2)$$

where

$$\mathbf{A} = \begin{pmatrix} \mathbf{0} & \mathbf{M} \\ \mathbf{M} & \mathbf{C} \end{pmatrix} \in \mathbb{R}^{2N \times 2N}, \quad \mathbf{B} = \begin{pmatrix} -\mathbf{M} & \mathbf{0} \\ \mathbf{0} & \mathbf{K} \end{pmatrix} \in \mathbb{R}^{2N \times 2N} \quad (2.3)$$

$$\mathbf{y}(t) = \begin{Bmatrix} \dot{\mathbf{x}}(t) \\ \mathbf{x}(t) \end{Bmatrix} \in \mathbb{R}^{2N}, \quad \mathbf{f}_s(t) = \begin{Bmatrix} \mathbf{0} \\ \mathbf{f}(t) \end{Bmatrix} \in \mathbb{R}^{2N}$$

It can be proved that  $\mathbf{A}$  and  $\mathbf{B}$  are non-singular, implying that both  $\mathbf{A}^{-1}$  and  $\mathbf{B}^{-1}$  exist. The proof is given in Appendix A. The associated eigen-equation with Equation (2.2) is given by

$$(\lambda\mathbf{A} + \mathbf{B})\boldsymbol{\psi} = \mathbf{0} \quad (2.4)$$

The solution to the above eigenvalue problem leads to a set of total  $2N$  eigenvalues (also known as eigen-roots or characteristic roots)  $\lambda_i \in \mathbb{C}$  (belong to complex field) and  $2N$  complex eigenvectors  $\boldsymbol{\psi}_i \in \mathbb{C}^{2N}$ . For a conventional structure or a structure enhanced with passive damping devices, a stable system is expected. In other words, the eigenvalues are either complex-valued with negative real parts or negative real-valued.

When the eigenvalues are complex-valued, the corresponding modes are under-damped and the eigenvalues and eigenvectors appear in complex-conjugated pairs, which can be easily proved as follows.

Supposing  $\lambda_i$  and  $\boldsymbol{\psi}_i$  are the  $i$ th complex eigenvalue and corresponding eigenvector, respectively,  $\lambda_i$  and  $\boldsymbol{\psi}_i$  therefore satisfy Equation (2.4). That is,

$$(\lambda_i \mathbf{A} + \mathbf{B}) \boldsymbol{\psi}_i = \mathbf{0} \quad (2.5)$$

Taking conjugate operation to both sides of Equation (2.5) and noting that  $\mathbf{A}$  and  $\mathbf{B}$  are both real-valued matrices,  $\mathbf{A} = \mathbf{A}^*$  and  $\mathbf{B} = \mathbf{B}^*$  (the superscript  $*$  denotes a conjugate operation), we have

$$(\lambda_i^* \mathbf{A} + \mathbf{B}) \boldsymbol{\psi}_i^* = \mathbf{0} \quad (2.6)$$

which means that  $\lambda_i^*$  and  $\boldsymbol{\psi}_i^*$  also satisfy Equation (2.4) and they are one pair of eigen-solution of Equation (2.4). Now assuming that there are  $N_C$  pairs, the corresponding eigenvalues and eigenvectors can be expressed as

$$\lambda_i, \lambda_i^* = -\xi_i \omega_i \pm j \omega_{di} \quad (i = 1, 2, 3 \dots N_C) \quad (2.7)$$

$$\boldsymbol{\psi}_i = \begin{Bmatrix} \lambda_i \boldsymbol{\phi}_i \\ \boldsymbol{\phi}_i \end{Bmatrix}, \boldsymbol{\psi}_i^* = \begin{Bmatrix} \lambda_i^* \boldsymbol{\phi}_i^* \\ \boldsymbol{\phi}_i^* \end{Bmatrix} \quad (2.8)$$

where  $\boldsymbol{\phi}_i \in \mathbb{C}^N$  or  $\boldsymbol{\phi}_i^* \in \mathbb{C}^N$  is the  $i$ th complex modal shape;  $\omega_i \in \mathbb{R}$  and  $\xi_i \in \mathbb{R}$  are called the  $i$ th modal circular frequency and  $i$ th damping ratio, respectively, and  $\omega_{di} = \sqrt{1 - \xi_i^2} \omega_i \in \mathbb{R}$  is called the  $i$ th damped modal circular frequency.

When the eigenvalues are real-valued, the corresponding modes are the properties of the over-damped first order subsystems which are no longer second-order oscillatory subsystems. For the sake of simplicity, all related variables, such as periods, modal shape and modal responses, to the over-damped subsystems are denoted by superscript or subscript “P” (“O” may be a better choice, but it is easily confused with “0”) is to distinguish them from the variables associated with complex modes.

Mathematically speaking, over-damped modes appear in pairs. However, based on the control theory, each over-damped mode must be considered as an independent basic unit. There are no functional relationships among all over-damped modes, mathematically or physically. Thus it would not be necessary to group them in pairs in

the analytical formulation process. In this report all over-damped modes are handled individually. Assuming that there are  $N_p [= 2(N - N_c)]$  real negative-valued eigenvalues:

$$\lambda_i^p = -\omega_i^p \in \mathbb{R} \quad (i = 1, 2, 3 \dots N_p) \quad (2.9)$$

where  $\omega_i^p > 0$ , which has dimension “rad/sec”, is defined as  $i$ th over-damped modal circular natural frequency. Each real eigenvalue  $\lambda_i^p$ , the corresponding eigenvector  $\boldsymbol{\psi}_i^p$  must be a real-valued vector, that is, imaginary part of  $\boldsymbol{\psi}_i^p$ ,  $\text{Im}(\boldsymbol{\psi}_i^p) = 0$ , which can be easily derived after substituting  $\lambda_i^p$  and  $\boldsymbol{\psi}_i^p$  into Equation (2.4) and taking imaginary parts operation for both sides of the consequent equation. Thus,  $\boldsymbol{\psi}_i^p \in \mathbb{R}^{2N}$  ( $i = 1, 2 \dots N_p$ ) and

$$\boldsymbol{\psi}_i^p = \begin{Bmatrix} \lambda_i^p \boldsymbol{\phi}_i^p \\ \boldsymbol{\phi}_i^p \end{Bmatrix} \in \mathbb{R}^{2N} \quad (2.10)$$

where  $\boldsymbol{\phi}_i^p \in \mathbb{R}^N$  is the  $i$ th “over-damped modal shape”.

The eigenvalue matrix, which is the assembly of all eigenvalues, is a diagonal matrix and is denoted as

$$\boldsymbol{\Lambda} = \text{diag}(\lambda_1, \lambda_2 \dots \lambda_{N_c}, \lambda_1^*, \lambda_2^* \dots \lambda_{N_c}^*, \lambda_1^p, \lambda_2^p \dots \lambda_{N_p}^p) \in \mathbb{C}^{2N \times 2N} \quad (2.11)$$

The eigenvector matrix, which is the assembly of all eigenvectors, is denoted as

$$\begin{aligned} \boldsymbol{\Psi} &= (\boldsymbol{\psi}_1, \boldsymbol{\psi}_2 \dots \boldsymbol{\psi}_{N_c}, \boldsymbol{\psi}_1^*, \boldsymbol{\psi}_2^* \dots \boldsymbol{\psi}_{N_c}^*, \boldsymbol{\psi}_1^p, \boldsymbol{\psi}_2^p \dots \boldsymbol{\psi}_{N_p}^p) \\ &= \begin{pmatrix} \boldsymbol{\Phi} \boldsymbol{\Lambda} \\ \boldsymbol{\Phi} \end{pmatrix} \in \mathbb{C}^{2N \times 2N} \end{aligned} \quad (2.12)$$

in which  $\boldsymbol{\Phi} = (\boldsymbol{\phi}_1, \boldsymbol{\phi}_2 \dots \boldsymbol{\phi}_{N_c}, \boldsymbol{\phi}_1^*, \boldsymbol{\phi}_2^* \dots \boldsymbol{\phi}_{N_c}^*, \boldsymbol{\phi}_1^p, \boldsymbol{\phi}_2^p \dots \boldsymbol{\phi}_{N_p}^p) \in \mathbb{C}^{N \times 2N}$  is the eigenvector matrix associated with the displacement vector (modal shape matrix) and  $\boldsymbol{\Phi} \boldsymbol{\Lambda}$  is the eigenvector matrix associated with the velocity vector.

## 2.4 Orthogonality

The eigenvectors corresponding to different eigenvalues can be shown to satisfy the following orthogonality conditions, in which no repeated eigenvalues condition is assumed. For simplicity of the proof of the orthogonality, denote  $(\lambda_r, \boldsymbol{\psi}_r)$  ( $r = 1, 2 \dots N$ ) or  $(\lambda_s, \boldsymbol{\psi}_s)$  ( $s = 1, 2 \dots N$ ) to express all general eigen-pairs. Thus,  $(\lambda_r, \boldsymbol{\psi}_r)$  and  $(\lambda_s, \boldsymbol{\psi}_s)$  satisfy the following two equations, respectively:

$$(\lambda_r \mathbf{A} + \mathbf{B}) \boldsymbol{\psi}_r = \mathbf{0} \in \mathbb{C}^{2N} \quad (2.13)$$

$$(\lambda_s \mathbf{A} + \mathbf{B}) \boldsymbol{\psi}_s = \mathbf{0} \in \mathbb{C}^{2N} \quad (2.14)$$

Pre-multiplying  $\boldsymbol{\psi}_s^T$  and  $\boldsymbol{\psi}_r^T$  to both sides of Equations (2.13) and (2.14), respectively, gives

$$\boldsymbol{\psi}_s^T (\lambda_r \mathbf{A} + \mathbf{B}) \boldsymbol{\psi}_r = 0 \in \mathbb{C} \quad (2.15)$$

$$\boldsymbol{\psi}_r^T (\lambda_s \mathbf{A} + \mathbf{B}) \boldsymbol{\psi}_s = 0 \in \mathbb{C} \quad (2.16)$$

Since  $\mathbf{A}$  and  $\mathbf{B}$  are symmetric matrices,  $\boldsymbol{\psi}_s^T \mathbf{A} \boldsymbol{\psi}_r = \boldsymbol{\psi}_r^T \mathbf{A} \boldsymbol{\psi}_s$  and  $\boldsymbol{\psi}_s^T \mathbf{B} \boldsymbol{\psi}_r = \boldsymbol{\psi}_r^T \mathbf{B} \boldsymbol{\psi}_s$ . Further, subtracting (2.15) from (2.16) gives

$$(\lambda_s - \lambda_r) \boldsymbol{\psi}_r^T \mathbf{A} \boldsymbol{\psi}_s = 0 \quad (2.17)$$

Assume that there are no repeated eigenvalues in the structural system, that is, if  $r = s$ ,  $\lambda_r \neq \lambda_s$ . Thus

$$\boldsymbol{\psi}_r^T \mathbf{A} \boldsymbol{\psi}_s = \boldsymbol{\psi}_r^T \mathbf{B} \boldsymbol{\psi}_s = 0, \text{ if } r \neq s \quad (2.18)$$

When  $r = s$ , the following relationships exist

$$\boldsymbol{\psi}_r^T \mathbf{A} \boldsymbol{\psi}_r = a_r \in \mathbb{C} \quad (2.19)$$

$$\boldsymbol{\psi}_r^T \mathbf{B} \boldsymbol{\psi}_r = b_r = -\lambda_r a_r \in \mathbb{C} \quad (2.20)$$

Equations (2.18) to (2.20) show that all eigenvectors are orthogonal with respect to the matrices  $\mathbf{A}$  and  $\mathbf{B}$ , respectively, under the conditions that no repeated eigenvalues exist. Note that a complex mode as denoted with subscript  $i$  as previously defined is composed of two eigen-pairs which are conjugated with each other. However, they actually belong to different eigen-pairs because their eigenvalues are unequal and their eigenvectors are orthogonal each other.

Combining Equations (2.18) to (2.20) and expanding the consequent equations with the help of Equation (2.3) as well as rewriting Equation (2.8) for  $r$  and  $s$ , respectively, as

$$\boldsymbol{\Psi}_r = \begin{Bmatrix} \lambda_r \boldsymbol{\Phi}_r \\ \boldsymbol{\Phi}_r \end{Bmatrix} \in \mathbb{C}^{2N} \quad (2.21)$$

and

$$\boldsymbol{\Psi}_s = \begin{Bmatrix} \lambda_s \boldsymbol{\Phi}_s \\ \boldsymbol{\Phi}_s \end{Bmatrix} \in \mathbb{C}^{2N} \quad (2.22)$$

we can have

$$\boldsymbol{\Psi}_r^T \mathbf{A} \boldsymbol{\Psi}_s = (\lambda_r + \lambda_s) \boldsymbol{\Phi}_r^T \mathbf{M} \boldsymbol{\Phi}_s + \boldsymbol{\Phi}_r^T \mathbf{C} \boldsymbol{\Phi}_s = \begin{cases} a_r & \text{if } r = s \\ 0 & \text{if } r \neq s \end{cases} \quad (2.23)$$

$$\boldsymbol{\Psi}_r^T \mathbf{B} \boldsymbol{\Psi}_s = -\lambda_r \lambda_s \boldsymbol{\Phi}_r^T \mathbf{M} \boldsymbol{\Phi}_s + \boldsymbol{\Phi}_r^T \mathbf{K} \boldsymbol{\Phi}_s = \begin{cases} b_r = -\lambda_r a_r & \text{if } r = s \\ 0 & \text{if } r \neq s \end{cases} \quad (2.24)$$

$$(r, s = 1, 2, 3 \dots N)$$

Supposing that  $r$  and  $s$  express the same complex mode (the  $i$ th order), that is,  $\lambda_r = \lambda_s^*$ ,  $\boldsymbol{\Phi}_r = \boldsymbol{\Phi}_s^*$ , and noting that  $(\lambda_i + \lambda_i^*) = -2\xi_i \omega_i$  and  $\lambda_i \lambda_i^* = \omega_i^2$  ( $i = 1, 2, 3 \dots N_C$ ), from Equations (2.23) and (2.24), we can obtain two useful formulas for calculating modal natural frequency  $\omega_i$  and modal damping ratio  $\xi_i$  of the system, respectively:

$$\omega_i = \sqrt{\frac{\boldsymbol{\Phi}_i^H \mathbf{K} \boldsymbol{\Phi}_i}{\boldsymbol{\Phi}_i^H \mathbf{M} \boldsymbol{\Phi}_i}} \in \mathbb{R} \quad (2.25)$$

and



$$\xi_i = \frac{\boldsymbol{\varphi}_i^H \mathbf{C} \boldsymbol{\varphi}_i}{(2\omega_i) \boldsymbol{\varphi}_i^H \mathbf{M} \boldsymbol{\varphi}_i} = \frac{\boldsymbol{\varphi}_i^H \mathbf{C} \boldsymbol{\varphi}_i}{2\sqrt{(\boldsymbol{\varphi}_i^H \mathbf{M} \boldsymbol{\varphi}_i)(\boldsymbol{\varphi}_i^H \mathbf{K} \boldsymbol{\varphi}_i)}} \in \mathbb{R} \quad (2.26)$$

$$(i = 1, 2, 3 \dots N_C)$$

where superscript ‘‘H’’ denotes Hermitian transpose, which is equivalent to conjugate and transpose operation. Note that since  $\mathbf{M}$  and  $\mathbf{K}$  are assumed positive-definite matrices and the structure is completely constrained,  $(\boldsymbol{\varphi}_i^H \mathbf{M} \boldsymbol{\varphi}_i) \neq 0$ ,  $(\boldsymbol{\varphi}_i^H \mathbf{K} \boldsymbol{\varphi}_i) \neq 0$  and  $\omega_i \neq 0$ .

Considering the orthogonality shown in Equations (2.23) and (2.24), the general orthogonal property can be re-expressed as

$$\hat{\mathbf{a}} = \boldsymbol{\Psi}^T \mathbf{A} \boldsymbol{\Psi} = \text{diag}(a_1, a_2 \dots a_{N_C}, a_1^*, a_2^* \dots a_{N_C}^*, a_1^P, a_2^P \dots a_{N_P}^P) \in \mathbb{C}^{2N \times 2N} \quad (2.27)$$

$$\hat{\mathbf{b}} = \boldsymbol{\Psi}^T \mathbf{B} \boldsymbol{\Psi} = \text{diag}(b_1, b_2 \dots b_{N_C}, b_1^*, b_2^* \dots b_{N_C}^*, b_1^P, b_2^P \dots b_{N_P}^P) \in \mathbb{C}^{2N \times 2N} \quad (2.28)$$

where

$$a_i = \boldsymbol{\psi}_i^T \mathbf{A} \boldsymbol{\psi}_i = \boldsymbol{\varphi}_i^T (2\lambda_i \mathbf{M} + \mathbf{C}) \boldsymbol{\varphi}_i \in \mathbb{C} \quad (2.29)$$

$$b_i = \boldsymbol{\psi}_i^T \mathbf{B} \boldsymbol{\psi}_i = \boldsymbol{\varphi}_i^T (-\lambda_i^2 \mathbf{M} + \mathbf{K}) \boldsymbol{\varphi}_i = -a_i \lambda_i \in \mathbb{C} \quad (2.30)$$

$$(i = 1, 2, 3 \dots N_C \text{ for complex modes})$$

and

$$a_i^P = (\boldsymbol{\psi}_i^P)^T \mathbf{A} \boldsymbol{\psi}_i^P = (\boldsymbol{\varphi}_i^P)^T (2\lambda_i^P \mathbf{M} + \mathbf{C}) \boldsymbol{\varphi}_i^P \in \mathbb{R} \quad (2.31)$$

$$b_i^P = (\boldsymbol{\psi}_i^P)^T \mathbf{B} \boldsymbol{\psi}_i^P = (\boldsymbol{\varphi}_i^P)^T [-(\lambda_i^P)^2 \mathbf{M} + \mathbf{K}] \boldsymbol{\varphi}_i^P = -a_i^P \lambda_i^P \in \mathbb{R} \quad (2.32)$$

$$(i = 1, 2, 3 \dots N_P \text{ for pseudo modes})$$

In Appendix A, the non-singular properties of  $\hat{\mathbf{a}}$  and  $\hat{\mathbf{b}}$  have been proven, which means that each element ( $a_i$ ,  $a_i^*$ ,  $b_i$ ,  $b_i^*$ ,  $a_i^P$  and  $b_i^P$ ) in diagonal matrices  $\hat{\mathbf{a}}$  and  $\hat{\mathbf{b}}$  is non-zero parameter.

## 2.5 Modal Decomposition and Superposition of Modal Responses

Equation (2.1) can be decoupled into  $2N$  independent modal equations, after taking congruent transformation to coefficient matrices in Equation (2.1) based on the orthogonality property shown in the previous section. Let

$$\mathbf{y}(t) = \begin{Bmatrix} \dot{\mathbf{x}}(t) \\ \mathbf{x}(t) \end{Bmatrix} = \mathbf{\Psi} \mathbf{z}(t) \in \mathbb{R}^{2N} \quad (2.33)$$

in which

$$\mathbf{z}(t) = \left[ z_1(t), z_2(t), \dots, z_{N_c}(t), z_1^*(t), z_2^*(t), \dots, z_{N_c}^*(t), z_1^p(t), z_2^p(t), \dots, z_{N_p}^p(t) \right]^T \in \mathbb{C}^{2N} \quad (2.34)$$

is the complex-valued modal coordinate vector in time domain.

Substituting Equation (2.33) into Equation (2.1) and pre-multiplying  $\mathbf{\Psi}^T$  to both sides of the resulting equation as well as making use of Equations (2.29) to (2.32), the following equations can be obtained

$$a_i \dot{z}_i(t) + b_i z_i(t) = \boldsymbol{\phi}_i^T \mathbf{f}(t) \in \mathbb{C} \quad (i = 1, 2, \dots, N_c) \quad (2.35)$$

$$a_i^* \dot{z}_i^*(t) + b_i^* z_i^*(t) = \boldsymbol{\phi}_i^H \mathbf{f}(t) \in \mathbb{C} \quad (i = 1, 2, \dots, N_c) \quad (2.36)$$

and 
$$a_i^p \dot{z}_i^p(t) + b_i^p z_i^p(t) = (\boldsymbol{\phi}_i^p)^T \mathbf{f}(t) \in \mathbb{R} \quad (i = 1, 2, \dots, N_p) \quad (2.37)$$

Equations (2.35) to (2.37) are all first-order complex numbered differential equations that can be readily solved using the standard digital algorithms. The solutions of (2.35) to (2.37) can be expressed as (Hart and Wong 1999)

$$z_i(t) = \frac{1}{a_i} \int_0^t e^{\lambda_i(t-\tau)} \boldsymbol{\phi}_i^T \mathbf{f}(\tau) d\tau \in \mathbb{C} \quad (2.37a)$$

$$z_i^*(t) = \frac{1}{a_i^*} \int_0^t e^{\lambda_i^*(t-\tau)} \boldsymbol{\phi}_i^H \mathbf{f}(\tau) d\tau \in \mathbb{C} \quad (2.37b)$$

$$z_i^p(t) = \frac{1}{a_i^p} \int_0^t e^{\lambda_i^p(t-\tau)} (\boldsymbol{\phi}_i^p)^T \mathbf{f}(\tau) d\tau \in \mathbb{R} \quad (2.37c)$$

Obviously, only one of Equations (2.37a) and (2.37b) is independent and needs to be solved.

After the modal responses are solved, the total responses are back-calculated by the superposition of the modal responses. Considering Equation (2.12) in Equation (2.33) gives the following two expressions:

$$\mathbf{x}(t) = \sum_{i=1}^{N_c} \left[ \boldsymbol{\varphi}_i z_i(t) + \boldsymbol{\varphi}_i^* z_i^*(t) \right] + \sum_{i=1}^{N_p} \boldsymbol{\varphi}_i^p z_i^p(t) \in \mathbb{R}^N \quad (2.38)$$

$$\dot{\mathbf{x}}(t) = \sum_{i=1}^{N_c} \left[ \lambda_i \boldsymbol{\varphi}_i z_i(t) + \lambda_i^* \boldsymbol{\varphi}_i^* z_i^*(t) \right] + \sum_{i=1}^{N_p} \lambda_i^p \boldsymbol{\varphi}_i^p z_i^p(t) \in \mathbb{R}^N \quad (2.39)$$

## 2.6 Expansion of System Matrices in terms of Modal Parameters

### 2.6.1 A Special Property of System Modal Shapes

Taking the time derivative of Equation (2.38) gives

$$\dot{\mathbf{x}}(t) = \sum_{i=1}^{N_c} \left[ \boldsymbol{\varphi}_i \dot{z}_i(t) + \boldsymbol{\varphi}_i^* \dot{z}_i^*(t) \right] + \sum_{i=1}^{N_p} \boldsymbol{\varphi}_i^p \dot{z}_i^p(t) \quad (2.40)$$

Substituting Equations (2.35) to (2.37) into Equation (2.40) accordingly leads to

$$\dot{\mathbf{x}}(t) = \sum_{i=1}^{N_c} \left[ \frac{\boldsymbol{\varphi}_i \boldsymbol{\varphi}_i^T \mathbf{f}(t)}{a_i} + \boldsymbol{\varphi}_i \lambda_i z_i(t) + \frac{\boldsymbol{\varphi}_i^* \boldsymbol{\varphi}_i^H \mathbf{f}(t)}{a_i^*} + \boldsymbol{\varphi}_i^* \lambda_i^* z_i^*(t) \right] + \sum_{i=1}^{N_p} \left[ \frac{\boldsymbol{\varphi}_i^p (\boldsymbol{\varphi}_i^p)^T \mathbf{f}(t)}{a_i^p} + \boldsymbol{\varphi}_i^p \lambda_i^p z_i^p(t) \right] \quad (2.41)$$

After comparing Equations (2.39) and (2.41), it can be observed that

$$\sum_{i=1}^{N_c} \left[ \frac{\boldsymbol{\varphi}_i \boldsymbol{\varphi}_i^T}{a_i} + \frac{\boldsymbol{\varphi}_i^* \boldsymbol{\varphi}_i^H}{a_i^*} \right] \mathbf{f}(t) + \sum_{i=1}^{N_p} \left[ \frac{\boldsymbol{\varphi}_i^p (\boldsymbol{\varphi}_i^p)^T}{a_i^p} \right] \mathbf{f}(t) = \mathbf{0} \in \mathbb{R}^N \quad (2.42)$$

As  $\mathbf{f}(t)$  is an arbitrary excitation force vector, it implies that

$$\sum_{i=1}^{N_c} \left[ \frac{\boldsymbol{\varphi}_i \boldsymbol{\varphi}_i^T}{a_i} + \frac{\boldsymbol{\varphi}_i^* \boldsymbol{\varphi}_i^H}{a_i^*} \right] + \sum_{i=1}^{N_p} \left[ \frac{\boldsymbol{\varphi}_i^p (\boldsymbol{\varphi}_i^p)^T}{a_i^p} \right] = \mathbf{0} \in \mathbb{R}^{N \times N} \quad (2.43)$$

which can be assembled in a simple matrix form as

$$\Phi \hat{\mathbf{a}}^{-1} \Phi^T = \mathbf{0} \quad (2.44)$$

Actually, Equations (2.42) and (2.44) are the result of the summation of the system residual matrix, which will be defined in details in the next chapter. This property is a key element in the derivation of other modal properties.

## 2.6.2 Expansion of the Mass Matrix $\mathbf{M}$ and Its Inverse $\mathbf{M}^{-1}$

Substituting Equation (2.12) into Equation (2.28) yields

$$\Psi^T \mathbf{B} \Psi = \begin{pmatrix} \Phi \Lambda \\ \Phi \end{pmatrix}^T \begin{pmatrix} -\mathbf{M} & \mathbf{0} \\ \mathbf{0} & \mathbf{K} \end{pmatrix} \begin{pmatrix} \Phi \Lambda \\ \Phi \end{pmatrix} = -\Lambda \Phi^T \mathbf{M} \Phi \Lambda + \Phi^T \mathbf{K} \Phi = \hat{\mathbf{b}} = -\hat{\mathbf{a}} \Lambda \quad (2.45)$$

that is, 
$$\Lambda \Phi^T \mathbf{M} \Phi \Lambda - \Phi^T \mathbf{K} \Phi = \hat{\mathbf{a}} \Lambda \quad (2.46)$$

Pre-multiplying  $\Phi \hat{\mathbf{a}}^{-1}$  and post-multiplying  $\hat{\mathbf{a}}^{-1} \Phi^T$  to both sides of Equation (2.46) leads to

$$\left( \Phi \hat{\mathbf{a}}^{-1} \Lambda \Phi^T \right) \mathbf{M} \left( \Phi \hat{\mathbf{a}}^{-1} \Lambda \Phi^T \right) - \left( \Phi \hat{\mathbf{a}}^{-1} \Phi^T \right) \mathbf{K} \left( \Phi \hat{\mathbf{a}}^{-1} \Phi^T \right) = \left( \Phi \Lambda \hat{\mathbf{a}}^{-1} \Phi^T \right) \quad (2.47)$$

Substituting Equation (2.44) into Equation (2.47), it can be simplified as

$$\left( \Phi \hat{\mathbf{a}}^{-1} \Lambda \Phi^T \right) \mathbf{M} \left( \Phi \Lambda \hat{\mathbf{a}}^{-1} \Phi^T \right) = \left( \Phi \Lambda \hat{\mathbf{a}}^{-1} \Phi^T \right) \quad (2.48)$$

Thus, 
$$\mathbf{M} = \left( \Phi \hat{\mathbf{a}}^{-1} \Lambda \Phi^T \right)^{-1} \quad (2.49)$$

and

$$\begin{aligned} \mathbf{M}^{-1} &= \Phi \hat{\mathbf{a}}^{-1} \Lambda \Phi^T = \sum_{i=1}^{N_c} \left( \frac{\lambda_i \boldsymbol{\varphi}_i \boldsymbol{\varphi}_i^T}{a_i} + \frac{\lambda_i^* \boldsymbol{\varphi}_i^* \boldsymbol{\varphi}_i^H}{a_i^*} \right) + \sum_{i=1}^{N_p} \frac{\lambda_i^p \boldsymbol{\varphi}_i^p (\boldsymbol{\varphi}_i^p)^T}{a_i^p} \\ &= 2 \sum_{i=1}^{N_c} \operatorname{Re} \left( \frac{\lambda_i \boldsymbol{\varphi}_i \boldsymbol{\varphi}_i^T}{a_i} \right) + \sum_{i=1}^{N_p} \frac{\lambda_i^p \boldsymbol{\varphi}_i^p (\boldsymbol{\varphi}_i^p)^T}{a_i^p} \end{aligned} \quad (2.50)$$

### 2.6.3 Expansion of the Damping Matrix $\mathbf{C}$

Substituting Equation (2.12) into Equation (2.27) yields

$$\begin{aligned}\Psi^T \mathbf{A} \Psi &= \begin{pmatrix} \Phi \Lambda \\ \Phi \end{pmatrix}^T \begin{pmatrix} \mathbf{0} & \mathbf{M} \\ \mathbf{M} & \mathbf{C} \end{pmatrix} \begin{pmatrix} \Phi \Lambda \\ \Phi \end{pmatrix} \\ &= \Phi^T \mathbf{M} \Phi \Lambda + \Lambda \Phi^T \mathbf{M} \Phi + \Phi^T \mathbf{C} \Phi = \hat{\mathbf{a}}\end{aligned}\quad (2.51)$$

that is, 
$$\Phi^T \mathbf{M} \Phi \Lambda + \Lambda \Phi^T \mathbf{M} \Phi + \Phi^T \mathbf{C} \Phi = \hat{\mathbf{a}} \quad (2.52)$$

Post-multiplying  $\Lambda \hat{\mathbf{a}}^{-1} \Phi^T$  to both sides of Equation (2.52) leads to

$$\Phi^T \mathbf{M} \Phi \Lambda^2 \hat{\mathbf{a}}^{-1} \Phi^T + \Lambda \Phi^T \mathbf{M} \Phi \Lambda \hat{\mathbf{a}}^{-1} \Phi^T + \Phi^T \mathbf{C} \Phi \Lambda \hat{\mathbf{a}}^{-1} \Phi^T = \Lambda \Phi^T \quad (2.53)$$

Using Equation (2.50), Equation (2.53) becomes

$$\Phi^T \mathbf{M} \Phi \Lambda^2 \hat{\mathbf{a}}^{-1} \Phi^T + \Lambda \Phi^T + \Phi^T \mathbf{C} \mathbf{M}^{-1} = \Lambda \Phi^T \quad (2.54)$$

That is,

$$\Phi^T (\mathbf{M} \Phi \Lambda^2 \hat{\mathbf{a}}^{-1} \Phi^T + \mathbf{C} \mathbf{M}^{-1}) = \mathbf{0} \quad (2.55)$$

Since  $\Phi \in \mathbb{C}^{N \times 2N}$  and  $\det[\Phi \Phi^T] \neq 0$ , we have

$$\mathbf{M} \Phi \Lambda^2 \hat{\mathbf{a}}^{-1} \Phi^T + \mathbf{C} \mathbf{M}^{-1} = \mathbf{0} \quad (2.56)$$

The damping matrix  $\mathbf{C}$  therefore can be expressed as

$$\mathbf{C} = -\mathbf{M} \Phi \Lambda^2 \hat{\mathbf{a}}^{-1} \Phi^T \mathbf{M} \quad (2.57)$$

Equation (2.57) can be further expanded as

$$\mathbf{C} = -\sum_{i=1}^{N_c} \left[ \frac{\lambda_i^2 \mathbf{M} \boldsymbol{\varphi}_i \boldsymbol{\varphi}_i^T \mathbf{M}}{a_i} + \frac{(\lambda_i^*)^2 \mathbf{M} \boldsymbol{\varphi}_i^* \boldsymbol{\varphi}_i^H \mathbf{M}}{a_i^*} \right] - \sum_{i=1}^{N_p} \left[ \frac{(\lambda_i^p)^2 \mathbf{M} \boldsymbol{\varphi}_i^p (\boldsymbol{\varphi}_i^p)^T \mathbf{M}}{a_i^p} \right] \quad (2.58)$$

### 2.6.4 Expansion of the Stiffness Matrix $\mathbf{K}$ and Flexibility Matrix $\mathbf{K}^{-1}$

To obtain the expansion of  $\mathbf{K}$ , we assemble the eigen-equation shown in Equation (2.4) as

$$\mathbf{M}\Phi\Lambda^2 + \mathbf{C}\Phi\Lambda + \mathbf{K}\Phi = \mathbf{0} \quad (2.59)$$

Substituting the expansion of  $\mathbf{C}$  shown in Equation (2.57) into Equation (2.59) gives

$$\begin{aligned} & \mathbf{M}\Phi\Lambda^2 - \mathbf{M}\Phi\Lambda^2\hat{\mathbf{a}}^{-1}\Phi^T\mathbf{M}\Phi\Lambda + \mathbf{K}\Phi \\ &= \mathbf{M}\Phi\Lambda^2(\mathbf{I} - \hat{\mathbf{a}}^{-1}\Phi^T\mathbf{M}\Phi\Lambda) + \mathbf{K}\Phi \\ &= \mathbf{0} \end{aligned} \quad (2.60)$$

where  $\mathbf{I}$  is a  $2N \times 2N$  identity matrix. Post-multiplying  $\Lambda\hat{\mathbf{a}}^{-1}\Phi^T$  to both sides of Equation (2.60) and using Equation (2.49) give

$$\begin{aligned} & \mathbf{M}\Phi\Lambda^2(\mathbf{I} - \hat{\mathbf{a}}^{-1}\Phi^T\mathbf{M}\Phi\Lambda)\Lambda\hat{\mathbf{a}}^{-1}\Phi^T + \mathbf{K}\Phi\Lambda\hat{\mathbf{a}}^{-1}\Phi^T \\ &= \mathbf{M}\Phi\Lambda^2(\mathbf{I} - \hat{\mathbf{a}}^{-1}\Phi^T\mathbf{M}\Phi\Lambda)\Lambda\hat{\mathbf{a}}^{-1}\Phi^T + \mathbf{K}\mathbf{M}^{-1} \\ &= \mathbf{0} \end{aligned} \quad (2.61)$$

As a result, the stiffness matrix  $\mathbf{K}$  can be expanded as

$$\mathbf{K} = -\mathbf{M}\Phi\Lambda^2(\mathbf{I} - \hat{\mathbf{a}}^{-1}\Phi^T\mathbf{M}\Phi\Lambda)\Lambda\hat{\mathbf{a}}^{-1}\Phi^T\mathbf{M} \quad (2.62)$$

To obtain the expansion of the structural  $\mathbf{K}^{-1}$ , pre-multiplying  $\Phi\hat{\mathbf{a}}^{-1}\Lambda^{-1}$  to both sides of Equation (2.46) leads to

$$(\Phi\hat{\mathbf{a}}^{-1}\Lambda^{-1}\Lambda\Phi^T)\mathbf{M}\Phi\Lambda - (\Phi\hat{\mathbf{a}}^{-1}\Lambda^{-1}\Phi^T)\mathbf{K}\Phi = \Phi\Lambda^{-1}\hat{\mathbf{a}}^{-1}\hat{\mathbf{a}}\Lambda \quad (2.63)$$

Using the residual matrix  $\Phi\hat{\mathbf{a}}^{-1}\Phi^T = \mathbf{0}$  shown in Equation (2.44), Equation (2.63) becomes

$$-\Phi\hat{\mathbf{a}}^{-1}\Lambda^{-1}\Phi^T\mathbf{K}\Phi = \Phi \quad (2.64)$$

Post-multiplying  $\Lambda \hat{\mathbf{a}}^{-1} \Phi^T$  to both sides of Equation (2.64) and using Equation (2.50), we have

$$-\Phi \hat{\mathbf{a}}^{-1} \Lambda^{-1} \Phi^T \mathbf{K} \mathbf{M}^{-1} = \mathbf{M}^{-1} \quad (2.65)$$

Thus, 
$$\mathbf{K}^{-1} = -\Phi \hat{\mathbf{a}}^{-1} \Lambda^{-1} \Phi^T \quad (2.66)$$

Equation (2.66) can be further expanded as

$$\mathbf{K}^{-1} = -\Phi \hat{\mathbf{a}}^{-1} \Lambda^{-1} \Phi^T = -\sum_{i=1}^{N_c} \left( \frac{\boldsymbol{\varphi}_i \boldsymbol{\varphi}_i^T}{\lambda_i a_i} + \frac{\boldsymbol{\varphi}_i^* \boldsymbol{\varphi}_i^H}{\lambda_i^* a_i^*} \right) - \sum_{i=1}^{N_p} \frac{\boldsymbol{\varphi}_i^p (\boldsymbol{\varphi}_i^p)^T}{\lambda_i^p a_i^p} \quad (2.67)$$

### 2.6.5 Expansion of the Total Mass of the System $M_\Sigma$

For a planar lumped-mass building system which may or may not have rotation moment of inertia, the total translational mass (or the total mass in the direction of seismic excitation) of the system is denoted as  $M_\Sigma$ , which can be represented by the following form.

$$M_\Sigma = \mathbf{J}^T \mathbf{M} \mathbf{J} \in \mathbb{R} \quad (2.68)$$

in which,  $\mathbf{J}$  is the ground motion influence vector. Note that when the system is a shear frame structure,  $\mathbf{J}$  is a  $N$ -dimensional ones vector (all  $N$  elements are unitary) while for a general planar structure, the elements corresponding to the rotation DOFs in  $\mathbf{J}$  are zero because in most cases rotation excitations from ground motion are ignored. The expansion of the total mass  $M_\Sigma$  can be shown in the following manner.

$$\begin{aligned} M_\Sigma &= \mathbf{J}^T \mathbf{M} \mathbf{J} \\ &= \mathbf{J}^T \mathbf{M} \mathbf{M}^{-1} \mathbf{M} \mathbf{J} \\ &= (\mathbf{M} \mathbf{J})^T \mathbf{M}^{-1} (\mathbf{M} \mathbf{J}) \end{aligned} \quad (2.69)$$

Substituting the inverse of the mass matrix  $\mathbf{M}^{-1}$  shown in Equation (2.50) into Equation (2.69) gives the expansion as

$$\begin{aligned}
M_\Sigma &= 2 \sum_{i=1}^{N_C} \operatorname{Re} \left( \frac{(\mathbf{M}\mathbf{J})^T \lambda_i \boldsymbol{\varphi}_i \boldsymbol{\varphi}_i^T \mathbf{M}\mathbf{J}}{a_i} \right) + \sum_{i=1}^{N_P} \frac{(\mathbf{M}\mathbf{J})^T \lambda_i^P \boldsymbol{\varphi}_i^P (\boldsymbol{\varphi}_i^P)^T \mathbf{M}\mathbf{J}}{a_i^P} \\
&= 2 \sum_{i=1}^{N_C} \operatorname{Re} \left( \frac{\lambda_i (\boldsymbol{\varphi}_i^T \mathbf{M}\mathbf{J})^2}{a_i} \right) + \sum_{i=1}^{N_P} \frac{\lambda_i^P ((\boldsymbol{\varphi}_i^P)^T \mathbf{M}\mathbf{J})^2}{a_i^P}
\end{aligned} \tag{2.70}$$

## 2.7 Reduction to Classically-Damped System

When a structure satisfies the Caughey criterion  $\mathbf{C}\mathbf{M}^{-1}\mathbf{K} = \mathbf{K}\mathbf{M}^{-1}\mathbf{C}$  (Caughey and O'Kelly 1965), all system mode shapes are real-valued and are consistent with those of an undamped system. In Appendix B, Caughey criterion has been extended to be used as the criterion for a system with over-damped subsystems. Thus, the modal shape proportional factors  $a_i$  for real modes ( $i=1, 2 \dots N_C$ ) expressed by Equation (2.29) can be simplified as

$$a_i = \boldsymbol{\varphi}_i^T (2\lambda_i \mathbf{M} + \mathbf{C}) \boldsymbol{\varphi}_i = 2m_i (\lambda_i + \xi_i \omega_i) = j2m_i \omega_{d_i} \tag{2.71a}$$

where  $m_i = \boldsymbol{\varphi}_i^T \mathbf{M} \boldsymbol{\varphi}_i$  is the  $i$ th real modal mass while  $a_i^P$  ( $i=1, 2 \dots N_P$ ) remains the same format. Substituting Equation (2.71a) into Equations (2.50), (2.58), (2.62), (2.67) and (2.70) we have

$$\mathbf{M}^{-1} = \sum_{i=1}^{N_C} \frac{\boldsymbol{\varphi}_i \boldsymbol{\varphi}_i^T}{m_i} - \sum_{i=1}^{N_P} \frac{\omega_i^P \boldsymbol{\varphi}_i^P (\boldsymbol{\varphi}_i^P)^T}{a_i^P} \tag{2.71b}$$

$$\mathbf{C} = \sum_{i=1}^{N_C} \frac{(2\xi_i \omega_i) \mathbf{M} \boldsymbol{\varphi}_i \boldsymbol{\varphi}_i^T \mathbf{M}}{m_i} - \sum_{i=1}^{N_P} \left[ \frac{(\omega_i^P)^2 \mathbf{M} \boldsymbol{\varphi}_i^P (\boldsymbol{\varphi}_i^P)^T \mathbf{M}}{a_i^P} \right] \tag{2.71c}$$

$$\mathbf{K} = \sum_{i=1}^{N_C} \frac{\omega_i^2 \mathbf{M} \boldsymbol{\varphi}_i \boldsymbol{\varphi}_i^T \mathbf{M}}{m_i} + \sum_{i=1}^{N_P} \frac{\omega_i^P \mathbf{M} \boldsymbol{\varphi}_i^P (\boldsymbol{\varphi}_i^P)^T \mathbf{M}}{a_i^P} \tag{2.71d}$$

$$\mathbf{K}^{-1} = \sum_{i=1}^{N_C} \frac{\boldsymbol{\varphi}_i \boldsymbol{\varphi}_i^T}{\omega_i^2 m_i} + \sum_{i=1}^{N_P} \frac{\boldsymbol{\varphi}_i^P (\boldsymbol{\varphi}_i^P)^T}{\omega_i^P a_i^P} \tag{2.71e}$$



$$M_{\Sigma} = \sum_{i=1}^{N_c} \frac{(\boldsymbol{\varphi}_i^T \mathbf{M} \mathbf{J})^2}{m_i} - \sum_{i=1}^{N_p} \frac{\omega_i^p ((\boldsymbol{\varphi}_i^p)^T \mathbf{M} \mathbf{J})^2}{a_i^p} \quad (2.71f)$$

If there are no over-damped modes existing in the system ( $N_p = 0$  and  $N_c = N$ ), the Equations (2.71a) to (2.71f) can be further simplified as

$$\mathbf{M}^{-1} = \sum_{i=1}^{N_c} \frac{\boldsymbol{\varphi}_i \boldsymbol{\varphi}_i^T}{m_i} \quad (2.71g)$$

$$\mathbf{C} = \sum_{i=1}^{N_c} \frac{(2\xi_i \omega_i) \mathbf{M} \boldsymbol{\varphi}_i \boldsymbol{\varphi}_i^T \mathbf{M}}{m_i} \quad (2.71h)$$

$$\mathbf{K} = \sum_{i=1}^{N_c} \frac{\omega_i^2 \mathbf{M} \boldsymbol{\varphi}_i \boldsymbol{\varphi}_i^T \mathbf{M}}{m_i} \quad (2.71i)$$

$$\mathbf{K}^{-1} = \sum_{i=1}^{N_c} \frac{\boldsymbol{\varphi}_i \boldsymbol{\varphi}_i^T}{\omega_i^2 m_i} \quad (2.71j)$$

$$M_{\Sigma} = \sum_{i=1}^{N_c} \frac{(\boldsymbol{\varphi}_i^T \mathbf{M} \mathbf{J})^2}{m_i} \quad (2.71k)$$

In Equation (2.71),  $(\boldsymbol{\varphi}_i^T \mathbf{M} \mathbf{J})^2 / m_i$  is the  $i$ th modal participation mass (Wilson 2004).



## **CHAPTER 3**

### **GENERAL MODAL RESPONSE HISTORY ANALYSIS**

#### **3.1 Introduction**

In Chapter 2, the dynamic response of a generally damped linear MDOF structure has been expressed by means of the superposition of its modal responses. However, it is expressed in complex-valued form without physical meaning. An improved general solution, completely expressed in real-valued form, for calculating seismic response history of the MDOF structure, is deduced in this chapter and the physical explanation of each resulting terms are given. In this formulation, the Laplace transformation approach is employed, by which the system original differential equations in time domain can be converted to algebraic equations in Laplacian domain, to show the intrinsic relationship among the system's parameters.

#### **3.2 Analytical Formulation**

A solution to the problem of obtaining the dynamic response of generally damped linear MDOF systems via the modal analysis approach is presented in this section. This formulation takes into consideration the presence of the over-damped modes (i.e., the eigenvalues associated with these modes are real-valued rather than complex-valued).

##### **3.2.1 Laplace Transform Operation**

To simplify further development, the Laplace transformation (Greenberg 1998) is employed first to transform the differential equations to the linear algebraic equations in Laplacian domain, by which the system response in Laplace domain can be easily expressed as the combination of the complete orders of the modal subsystems (composed by the corresponding modal parameters). The responses in the time domain for the complete system and all sub-systems are easily retrieved through the inverse-Laplace transform.

Applying Laplace transform to Equations (2.33) and (2.35) to (2.37) under zero initial conditions, respectively, yields

$$\mathbf{Y}(s) = \begin{Bmatrix} \dot{\mathbf{X}}(s) \\ \mathbf{X}(s) \end{Bmatrix} = \begin{Bmatrix} s\mathbf{X}(s) \\ \mathbf{X}(s) \end{Bmatrix} = \boldsymbol{\Psi} \mathbf{Z}(s) \in \mathbb{C}^{2N \times 2N} \quad (3.1)$$

$$(a_i s + b_i) Z_i(s) = \boldsymbol{\varphi}_i^T \mathbf{F}(s) \in \mathbb{C} \quad (i=1, 2 \dots N_C) \quad (3.2)$$

$$(a_i^* s + b_i^*) Z_i^*(s) = \boldsymbol{\varphi}_i^H \mathbf{F}(s) \in \mathbb{C} \quad (i=1, 2 \dots N_C) \quad (3.3)$$

and  $(a_i^P s + b_i^P) Z_i^P(s) = (\boldsymbol{\varphi}_i^P)^T \mathbf{F}(s) \in \mathbb{C} \quad (i=1, 2 \dots N_p) \quad (3.4)$

where  $s$  is the Laplace parameter and

$$\mathbf{Z}(s) = \left[ Z_1(s), Z_2(s) \dots Z_{N_C}(s), Z_1^*(s), Z_2^*(s) \dots Z_{N_C}^*(s), Z_1^P(s), Z_2^P(s) \dots Z_{N_p}^P(s) \right]^T \quad (3.5)$$

is the modal coordinates vector expressed in Laplace domain and  $\mathbf{Z}(s) \in \mathbb{C}^{2N \times 2N}$ .  $\mathbf{X}(s)$  is the Laplace transformation of the displacement vector  $\mathbf{x}(t)$ ,  $\dot{\mathbf{X}}(s)$  is the Laplace transformation of the velocity vector  $\dot{\mathbf{x}}(t)$  and  $\mathbf{F}(s)$  is the Laplace transformation of the force vector  $\mathbf{f}(t)$ .

Solving  $Z_i(s)$ ,  $Z_i^*(s)$  and  $Z_i^P$  from Equations (3.2) to (3.4), respectively, and substituting the resulting solutions into Equation (3.1) as well as using Equations (2.30) and (2.32) result in

$$\begin{aligned} \mathbf{X}(s) &= \left\{ \sum_{i=1}^{N_C} \left[ \frac{\boldsymbol{\varphi}_i \boldsymbol{\varphi}_i^T}{a_i(s - \lambda_i)} + \frac{\boldsymbol{\varphi}_i^* \boldsymbol{\varphi}_i^H}{a_i^*(s - \lambda_i^*)} \right] + \sum_{i=1}^{N_p} \frac{\boldsymbol{\varphi}_i^P (\boldsymbol{\varphi}_i^P)^T}{a_i^P(s - \lambda_i^P)} \right\} \mathbf{F}(s) \\ &= \left[ \sum_{i=1}^{N_C} \left( \frac{\mathbf{R}_i}{s - \lambda_i} + \frac{\mathbf{R}_i^*}{s - \lambda_i^*} \right) + \sum_{i=1}^{N_p} \frac{\mathbf{R}_i^P}{s - \lambda_i^P} \right] \mathbf{F}(s) \in \mathbb{C}^N \end{aligned} \quad (3.6)$$

and 
$$\begin{aligned} \dot{\mathbf{X}}(s) = s\mathbf{X}(s) &= \left\{ \sum_{i=1}^{N_C} \left[ \frac{\lambda_i \boldsymbol{\varphi}_i \boldsymbol{\varphi}_i^T}{a_i(s - \lambda_i)} + \frac{\lambda_i^* \boldsymbol{\varphi}_i^* \boldsymbol{\varphi}_i^H}{a_i^*(s - \lambda_i^*)} \right] + \sum_{i=1}^{N_p} \frac{\lambda_i^P \boldsymbol{\varphi}_i^P (\boldsymbol{\varphi}_i^P)^T}{a_i^P(s - \lambda_i^P)} \right\} \mathbf{F}(s) \\ &= \left[ \sum_{i=1}^{N_C} \left( \frac{\lambda_i \mathbf{R}_i}{s - \lambda_i} + \frac{\lambda_i^* \mathbf{R}_i^*}{s - \lambda_i^*} \right) + \sum_{i=1}^{N_p} \frac{\lambda_i^P \mathbf{R}_i^P}{s - \lambda_i^P} \right] \mathbf{F}(s) \in \mathbb{C}^N \end{aligned} \quad (3.7)$$

where

$$\mathbf{R}_i = \mathbf{R}_i^R + j\mathbf{R}_i^I = \frac{\boldsymbol{\varphi}_i \boldsymbol{\varphi}_i^T}{a_i} \in \mathbb{C}^{N \times N} \quad (i = 1, 2 \dots N_C) \quad (3.8)$$

$$\mathbf{R}_i^* = \mathbf{R}_i^R - j\mathbf{R}_i^I = \frac{\boldsymbol{\varphi}_i^* \boldsymbol{\varphi}_i^H}{a_i^*} \in \mathbb{C}^{N \times N} \quad (i = 1, 2 \dots N_C) \quad (3.9)$$

$$\mathbf{R}_i^P = \frac{\boldsymbol{\varphi}_i^P (\boldsymbol{\varphi}_i^P)^T}{a_i^P} \in \mathbb{R}^{N \times N} \quad (i = 1, 2 \dots N_p) \quad (3.10)$$

$\mathbf{R}_i$ ,  $\mathbf{R}_i^*$  and  $\mathbf{R}_i^P$  are the system residual matrices corresponding to the eigenvalues  $\lambda_i$ ,  $\lambda_i^*$  and  $\lambda_i^P$ , respectively. Note that all residual matrices are intrinsic and invariant to a linear structural system, although modal shapes may be varied along with the corresponding changes of modal normalized factors (proportional multipliers)  $a_i$ ,  $a_i^*$  or  $a_i^P$ . In addition, referring to Equations (2.43) or (2.44), it has been proved that the summation for all residual matrixes is a zero matrix, that is,

$$\sum_{i=1}^{N_C} [\mathbf{R}_i + \mathbf{R}_i^*] + \sum_{i=1}^{N_p} \mathbf{R}_i^P = \mathbf{0} \in \mathbb{R}^{N \times N} \quad (3.10a)$$

or

$$2 \sum_{i=1}^{N_C} \mathbf{R}_i^R + \sum_{i=1}^{N_p} \mathbf{R}_i^P = \mathbf{0} \in \mathbb{R}^{N \times N} \quad (3.10b)$$

Now suppose that the structure is excited by the earthquake ground motion acceleration  $\ddot{x}_g(t)$ , the force vector  $\mathbf{F}(s)$  can be described as

$$\mathbf{F}(s) = -\mathbf{M}\mathbf{J}\ddot{X}_g(s) \in \mathbb{C}^N \quad (3.11)$$

in which  $\mathbf{J} \in \mathbb{R}^N$  is the influence vector which couples the ground motion to the DOF of the systems and  $\ddot{X}_g(s) \in \mathbb{C}$  is the Laplace transformation of the ground acceleration  $\ddot{x}_g(t)$ . As mentioned in Chapter 2 when the system is considered as a shear frame building,  $\mathbf{J}$  will be a column vector of unity. Substituting Equation (3.11) into Equation (3.6), the following equation can be obtained

$$\begin{aligned} \mathbf{X}(s) &= - \left[ \sum_{i=1}^{N_C} \left( \frac{\mathbf{R}_i}{s - \lambda_i} + \frac{\mathbf{R}_i^*}{s - \lambda_i^*} \right) \mathbf{M}\mathbf{J} + \sum_{i=1}^{N_p} \frac{\mathbf{R}_i^p \mathbf{M}\mathbf{J}}{s - \lambda_i^p} \right] \ddot{X}_g(s) \\ &= \sum_{i=1}^{N_C} \mathbf{X}_i(s) + \sum_{i=1}^{N_p} \mathbf{X}_i^p(s) \end{aligned} \quad (3.12)$$

where

$$\mathbf{X}_i(s) = - \left( \frac{\mathbf{R}_i}{s - \lambda_i} + \frac{\mathbf{R}_i^*}{s - \lambda_i^*} \right) \mathbf{M}\mathbf{J} \ddot{X}_g(s) \in \mathbb{C}^N \quad (3.13)$$

is the  $i$ th complex modal structural response vector in Laplace domain and

$$\mathbf{X}_i^p(s) = - \frac{\mathbf{R}_i^p \mathbf{M}\mathbf{J}}{s - \lambda_i^p} \ddot{X}_g(s) \in \mathbb{C}^N \quad (3.14)$$

is the  $i$ th over-damped modal structural response vector in Laplacian form. Considering the complex-valued eigenvalues and the residual matrices shown in Equations (2.7), (3.8) and (3.9), respectively, Equation (3.13) becomes

$$\begin{aligned} \mathbf{X}_i(s) &= - \left[ \frac{\mathbf{R}_i^R + j\mathbf{R}_i^I}{s - (-\xi_i \omega_i + j\omega_{di})} + \frac{\mathbf{R}_i^R - j\mathbf{R}_i^I}{s - (-\xi_i \omega_i - j\omega_{di})} \right] \mathbf{M}\mathbf{J} \ddot{X}_g(s) \\ &= - \left( \frac{\mathbf{A}_{Di} s}{s^2 + 2\xi_i \omega_i s + \omega_i^2} + \frac{\mathbf{B}_{Di}}{s^2 + 2\xi_i \omega_i s + \omega_i^2} \right) \ddot{X}_g(s) \quad (i = 1, 2, 3 \dots N_C) \end{aligned} \quad (3.15)$$

where

$$\mathbf{A}_{Di} = 2\mathbf{R}_i^R \mathbf{M}\mathbf{J} \in \mathbb{R}^N \quad (3.16)$$

$$\mathbf{B}_{D_i} = 2\omega_i \left( \xi_i \mathbf{R}_i^R - \sqrt{1 - \xi_i^2} \mathbf{R}_i^I \right) \mathbf{M} \mathbf{J} \in \mathbb{R}^N \quad (3.17)$$

Substituting Equations (2.9) and (3.10) into Equation (3.14) yields

$$\mathbf{X}_i^P(s) = -\frac{\mathbf{A}_{D_i}^P}{s + \omega_i^P} \ddot{X}_g(s) \quad (i = 1, 2, 3 \dots N_p) \quad (3.18)$$

in which 
$$\mathbf{A}_{D_i}^P = \mathbf{R}_i^P \mathbf{M} \mathbf{J} \in \mathbb{R}^N \quad (3.19)$$

Furthermore, denoting

$$Q_i(s) = H_i(s) \ddot{X}_g(s) \in \mathbb{C} \quad \text{and} \quad Q_{v_i}(s) = H_{v_i}(s) \ddot{X}_g(s) \in \mathbb{C} \quad (3.20)$$

where

$$H_i(s) = -\frac{1}{s^2 + 2\xi_i \omega_i s + \omega_i^2} \in \mathbb{C} \quad (3.21)$$

$$H_{v_i}(s) = s H_i(s) = -\frac{s}{s^2 + 2\xi_i \omega_i s + \omega_i^2} \in \mathbb{C} \quad (3.22)$$

are the displacement and velocity transfer function of a SDOF system with the  $i$ th complex modal damping ratio  $\xi_i$  and natural frequency  $\omega_i$  and excited by input  $\ddot{X}_g(s)$ . In fact, Equation (3.20) can be considered as the resulting Laplace transformation of the following SDOF differential equation expressed in time domain

$$\ddot{q}_i(t) + 2\xi_i \omega_i \dot{q}_i(t) + \omega_i^2 q_i(t) = -\ddot{x}_g(t) \quad (3.23)$$

where 
$$q_i(t) = \mathcal{L}^{-1}[Q_i(s)] \in \mathbb{R} \quad \text{and} \quad \dot{q}_i(t) = \mathcal{L}^{-1}[Q_{v_i}(s)] \in \mathbb{R} \quad (3.24)$$

in Equation (3.24),  $\mathcal{L}^{-1}$  stands for the inverse Laplace transformation operator. Taking the inverse Laplace transform of Equation (3.21) leads to

$$h_i(t) = \mathcal{L}^{-1}[H_i(s)] \in \mathbb{R} \quad (3.25)$$

$$h_{v_i}(t) = \mathcal{L}^{-1}[H_{v_i}(s)] = \in \mathbb{R} \quad (3.25a)$$

where  $h_i(t)$  and  $h_{v_i}(t)$  are the unit impulse response functions for displacement and velocity responses, respectively, of a SDOF system. It can be shown that

$$h_i(t) = -\frac{1}{\omega_{di}} e^{-\xi_i \omega_i t} \sin(\omega_{di} t) \in \mathbb{R} \quad (3.25b)$$

Thus, the  $i$ th modal displacement response  $q_i(t)$  can be written as

$$\begin{aligned} q_i(t) &= L^{-1}[Q_i(s)] = L^{-1}\left[H_i(s)\ddot{X}_g(s)\right] = \int_0^t h_i(t-\tau)\ddot{x}_g(\tau) d\tau \\ &= -\frac{1}{\omega_{di}} \int_0^t e^{-\xi_i \omega_i (t-\tau)} \sin \omega_{di}(t-\tau) \ddot{x}_g(\tau) d\tau \end{aligned} \quad (3.26)$$

For the case of over-damped modes, denoting

$$Q_i^p(s) = H_i^p(s)\ddot{X}_g(s) \in \mathbb{C} \quad (3.27)$$

in which

$$H_i^p(s) = -\frac{1}{s + \omega_i^p} \in \mathbb{C} \quad (3.28)$$

Similar to the transforming procedure of the complex mode case, Equation (3.27) is the Laplace transformation of the following first-order differential equation

$$\dot{q}_i^p(t) + \omega_i^p q_i^p(t) = -\ddot{x}_g(t) \quad (3.29)$$

where

$$q_i^p(t) = L^{-1}\left[Q_i^p(s)\right] \in \mathbb{R} \quad (3.30)$$

is the  $i$ th over-damped modal response. Note that  $q_i^p(t)$  has the dimension of velocity.

The inverse Laplace transformation of  $H_i^p(s)$  is given by

$$h_i^p(t) = -e^{-\omega_i^p t} \in \mathbb{R} \quad (3.31)$$



As a result, the  $i$ th over-damped modal response can be written as

$$\begin{aligned} q_i^p(t) &= L^{-1} [Q_i^p(s)] = L^{-1} [H_i^p(s) \ddot{X}_g(s)] = \int_0^t h_i^p(t-\tau) \ddot{x}_g(\tau) d\tau \\ &= -\int_0^t e^{-\omega_i^p(t-\tau)} \ddot{x}_g(\tau) d\tau \end{aligned} \quad (3.32)$$

### 3.2.2 Frequency Response Functions

Letting  $s = j\omega$  in Equations (3.21), (3.22) and (3.28), these transfer functions in Laplace domain are transformed to their corresponding Frequency Response Functions (FRF) in the frequency domain, which also can be considered as the resulting equations by taking Fourier transformation of  $h_i(t)$ ,  $h_{v_i}(t)$  and  $h_i^p(t)$ , respectively. That is,

$$H_i(j\omega) = \int_{-\infty}^{+\infty} h_i(t) e^{-j\omega t} dt = -\frac{1}{-\omega^2 + j2\xi_i\omega_i\omega + \omega_i^2} \quad (3.33)$$

$$H_{v_i}(j\omega) = \int_{-\infty}^{+\infty} h_{v_i}(t) e^{-j\omega t} dt = -\frac{j\omega}{-\omega^2 + j2\xi_i\omega_i\omega + \omega_i^2} \quad (3.34)$$

$$H_i^p(j\omega) = \int_{-\infty}^{+\infty} h_i^p(t) e^{-j\omega t} dt = -\frac{1}{j\omega + \omega_i^p} \quad (3.35)$$

Figure 3.1 shows the modulus of displacement FRF via Equation (3.33) considering natural periods equal 0.2s, 0.4s, 0.6s, 0.8s, 1.0s, 2.0s, 3.0s and 5.0s for damping ratio selected to be 5%. These natural periods are representative of the periods that are usually encountered in civil engineering structures. The 5% damping is often assumed in conventional structures as appropriate. Figure 3.2 presents the modulus of displacement FRF via Equation (3.33) using the damping ratios equal 2%, 5%, 10%, 20%, 50% and 80% while the period is 1 sec. These damping ratios are representatives of the modal damping ratios when structures are enhanced with damping devices. Similarly, the modulus of over-damped modal response via Equation (3.35) is presented in Figure 3.3 with respect to different over-damped modal periods, which are selected to be the same as those used in Figure 3.1. From Figure 3.1 to Figure 3.3, it may be observed that the order of the magnitude of the over-damped modal response FRF is at the same level as those of

the displacement modal response. This implies that the over-damped modes may be important for structural systems in which the over-damped modes exist.

### 3.2.3 Response Solutions to Displacement, Velocity and Absolute Acceleration

The displacement  $\mathbf{x}(t)$ , velocity  $\dot{\mathbf{x}}(t)$  and absolute acceleration  $\ddot{\mathbf{x}}_A(t)$  vectors in the time domain can be obtained as follows.

#### 3.2.3.1 Displacement Response Vector $\mathbf{x}(t)$

Applying inverse Laplace transform to Equations (3.15) and (3.18) and using Equations (3.24) and (3.30), the  $i$ th modal structural displacement response history vector for the complex modes and the  $i$ th modal structural response history vector for the over-damped modes can be derived as

$$\mathbf{x}_i(t) = \mathbf{A}_{D_i} \dot{q}_i(t) + \mathbf{B}_{D_i} q_i(t) \in \mathbb{R}^N \quad (i = 1, 2, 3 \dots N_C) \quad (3.36)$$

$$\mathbf{x}_i^P(t) = \mathbf{A}_{D_i}^P q_i^P(t) \in \mathbb{R}^N \quad (i = 1, 2, 3 \dots N_P) \quad (3.37)$$

Therefore, the complete structural displacement response history vector can be obtained by the modal superposition method via Equation (3.12) as

$$\mathbf{x}(t) = \sum_{i=1}^{N_C} [\mathbf{A}_{D_i} \dot{q}_i(t) + \mathbf{B}_{D_i} q_i(t)] + \sum_{i=1}^{N_P} \mathbf{A}_{D_i}^P q_i^P(t) \in \mathbb{R}^N \quad (3.38)$$

If all modes of the structure are under-damped (*i.e.*,  $N_C = N$  and  $N_P = 0$ ), the over-damped modal terms associated with  $q_i^P(t)$  disappear and Equation (3.38) can be reduced to

$$\mathbf{x}(t) = \sum_{i=1}^N [\mathbf{A}_{D_i} \dot{q}_i(t) + \mathbf{B}_{D_i} q_i(t)] \quad (3.39)$$

### 3.2.3.2 Velocity Response Vector $\dot{\mathbf{x}}(t)$

Intuitively, the structural velocity response vector can be obtained directly by taking the derivative of Equation (3.38) with respect to the time variable  $t$ , and it is given as

$$\dot{\mathbf{x}}(t) = \sum_{i=1}^{N_c} [\mathbf{A}_{D_i} \ddot{q}_i(t) + \mathbf{B}_{D_i} \dot{q}_i(t)] + \sum_{i=1}^{N_p} \mathbf{A}_{D_i}^p \dot{q}_i^p(t) \in \mathbb{R}^N \quad (3.40)$$

This approach seems to be simple and has been used by other researchers such as Takewaki (2004). However, this formulation requires the incorporation of two additional responses  $\ddot{q}_i(t)$  and  $\dot{q}_i^p(t)$ . A different approach to derive the expression of the relative velocity vector is given as follows.

Substituting Equations (2.7), (2.9) and (3.8) to (3.11) into Equation (3.7) and simplifying the resulting equation, the following expression can be obtained

$$\dot{\mathbf{X}}(s) = -\sum_{i=1}^{N_c} \left( \frac{\mathbf{A}_{V_i} s}{s^2 + 2\xi_i \omega_i s + \omega_i^2} + \frac{\mathbf{B}_{V_i}}{s^2 + 2\xi_i \omega_i s + \omega_i^2} \right) \ddot{X}_g(s) - \sum_{i=1}^{N_p} \frac{\mathbf{A}_{V_i}^p \ddot{X}_g(s)}{s + \omega_i^p} \quad (3.41)$$

where

$$\begin{aligned} \mathbf{A}_{V_i} &= -2\omega_i \left( \xi_i \mathbf{R}_i^R + \sqrt{1 - \xi_i^2} \mathbf{R}_i^I \right) \mathbf{M} \mathbf{J} \in \mathbb{R}^N \\ \mathbf{B}_{V_i} &= -2\omega_i^2 \mathbf{R}_i^R \mathbf{M} \mathbf{J} \in \mathbb{R}^N \\ \mathbf{A}_{V_i}^p &= -\omega_i^p \mathbf{R}_i^p \mathbf{M} \mathbf{J} \in \mathbb{R}^N \end{aligned} \quad (3.42)$$

Applying inverse Laplace transform to Equation (3.41) and considering Equations (3.24) and (3.30), the structural velocity response vector  $\dot{\mathbf{x}}(t)$  can be expressed as

$$\dot{\mathbf{x}}(t) = \sum_{i=1}^{N_c} [\mathbf{A}_{V_i} \dot{q}_i(t) + \mathbf{B}_{V_i} q_i(t)] + \sum_{i=1}^{N_p} \mathbf{A}_{V_i}^p q_i^p(t) \in \mathbb{R}^N \quad (3.43)$$

Equation (3.43) indicates that the structural relative velocity vector can also be expressed as a summation of all modal general responses. Noted that Equations (3.40) and (3.43) are equivalent. This is assured by the modal property which is introduced in

the following. However, Equation (3.43) is preferred in this study since the two additional modal responses  $\ddot{q}_i(t)$  and  $\dot{q}_i^p(t)$  are not needed in the expression.

Post-multiplying  $\mathbf{MJ}$  to both sides of Equation (3.10b) and further utilizing the relationships (3.16), (3.17) and (3.19), we have

$$2\sum_{i=1}^{N_C} \mathbf{R}_i^R \mathbf{MJ} + \sum_{i=1}^{N_P} \mathbf{R}_i^P \mathbf{MJ} = \mathbf{0} \in \mathbb{R}^N \quad (3.43a)$$

and

$$\sum_{i=1}^{N_C} \mathbf{A}_{D_i} + \sum_{i=1}^{N_P} \mathbf{A}_{D_i}^P = \mathbf{0} \in \mathbb{R}^N \quad (3.43b)$$

Equation (3.43b) shows that the summation of coefficient vectors  $\mathbf{A}_{D_i}$  and  $\mathbf{A}_{D_i}^P$  for all modes equals to a zero vector. Representing Equations (3.23) and (3.29), respectively, as

$$\ddot{q}_i(t) = -2\xi_i \omega_i \dot{q}_i(t) - \omega_i^2 q_i(t) - \ddot{x}_g(t) \in \mathbb{R} \quad (3.44)$$

$$\dot{q}_i^p(t) = -\omega_i^p q_i^p(t) - \ddot{x}_g(t) \in \mathbb{R} \quad (3.45)$$

and substituting them into Equation (3.40),  $\dot{\mathbf{x}}(t)$  can be expressed as

$$\begin{aligned} \dot{\mathbf{x}}(t) = & \sum_{i=1}^{N_C} \left\{ \left[ \mathbf{B}_{D_i} - 2\xi_i \omega_i \mathbf{A}_{D_i} \right] \dot{q}_i(t) - \omega_i^2 \mathbf{A}_{D_i} q_i(t) \right\} + \sum_{i=1}^{N_P} \left[ -\omega_i^p \mathbf{A}_{D_i}^P q_i^p(t) \right] \\ & - \left[ \sum_{i=1}^{N_C} \mathbf{A}_{D_i} + \sum_{i=1}^{N_P} \mathbf{A}_{D_i}^P \right] \ddot{x}_g(t) \end{aligned} \quad (3.46)$$

Utilizing Equations (3.42) and (3.43b), Equation (3.46) becomes

$$\dot{\mathbf{x}}(t) = \sum_{i=1}^{N_C} \left[ \mathbf{A}_{V_i} \dot{q}_i(t) + \mathbf{B}_{V_i} q_i(t) \right] + \sum_{i=1}^{N_P} \mathbf{A}_{V_i}^P q_i^p(t) \quad (3.47)$$

which is exactly same as Equation (3.43).

### 3.2.3.3 Absolute Acceleration Response Vector $\ddot{\mathbf{x}}_A(t)$

In the following, the expression for the absolute acceleration response is established in the general modal responses superposition form, which is similar to those obtained for the relative displacement and velocity responses.

Taking derivative to both sides of Equation (3.43) yields

$$\ddot{\mathbf{x}}(t) = \sum_{i=1}^{N_C} [\mathbf{A}_{V_i} \ddot{q}_i(t) + \mathbf{B}_{V_i} \dot{q}_i(t)] + \sum_{i=1}^{N_P} \mathbf{A}_{V_i}^P \dot{q}_i^P(t) \in \mathbb{R}^N \quad (3.48)$$

Substituting Equations (3.44) and (3.45) into Equation (3.48) leads to

$$\ddot{\mathbf{x}}(t) = \sum_{i=1}^{N_C} [\mathbf{A}_{A_i} \dot{q}_i(t) + \mathbf{B}_{A_i} q_i(t)] + \sum_{i=1}^{N_P} \mathbf{A}_{A_i}^P q_i^P(t) - \left[ \sum_{i=1}^{N_C} \mathbf{A}_{V_i} + \sum_{i=1}^{N_P} \mathbf{A}_{V_i}^P \right] \ddot{\mathbf{x}}_g(t) \quad (3.49)$$

where

$$\begin{aligned} \mathbf{A}_{A_i} &= 2\omega_i^2 \left[ (2\xi_i^2 - 1) \mathbf{R}_i^R + 2\xi_i \sqrt{1 - \xi_i^2} \mathbf{R}_i^I \right] \mathbf{M} \mathbf{J} \in \mathbb{R}^N \\ \mathbf{B}_{A_i} &= 2\omega_i^3 \left( \xi_i \mathbf{R}_i^R + \sqrt{1 - \xi_i^2} \mathbf{R}_i^I \right) \mathbf{M} \mathbf{J} \in \mathbb{R}^N \\ \mathbf{A}_{A_i}^P &= (\omega_i^P)^2 \mathbf{R}_i^P \mathbf{M} \mathbf{J} \in \mathbb{R}^N \end{aligned} \quad (3.50)$$

Post-multiplying  $\mathbf{M} \mathbf{J}$  to the both sides of the Equation (2.50) results in

$$\mathbf{J} = \sum_{i=1}^{N_C} \left( \frac{\lambda_i \boldsymbol{\varphi}_i \boldsymbol{\varphi}_i^T \mathbf{M} \mathbf{J}}{a_i} \right) + \sum_{i=1}^{N_P} \frac{\lambda_i^P \boldsymbol{\varphi}_i^P (\boldsymbol{\varphi}_i^P)^T \mathbf{M} \mathbf{J}}{a_i^P} \quad (3.51)$$

Equation (3.51) indicates another important property of the structural system. Using the definitions of system modal residual matrices in Equations (3.8) to (3.9), the modal property expressed in (3.51) can be rewritten as

$$\begin{aligned} \mathbf{J} &= \sum_{i=1}^{N_C} (\lambda_i \mathbf{R}_i \mathbf{M} \mathbf{J} + \lambda_i^* \mathbf{R}_i^* \mathbf{M} \mathbf{J}) + \sum_{i=1}^{N_P} \lambda_i^P \mathbf{R}_i^P \mathbf{M} \mathbf{J} \\ &= -2 \sum_{i=1}^{N_C} (\xi_i \omega_i \mathbf{R}_i^R + \omega_{di} \mathbf{R}_i^I) \mathbf{M} \mathbf{J} - \sum_{i=1}^{N_P} \omega_i^P \mathbf{R}_i^P \mathbf{M} \mathbf{J} \end{aligned} \quad (3.51a)$$

Further considering the notations for  $\mathbf{A}_{Vi}$  and  $\mathbf{A}_{Vi}^P$  defined in Equation (3.42), Equation (3.51a) can be simplified as

$$\sum_{i=1}^{N_C} \mathbf{A}_{Vi} + \sum_{i=1}^{N_P} \mathbf{A}_{Vi}^P = \mathbf{J} \in \mathbb{R}^N \quad (3.51b)$$

which indicates that the summation of coefficient vectors  $\mathbf{A}_{Vi}$  and  $\mathbf{A}_{Vi}^P$  for all modes equals to the ground motion influence vector. Thus

$$\left[ \sum_{i=1}^{N_C} \mathbf{A}_{Vi} + \sum_{i=1}^{N_P} \mathbf{A}_{Vi}^P \right] \ddot{\mathbf{x}}_g(t) = \mathbf{J} \ddot{\mathbf{x}}_g(t) \quad (3.52)$$

Substituting Equation (3.52) into Equation (3.49) and denoting the structural absolute acceleration vector as  $\ddot{\mathbf{x}}_A(t) \in \mathbb{R}^N$ , which can be expressed as  $\ddot{\mathbf{x}}_A(t) = \ddot{\mathbf{x}}(t) + \mathbf{J} \ddot{\mathbf{x}}_g(t)$  for a planar structure, Equation (3.49) becomes

$$\ddot{\mathbf{x}}_A(t) = \sum_{i=1}^{N_C} \left[ \mathbf{A}_{Ai} \dot{q}_i(t) + \mathbf{B}_{Ai} q_i(t) \right] + \sum_{i=1}^{N_P} \mathbf{A}_{Ai}^P q_i^P(t) \quad (3.53)$$

Note that in practical earthquake engineering application, the rotations effect of an earthquake ground motion are always ignored (Wilson 2004), thus the absolute acceleration for a structural rotation DOF always equals to the relative acceleration for the same DOF. The Equation (3.53) can be applied to either shear-frame type or non shear-frame type plane structure excited by single direction seismic acceleration. The difference lies on the ground motion influence vector  $\mathbf{J}$ . For the former, all elements in  $\mathbf{J}$  are “1”; while for the latter, the elements in  $\mathbf{J}$  may be “1” or may be “0”, which corresponds to translation DOFs and rotation DOFs, respectively.

By comparing the expressions of  $\mathbf{x}(t)$ ,  $\dot{\mathbf{x}}(t)$  and  $\ddot{\mathbf{x}}_A(t)$  derived above, it is found that these formulations are consistent and simple and computations of the modal responses  $q_i(t)$ ,  $\dot{q}_i(t)$  and  $q_i^P(t)$  are only required. These modal responses can be evaluated in the time domain for the specific ground motions using well-established

numerical methods. Note that the modal relative acceleration  $\ddot{q}_i(t)$  and the ground acceleration  $\ddot{x}_g(t)$  are not involved in the computation of the absolute acceleration.

### 3.3 A Unified Form for Structural Responses

In addition to the displacement, velocity and absolute acceleration vectors, a number of other response quantities are also important from the view point of seismic design. In this section, a unified form describing several response quantities of a shear planar building enhanced with damping devices is given. This form only incorporates the modal responses  $q_i(t)$ ,  $\dot{q}_i(t)$  and  $q_i^p(t)$ . For illustrative purpose, the response quantities discussed include (1) inter-story drift, (2) inter-story shear, (3) general inter-story shear (including the damping forces as appropriate), (4) inter-story moments, (5) general inter-story moment (including the moment caused by the damper forces as appropriate), and (6) damper forces.

To develop the unified form of dynamic responses, three transformation matrices established in the global structural coordinates are defined as follows

$$\mathbf{T}_D = \begin{pmatrix} 1/h_1 & 0 & 0 & \dots & \dots & 0 \\ -1/h_2 & 1/h_2 & 0 & \dots & \dots & 0 \\ 0 & -1/h_3 & 1/h_3 & \dots & \dots & 0 \\ \dots & \dots & \dots & \dots & \dots & \dots \\ 0 & 0 & 0 & \dots & -1/h_N & 1/h_N \end{pmatrix} \in \mathbb{R}^{N \times N} \quad (3.54)$$

$$\mathbf{T}_S = \begin{pmatrix} 1 & 1 & 1 & \dots & \dots & 1 \\ 0 & 1 & 1 & \dots & \dots & 1 \\ 0 & 0 & 1 & \dots & \dots & 1 \\ \dots & \dots & \dots & \dots & \dots & \dots \\ 0 & 0 & 0 & \dots & 0 & 1 \end{pmatrix} \in \mathbb{R}^{N \times N} \quad (3.55)$$

$$\mathbf{T}_M = \begin{pmatrix} h_1 & h_2 & h_3 & \dots & \dots & h_N \\ 0 & h_2 & h_3 & \dots & \dots & h_N \\ 0 & 0 & h_3 & \dots & \dots & h_N \\ \dots & \dots & \dots & \dots & \dots & \dots \\ 0 & 0 & 0 & \dots & 0 & h_N \end{pmatrix} \in \mathbb{R}^{N \times N} \quad (3.56)$$

in which  $h_i (i = 1, 2, 3 \dots N)$  is the  $i$ th story height. These three matrices will be used in transforming  $\mathbf{x}(t)$ ,  $\dot{\mathbf{x}}(t)$  and  $\ddot{\mathbf{x}}_A(t)$  to the corresponding response quantities of interest.

### 3.3.1 Inter-Story Drift

The inter-story drift is denoted by  $\mathbf{D}_{ID}(t) \in \mathbb{R}^N$ , which can be derived by multiplying  $\mathbf{T}_D$  with  $\mathbf{x}(t)$  as

$$\begin{aligned} \mathbf{D}_{ID}(t) &= \mathbf{T}_D \mathbf{x}(t) = \sum_{i=1}^{N_C} \left[ \mathbf{T}_D \mathbf{A}_{Di} \dot{q}_i(t) + \mathbf{T}_D \mathbf{B}_{Di} q_i(t) \right] + \sum_{i=1}^{N_P} \mathbf{T}_D \mathbf{A}_{Di}^P q_i^P(t) \\ &= \sum_{i=1}^{N_C} \left[ \mathbf{A}_{IDi} \dot{q}_i(t) + \mathbf{B}_{IDi} q_i(t) \right] + \sum_{i=1}^{N_P} \mathbf{A}_{IDi}^P q_i^P(t) \in \mathbb{R}^N \end{aligned} \quad (3.57)$$

where  $\mathbf{A}_{IDi} = \mathbf{T}_D \mathbf{A}_{Di} \in \mathbb{R}^N$ ,  $\mathbf{B}_{IDi} = \mathbf{T}_D \mathbf{B}_{Di} \in \mathbb{R}^N$  and  $\mathbf{A}_{IDi}^P = \mathbf{T}_D \mathbf{A}_{Di}^P \in \mathbb{R}^N$ .

### 3.3.2 Inter-story shear

The inter-story shear is denoted by  $\mathbf{F}_{IS}(t)$ , which can be derived by

$$\mathbf{F}_{IS}(t) = \mathbf{T}_S \mathbf{K} \mathbf{x}(t) = \sum_{i=1}^{N_C} \left[ \mathbf{A}_{ISi} \dot{q}_i(t) + \mathbf{B}_{ISi} q_i(t) \right] + \sum_{i=1}^{N_P} \mathbf{A}_{ISi}^P q_i^P(t) \in \mathbb{R}^N \quad (3.58)$$

where  $\mathbf{A}_{ISi} = \mathbf{T}_S \mathbf{K} \mathbf{A}_{Di} \in \mathbb{R}^N$ ,  $\mathbf{B}_{ISi} = \mathbf{T}_S \mathbf{K} \mathbf{B}_{Di} \in \mathbb{R}^N$  and  $\mathbf{A}_{ISi}^P = \mathbf{T}_S \mathbf{K} \mathbf{A}_{Di}^P \in \mathbb{R}^N$ .

Supposing that the second floor is designated as the first DOF of the shear building, the first element of  $\mathbf{F}_{IS}(t)$  represents the base shear, which is the primary concern in design.

### 3.3.3 General Inter-Story Shear

The general inter-story shear vector is defined as the inter-story shear forces adding the elastic restoring forces and damping forces, termed as  $\mathbf{F}_{GS}(t)$ .

$$\mathbf{F}_{GS}(t) = \mathbf{T}_S [\mathbf{C} \dot{\mathbf{x}}(t) + \mathbf{K} \mathbf{x}(t)] = \sum_{i=1}^{N_C} \left[ \mathbf{A}_{GSi} \dot{q}_i(t) + \mathbf{B}_{GSi} q_i(t) \right] + \sum_{i=1}^{N_P} \mathbf{A}_{GSi}^P q_i^P(t) \in \mathbb{R}^N \quad (3.59)$$



where  $\mathbf{A}_{GSi} = \mathbf{T}_S(\mathbf{C}\mathbf{A}_{Vi} + \mathbf{K}\mathbf{A}_{Di}) \in \mathbb{R}^N$  ,  $\mathbf{B}_{GSi} = \mathbf{T}_S(\mathbf{C}\mathbf{B}_{Vi} + \mathbf{K}\mathbf{B}_{Di}) \in \mathbb{R}^N$  and  $\mathbf{A}_{GSi}^P = \mathbf{T}_S(\mathbf{C}\mathbf{A}_{Vi}^P + \mathbf{K}\mathbf{A}_{Di}^P) \in \mathbb{R}^N$  .

Similar to the inter-story shear, the first element of  $\mathbf{F}_{GS}(t)$  is the general base shear, which can be called foundation shear (Lin and Chopra 2003). If the structure is lightly damped,  $\mathbf{F}_{GS}(t) \approx \mathbf{F}_{IS}(t)$ .

### 3.3.4 Inter-Story Moment

The inter-story moment vector is defined as the resulting moment caused by elastic restoring forces, defined as  $\mathbf{M}_{IM}(t)$  .

$$\mathbf{M}_{IM}(t) = \mathbf{T}_M \mathbf{T}_S \mathbf{K} \mathbf{x}(t) = \sum_{i=1}^{N_C} [\mathbf{A}_{IMi} \dot{q}_i(t) + \mathbf{B}_{IMi} q_i(t)] + \sum_{i=1}^{N_P} \mathbf{A}_{IMi}^P q_i^P(t) \in \mathbb{R}^N \quad (3.60)$$

where  $\mathbf{A}_{IMi} = \mathbf{T}_M \mathbf{T}_S \mathbf{K} \mathbf{A}_{Di} \in \mathbb{R}^N$  ,  $\mathbf{B}_{IMi} = \mathbf{T}_M \mathbf{T}_S \mathbf{K} \mathbf{B}_{Di} \in \mathbb{R}^N$  and  $\mathbf{A}_{IMi}^P = \mathbf{T}_M \mathbf{T}_S \mathbf{K} \mathbf{A}_{Di}^P \in \mathbb{R}^N$  .

Note that the first element of  $\mathbf{M}_{IM}(t)$  is the base turning moment, which is also a critical quantity in design.

### 3.3.5 General Inter-Story Moment

Similar to the general inter-story shear, the general inter-story moment is defined as the story moments with contributions from both elastic restoring forces and damping forces, denoted as  $\mathbf{M}_{GM}(t)$  .

$$\mathbf{M}_{GM}(t) = \mathbf{T}_M \mathbf{T}_S [\mathbf{C}\dot{\mathbf{x}}(t) + \mathbf{K}\mathbf{x}(t)] = \sum_{i=1}^{N_C} [\mathbf{A}_{GMi} \dot{q}_i(t) + \mathbf{B}_{GMi} q_i(t)] + \sum_{i=1}^{N_P} \mathbf{A}_{GMi}^P q_i^P(t) \in \mathbb{R}^N \quad (3.61)$$

where  $\mathbf{A}_{GMi} = \mathbf{T}_M \mathbf{T}_S (\mathbf{C} \mathbf{A}_{Vi} + \mathbf{K} \mathbf{A}_{Di}) \in \mathbb{R}^N$ ,  $\mathbf{B}_{GMi} = \mathbf{T}_M \mathbf{T}_S (\mathbf{C} \mathbf{B}_{Vi} + \mathbf{K} \mathbf{B}_{Di}) \in \mathbb{R}^N$  and  $\mathbf{A}_{GMi}^P = \mathbf{T}_M \mathbf{T}_S (\mathbf{C} \mathbf{A}_{Vi}^P + \mathbf{K} \mathbf{A}_{Di}^P) \in \mathbb{R}^N$ .

### 3.3.6 Damper Forces

The damper forces  $\mathbf{F}_{DR}(t)$  are defined as the force of each damper installed (the structural inherent damping is assumed to be very small, say, less than 5%, and can be ignored, i.e., damping matrix  $\mathbf{C}$  is formed completely by the supplemental dampers). A second transformation matrix,  $\mathbf{T}_{DC}$ , was introduced here to obtain the damper forces. This matrix represents the damper installation configuration in a shear building. It depends on the locations and the installation configurations of the dampers. The common damper configurations are given by Figure 7.2 in Ramirez et al. (2000). The  $\mathbf{T}_{DC}$  can be determined accordingly. As a result,

$$\mathbf{F}_{DR}(t) = \mathbf{T}_{DC} \mathbf{T}_S \mathbf{C} \mathbf{x}(t) = \sum_{i=1}^{N_C} [\mathbf{A}_{DRi} \dot{q}_i(t) + \mathbf{B}_{DRi} q_i(t)] + \sum_{i=1}^{N_p} \mathbf{A}_{DRi}^P q_i^P(t) \in \mathbb{R}^N \quad (3.62)$$

where  $\mathbf{A}_{DRi} = \mathbf{T}_{DC} \mathbf{T}_S \mathbf{C} \mathbf{A}_{Vi} \in \mathbb{R}^N$ ,  $\mathbf{B}_{DRi} = \mathbf{T}_{DC} \mathbf{T}_S \mathbf{C} \mathbf{B}_{Vi} \in \mathbb{R}^N$  and  $\mathbf{A}_{DRi}^P = \mathbf{T}_{DC} \mathbf{T}_S \mathbf{C} \mathbf{A}_{Vi}^P \in \mathbb{R}^N$ .

### 3.3.7 Generalization

From above derivations, it is noted that all the response quantities can be expressed as the combination of modal responses  $q_i(t)$ ,  $\dot{q}_i(t)$  and  $q_i^P(t)$ . They only differ in the coefficients vectors in front of each modal response. That is, these response quantities can be expressed in a similar manner as follows.

$$\mathbf{x}_0(t) = \sum_{i=1}^{N_C} [\mathbf{A}_{0i} \dot{q}_i(t) + \mathbf{B}_{0i} q_i(t)] + \sum_{i=1}^{N_p} \mathbf{A}_{0i}^P q_i^P(t) \in \mathbb{R}^N \quad (3.63)$$

in which  $\mathbf{x}_0(t)$  represents any response quantity discussed in this report and  $\mathbf{A}_{0i} \in \mathbb{R}^N$ ,  $\mathbf{B}_{0i} \in \mathbb{R}^N$  and  $\mathbf{A}_{0i}^P \in \mathbb{R}^N$  are the coefficient vectors corresponding to different response quantities. This unified response form is a suitable platform for developing the modal combination rule for the response spectrum method presented in a later chapter. In

addition, it is worthwhile to note that when using Equation (3.63), if the DOFs of the structures are very large, there is in general no need to consider all modal responses in the modal superposition because higher order modes may contribute very little to the corresponding total structural responses. This leads to the issue of modal truncation for a generally damped linear structure, which will be discussed in a later chapter. For now, it is simply assumed that the first  $N'_c$  complex modes and first  $N'_p$  over-damped modes are reserved  $\left[ (N'_c + N'_p) \ll N \right]$ ; consequently, Equation (3.63) can then be rewritten as

$$\mathbf{x}_0(t) \cong \sum_{i=1}^{N'_c} [\mathbf{A}_{0i} \dot{q}_i(t) + \mathbf{B}_{0i} q_i(t)] + \sum_{i=1}^{N'_p} \mathbf{A}_{0i}^p q_i^p(t) \quad (3.64)$$

### 3.4 Reduction to Classically Damped Systems

The formulation above is applicable to all linear 2D structures regardless of the damping distribution. To partly verify the above formulation, a classical damping condition was imposed on the formulation and the general response form can be reduced to the case of the well-established modal analysis solution for classically damped structures.

When a system satisfies the Caughey criterion  $\mathbf{C}\mathbf{M}^{-1}\mathbf{K} = \mathbf{K}\mathbf{M}^{-1}\mathbf{C}$  (Caughey and O'Kelly 1965), its mode shapes  $\boldsymbol{\varphi}_i$  are real-valued and are consistent with those of an undamped system. Further, the equation of motion of the systems can be decoupled into  $N_c + N_p$  independent equations of motion in terms of modal displacement coordinates only. The associated eigenvalues for complex modes are still equal to Equations (2.7) and (2.9).

Utilizing Equation (2.71a) and revisiting Equation (3.8), the residual matrices become

$$\mathbf{R}_i^R = \text{Re} \left( \frac{\boldsymbol{\varphi}_i \boldsymbol{\varphi}_i^T}{a_i} \right) = \mathbf{0} \in \mathbb{R}^{N \times N} \quad \text{and} \quad \mathbf{R}_i^I = \text{Im} \left( \frac{\boldsymbol{\varphi}_i \boldsymbol{\varphi}_i^T}{a_i} \right) = -\frac{\boldsymbol{\varphi}_i \boldsymbol{\varphi}_i^T}{2m_i \omega_{di}} \in \mathbb{R}^{N \times N} \quad (3.65)$$

Substituting Equation (3.65) into the displacement coefficient vectors shown in Equations (3.16) and (3.17), respectively, gives

$$\mathbf{A}_{Di} = \mathbf{0} \in \mathbb{R}^N \quad (3.66)$$

$$\mathbf{B}_{Di} = -2\omega_{di} \mathbf{R}_i^l \mathbf{M} \mathbf{J} = \frac{\boldsymbol{\varphi}_i \boldsymbol{\varphi}_i^T \mathbf{M} \mathbf{J}}{m_i} = \Gamma_i \boldsymbol{\varphi}_i \in \mathbb{R}^N \quad (i=1,2,\dots,N_C) \quad (3.67)$$

where  $\Gamma_i = \frac{\boldsymbol{\varphi}_i^T \mathbf{M} \mathbf{J}}{m_i} \in \mathbb{R}$  is the  $i$ th modal participation factor defined for the classically damped structures and  $m_i = (\boldsymbol{\varphi}_i)^T \mathbf{M} \boldsymbol{\varphi}_i \in \mathbb{R}$  is the  $i$ th modal mass. Also the over-damped modes may exist even in classically damped structures. When this situation takes place, both  $\mathbf{R}_i^p$  and  $\mathbf{A}_{Di}^p$  remain the same as Equations (3.10) and (3.19), respectively. As a result, substituting Equations (3.66) and (3.67) in Equation (3.38), the displacement response vector  $\mathbf{x}(t)$  reduces to

$$\mathbf{x}(t) = \sum_{i=1}^{N_C} \Gamma_i \boldsymbol{\varphi}_i q_i(t) + \sum_{i=1}^{N_p} \Gamma_i^p \boldsymbol{\varphi}_i^p q_i^p(t) \quad (3.68)$$

where

$$\Gamma_i^p = \frac{(\boldsymbol{\varphi}_i^p)^T \mathbf{M} \mathbf{J}}{m_i^p} \in \mathbb{R} \quad (i=1,2,\dots,N_p) \quad (3.68a)$$

and

$$m_i^p = (\boldsymbol{\varphi}_i^p)^T (-2\omega_i^p \mathbf{M} + \mathbf{C}) \boldsymbol{\varphi}_i^p \in \mathbb{R} \quad (3.68b)$$

are the  $i$ th over-damped modal participation factor and the  $i$ th over-damped modal mass, respectively. If the classically damped structure is under-damped ( $N_c = N$  and  $N_p = 0$ ), the over-damped mode terms associated with  $q_i^p(t)$  can be eliminated and Equation (3.68) can be further reduced to

$$\mathbf{x}(t) = \sum_{i=1}^N \Gamma_i \boldsymbol{\phi}_i q_i(t) \quad (3.69)$$

Equation (3.69) is identical to the well-known displacement modal response solution for the classically damped structures (Chopra 2001 and Clough and Penzien 1993). With the same conditions and approaches used for obtaining Equation (3.69), the structural velocity and absolute acceleration vectors can be written as

$$\dot{\mathbf{x}}(t) = \sum_{i=1}^N \Gamma_i \boldsymbol{\phi}_i \dot{q}_i(t) \quad (3.70)$$

$$\begin{aligned} \ddot{\mathbf{x}}_A(t) &= -\sum_{i=1}^N [2\xi_i \omega_i \dot{q}_i(t) + \omega_i^2 q_i(t)] \Gamma_i \boldsymbol{\phi}_i \\ &= \sum_{i=1}^N \ddot{q}_{Ai}(t) \Gamma_i \boldsymbol{\phi}_i \end{aligned} \quad (3.71)$$

It may be observed from Equation (3.71) that the structural absolute acceleration vector of a classically under-damped structure is the summation of the absolute acceleration response of a series of SDOF systems  $\ddot{q}_{Ai}(t) = \ddot{q}_i(t) + \ddot{x}_g(t) = -2\xi_i \omega_i \dot{q}_i(t) - \omega_i^2 q_i(t)$  in combination with the corresponding modal participation factors and mode shapes.

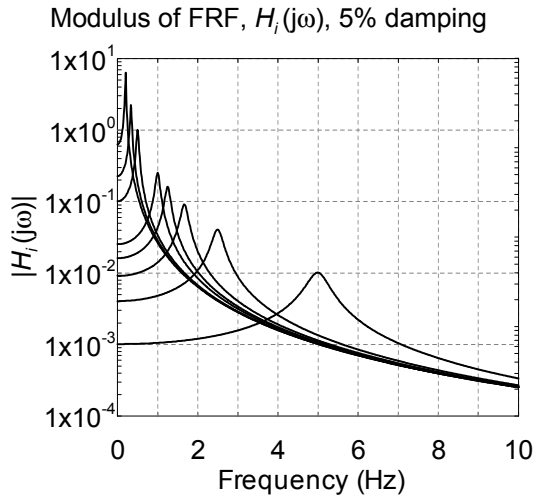


Figure 3.1 FRF of modal displacement response (periods equal to 0.2s, 0.4s, 0.6s, 0.8s, 1.0s, 2.0s, 3.0s and 5.0s; damping ratio=5%)

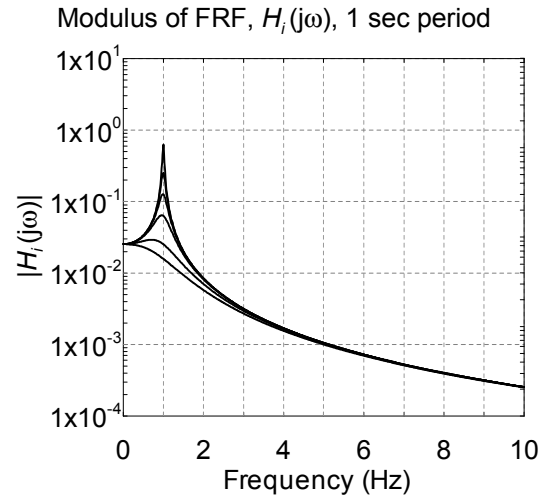


Figure 3.2 FRF of modal displacement response (damping ratios equal to 2%, 5%, 10%, 20%, 50% and 80%; period=1 sec)

Modulus of FRF  $H_i^p(j\omega)$  of over-damped mode, over-damped period

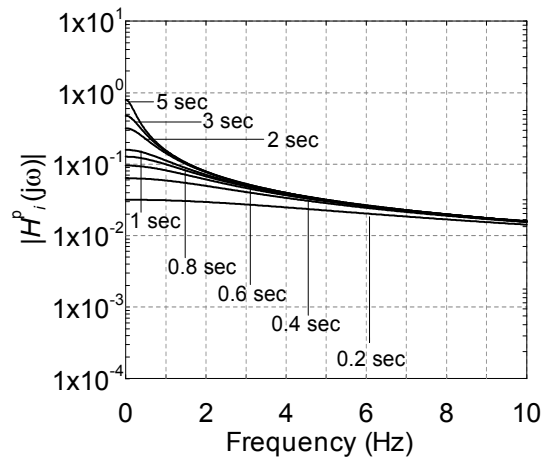


Figure 3.3 FRF of over-damped modal displacement response (over-damped modal periods equal to 0.2s, 0.4s, 0.6s, 0.8s, 1.0s, 2.0s, 3.0s and 5.0s)

# CHAPTER 4

## GENERAL MODAL COORDINATE TRANSFORMATION AND MODAL ENERGY

### 4.1 Introduction

In Chapter 3, a unified formulation for seismic responses formulated by superposition of its modal responses for a generally damped linear MDOF system has been developed. The displacement response vector and velocity response vector expressed in Equations (3.38) and (3.43) can be assembled into the state vector format in terms of the original physical coordinates and the general modal coordinates. Between the coordinates, a general real-valued transformation matrix can be established, which possesses a number of special properties that will be discussed in detail in this chapter.

### 4.2 General Modal Transformation Matrix

From the formulation in Chapter 3, the response state vector  $\mathbf{y}(t)$  can be expressed as

$$\mathbf{y}(t) = \begin{Bmatrix} \dot{\mathbf{x}}(t) \\ \mathbf{x}(t) \end{Bmatrix} = \mathbf{A}_T \mathbf{u}(t) \quad (4.1)$$

where

$$\mathbf{u}(t) = \begin{Bmatrix} \dot{\mathbf{q}}(t) \\ \mathbf{q}(t) \\ \mathbf{q}^p(t) \end{Bmatrix} \in \mathbb{R}^{2N} \quad (4.2)$$

is defined as the general modal coordinate vector in which  $\mathbf{q}(t) = [q_1(t), q_2(t) \cdots q_{N_c}(t)]^T \in \mathbb{R}^{N_c}$  and  $\mathbf{q}^p(t) = [q_1^p(t), q_2^p(t) \cdots q_{N_p}^p(t)] \in \mathbb{R}^{N_p}$ , and

$$\mathbf{A}_T = \begin{pmatrix} \mathbf{A}_V & \mathbf{B}_V & \mathbf{A}_V^p \\ \mathbf{A}_D & \mathbf{B}_D & \mathbf{A}_D^p \end{pmatrix} \in \mathbb{R}^{2N \times 2N} \quad (4.3)$$

Equation (4.3) is termed as the general modal coordinate transformation matrix, in which

$$\begin{aligned}
\mathbf{A}_V &= (\mathbf{A}_{V1}, \mathbf{A}_{V2} \cdots \mathbf{A}_{VN_C}) \in \mathbb{R}^{N \times N_C} \\
\mathbf{B}_V &= (\mathbf{B}_{V1}, \mathbf{B}_{V2} \cdots \mathbf{B}_{VN_C}) \in \mathbb{R}^{N \times N_C} \\
\mathbf{A}_D &= (\mathbf{A}_{D1}, \mathbf{A}_{D2} \cdots \mathbf{A}_{DN_C}) \in \mathbb{R}^{N \times N_C} \\
\mathbf{B}_D &= (\mathbf{B}_{D1}, \mathbf{B}_{D2} \cdots \mathbf{B}_{DN_C}) \in \mathbb{R}^{N \times N_C} \\
\mathbf{A}_V^P &= (\mathbf{A}_{V1}^P, \mathbf{A}_{V2}^P \cdots \mathbf{A}_{VN_P}^P) \in \mathbb{R}^{N \times N_P} \\
\mathbf{A}_D^P &= (\mathbf{A}_{D1}^P, \mathbf{A}_{D2}^P \cdots \mathbf{A}_{DN_P}^P) \in \mathbb{R}^{N \times N_P}
\end{aligned} \tag{4.4}$$

and

$$\mathbf{A}_{Di} = (\mathbf{R}_i \mathbf{M} \mathbf{J} + \mathbf{R}_i^* \mathbf{M} \mathbf{J}) = \left( \frac{\boldsymbol{\varphi}_i \boldsymbol{\varphi}_i^T}{a_i} + \frac{\boldsymbol{\varphi}_i^* \boldsymbol{\varphi}_i^H}{a_i^*} \right) \mathbf{M} \mathbf{J} \in \mathbb{R}^N \tag{4.5}$$

$$\mathbf{B}_{Di} = -(\lambda_i^* \mathbf{R}_i \mathbf{M} \mathbf{J} + \lambda_i \mathbf{R}_i^* \mathbf{M} \mathbf{J}) = -\left( \frac{\lambda_i^* \boldsymbol{\varphi}_i \boldsymbol{\varphi}_i^T}{a_i} + \frac{\lambda_i \boldsymbol{\varphi}_i^* \boldsymbol{\varphi}_i^H}{a_i^*} \right) \mathbf{M} \mathbf{J} \in \mathbb{R}^N \tag{4.6}$$

$$\mathbf{A}_{Di}^P = \mathbf{R}_i^P \mathbf{D}_i^P = \frac{\boldsymbol{\varphi}_i^P (\boldsymbol{\varphi}_i^P)^T \mathbf{M} \mathbf{J}}{a_i^P} \in \mathbb{R}^N \tag{4.7}$$

$$\mathbf{A}_{Vi} = (\lambda_i \mathbf{R}_i \mathbf{M} \mathbf{J} + \lambda_i^* \mathbf{R}_i^* \mathbf{M} \mathbf{J}) = \left( \frac{\lambda_i \boldsymbol{\varphi}_i \boldsymbol{\varphi}_i^T}{a_i} + \frac{\lambda_i^* \boldsymbol{\varphi}_i^* \boldsymbol{\varphi}_i^H}{a_i^*} \right) \mathbf{M} \mathbf{J} \in \mathbb{R}^N \tag{4.8}$$

$$\mathbf{B}_{Vi} = -\lambda_i \lambda_i^* (\mathbf{R}_i \mathbf{M} \mathbf{J} + \mathbf{R}_i^* \mathbf{M} \mathbf{J}) = -\lambda_i \lambda_i^* \left( \frac{\boldsymbol{\varphi}_i \boldsymbol{\varphi}_i^T}{a_i} + \frac{\boldsymbol{\varphi}_i^* \boldsymbol{\varphi}_i^H}{a_i^*} \right) \mathbf{M} \mathbf{J} \in \mathbb{R}^N \tag{4.9}$$

$$\mathbf{A}_{Vi}^P = \lambda_i^P \mathbf{R}_i^P \mathbf{M} \mathbf{J} = \frac{\lambda_i^P \boldsymbol{\varphi}_i^P (\boldsymbol{\varphi}_i^P)^T \mathbf{M} \mathbf{J}}{a_i^P} \in \mathbb{R}^N \tag{4.10}$$

From Equations (4.4) to (4.10), it can be seen that all elements of  $\mathbf{A}_T$  are real numbers and are only specified by structural system's parameters, including modal parameters, mass matrix  $\mathbf{M}$  and ground motion influence vector  $\mathbf{J}$ ; and are independent from the loading type of the excitation and how the mode shapes are normalized.  $\mathbf{J}$  is a



time-invariable vector and is related to the spatial distribution of the excitation load caused by the ground motion. When a structural system and the type of external loading are determined,  $\mathbf{J}$  is also determined and can be considered as a system parameter vector.

Equation (4.1) gives the modal expansion of the response vector  $\mathbf{y}(t)$  in terms of the real-valued modal coordinate vector  $\mathbf{u}(t)$ . Intuitively, using Equation (4.1), the coupled equations defined by Equation (2.2) can be transformed into a set of uncoupled equations expressed in terms of real-valued quantities. This hypothesis is proved mathematically in the next section, where some intermediary formulas are used and discussed to further expose characteristics of the general transformation matrix.

### 4.3 Proof of Modal Decoupling

For the sake of simplicity for decoupling proof, we reset the arrangement of the vectors in the matrix  $\mathbf{A}_T$  and the elements in the modal coordinate vector without interference to the transformation results. Denote

$$\mathbf{y}(t) = \mathbf{A}_{ST} \mathbf{u}_S(t) \in \mathbb{R}^{2N} \quad (4.11)$$

where  $\mathbf{y} = (\dot{\mathbf{x}}^T, \mathbf{x}^T)^T \in \mathbb{R}^{2N}$  remains the same as the definition in Equation (4.1); and

$$\mathbf{A}_{ST} = \begin{pmatrix} \mathbf{A}_{v1} & \mathbf{B}_{v1} & \mathbf{A}_{v2} & \mathbf{B}_{v2} & \cdots & \mathbf{A}_{vN_c} & \mathbf{B}_{vN_c} & \mathbf{A}_{v1}^p & \mathbf{A}_{v2}^p & \cdots & \mathbf{A}_{vN_p}^p \\ \mathbf{A}_{d1} & \mathbf{B}_{d1} & \mathbf{A}_{d2} & \mathbf{B}_{d2} & \cdots & \mathbf{A}_{dN_c} & \mathbf{B}_{dN_c} & \mathbf{A}_{d1}^p & \mathbf{A}_{d2}^p & \cdots & \mathbf{A}_{dN_p}^p \end{pmatrix} \in \mathbb{R}^{2N \times 2N} \quad (4.12)$$

$$\mathbf{u}_S(t) = [\dot{q}_1(t), q_1(t), \dot{q}_2(t), q_2(t), \cdots, \dot{q}_{N_c}(t), q_{N_c}(t), q_1^p(t), q_2^p(t), \cdots, q_{N_p}^p(t)]^T \in \mathbb{R}^{2N} \quad (4.13)$$

For each column in Equation (4.12),

$$\begin{aligned}
\begin{Bmatrix} \mathbf{A}_{Vi} \\ \mathbf{A}_{Di} \end{Bmatrix} &= \begin{Bmatrix} \left( \frac{\lambda_i \boldsymbol{\varphi}_i \boldsymbol{\varphi}_i^T + \lambda_i^* \boldsymbol{\varphi}_i^* \boldsymbol{\varphi}_i^{*H}}{a_i} \right) \mathbf{M} \mathbf{J} \\ \left( \frac{\boldsymbol{\varphi}_i \boldsymbol{\varphi}_i^T + \boldsymbol{\varphi}_i^* \boldsymbol{\varphi}_i^{*H}}{a_i} \right) \mathbf{M} \mathbf{J} \end{Bmatrix} = \begin{Bmatrix} \lambda_i \boldsymbol{\varphi}_i & \lambda_i^* \boldsymbol{\varphi}_i^* \\ \boldsymbol{\varphi}_i & \boldsymbol{\varphi}_i^* \end{Bmatrix} \begin{Bmatrix} \frac{\boldsymbol{\varphi}_i^T \mathbf{M} \mathbf{J}}{a_i} \\ \frac{\boldsymbol{\varphi}_i^H \mathbf{M} \mathbf{J}}{a_i^*} \end{Bmatrix} \\
&= (\boldsymbol{\Psi}_i, \boldsymbol{\Psi}_i^*) \begin{Bmatrix} \frac{\boldsymbol{\varphi}_i^T \mathbf{M} \mathbf{J}}{a_i} \\ \frac{\boldsymbol{\varphi}_i^H \mathbf{M} \mathbf{J}}{a_i^*} \end{Bmatrix} \in \mathbb{R}^{2N}
\end{aligned} \tag{4.14}$$

$$\begin{aligned}
\begin{Bmatrix} \mathbf{B}_{Vi} \\ \mathbf{B}_{Di} \end{Bmatrix} &= - \begin{Bmatrix} \lambda_i \lambda_i^* \left( \frac{\boldsymbol{\varphi}_i \boldsymbol{\varphi}_i^T + \boldsymbol{\varphi}_i^* \boldsymbol{\varphi}_i^{*H}}{a_i} \right) \mathbf{M} \mathbf{J} \\ \left( \frac{\lambda_i^* \boldsymbol{\varphi}_i \boldsymbol{\varphi}_i^T + \lambda_i \boldsymbol{\varphi}_i^* \boldsymbol{\varphi}_i^{*H}}{a_i} \right) \mathbf{M} \mathbf{J} \end{Bmatrix} \\
&= - \begin{Bmatrix} \lambda_i \boldsymbol{\varphi}_i & \lambda_i^* \boldsymbol{\varphi}_i^* \\ \boldsymbol{\varphi}_i & \boldsymbol{\varphi}_i^* \end{Bmatrix} \begin{Bmatrix} \frac{\lambda_i^* \boldsymbol{\varphi}_i^T \mathbf{M} \mathbf{J}}{a_i} \\ \frac{\lambda_i \boldsymbol{\varphi}_i^H \mathbf{M} \mathbf{J}}{a_i^*} \end{Bmatrix} = - (\boldsymbol{\Psi}_i, \boldsymbol{\Psi}_i^*) \begin{Bmatrix} \frac{\lambda_i^* \boldsymbol{\varphi}_i^T \mathbf{M} \mathbf{J}}{a_i} \\ \frac{\lambda_i \boldsymbol{\varphi}_i^H \mathbf{M} \mathbf{J}}{a_i^*} \end{Bmatrix} \in \mathbb{R}^{2N}
\end{aligned} \tag{4.15}$$

$$\begin{aligned}
\begin{Bmatrix} \mathbf{A}_{Vi}^P \\ \mathbf{A}_{Di}^P \end{Bmatrix} &= \begin{Bmatrix} \frac{\lambda_i^P \boldsymbol{\varphi}_i^P (\boldsymbol{\varphi}_i^P)^T \mathbf{M} \mathbf{J}}{a_i^P} \\ \frac{\boldsymbol{\varphi}_i^P (\boldsymbol{\varphi}_i^P)^T \mathbf{M} \mathbf{J}}{a_i^P} \end{Bmatrix} = \begin{Bmatrix} \lambda_i^P \boldsymbol{\varphi}_i^P \\ \boldsymbol{\varphi}_i^P \end{Bmatrix} \frac{[(\boldsymbol{\varphi}_i^P)^T \mathbf{M} \mathbf{J}]}{a_i^P} = \boldsymbol{\Psi}_i^P \left[ \frac{(\boldsymbol{\varphi}_i^P)^T \mathbf{M} \mathbf{J}}{a_i^P} \right] \in \mathbb{R}^{2N}
\end{aligned} \tag{4.16}$$

Thus  $\mathbf{A}_{ST}$  can be rewritten as

$$\mathbf{A}_{ST} = \boldsymbol{\Psi}_S \boldsymbol{\Gamma} = \begin{Bmatrix} \boldsymbol{\Phi}_S \boldsymbol{\Lambda}_S \\ \boldsymbol{\Phi}_S \end{Bmatrix} \boldsymbol{\Gamma} \tag{4.17}$$

where

$$\boldsymbol{\Phi}_S = (\boldsymbol{\varphi}_1, \boldsymbol{\varphi}_1^*, \boldsymbol{\varphi}_2, \boldsymbol{\varphi}_2^* \cdots \boldsymbol{\varphi}_{N_C}, \boldsymbol{\varphi}_{N_C}^*, \boldsymbol{\varphi}_1^P, \boldsymbol{\varphi}_2^P \cdots \boldsymbol{\varphi}_{N_P}^P) \in \mathbb{C}^{N \times 2N} \tag{4.18}$$

$$\boldsymbol{\Lambda}_S = \text{diag}(\lambda_1, \lambda_1^*, \lambda_2, \lambda_2^* \cdots \lambda_{N_C}, \lambda_{N_C}^*, \lambda_1^P, \lambda_2^P \cdots \lambda_{N_P}^P) \in \mathbb{C}^{2N \times 2N} \tag{4.18a}$$

$$\boldsymbol{\psi}_S = (\boldsymbol{\psi}_1, \boldsymbol{\psi}_1^*, \boldsymbol{\psi}_2, \boldsymbol{\psi}_2^* \cdots \boldsymbol{\psi}_{N_C}, \boldsymbol{\psi}_{N_C}^*, \boldsymbol{\psi}_1^P, \boldsymbol{\psi}_2^P \cdots \boldsymbol{\psi}_{N_P}^P) \in \mathbb{C}^{2N \times 2N} \quad (4.19)$$

$$\boldsymbol{\Gamma} = \begin{pmatrix} \boldsymbol{\Gamma}_{C1} & & & & & & & \mathbf{0} \\ & \boldsymbol{\Gamma}_{C2} & & & & & & \\ & & \ddots & & & & & \\ & & & \boldsymbol{\Gamma}_{CN_C} & & & & \\ & \mathbf{0} & & & \boldsymbol{\Gamma}_1^P & & \ddots & \\ & & & & & & & \boldsymbol{\Gamma}_{N_P}^P \end{pmatrix} \in \mathbb{C}^{2N \times 2N} \quad (4.20)$$

$$\boldsymbol{\Gamma}_{Ci} = \begin{pmatrix} \frac{\boldsymbol{\phi}_i^T \mathbf{M} \mathbf{J}}{a_i} & -\frac{\lambda_i^* \boldsymbol{\phi}_i^T \mathbf{M} \mathbf{J}}{a_i} \\ \frac{\boldsymbol{\phi}_i^H \mathbf{M} \mathbf{J}}{a_i^*} & -\frac{\lambda_i \boldsymbol{\phi}_i^H \mathbf{M} \mathbf{J}}{a_i^*} \end{pmatrix} \in \mathbb{C}^{2 \times 2} \quad (4.21)$$

$$\boldsymbol{\Gamma}_i^P = \frac{1}{a_i^P} [(\boldsymbol{\phi}_i^P)^T \mathbf{M} \mathbf{J}] \in \mathbb{R} \quad (4.22)$$

Analogous to the formula defined for classically damped systems (Clough and Penzien 1993 and Chopra 2001),  $\boldsymbol{\Gamma}_{Ci}$  and  $\boldsymbol{\Gamma}_i^P$  can be termed as  $i$ th modal participation factor matrix and over-damped modal participation factor, respectively.

According to the orthogonality of eigen-matrix proved in Chapter 2, Equations (2.27) and (2.28) can be rewritten as

$$\hat{\mathbf{a}}_s = \boldsymbol{\psi}_S^T \mathbf{A} \boldsymbol{\psi}_S = \text{diag}(a_1, a_1^*, a_2, a_2^* \cdots a_{N_C}, a_{N_C}^*, a_1^P, a_2^P \cdots a_{N_P}^P) \in \mathbb{C}^{2N \times 2N} \quad (4.23)$$

$$\hat{\mathbf{b}}_s = \boldsymbol{\psi}_S^T \mathbf{B} \boldsymbol{\psi}_S = \text{diag}(b_1, b_1^*, b_2, b_2^* \cdots b_{N_C}, b_{N_C}^*, b_1^P, b_2^P \cdots b_{N_P}^P) \in \mathbb{C}^{2N \times 2N} \quad (4.24)$$

For simplicity, the equation of motion of the structure represented in the state space form shown in Equation (2.2) is revisited here

$$\mathbf{A} \dot{\mathbf{y}}(t) + \mathbf{B} \mathbf{y}(t) = \mathbf{f}_s(t) \quad (4.25)$$



and

$$\begin{aligned}
\mathbf{A}_{ST}^T \mathbf{f}_s(t) &= \begin{Bmatrix} \mathbf{0} \\ \mathbf{f}(t) \end{Bmatrix} = -\mathbf{\Gamma}^T (\mathbf{\Phi}_S^T \mathbf{M} \mathbf{J}) \ddot{\mathbf{x}}_g(t) \quad (\in \mathbb{R}^{2N \times 1}) \\
&= \left\{ \begin{array}{c} \left[ 2 \operatorname{Re} \left[ \frac{(\boldsymbol{\varphi}_1^T \mathbf{M} \mathbf{J})^2}{a_1} \right] \right]^T \\ \left[ -2 \operatorname{Re} \left[ \frac{\lambda_1^* (\boldsymbol{\varphi}_1^T \mathbf{M} \mathbf{J})^2}{a_1} \right] \right]^T \end{array} \right\}, \left\{ \begin{array}{c} \left[ 2 \operatorname{Re} \left[ \frac{(\boldsymbol{\varphi}_2^T \mathbf{M} \mathbf{J})^2}{a_2} \right] \right]^T \\ \left[ -2 \operatorname{Re} \left[ \frac{\lambda_2^* (\boldsymbol{\varphi}_2^T \mathbf{M} \mathbf{J})^2}{a_2} \right] \right]^T \end{array} \right\} \dots \left\{ \begin{array}{c} \left[ 2 \operatorname{Re} \left[ \frac{(\boldsymbol{\varphi}_{N_c}^T \mathbf{M} \mathbf{J})^2}{a_{N_c}} \right] \right]^T \\ \left[ -2 \operatorname{Re} \left[ \frac{\lambda_{N_c}^* (\boldsymbol{\varphi}_{N_c}^T \mathbf{M} \mathbf{J})^2}{a_{N_c}} \right] \right]^T \end{array} \right\}, \quad (4.29) \\
&\quad \left( \frac{(\boldsymbol{\varphi}_1^p \mathbf{M} \mathbf{J})^2}{a_1^p}, \frac{(\boldsymbol{\varphi}_2^p \mathbf{M} \mathbf{J})^2}{a_2^p} \dots \frac{(\boldsymbol{\varphi}_{N_p}^p \mathbf{M} \mathbf{J})^2}{a_{N_p}^p} \right)^T [-\ddot{\mathbf{x}}_g(t)]
\end{aligned}$$

After substituting Equations (4.27) to (4.29) back into Equation (4.26), the corresponding  $i$ th block element for the complex mode and over-damped mode for the both sides of the resulting equation can be further manipulated as

$$\begin{aligned}
\mathbf{\Gamma}_{c_i}^T \begin{pmatrix} a_i & 0 \\ 0 & a_i^* \end{pmatrix} \mathbf{\Gamma}_{c_i} \begin{Bmatrix} \ddot{q}_i \\ \dot{q}_i \end{Bmatrix} + \mathbf{\Gamma}_{c_i}^T \begin{pmatrix} b_i & 0 \\ 0 & b_i^* \end{pmatrix} \mathbf{\Gamma}_{c_i} \begin{Bmatrix} \dot{q}_i \\ q_i \end{Bmatrix} &= \left\{ \begin{array}{c} \left[ 2 \operatorname{Re} \left[ \frac{(\boldsymbol{\varphi}_i^T \mathbf{M} \mathbf{J})^2}{a_i} \right] \right]^T \\ \left[ 2 \operatorname{Re} \left[ \frac{\lambda_i^* (\boldsymbol{\varphi}_i^T \mathbf{M} \mathbf{J})^2}{a_i} \right] \right]^T \end{array} \right\} [-\ddot{\mathbf{x}}_g(t)] \quad (4.30) \\
&\quad (i = 1, 2 \dots N_c)
\end{aligned}$$

$$a_i^p (\Gamma_i^p)^2 (\dot{q}_i^p + \omega_i^p q_i^p) = \frac{(\boldsymbol{\varphi}_i^p \mathbf{M} \mathbf{J})^2}{a_i^p} [-\ddot{\mathbf{x}}_g(t)] \quad (4.31)$$

$(i = 1, 2 \dots N_p)$

In Equation (4.30),

$$\begin{aligned}
\mathbf{\Gamma}_{C_i}^T \begin{pmatrix} a_i & 0 \\ 0 & a_i^* \end{pmatrix} \mathbf{\Gamma}_{C_i} &= \begin{pmatrix} \frac{(\boldsymbol{\varphi}_i^T \mathbf{M} \mathbf{J})}{a_i} & \frac{(\boldsymbol{\varphi}_i^H \mathbf{M} \mathbf{J})}{a_i^*} \\ -\frac{\lambda_i^*(\boldsymbol{\varphi}_i^T \mathbf{M} \mathbf{J})}{a_i} & -\frac{\lambda_i(\boldsymbol{\varphi}_i^H \mathbf{M} \mathbf{J})}{a_i^*} \end{pmatrix} \begin{pmatrix} a_i & 0 \\ 0 & a_i^* \end{pmatrix} \begin{pmatrix} \frac{(\boldsymbol{\varphi}_i^T \mathbf{M} \mathbf{J})}{a_i} & -\frac{\lambda_i^*(\boldsymbol{\varphi}_i^T \mathbf{M} \mathbf{J})}{a_i} \\ \frac{(\boldsymbol{\varphi}_i^H \mathbf{M} \mathbf{J})}{a_i^*} & -\frac{\lambda_i(\boldsymbol{\varphi}_i^H \mathbf{M} \mathbf{J})}{a_i^*} \end{pmatrix} \\
&= \begin{pmatrix} \boldsymbol{\varphi}_i^T \mathbf{M} \mathbf{J} & \boldsymbol{\varphi}_i^H \mathbf{M} \mathbf{J} \\ -\lambda_i^* \boldsymbol{\varphi}_i^T \mathbf{M} \mathbf{J} & -\lambda_i \boldsymbol{\varphi}_i^H \mathbf{M} \mathbf{J} \end{pmatrix} \begin{pmatrix} \frac{(\boldsymbol{\varphi}_i^T \mathbf{M} \mathbf{J})}{a_i} & -\frac{\lambda_i^*(\boldsymbol{\varphi}_i^T \mathbf{M} \mathbf{J})}{a_i} \\ \frac{(\boldsymbol{\varphi}_i^H \mathbf{M} \mathbf{J})}{a_i^*} & -\frac{\lambda_i(\boldsymbol{\varphi}_i^H \mathbf{M} \mathbf{J})}{a_i^*} \end{pmatrix} \\
&= \begin{pmatrix} \frac{(\boldsymbol{\varphi}_i^T \mathbf{M} \mathbf{J})^2}{a_i} + \frac{(\boldsymbol{\varphi}_i^H \mathbf{M} \mathbf{J})^2}{a_i^*} & -\frac{\lambda_i^*(\boldsymbol{\varphi}_i^T \mathbf{M} \mathbf{J})^2}{a_i} - \frac{\lambda_i(\boldsymbol{\varphi}_i^H \mathbf{M} \mathbf{J})^2}{a_i^*} \\ -\frac{\lambda_i^*(\boldsymbol{\varphi}_i^T \mathbf{M} \mathbf{J})^2}{a_i} - \frac{\lambda_i(\boldsymbol{\varphi}_i^H \mathbf{M} \mathbf{J})^2}{a_i^*} & \frac{(\lambda_i^*)^2 (\boldsymbol{\varphi}_i^T \mathbf{M} \mathbf{J})^2}{a_i} + \frac{(\lambda_i)^2 (\boldsymbol{\varphi}_i^H \mathbf{M} \mathbf{J})^2}{a_i^*} \end{pmatrix} \\
&= 2 \begin{pmatrix} \operatorname{Re} \left[ \frac{(\boldsymbol{\varphi}_i^T \mathbf{M} \mathbf{J})^2}{a_i} \right] & -\operatorname{Re} \left[ \frac{\lambda_i^*(\boldsymbol{\varphi}_i^T \mathbf{M} \mathbf{J})^2}{a_i} \right] \\ -\operatorname{Re} \left[ \frac{\lambda_i^*(\boldsymbol{\varphi}_i^T \mathbf{M} \mathbf{J})^2}{a_i} \right] & \operatorname{Re} \left[ \frac{(\lambda_i^*)^2 (\boldsymbol{\varphi}_i^T \mathbf{M} \mathbf{J})^2}{a_i} \right] \end{pmatrix} \in \mathbb{R}^{2 \times 2} \tag{4.32}
\end{aligned}$$

and

$$\begin{aligned}
\Gamma_{C_i}^T \begin{pmatrix} b_i & 0 \\ 0 & b_i^* \end{pmatrix} \Gamma_{C_i} &= \Gamma_{C_i}^T \begin{pmatrix} -\lambda_i a_i & 0 \\ 0 & -\lambda_i^* a_i^* \end{pmatrix} \Gamma_{C_i} \\
&= \begin{pmatrix} \frac{(\boldsymbol{\varphi}_i^T \mathbf{M} \mathbf{J})}{a_i} & \frac{(\boldsymbol{\varphi}_i^H \mathbf{M} \mathbf{J})}{a_i^*} \\ -\frac{\lambda_i^* (\boldsymbol{\varphi}_i^T \mathbf{M} \mathbf{J})}{a_i} & -\frac{\lambda_i (\boldsymbol{\varphi}_i^H \mathbf{M} \mathbf{J})}{a_i^*} \end{pmatrix} \begin{pmatrix} -\lambda_i a_i & 0 \\ 0 & -\lambda_i^* a_i^* \end{pmatrix} \begin{pmatrix} \frac{(\boldsymbol{\varphi}_i^T \mathbf{M} \mathbf{J})}{a_i} & -\frac{\lambda_i^* (\boldsymbol{\varphi}_i^T \mathbf{M} \mathbf{J})}{a_i} \\ \frac{(\boldsymbol{\varphi}_i^H \mathbf{M} \mathbf{J})}{a_i^*} & -\frac{\lambda_i (\boldsymbol{\varphi}_i^H \mathbf{M} \mathbf{J})}{a_i^*} \end{pmatrix} \\
&= \begin{pmatrix} -\lambda_i \boldsymbol{\varphi}_i^T \mathbf{M} \mathbf{J} & -\lambda_i^* \boldsymbol{\varphi}_i^H \mathbf{M} \mathbf{J} \\ \lambda_i \lambda_i^* \boldsymbol{\varphi}_i^T \mathbf{M} \mathbf{J} & \lambda_i \lambda_i^* \boldsymbol{\varphi}_i^H \mathbf{M} \mathbf{J} \end{pmatrix} \begin{pmatrix} \frac{(\boldsymbol{\varphi}_i^T \mathbf{M} \mathbf{J})}{a_i} & -\frac{\lambda_i^* (\boldsymbol{\varphi}_i^T \mathbf{M} \mathbf{J})}{a_i} \\ \frac{(\boldsymbol{\varphi}_i^H \mathbf{M} \mathbf{J})}{a_i^*} & -\frac{\lambda_i (\boldsymbol{\varphi}_i^H \mathbf{M} \mathbf{J})}{a_i^*} \end{pmatrix} \\
&= \begin{pmatrix} \frac{\lambda_i (\boldsymbol{\varphi}_i^T \mathbf{M} \mathbf{J})^2}{a_i} - \frac{\lambda_i^* (\boldsymbol{\varphi}_i^H \mathbf{M} \mathbf{J})^2}{a_i^*} & \frac{\lambda_i \lambda_i^* (\boldsymbol{\varphi}_i^T \mathbf{M} \mathbf{J})^2}{a_i} + \frac{\lambda_i \lambda_i^* (\boldsymbol{\varphi}_i^H \mathbf{M} \mathbf{J})^2}{a_i^*} \\ \frac{\lambda_i \lambda_i^* (\boldsymbol{\varphi}_i^T \mathbf{M} \mathbf{J})^2}{a_i} + \frac{\lambda_i \lambda_i^* (\boldsymbol{\varphi}_i^H \mathbf{M} \mathbf{J})^2}{a_i^*} & -\frac{\lambda_i (\lambda_i^*)^2 (\boldsymbol{\varphi}_i^T \mathbf{M} \mathbf{J})^2}{a_i} - \frac{\lambda_i^* (\lambda_i)^2 (\boldsymbol{\varphi}_i^H \mathbf{M} \mathbf{J})^2}{a_i^*} \end{pmatrix} \\
&= 2 \begin{pmatrix} -\operatorname{Re} \left[ \frac{\lambda_i (\boldsymbol{\varphi}_i^T \mathbf{M} \mathbf{J})^2}{a_i} \right] & \operatorname{Re} \left[ \frac{\lambda_i \lambda_i^* (\boldsymbol{\varphi}_i^T \mathbf{M} \mathbf{J})^2}{a_i} \right] \\ \operatorname{Re} \left[ \frac{\lambda_i \lambda_i^* (\boldsymbol{\varphi}_i^T \mathbf{M} \mathbf{J})^2}{a_i} \right] & -\operatorname{Re} \left[ \frac{\lambda_i (\lambda_i^*)^2 (\boldsymbol{\varphi}_i^T \mathbf{M} \mathbf{J})^2}{a_i} \right] \end{pmatrix} \\
&= 2 \begin{pmatrix} -\operatorname{Re} \left[ \frac{\lambda_i (\boldsymbol{\varphi}_i^T \mathbf{M} \mathbf{J})^2}{a_i} \right] & \omega_i^2 \operatorname{Re} \left[ \frac{(\boldsymbol{\varphi}_i^T \mathbf{M} \mathbf{J})^2}{a_i} \right] \\ \omega_i^2 \operatorname{Re} \left[ \frac{(\boldsymbol{\varphi}_i^T \mathbf{M} \mathbf{J})^2}{a_i} \right] & -\omega_i^2 \operatorname{Re} \left[ \frac{\lambda_i^* (\boldsymbol{\varphi}_i^T \mathbf{M} \mathbf{J})^2}{a_i} \right] \end{pmatrix} \in \mathbb{R}^{2 \times 2} \tag{4.33}
\end{aligned}$$

Substituting Equations (4.32) and (4.33) into the left side of Equation (4.30) leads to:

$$\begin{aligned}
& \left( \begin{array}{cc} \frac{(\boldsymbol{\varphi}_i^T \mathbf{M} \mathbf{J})^2}{a_i} + \frac{(\boldsymbol{\varphi}_i^H \mathbf{M} \mathbf{J})^2}{a_i^*} & -\frac{\lambda_i^*(\boldsymbol{\varphi}_i^T \mathbf{M} \mathbf{J})^2}{a_i} - \frac{\lambda_i(\boldsymbol{\varphi}_i^H \mathbf{M} \mathbf{J})^2}{a_i^*} \\ -\frac{\lambda_i^*(\boldsymbol{\varphi}_i^T \mathbf{M} \mathbf{J})^2}{a_i} - \frac{\lambda_i(\boldsymbol{\varphi}_i^H \mathbf{M} \mathbf{J})^2}{a_i^*} & \frac{(\lambda_i^*)^2(\boldsymbol{\varphi}_i^T \mathbf{M} \mathbf{J})^2}{a_i} + \frac{(\lambda_i)^2(\boldsymbol{\varphi}_i^H \mathbf{M} \mathbf{J})^2}{a_i^*} \end{array} \right) \begin{Bmatrix} \ddot{q}_i \\ \dot{q}_i \end{Bmatrix} \\
& + \left( \begin{array}{cc} -\frac{\lambda_i(\boldsymbol{\varphi}_i^T \mathbf{M} \mathbf{J})^2}{a_i} - \frac{\lambda_i^*(\boldsymbol{\varphi}_i^H \mathbf{M} \mathbf{J})^2}{a_i^*} & \frac{\lambda_i \lambda_i^*(\boldsymbol{\varphi}_i^T \mathbf{M} \mathbf{J})^2}{a_i} + \frac{\lambda_i \lambda_i^*(\boldsymbol{\varphi}_i^H \mathbf{M} \mathbf{J})^2}{a_i^*} \\ \frac{\lambda_i \lambda_i^*(\boldsymbol{\varphi}_i^T \mathbf{M} \mathbf{J})^2}{a_i} + \frac{\lambda_i \lambda_i^*(\boldsymbol{\varphi}_i^H \mathbf{M} \mathbf{J})^2}{a_i^*} & -\frac{\lambda_i(\lambda_i^*)^2(\boldsymbol{\varphi}_i^T \mathbf{M} \mathbf{J})^2}{a_i} - \frac{\lambda_i^*(\lambda_i)^2(\boldsymbol{\varphi}_i^H \mathbf{M} \mathbf{J})^2}{a_i^*} \end{array} \right) \begin{Bmatrix} \dot{q}_i \\ q_i \end{Bmatrix} \\
& = \begin{Bmatrix} 2 \operatorname{Re} \left[ \frac{(\boldsymbol{\varphi}_i^T \mathbf{M} \mathbf{J})^2}{a_i} \right] \\ 2 \operatorname{Re} \left[ \frac{\lambda_i^*(\boldsymbol{\varphi}_i^T \mathbf{M} \mathbf{J})^2}{a_i} \right] \end{Bmatrix} \begin{Bmatrix} -\ddot{x}_g(t) \\ \end{Bmatrix} \in \mathbb{R}^2 \tag{4.34}
\end{aligned}$$

It is easy to be seen that Equation (4.34) corresponds to two equations, the first one is that

$$\begin{aligned}
& \left[ \frac{(\boldsymbol{\varphi}_i^T \mathbf{M} \mathbf{J})^2}{a_i} + \frac{(\boldsymbol{\varphi}_i^H \mathbf{M} \mathbf{J})^2}{a_i^*} \right] \ddot{q}_i + \left[ -\frac{\lambda_i^*(\boldsymbol{\varphi}_i^T \mathbf{M} \mathbf{J})^2}{a_i} - \frac{\lambda_i(\boldsymbol{\varphi}_i^H \mathbf{M} \mathbf{J})^2}{a_i^*} - \frac{\lambda_i(\boldsymbol{\varphi}_i^T \mathbf{M} \mathbf{J})^2}{a_i} - \frac{\lambda_i^*(\boldsymbol{\varphi}_i^H \mathbf{M} \mathbf{J})^2}{a_i^*} \right] \dot{q}_i \\
& - \left[ \frac{\lambda_i \lambda_i^*(\boldsymbol{\varphi}_i^T \mathbf{M} \mathbf{J})^2}{a_i} + \frac{\lambda_i \lambda_i^*(\boldsymbol{\varphi}_i^H \mathbf{M} \mathbf{J})^2}{a_i^*} \right] q_i = \left[ \frac{(\boldsymbol{\varphi}_i^T \mathbf{M} \mathbf{J})^2}{a_i} + \frac{(\boldsymbol{\varphi}_i^H \mathbf{M} \mathbf{J})^2}{a_i^*} \right] \left[ \ddot{q}_i + (-\lambda_i - \lambda_i^*) \dot{q}_i + \omega_i^2 q_i \right] \\
& = \left[ \frac{(\boldsymbol{\varphi}_i^T \mathbf{M} \mathbf{J})^2}{a_i} + \frac{(\boldsymbol{\varphi}_i^H \mathbf{M} \mathbf{J})^2}{a_i^*} \right] \left[ \ddot{q}_i + 2\zeta_i \omega_i \dot{q}_i + \omega_i^2 q_i \right] = 2 \operatorname{Re} \left[ \frac{(\boldsymbol{\varphi}_i^T \mathbf{M} \mathbf{J})^2}{a_i} \right] \left[ -\ddot{x}_g(t) \right] \in \mathbb{R}
\end{aligned}$$



while the second one is expressed as

$$\begin{aligned}
& \left[ -\frac{\lambda_i^*(\boldsymbol{\varphi}_i^T \mathbf{M} \mathbf{J})^2}{a_i} - \frac{\lambda_i(\boldsymbol{\varphi}_i^H \mathbf{M} \mathbf{J})^2}{a_i^*} \right] \ddot{q}_i + \left[ \frac{(\lambda_i^*)^2 (\boldsymbol{\varphi}_i^T \mathbf{M} \mathbf{J})^2}{a_i} + \frac{(\lambda_i)^2 (\boldsymbol{\varphi}_i^H \mathbf{M} \mathbf{J})^2}{a_i^*} + \frac{\lambda_i \lambda_i^* (\boldsymbol{\varphi}_i^T \mathbf{M} \mathbf{J})^2}{a_i} + \frac{\lambda_i \lambda_i^* (\boldsymbol{\varphi}_i^H \mathbf{M} \mathbf{J})^2}{a_i^*} \right] \dot{q}_i \\
& + \left[ \frac{\lambda_i (\lambda_i^*)^2 (\boldsymbol{\varphi}_i^T \mathbf{M} \mathbf{J})^2}{a_i} + \frac{\lambda_i^* (\lambda_i)^2 (\boldsymbol{\varphi}_i^H \mathbf{M} \mathbf{J})^2}{a_i^*} \right] q_i = - \left[ \frac{\lambda_i^* (\boldsymbol{\varphi}_i^T \mathbf{M} \mathbf{J})^2}{a_i} + \frac{\lambda_i (\boldsymbol{\varphi}_i^H \mathbf{M} \mathbf{J})^2}{a_i^*} \right] [\ddot{q}_i + 2\xi_i \omega_i \dot{q}_i + \omega_i^2 q_i] \\
& = -2 \operatorname{Re} \left[ \frac{\lambda_i^* (\boldsymbol{\varphi}_i^T \mathbf{M} \mathbf{J})^2}{a_i} \right] [-\ddot{x}_g(t)] \in \mathbb{R}
\end{aligned}$$

After simplifying the above two equations, the  $i$ th complex modal equations are:

$$\operatorname{Re} \left[ \frac{2(\boldsymbol{\varphi}_i^T \mathbf{M} \mathbf{J})^2}{a_i} \right] [\ddot{q}_i + 2\xi_i \omega_i \dot{q}_i + \omega_i^2 q_i] = \operatorname{Re} \left[ \frac{2(\boldsymbol{\varphi}_i^T \mathbf{M} \mathbf{J})^2}{a_i} \right] [-\ddot{x}_g(t)] \quad (4.35)$$

$$\operatorname{Re} \left[ \frac{-2\lambda_i^* (\boldsymbol{\varphi}_i^T \mathbf{M} \mathbf{J})^2}{a_i} \right] [\ddot{q}_i + 2\xi_i \omega_i \dot{q}_i + \omega_i^2 q_i] = -\operatorname{Re} \left[ \frac{-2\lambda_i^* (\boldsymbol{\varphi}_i^T \mathbf{M} \mathbf{J})^2}{a_i} \right] [-\ddot{x}_g(t)] \quad (4.36)$$

Comparing Equation (4.35) and (4.36), it can be easily found that these two equations are identical to modal responses no matter  $(\boldsymbol{\varphi}_i^T \mathbf{M} \mathbf{J}) \neq 0$ . When  $(\boldsymbol{\varphi}_i^T \mathbf{M} \mathbf{J}) \neq 0$ , either Equation (4.35) or (4.36) can be simplified as a second order governing motion differential equation for a pure SDOF system with the  $i$ th modal frequency and damping ratio:

$$\ddot{q}_i + 2\xi_i \omega_i \dot{q}_i + \omega_i^2 q_i = -\ddot{x}_g(t) \in \mathbb{R} \quad (i=1,2,\dots,N_c) \quad (4.36a)$$

It is found that Equation (4.36a) is exactly same as Equation (3.23).

For the over-damped modes, substituting Equation (4.22) into Equation (4.31), we have

$$\frac{1}{a_i^p} [(\boldsymbol{\varphi}_i^p)^T \mathbf{M} \mathbf{J}]^2 (\dot{q}_i^p + \omega_i^p q_i^p) = \frac{1}{a_i^p} [(\boldsymbol{\varphi}_i^p)^T \mathbf{M} \mathbf{J}]^2 [-\ddot{x}_g(t)] \in \mathbb{R} \quad (4.37)$$

If  $\left[ (\boldsymbol{\Phi}_i^p)^T \mathbf{M} \mathbf{J} \right] \neq 0$ , Equation (4.37) can be further simplified as a pure, first-order differential equation for an over-damped mode

$$\dot{q}_i^p + \omega_i^p q_i^p = -\ddot{x}_g(t) \in \mathbb{R} \quad (i=1, 2 \dots N_p) \quad (4.38)$$

which is exactly the same as Equation (3.29). Now, we have shown that the general transformation matrix  $\mathbf{A}_T$  can decouple the original MDOF structural motion differential equation.

After the original motion equation is decoupled, the computational burden for response solutions of a structure with a large number of DOFs can be considerably reduced by applying the modal truncation techniques, which will be discussed in the next chapter. In the unified formula for structural responses of interest for seismic analysis and structural design shown in the Chapter 3, the velocity responses  $\dot{q}_i(t)$  for complex modes are required. However, mathematically speaking, both  $\dot{q}_i(t)$  and  $q_i(t)$  are the complete solution set of the Equation (4.36a), and the computation demand is comparable to the one required for the classically damped cases. The only additional effort is in solving the eigenvalue problem shown in Equation (2.4) whose size is doubled compared to the size in the classically damped cases. However, this demand is minimal beyond the computation for classically damped cases.

Furthermore, it can be predicted that the general coordinate transformation matrix  $\mathbf{A}_T$  established in this study has significant values in many respects, such as the seismic structural analysis and design, structural response analysis to initial conditions, supplemental damping design, reserved modal order determination (modal truncation), modal energy transfer analysis and structural active/semi-active control based on independent modal space approach (IMSC) as well as the physical interpretations of the complex modal analysis.

#### 4.4 Non-Singularity Analysis for General Transformation Matrix

Taking determinant operation for both sides of Equation (4.27) and considering Equations (4.17) and (4.23), we have

$$\begin{aligned} \det[\mathbf{A}_{ST}^T \mathbf{A} \mathbf{A}_{ST}] &= [\det(\mathbf{A}_{ST})]^2 \cdot \det(\mathbf{A}) = \det[\mathbf{\Gamma}^T (\boldsymbol{\Psi}_S^T \mathbf{A} \boldsymbol{\Psi}_S) \mathbf{\Gamma}] \\ &= [\det(\mathbf{\Gamma})]^2 \det(\boldsymbol{\Psi}_S^T \mathbf{A} \boldsymbol{\Psi}_S) = [\det(\mathbf{\Gamma})]^2 \det(\hat{\mathbf{a}}_s) \end{aligned} \quad (4.39)$$

In Appendix A, it has been proved that  $\det(\mathbf{A}) \neq 0$  and  $\det(\hat{\mathbf{a}}) [= \det(\hat{\mathbf{a}}_s)] \neq 0$ .

Thus Equation (4.39) becomes

$$[\det(\mathbf{A}_{ST})]^2 = \frac{\det(\hat{\mathbf{a}}_s)}{\det(\mathbf{A})} [\det(\mathbf{\Gamma})]^2 \in \mathbb{R} \quad (4.40)$$

Using the relationships (4.20) to (4.22),  $\det(\mathbf{\Gamma})$  can be expressed as

$$\begin{aligned} \det(\mathbf{\Gamma}) &= \det \begin{pmatrix} \mathbf{\Gamma}_{C1} & & & & & \\ & \mathbf{\Gamma}_{C2} & & & & \\ & & \ddots & & & \\ & & & \mathbf{\Gamma}_{CN_C} & & \\ & & & & \mathbf{\Gamma}_1^P & \\ \mathbf{0} & & & & & \ddots \\ & & & & & & \mathbf{\Gamma}_{N_P}^P \end{pmatrix} \\ &= \prod_{i=1}^{N_C} \det(\mathbf{\Gamma}_{C_i}) \cdot \prod_{i=1}^{N_P} \det(\mathbf{\Gamma}_i^P) \in \mathbb{C} \end{aligned} \quad (4.41)$$

in which

$$\det(\mathbf{\Gamma}_{C_i}) = \det \begin{pmatrix} \frac{\boldsymbol{\Phi}_i^T \mathbf{M} \mathbf{J}}{a_i} & -\frac{\lambda_i^* \boldsymbol{\Phi}_i^T \mathbf{M} \mathbf{J}}{a_i} \\ \frac{\boldsymbol{\Phi}_i^H \mathbf{M} \mathbf{J}}{a_i^*} & -\frac{\lambda_i \boldsymbol{\Phi}_i^H \mathbf{M} \mathbf{J}}{a_i^*} \end{pmatrix} = (\lambda_i^* - \lambda_i) \left| \frac{\boldsymbol{\Phi}_i^T \mathbf{M} \mathbf{J}}{a_i} \right|^2 = -j2\omega_{di} \left| \frac{\boldsymbol{\Phi}_i^T \mathbf{M} \mathbf{J}}{a_i} \right|^2 \quad (4.42)$$

$$\det(\mathbf{\Gamma}_i^P) = \frac{1}{a_i^P} [(\boldsymbol{\Phi}_i^P)^T \mathbf{M} \mathbf{J}] \quad (4.43)$$

From Equations (4.40) to (4.43), it can be easily concluded that whether or not  $\det(\mathbf{A}_{\text{ST}}) = 0$  only depends on the term  $\det(\mathbf{\Gamma})$  and further depends on  $[\boldsymbol{\varphi}_i^{\text{T}} \mathbf{M} \mathbf{J}]$  for all complex modes and  $[(\boldsymbol{\varphi}_i^{\text{P}})^{\text{T}} \mathbf{M} \mathbf{J}]$  for all over-damped modes. If

$$[\boldsymbol{\varphi}_i^{\text{T}} \mathbf{M} \mathbf{J}] \neq 0 \quad (i = 1, 2 \cdots N_c) \quad (4.43a)$$

and

$$[(\boldsymbol{\varphi}_i^{\text{P}})^{\text{T}} \mathbf{M} \mathbf{J}] \neq 0 \quad (i = 1, 2 \cdots N_p) \quad (4.43b)$$

, we can have  $\det(\mathbf{A}_{\text{ST}}) \neq 0$ , that is, the general modal transformation matrix  $\mathbf{A}_{\text{ST}}$  is non-singular. On the other hand, if  $\det(\mathbf{A}_{\text{ST}}) = 0$ , there is at least one mode in the system that causes  $[\boldsymbol{\varphi}_i^{\text{T}} \mathbf{M} \mathbf{J}] = 0$  or  $[(\boldsymbol{\varphi}_i^{\text{P}})^{\text{T}} \mathbf{M} \mathbf{J}] = 0$ .

Theoretically speaking, for an arbitrary linear structure with complete constraints (without zero and repeated eigenvalues), there is no guarantee that the conditions (4.43a) and (4.43b) are satisfied.

From mathematical point of view,  $[\boldsymbol{\varphi}_i^{\text{T}} \mathbf{M} \mathbf{J}] = 0$  and/or  $[(\boldsymbol{\varphi}_i^{\text{P}})^{\text{T}} \mathbf{M} \mathbf{J}] = 0$  implies that the vector  $\boldsymbol{\varphi}_i$  or  $\boldsymbol{\varphi}_i^{\text{P}}$  is orthogonal to the vector  $\mathbf{M} \mathbf{J}$  and that the corresponding modes do not have contributions to the structural responses, which may happen to a symmetric structure. In earthquake engineering, especially for the tower type of building structures (the cantilever type of structures), a few number of lower modes, say 20 modes, dominate the structural dynamic behaviors, and further for these lower order modes of the structures, the conditions (4.43a) and (4.43b) for all modes may be satisfied, which should be examined after the system's eigen-solutions are obtained.

Assuming that when modal order  $r_0 = r_1, r_2 \cdots r_n$  ( $N_c \geq r_0 \geq 1$  and  $N_c \geq n \geq 1$ ),  $[\boldsymbol{\varphi}_{r_i}^{\text{T}} \mathbf{M} \mathbf{J}] = 0$  and/or when over-damped modal order  $r_0^{\text{P}} = r_1^{\text{P}}, r_2^{\text{P}} \cdots r_{n_p}^{\text{P}}$  ( $N_p \geq r_0^{\text{P}} \geq 1$  and  $N_p \geq n_p \geq 1$ ),  $[(\boldsymbol{\varphi}_{r_i^{\text{P}}}^{\text{P}})^{\text{T}} \mathbf{M} \mathbf{J}] = 0$ , the terms and vectors concerning these modes should be removed from the modal superposition expressions for varied types of structural

responses and from the general modal transformation matrix  $\mathbf{A}_T$ , respectively. Referring to the unified structural response form expressed in Equation (3.63), we have

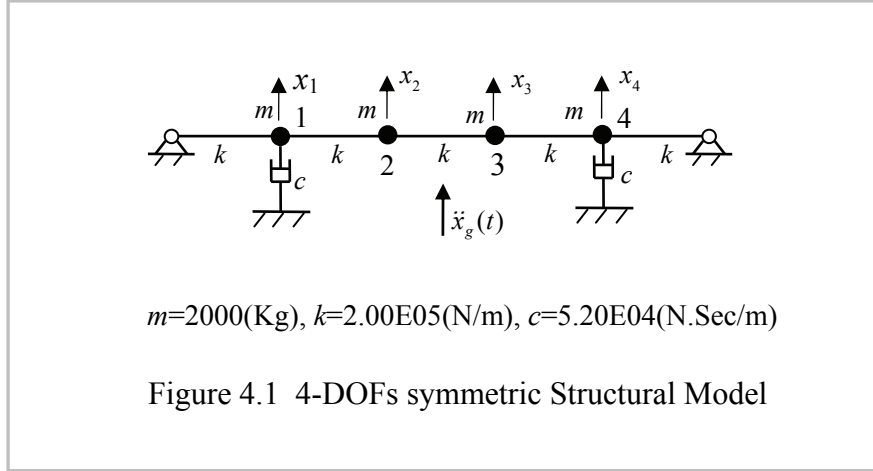
$$\mathbf{x}_0(t) = \sum_{\substack{i=1 \\ i \neq n_0}}^{N_C} [\mathbf{A}_{0i} \dot{q}_i(t) + \mathbf{B}_{0i} q_i(t)] + \sum_{\substack{i=1 \\ i \neq n_0^P}}^{N_p} \mathbf{A}_{0i}^P q_i^P(t) \quad (4.44)$$

The  $\mathbf{A}_T$  expressed in Equation (4.3), as the consequence, which is denoted as  $\mathbf{A}'_T$ , will no longer be a square matrix. Instead, it becomes a matrix with  $(2N) \times (2N - 2n - n_p)$  dimension, that is,  $\mathbf{A}'_T \in \mathbb{R}^{(2N) \times (2N - 2n - n_p)}$ . However, the vectors in  $\mathbf{A}'_T$  are kept linear independent with respect to each other, which can still be used to decouple the system original differential equation. The difference lies on that only  $(N - n - n_p)$  independent pure modal equations are available.

#### 4.5 Numerical Example for General Modal Responses

Figure 4.1 shows a simple symmetric structural example model with four lumped masses (4 DOFs). The structural mass, stiffness and damping matrices are

$$\mathbf{M} = \begin{pmatrix} m & & & \\ & m & & \\ & & m & \\ & & & m \end{pmatrix}, \quad \mathbf{K} = \begin{pmatrix} 2k & -k & & \\ -k & 2k & -k & \\ & -k & 2k & -k \\ & & -k & 2k \end{pmatrix}, \quad \mathbf{C} = \begin{pmatrix} c & & & \\ & 0 & & \\ & & 0 & \\ & & & c \end{pmatrix}$$



According to Caughey criterion, it is found that

$$\mathbf{CM}^{-1}\mathbf{K} = \begin{pmatrix} 1.04\text{E}7 & 0 & 0 & 0 \\ -5.20\text{E}6 & 0 & 0 & 0 \\ 0 & 0 & 0 & -5.20\text{E}6 \\ 0 & 0 & 0 & 1.04\text{E}7 \end{pmatrix} \neq \mathbf{KM}^{-1}\mathbf{C} = \begin{pmatrix} 1.04\text{E}7 & -5.20\text{E}6 & 0 & 0 \\ 0 & 0 & 0 & 0 \\ 0 & 0 & 0 & 0 \\ 0 & 0 & -5.20\text{E}6 & 1.04\text{E}7 \end{pmatrix}$$

Thus this structure is a non-classically damped system. From  $\mathbf{M}$ ,  $\mathbf{K}$  and  $\mathbf{C}$ , we can further obtain system state coefficient matrix  $\mathbf{A}_s$ , which is defined in Equation (A.4) of Appendix A:

$$\mathbf{A}_s = \begin{pmatrix} -\mathbf{M}^{-1}\mathbf{C} & -\mathbf{M}^{-1}\mathbf{K} \\ \mathbf{I} & \mathbf{0} \end{pmatrix} = \begin{pmatrix} -c/m & 0 & 0 & 0 & -2k/m & k/m & 0 & 0 \\ 0 & 0 & 0 & 0 & k/m & -2k/m & k/m & 0 \\ 0 & 0 & 0 & 0 & 0 & k/m & -2k/m & k/m \\ 0 & 0 & 0 & -c/m & 0 & 0 & k/m & -2k/m \\ 1 & 0 & 0 & 0 & 0 & 0 & 0 & 0 \\ 0 & 1 & 0 & 0 & 0 & 0 & 0 & 0 \\ 0 & 0 & 1 & 0 & 0 & 0 & 0 & 0 \\ 0 & 0 & 0 & 1 & 0 & 0 & 0 & 0 \end{pmatrix}$$

Substituting values of  $m$ ,  $k$  and  $c$  listed in Figure 4.1 and then calculating eigen-solutions of the matrix  $\mathbf{A}_s$ , we found that there are three complex modes and two over-

damped modes for this structure under current parameter assumption. The modal frequencies, periods and damping ratios for all modes are listed in Table 4.1, while the modal shape matrix and their plots are shown in Equation (4.45) and Figure 4.2(a) and (b), respectively.

$$\Phi = \begin{pmatrix} 1.0000 & 0.5664-0.3461j & 1.0000+1.0000j & 1.0000 & -0.1536+ 0.2737j \\ 0.6724 & 1.0000+1.0000j & 0.1811+0.2564j & 0.3276 & -1.0000- 1.0000j \\ 0.6724 & 1.0000+1.0000j & -0.1811- 0.2564j & 0.3276 & 1.0000+ 1.0000j \\ 1.0000 & 0.5664- 0.3461j & -1.0000- 1.0000j & 1.0000 & 0.1536- 0.2737j \end{pmatrix} \quad (4.45)$$

Note that each modal shape has normalized based on the following relationships for complex modes and over-damped modes, respectively:

$$\phi'_i = \frac{(1+j)\phi_i}{\max_{l=1,2,\dots,N}(|\phi_{li}|)} \in \mathbb{C}^N \quad (4.46)$$

$$(\phi_i^p)' = \frac{\phi_i^p}{\max_{l=1,2,\dots,N}(|\phi_{li}^p|)} \in \mathbb{R}^N \quad (4.47)$$

in which  $\phi_{li}$  and  $\phi_{li}^p$  are the  $l^{\text{th}}$  ( $l=1, 2, \dots, N$ ) element in the  $i^{\text{th}}$  complex and over-damped modal shape vector, respectively. For the complex modes, only those corresponding to complex eigenvalues with positive imagine parts are shown in Equation (4.45) and Figure 4.2.

Table 4.1 Modal Frequency, Period and Damping Ratio

Mode Order	Mode Type	Frequency (Hz)	Period (Sec.)	Damping Ratio (100%)
1	1 <sup>st</sup> over-damped	1.1109	0.9002	N/A
2	1 <sup>st</sup> Complex	1.5915	0.6283	23.4669
3	2 <sup>nd</sup> Complex	2.0320	0.4921	97.0430
4	2 <sup>nd</sup> over-damped	2.2801	0.4386	N/A
5	3 <sup>rd</sup> Complex	2.7875	0.3587	3.4852

From the modal shape data in  $\Phi$  and Figure 4.2(a) and (b), it can be observed that the 1<sup>st</sup> complex modal shapes, both real parts and imaginary parts, are symmetric with

respect to the structural symmetric line, while those of 2<sup>nd</sup> and 3<sup>rd</sup> complex modes are anti-symmetric to the structural symmetric line and two over-damped modal shapes are symmetric with respect to the structural symmetric line. Thus the 2<sup>nd</sup> and 3<sup>rd</sup> complex modes will not contribute to the structural responses. In this instance, the structural displacement and velocity vector can be expressed as

$$\mathbf{x}(t) = (x_1, x_2, x_3, x_4)^T = [\mathbf{A}_{D1}\dot{q}_1(t) + \mathbf{B}_{D1}q_1(t)] + [\mathbf{A}_{D1}^P q_1^P(t)] + [\mathbf{A}_{D2}^P q_2^P(t)] \quad (4.48)$$

$$\dot{\mathbf{x}}(t) = (\dot{x}_1, \dot{x}_2, \dot{x}_3, \dot{x}_4)^T = [\mathbf{A}_{V1}\dot{q}_1(t) + \mathbf{B}_{V1}q_1(t)] + [\mathbf{A}_{V1}^P q_1^P(t)] + [\mathbf{A}_{V2}^P q_2^P(t)] \quad (4.49)$$

and the general modal transformation relationships are

$$\mathbf{A}_T = \begin{pmatrix} \mathbf{A}_{V1} & \mathbf{B}_{V1} & \mathbf{0} & \mathbf{0} & \mathbf{0} & \mathbf{0} & \mathbf{A}_{V1}^P & \mathbf{A}_{V2}^P \\ \mathbf{A}_{D1} & \mathbf{B}_{D1} & \mathbf{0} & \mathbf{0} & \mathbf{0} & \mathbf{0} & \mathbf{A}_{D1}^P & \mathbf{A}_{D2}^P \end{pmatrix} \in \mathbb{R}^{8 \times 8} \quad (4.50)$$

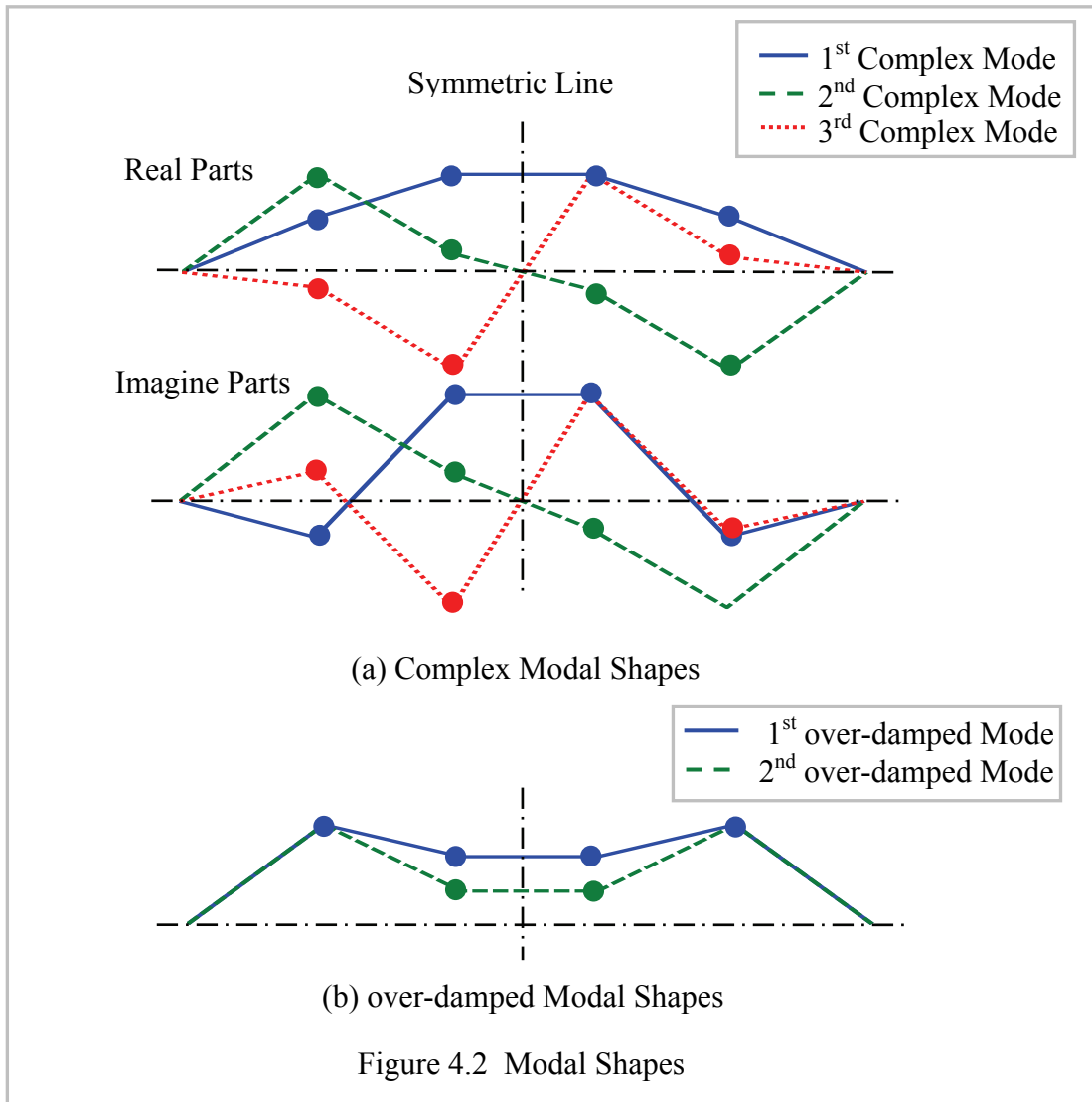
$$\mathbf{A}'_T = \begin{pmatrix} \mathbf{A}_{V1} & \mathbf{B}_{V1} & \mathbf{A}_{V1}^P & \mathbf{A}_{V2}^P \\ \mathbf{A}_{D1} & \mathbf{B}_{D1} & \mathbf{A}_{D1}^P & \mathbf{A}_{D2}^P \end{pmatrix} \in \mathbb{R}^{8 \times 4} \quad (4.51)$$

$$\mathbf{u}'(t) = (\dot{q}_1(t), q_1(t), q_1^P(t), q_2^P(t))^T \in \mathbb{R}^4 \quad (4.52)$$

Utilizing Equations (3.16), (3.17) (3.19) and (3.42), we can calculate the values of matrix  $\mathbf{A}'_T$ :

$$\mathbf{A}'_T = \begin{pmatrix} -0.2825 & 6.0193 & -0.3844 & 1.1248 \\ 1.2825 & 12.0386 & -0.2585 & 0.3685 \\ 1.2825 & 12.0386 & -0.2585 & 0.3685 \\ -0.2825 & 6.0193 & -0.3844 & 1.1248 \\ -0.0602 & -0.5650 & 0.0551 & -0.0785 \\ -0.1204 & 0.7175 & 0.0370 & -0.0257 \\ -0.1204 & 0.7175 & 0.0370 & -0.0257 \\ -0.0602 & -0.5650 & 0.0551 & -0.0785 \end{pmatrix} \in \mathbb{R}^{8 \times 4} \quad (4.53)$$

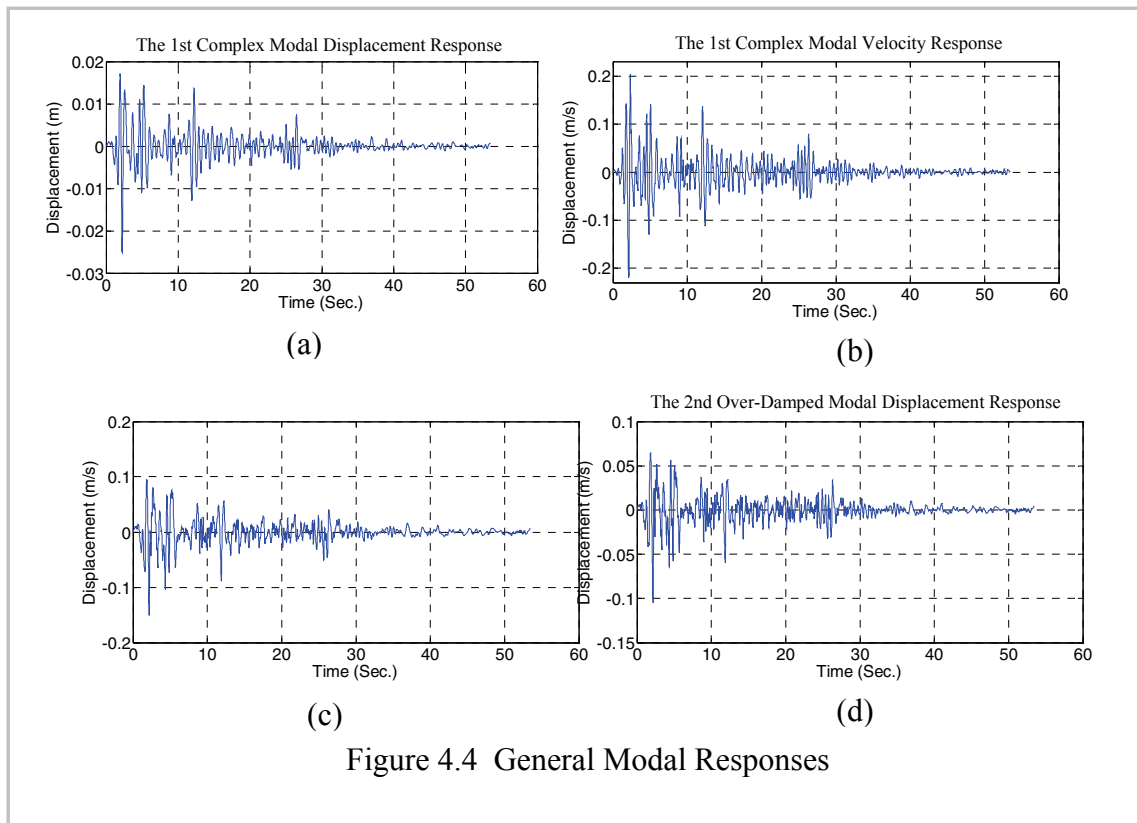
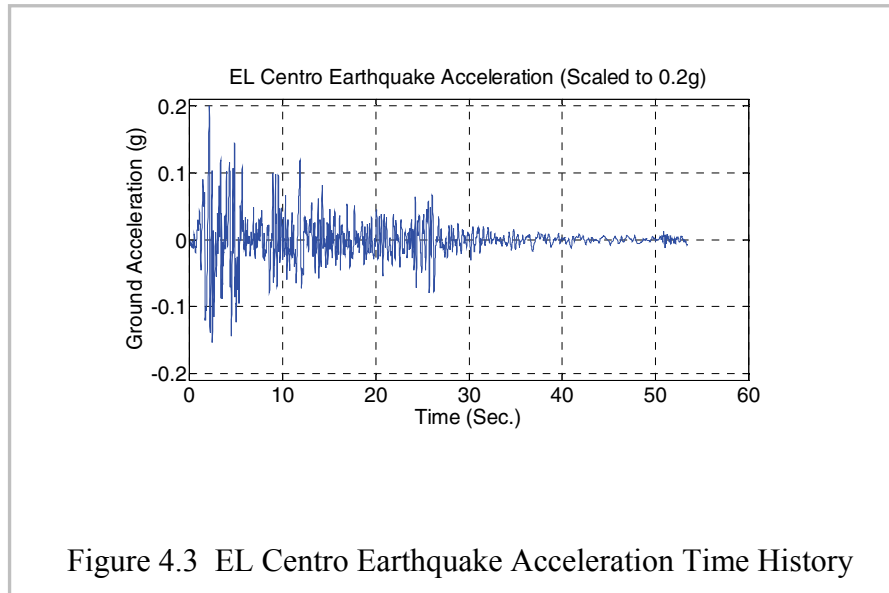




Similar to Equations (4.48) and (4.49), the structural absolute acceleration can also be expressed as

$$\ddot{\mathbf{x}}_A(t) = (\ddot{x}_{A1}, \ddot{x}_{A2}, \ddot{x}_{A3}, \ddot{x}_{A4})^T = [\mathbf{A}_{A1}\dot{q}_1(t) + \mathbf{B}_{A1}q_1(t)] + [\mathbf{A}_{A1}^p q_1^p(t)] + [\mathbf{A}_{A2}^p q_2^p(t)] \quad (4.54)$$

Now the El Centro earthquake ground motion acceleration with peak value of 0.2g (0.2g PGA) is assumed applying to the example model. The acceleration history plot is shown in Figure 4.3. Utilizing Equations (4.36a) and (4.38), we can solve the general modal responses for three effective modes (the modes that satisfied conditions (4.43a) and (4.43b)).

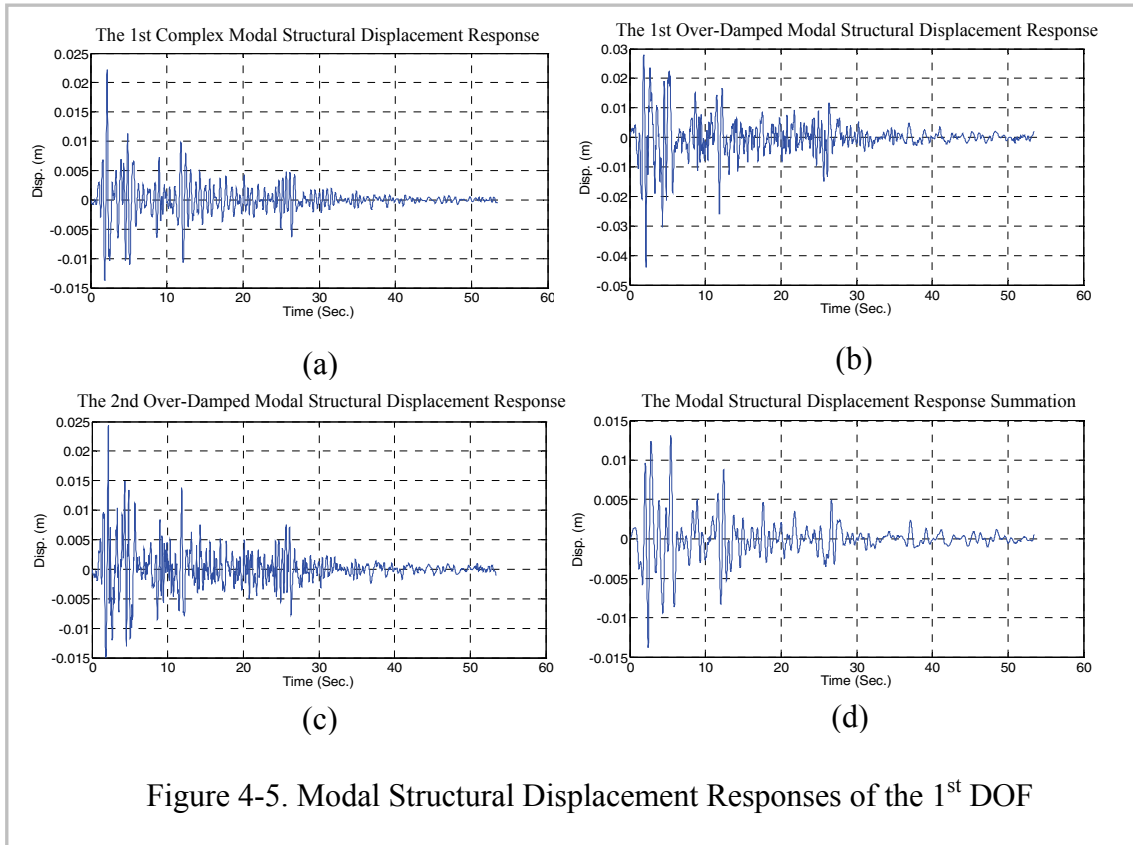


The corresponding response plots are shown in Figure 4.4 (a) to (b). As similar as the definitions in Equation (3.13) and (3.14), each term in square bracket in Equations (4.48) and (4.49) is named as the modal structural response, such as:  $\mathbf{x}_1(t) = \mathbf{A}_{D1}\dot{q}_1(t) + \mathbf{B}_{D1}q_1(t)$  ,  $\dot{\mathbf{x}}_1(t) = \mathbf{A}_{V1}\dot{q}_1(t) + \mathbf{B}_{V1}q_1(t)$  and  $\ddot{\mathbf{x}}_{A1}(t) = \mathbf{A}_{A1}\dot{q}_1(t) + \mathbf{B}_{A1}q_1(t)$  are called as the 1<sup>st</sup> complex modal structural displacement, velocity and absolute acceleration vectors, respectively, while  $\mathbf{x}_1^P(t) = \mathbf{A}_{D1}^P q_1^P(t)$  ,  $\dot{\mathbf{x}}_1^P = \mathbf{A}_{V1}^P q_1^P(t)$  ,  $\ddot{\mathbf{x}}_{A1}^P = \mathbf{A}_{A1}^P q_1^P(t)$  ,  $\mathbf{x}_2^P(t) = \mathbf{A}_{D2}^P q_2^P(t)$  ,  $\dot{\mathbf{x}}_2^P = \mathbf{A}_{V2}^P q_2^P(t)$  and  $\ddot{\mathbf{x}}_{A2}^P = \mathbf{A}_{A2}^P q_2^P(t)$  are the 1<sup>st</sup> and 2<sup>nd</sup> over-damped modal structural displacement vector, velocity vector and absolute acceleration vector, respectively. Thus, (4.48), (4.49) and (4.54) can be rewritten as:

$$\mathbf{x}(t) = \mathbf{x}_1(t) + \mathbf{x}_1^P(t) + \mathbf{x}_2^P(t) \in \mathbb{R}^N \quad (4.55)$$

$$\dot{\mathbf{x}}(t) = \dot{\mathbf{x}}_1(t) + \dot{\mathbf{x}}_1^P(t) + \dot{\mathbf{x}}_2^P(t) \in \mathbb{R}^N \quad (4.56)$$

$$\ddot{\mathbf{x}}_A(t) = \ddot{\mathbf{x}}_{A1}(t) + \ddot{\mathbf{x}}_{A1}^P(t) + \ddot{\mathbf{x}}_{A2}^P(t) \in \mathbb{R}^N \quad (4.56a)$$



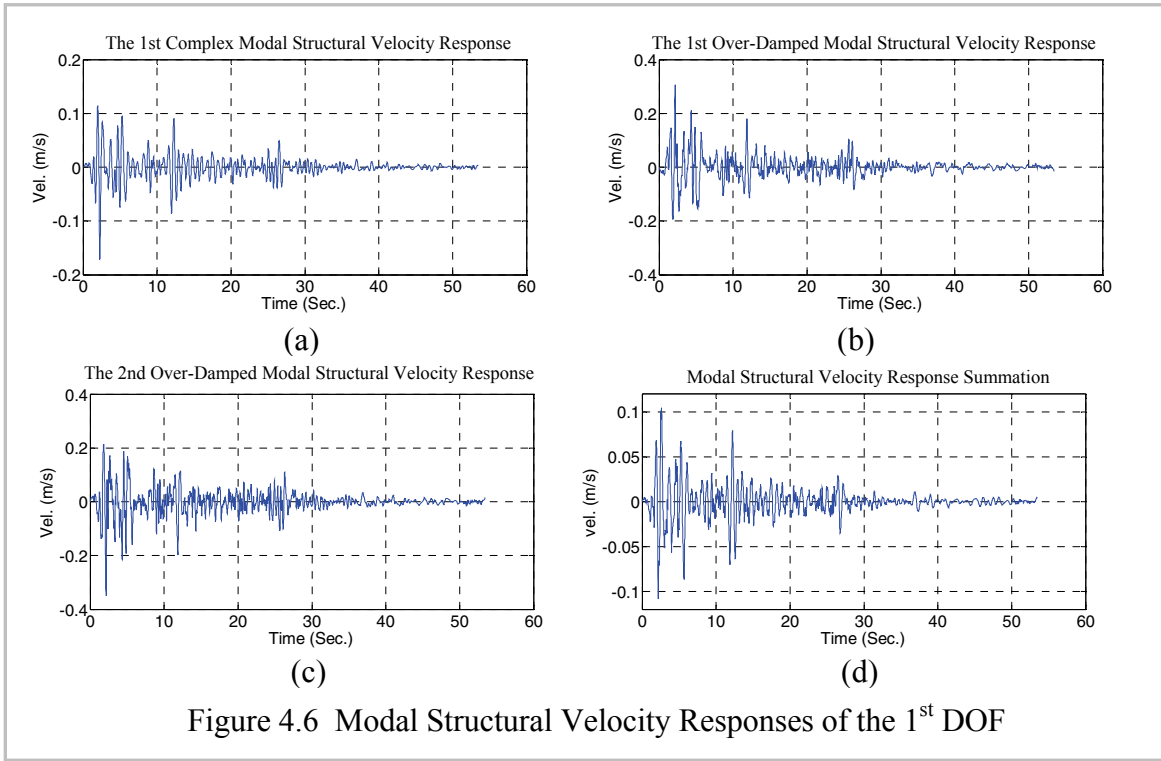


Figure 4.6 Modal Structural Velocity Responses of the 1<sup>st</sup> DOF

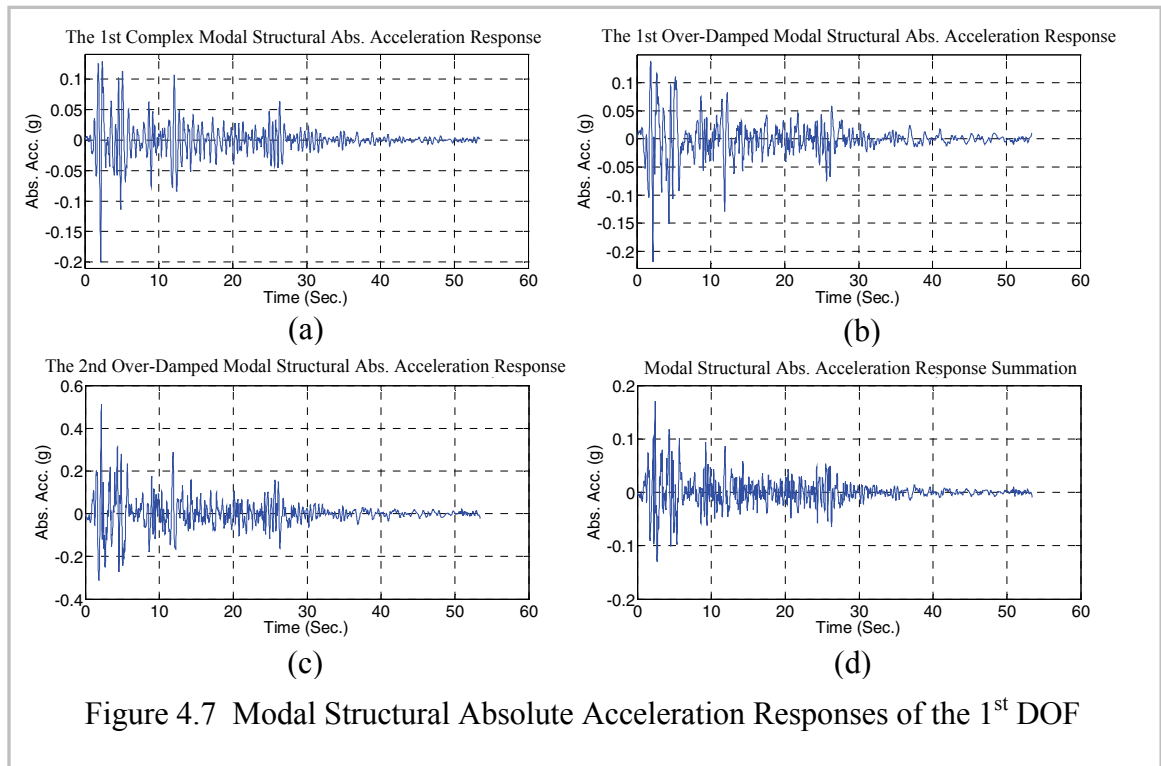
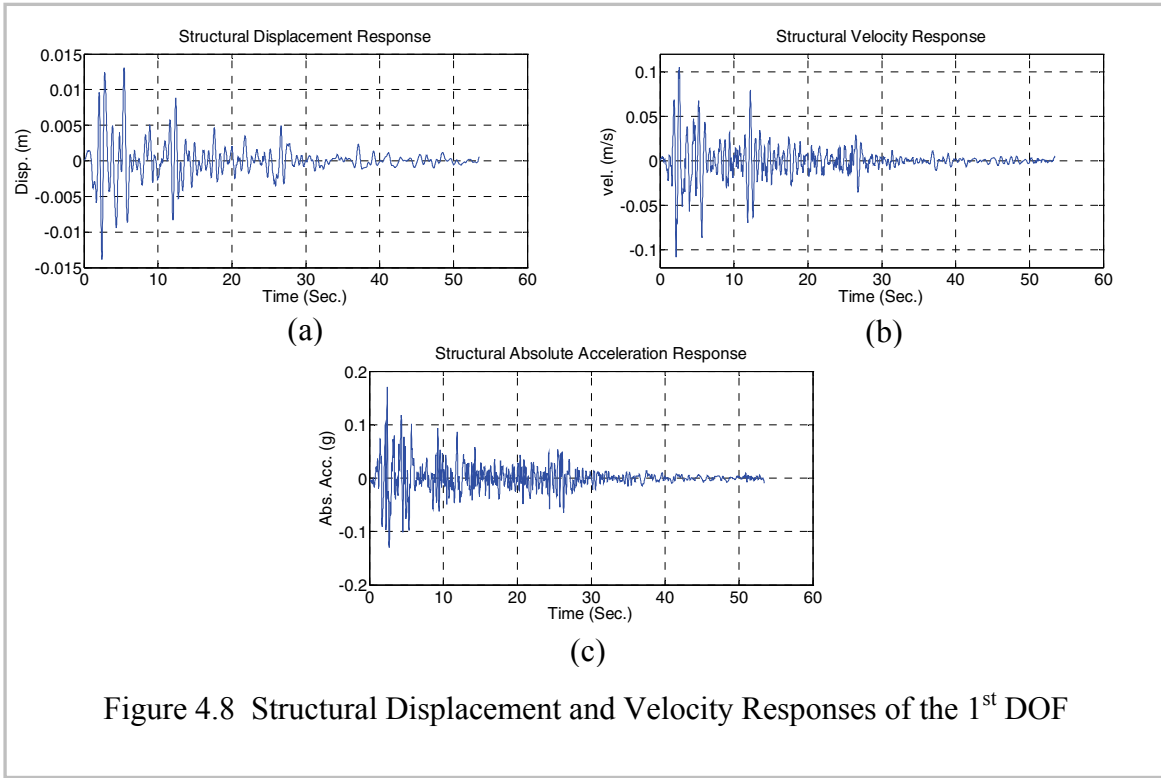


Figure 4.7 Modal Structural Absolute Acceleration Responses of the 1<sup>st</sup> DOF



As an example to illustrate the responses of the structure, the modal structural displacement responses for the first DOF of the structure and for the three general modes are shown in Figure 4.5 (a) to (c). Their summation is given in Figure 4.5 (d), while the modal structural velocity and absolute acceleration responses and their corresponding summation are shown in Figure 4.6 (a) to (d) and Figure 4.7 (a) to (d).

The Figure 4.8 (a) to (c) also show the structural displacement, velocity and absolute acceleration response plots of the 1<sup>st</sup> DOF, respectively. These three responses are calculated directly based on the complete state space equation of the structural system that is expressed as the following, other than via modal decoupling approach.

$$\begin{Bmatrix} \ddot{\mathbf{x}}(t) \\ \dot{\mathbf{x}}(t) \end{Bmatrix} = \begin{pmatrix} -\mathbf{M}^{-1}\mathbf{C} & -\mathbf{M}^{-1}\mathbf{K} \\ \mathbf{I} & \mathbf{0} \end{pmatrix} \begin{Bmatrix} \dot{\mathbf{x}}(t) \\ \mathbf{x}(t) \end{Bmatrix} + \begin{Bmatrix} -\mathbf{J}\ddot{\mathbf{x}}_g(t) \\ \mathbf{0} \end{Bmatrix} \in \mathbb{R}^{2N} \quad (4.57)$$

$$\ddot{\mathbf{x}}_A(t) = -(\mathbf{M}^{-1}\mathbf{C})\dot{\mathbf{x}}(t) - (\mathbf{M}^{-1}\mathbf{K})\mathbf{x}(t) \in \mathbb{R}^N \quad (4.58)$$

The major purpose of doing so is for comparison of responses obtained from different approaches and for further validation of formulas developed in this study. Comparing Figures 4.5(d), 4.6(d) and 4.7(d) with Figure 4.8(a), (b) and (c), respectively, it can be observed that the corresponding pairs of plots are exactly same.

#### 4.6 General Modal Responses to Initial Conditions

If the applied earthquake force to the structure is  $\mathbf{f}(t) = \mathbf{0} \in \mathbb{R}^N$ , Equations (2.1) and (2.2) become,

$$\mathbf{M}\ddot{\mathbf{x}}(t) + \mathbf{C}\dot{\mathbf{x}}(t) + \mathbf{K}\mathbf{x}(t) = \mathbf{0} \in \mathbb{R}^N \quad (4.59)$$

$$\mathbf{A}\dot{\mathbf{y}}(t) + \mathbf{B}\mathbf{y}(t) = \mathbf{0} \in \mathbb{R}^{2N} \quad (4.60)$$

However, if at the zero instant ( $t = 0^+$ ), the structure is subjected to an initial displacement vector  $\mathbf{x}_0 \in \mathbb{R}^N$  and a velocity vector  $\dot{\mathbf{x}}_0 \in \mathbb{R}^N$ , the structure will oscillate around its equilibrium position until the vibration level decays to zero (suppose that damping always exists more or less in the structure). The initial conditions can be expressed as state vector format, which is

$$\mathbf{y}_0 = \begin{Bmatrix} \dot{\mathbf{x}}_0 \\ \mathbf{x}_0 \end{Bmatrix} \in \mathbb{R}^{2N} \quad (4.61)$$

In the following, the general modal transformation matrix  $\mathbf{A}_{ST}$  is used to convert the initial conditions  $\mathbf{x}_0$  and  $\dot{\mathbf{x}}_0$  or  $\mathbf{y}_0$  in the original coordinates to those in general modal coordinates:

$$\mathbf{u}_{S0} = \left( \dot{q}_{01}, q_{01}, \dot{q}_{02}, q_{02}, \dots, \dot{q}_{0N_C}, q_{0N_C}, q_{01}^P, \dots, q_{0N_P}^P \right)^T \in \mathbb{R}^{2N} \quad (4.62)$$

According to Equation (4.11),  $\mathbf{y}_0$  and  $\mathbf{u}_{S0}$  satisfies the following relationship:

$$\mathbf{y}_0(t) = \mathbf{A}_{ST}\mathbf{u}_{S0}(t) \quad (4.63)$$

Pre-multiplying  $\mathbf{A}_{ST}^T \mathbf{B}$  to both sides of Equation (4.63) brings out

$$\mathbf{A}_{ST}^T \mathbf{B} \mathbf{y}_0 = (\mathbf{A}_{ST}^T \mathbf{B} \mathbf{A}_{ST}) \mathbf{u}_{s0} \in \mathbb{R}^{2N} \quad (4.64)$$

The left hand side of Equation (4.64) can be expanded as

$$\begin{aligned} \mathbf{A}_{ST}^T \mathbf{B} \mathbf{y}_0 &= \mathbf{A}_{ST}^T \begin{pmatrix} -\mathbf{M} & \mathbf{0} \\ \mathbf{0} & \mathbf{K} \end{pmatrix} \begin{Bmatrix} \dot{\mathbf{x}}_0 \\ \mathbf{x}_0 \end{Bmatrix} = \mathbf{\Gamma}^T \mathbf{\Psi}^T \begin{Bmatrix} -\mathbf{M} \dot{\mathbf{x}}_0 \\ \mathbf{K} \mathbf{x}_0 \end{Bmatrix} \\ &= \mathbf{\Gamma}^T \left[ -\Lambda_S \mathbf{\Phi}_S^T \mathbf{M} \dot{\mathbf{x}}_0 + \mathbf{\Phi}_S^T \mathbf{K} \mathbf{x}_0 \right] \end{aligned} \quad (4.65)$$

Based on Equation (4.28), the right side of Equation (4.64) becomes

$$(\mathbf{A}_{ST}^T \mathbf{B} \mathbf{A}_{ST}) \mathbf{u}_{s0} = (\mathbf{\Gamma}^T \hat{\mathbf{b}}_S \mathbf{\Gamma}) \mathbf{u}_{s0} \in \mathbb{R}^{2N} \quad (4.66)$$

Thus

$$\begin{aligned} \mathbf{u}_{s0} &= [\mathbf{A}_{ST}^T \mathbf{B} \mathbf{A}_{ST}]^{-1} \mathbf{A}_{ST}^T \mathbf{B} \mathbf{y}_0 = \mathbf{\Gamma}^{-1} \hat{\mathbf{b}}_S^{-1} \mathbf{\Gamma}^{-T} \mathbf{\Gamma}^T \left[ -\Lambda_S \mathbf{\Phi}_S^T \mathbf{M} \dot{\mathbf{x}}_0 + \mathbf{\Phi}_S^T \mathbf{K} \mathbf{x}_0 \right] \\ &= \mathbf{\Gamma}^{-1} \hat{\mathbf{b}}_S^{-1} \left[ -\Lambda_S \mathbf{\Phi}_S^T \mathbf{M} \dot{\mathbf{x}}_0 + \mathbf{\Phi}_S^T \mathbf{K} \mathbf{x}_0 \right] = \mathbf{\Gamma}^{-1} \hat{\mathbf{a}}_S^{-1} \left[ \mathbf{\Phi}_S^T \mathbf{M} \dot{\mathbf{x}}_0 - \Lambda_S^{-1} \mathbf{\Phi}_S^T \mathbf{K} \mathbf{x}_0 \right] \end{aligned} \quad (4.67)$$

in which

$$\mathbf{\Gamma}^{-1} \hat{\mathbf{a}}_S^{-1} = \begin{pmatrix} \text{diag} \left[ \frac{1}{j2\omega_{di}} \begin{pmatrix} \frac{\lambda_i}{(\boldsymbol{\varphi}_i^T \mathbf{M} \mathbf{J})} & -\frac{\lambda_i^*}{(\boldsymbol{\varphi}_i^H \mathbf{M} \mathbf{J})} \\ \frac{1}{(\boldsymbol{\varphi}_i^T \mathbf{M} \mathbf{J})} & -\frac{1}{(\boldsymbol{\varphi}_i^H \mathbf{M} \mathbf{J})} \end{pmatrix} \right] & \mathbf{0} \\ \mathbf{0} & \text{diag} \left( \frac{1}{(\boldsymbol{\varphi}_i^p)^T \mathbf{M} \mathbf{J}} \right) \end{pmatrix} \in \mathbb{C}^{2N \times 2N} \quad (4.68)$$

Substituting Equation (4.68) into (4.67) leads to

$$\begin{aligned} \dot{q}_{0i} &= \frac{1}{j2\omega_{di}} \left[ \left( \frac{\lambda_i \boldsymbol{\varphi}_i^T \mathbf{M}}{\boldsymbol{\varphi}_i^T \mathbf{M} \mathbf{J}} - \frac{\lambda_i^* \boldsymbol{\varphi}_i^H \mathbf{M}}{\boldsymbol{\varphi}_i^H \mathbf{M} \mathbf{J}} \right) \dot{\mathbf{x}}_0 - \left( \frac{\boldsymbol{\varphi}_i^T \mathbf{K}}{\boldsymbol{\varphi}_i^T \mathbf{M} \mathbf{J}} - \frac{\boldsymbol{\varphi}_i^H \mathbf{K}}{\boldsymbol{\varphi}_i^H \mathbf{M} \mathbf{J}} \right) \mathbf{x}_0 \right] \\ &= \frac{1}{\omega_{di}} \operatorname{Im} \left( \frac{\lambda_i \boldsymbol{\varphi}_i^T \mathbf{M}}{\boldsymbol{\varphi}_i^T \mathbf{M} \mathbf{J}} \right) \dot{\mathbf{x}}_0 - \frac{1}{\omega_{di}} \operatorname{Im} \left( \frac{\boldsymbol{\varphi}_i^T \mathbf{K}}{\boldsymbol{\varphi}_i^T \mathbf{M} \mathbf{J}} \right) \mathbf{x}_0 \in \mathbb{R} \end{aligned} \quad (4.69)$$

$$\begin{aligned} q_{0i} &= \frac{1}{j2\omega_{di}} \left[ \left( \frac{\boldsymbol{\varphi}_i^T \mathbf{M}}{\boldsymbol{\varphi}_i^T \mathbf{M} \mathbf{J}} - \frac{\boldsymbol{\varphi}_i^H \mathbf{M}}{\boldsymbol{\varphi}_i^H \mathbf{M} \mathbf{J}} \right) \dot{\mathbf{x}}_0 - \left( \frac{\boldsymbol{\varphi}_i^T \mathbf{K}}{\lambda_i \boldsymbol{\varphi}_i^T \mathbf{M} \mathbf{J}} - \frac{\boldsymbol{\varphi}_i^H \mathbf{K}}{\lambda_i^* \boldsymbol{\varphi}_i^H \mathbf{M} \mathbf{J}} \right) \mathbf{x}_0 \right] \\ &= \frac{1}{\omega_{di}} \operatorname{Im} \left( \frac{\boldsymbol{\varphi}_i^T \mathbf{M}}{\boldsymbol{\varphi}_i^T \mathbf{M} \mathbf{J}} \right) \dot{\mathbf{x}}_0 - \frac{1}{\omega_{di}} \operatorname{Im} \left( \frac{\boldsymbol{\varphi}_i^T \mathbf{K}}{\lambda_i \boldsymbol{\varphi}_i^T \mathbf{M} \mathbf{J}} \right) \mathbf{x}_0 \in \mathbb{R} \end{aligned} \quad (4.70)$$

$$q_{0i}^p = \frac{(\boldsymbol{\varphi}_i^p)^T \mathbf{M}}{(\boldsymbol{\varphi}_i^p)^T \mathbf{M} \mathbf{J}} \dot{\mathbf{x}}_0 + \frac{(\boldsymbol{\varphi}_i^p)^T \mathbf{K}}{\omega_i^p (\boldsymbol{\varphi}_i^p)^T \mathbf{M} \mathbf{J}} \mathbf{x}_0 \in \mathbb{R} \quad (4.71)$$

Note that if conditions (4.43a) and (4.43b) for certain modes cannot be satisfied, similar to that described in the Section 4.4, the modal coordinate transformation for initial conditions expressed in Equation (4.63) must be changed as

$$\mathbf{y}_0(t) = \mathbf{A}'_{\text{ST}} \mathbf{u}_{s0}(t) \quad (4.72)$$

in which  $\mathbf{A}'_{\text{ST}}$  is the same as  $\mathbf{A}_{\text{ST}}$  except that it excludes modes  $r_0 = r_1, r_2 \cdots r_n$  and/or  $r_0^p = r_1^p, r_2^p \cdots r_{n_p}^p$ . It is easy to predict that if we follow the procedure for formulation from (4.63) to (4.71), the final formulas for the initial conditions expressed in terms of general modal coordinates are same as those in (4.63) to (4.71), except  $i \neq r_0$  for complex modes and/or  $i \neq r_0^p$  for over-damped modes. This means that no assignments of initial conditions to these modes are needed. In other words, these modes do not have contributions to the structural initial conditions expressed in the structural original coordinates. In the following, we only focus on the discussion for Equations (4.63) to (4.71). For the cases that  $i = r_0$  and/or  $i = r_0^p$ , the analysis and the conclusions are similar. From Equations (4.69) and (4.70), supposing that only initial structural displacement  $\mathbf{x}_0$



exists or only initial structural velocity  $\dot{\mathbf{x}}_0$  exists, we have following two sets of simplified equations, respectively,

$$\dot{q}_{0i} = -\frac{1}{\omega_{di}} \text{Im} \left( \frac{\boldsymbol{\phi}_i^T \mathbf{K}}{\boldsymbol{\phi}_i^T \mathbf{M} \mathbf{J}} \right) \mathbf{x}_0 \quad (4.73)$$

and

$$q_{0i} = -\frac{1}{\omega_{di}} \text{Im} \left( \frac{\boldsymbol{\phi}_i^T \mathbf{K}}{\lambda_i \boldsymbol{\phi}_i^T \mathbf{M} \mathbf{J}} \right) \mathbf{x}_0 \quad (4.74)$$

or

$$\dot{q}_{0i} = \frac{1}{\omega_{di}} \text{Im} \left( \frac{\lambda_i \boldsymbol{\phi}_i^T \mathbf{M}}{\boldsymbol{\phi}_i^T \mathbf{M} \mathbf{J}} \right) \dot{\mathbf{x}}_0 \quad (4.75)$$

and

$$q_{0i} = \frac{1}{\omega_{di}} \text{Im} \left( \frac{\boldsymbol{\phi}_i^T \mathbf{M}}{\boldsymbol{\phi}_i^T \mathbf{M} \mathbf{J}} \right) \dot{\mathbf{x}}_0 \quad (4.76)$$

from which, we can see that sole  $\mathbf{x}_0$  or sole  $\dot{\mathbf{x}}_0$  will cause both complex modal initial displacement and velocity simultaneously for most cases. This is a special characteristic brought out from complex modes. From (4.71), we can notice that either  $\mathbf{x}_0$  or  $\dot{\mathbf{x}}_0$  or their combination will only lead over-damped modal displacement, which is due to the first order differential equation for the over-damped modes.

Now let us recall the earthquake loading expression  $f(t) = -\mathbf{M} \mathbf{J} \ddot{x}_g(t)$  and further suppose  $[-\ddot{x}_g(t)] = \alpha$  ( $\alpha \in \mathbb{R}$  and  $\alpha \neq 0$ ), which leads  $f_0 = \alpha \mathbf{M} \mathbf{J}$  and  $f_0$  can be considered as general static force vector due to constant ground motion acceleration. If  $\mathbf{x}_0$  is the structural initial displacement vector that is caused by applying  $f_0$  to the structure, we can express  $\mathbf{x}_0$  as

$$\mathbf{x}_0 = \alpha \mathbf{K}^{-1} \mathbf{M} \mathbf{J} \quad (4.77)$$

Substituting Equation (4.77) into Equations (4.73), (4.74) and (4.71), we have

$$\dot{q}_{0i} = -\frac{\alpha}{\omega_{di}} \operatorname{Im} \left( \frac{\boldsymbol{\varphi}_i^T \mathbf{K} \mathbf{K}^{-1} \mathbf{M} \mathbf{J}}{\boldsymbol{\varphi}_i^T \mathbf{M} \mathbf{J}} \right) = 0 \quad (4.78)$$

and

$$q_{0i} = -\frac{\alpha}{\omega_{di}} \operatorname{Im} \left( \frac{\boldsymbol{\varphi}_i^T \mathbf{K} \mathbf{K}^{-1} \mathbf{M} \mathbf{J}}{\lambda_i \boldsymbol{\varphi}_i^T \mathbf{M} \mathbf{J}} \right) = -\frac{\alpha}{\omega_{di}} \operatorname{Im} \left( \frac{1}{\lambda_i} \right) = \frac{\alpha}{\omega_i^2} \quad (4.79)$$

$$q_{0i}^p = \frac{\alpha (\boldsymbol{\varphi}_i^p)^T \mathbf{K} \mathbf{K}^{-1} \mathbf{M} \mathbf{J}}{\omega_i^p (\boldsymbol{\varphi}_i^p)^T \mathbf{M} \mathbf{J}} = \frac{\alpha}{\omega_i^p} \quad (4.80)$$

Equations (4.78) and (4.79) show that when the structure has only initial displacement  $\mathbf{x}_0$  and  $\mathbf{x}_0$  satisfies Equation (4.77), only initial displacement for a complex mode can be obtained through the coordinate transformation proposed in this study. In addition, from Equation (4.79), we can notice that the term  $1/\omega_i^2$  and its reciprocal  $\omega_i^2$  act as flexibility and stiffness, respectively, of a SDOF system with a unit mass, which is governed by Equation (4.36a).

On the other hand, if supposing that the ground suddenly generates a velocity  $(-\beta)$  (m/sec.) at  $t = 0$ , the structure will be subjected to a relative initial velocity vector

$$\dot{\mathbf{x}}_0 = \beta \mathbf{J} \quad (4.81)$$

Substituting Equation (4.81) into Equations (4.75), (4.76) and (4.71), we have

$$\dot{q}_{0i} = \frac{\beta}{\omega_{di}} \operatorname{Im} \left( \frac{\lambda_i \boldsymbol{\varphi}_i^T \mathbf{M} \mathbf{J}}{\boldsymbol{\varphi}_i^T \mathbf{M} \mathbf{J}} \right) = \beta \quad (4.82)$$

and

$$q_{0i} = \frac{\beta}{\omega_{di}} \operatorname{Im} \left( \frac{\boldsymbol{\varphi}_i^T \mathbf{M} \mathbf{J}}{\boldsymbol{\varphi}_i^T \mathbf{M} \mathbf{J}} \right) = 0 \quad (4.83)$$

and

$$q_{0i}^p = \frac{\beta(\boldsymbol{\varphi}_i^p)^T \mathbf{M}\mathbf{J}}{(\boldsymbol{\varphi}_i^p)^T \mathbf{M}\mathbf{J}} = \beta \quad (4.84)$$

If  $\mathbf{x}_0 = \alpha \mathbf{K}^{-1} \mathbf{M}\mathbf{J}$  and  $\dot{\mathbf{x}}_0 = \beta \mathbf{J}$  exist simultaneously, the following relationships can be easily derived:

$$\dot{q}_{0i} = \beta \quad (4.85)$$

$$q_{0i} = \frac{\alpha}{\omega_i^2} \quad (4.86)$$

and

$$q_{0i}^p = \frac{\alpha}{\omega_i^p} + \beta \quad (4.87)$$

Subjected to initial conditions, after  $t > 0$ , each complex mode responds in a free decay vibration of an under-damped SDOF system, which is the solution of the homogeneous format of Equation (4.36a) and can be represented by following formulas (Clough and Penzien 1993):

$$q_i(t) = e^{-\xi_i \omega_i t} \left[ q_{0i} \cos(\omega_{di} t) + \frac{\dot{q}_{0i} + \xi_i \omega_i q_{0i}}{\omega_{di}} \sin(\omega_{di} t) \right] \quad (4.88)$$

$$\dot{q}_i(t) = e^{-\xi_i \omega_i t} \left[ \dot{q}_{0i} \cos(\omega_{di} t) - \frac{(\xi_i \dot{q}_{0i} + \omega_i q_{0i})}{\sqrt{1 - \xi_i^2}} \sin(\omega_{di} t) \right] \quad (4.89)$$

Substituting Equations (4.85) and (4.86) into the above two expressions yields

$$q_i(t) = \frac{\alpha \sqrt{1 - \xi_i^2} \cos(\omega_{di} t) + (\alpha \xi_i + \beta \omega_i) \sin(\omega_{di} t)}{\sqrt{1 - \xi_i^2} \omega_i^2} e^{-\xi_i \omega_i t} \quad (4.90)$$

$$\dot{q}_i(t) = \frac{\beta\omega_{di} \cos(\omega_{di}t) - (\alpha + \beta\xi_i\omega_i) \sin(\omega_{di}t)}{\omega_{di}} e^{-\xi_i\omega_i t} \quad (4.91)$$

Following the same procedure for over-damped modes as that for the complex modes, we have the solution of the homogeneous format of Equation (4.38), which are

$$q_i^p(t) = q_{0i}^p e^{-\omega_i^p t} \quad (4.92)$$

and

$$q_i^p(t) = \frac{(\alpha + \beta\omega_i^p)}{\omega_i^p} e^{-\omega_i^p t} \quad (4.93)$$

Notice that sinusoidal and co-sinusoidal terms in Equations (4.92) and (4.93) do not exist, which implies that the free motion response of an over-damped mode to the initial conditions is a non-oscillatory motion. From the physical viewpoint, in an over-damped (or first order) subsystem, only one energy storage element exists, which differs from a second-order subsystem (consistence with an under-damped SDOF system). The latter has two different types of energy storage elements, i.e., mass (for kinematical energy) and stiffness (for potential energy) and these two types of energy are mutually transformable internally during vibrations. However, this internal energy transformation mechanism does not exist in a first order subsystem. Figure 4.9 shows four typical examples of first order subsystem composed of both mechanical and electric components. Note that the so-called “over-damped modal period” here is in correspondence with the term “time constant” in the control theory.

Take the structural model shown in Figure 4.1 as a numerical example again and suppose  $\alpha = 0.1g$  and  $\beta = 0.4$  (m/s) for structural initial conditions expressed in Equations (4.77) and (4.81).

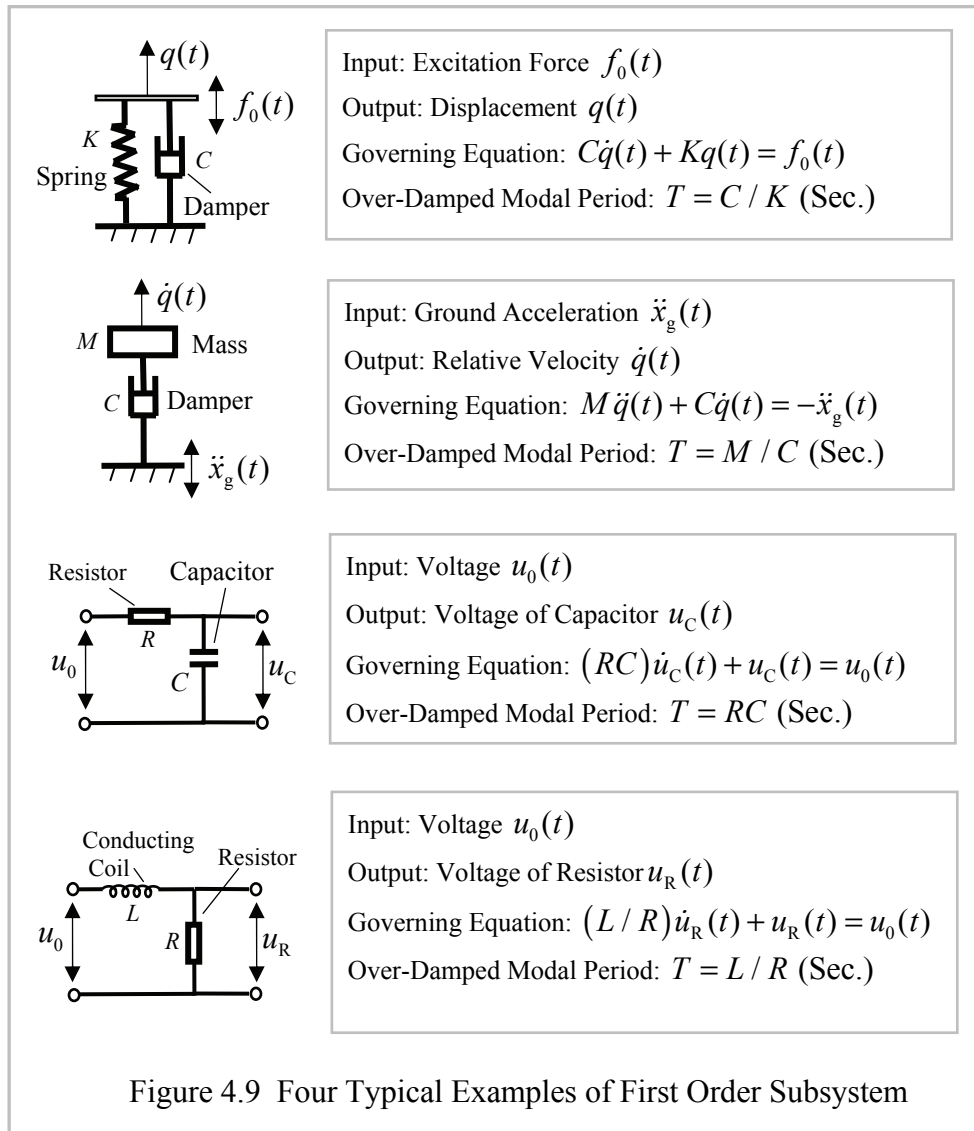


Figure 4.9 Four Typical Examples of First Order Subsystem

Using Equations (4.90) to (4.93), we can obtain the free responses to the initial conditions for each mode. The response plots are shown in Figure 4.10. Figure 4.11 shows structural displacement and velocity responses of the 1<sup>st</sup> and 2<sup>nd</sup> DOFs, while Figure 4.12 shows structural displacement and velocity responses of the 1<sup>st</sup> and 2<sup>nd</sup> DOFs which are combined results for all modes based on Equations (4.55) and (4.56).

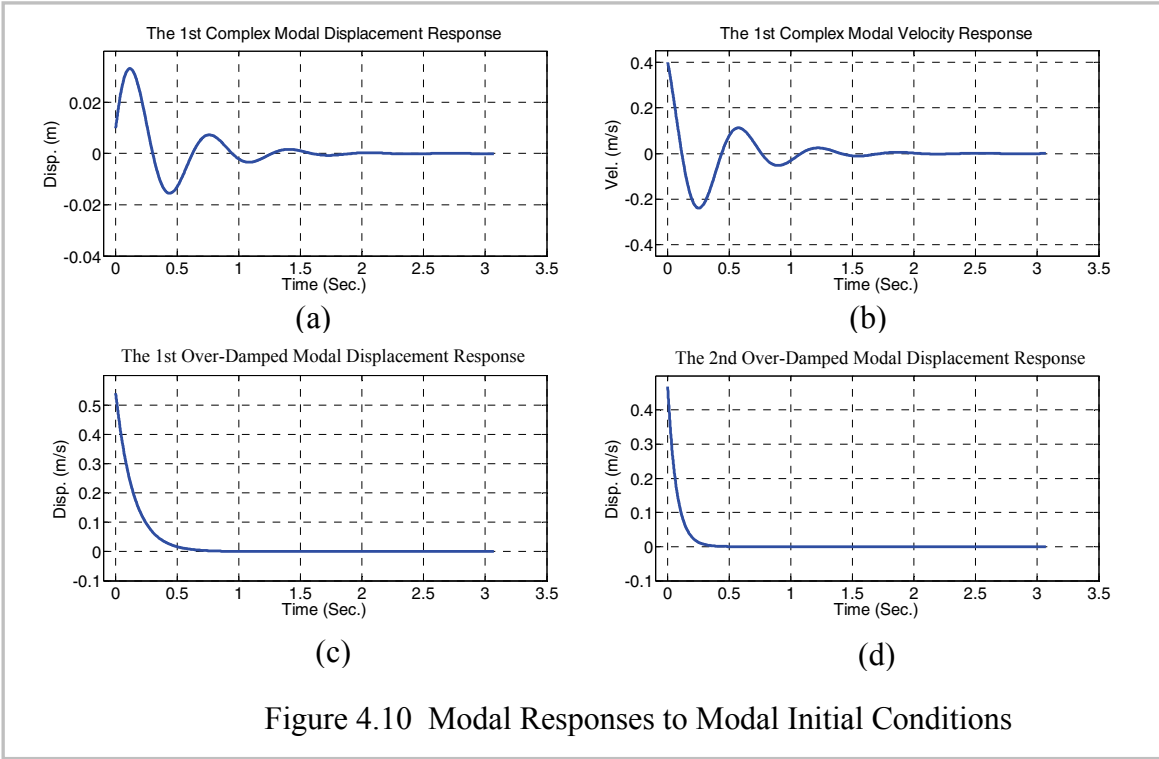


Figure 4.10 Modal Responses to Modal Initial Conditions

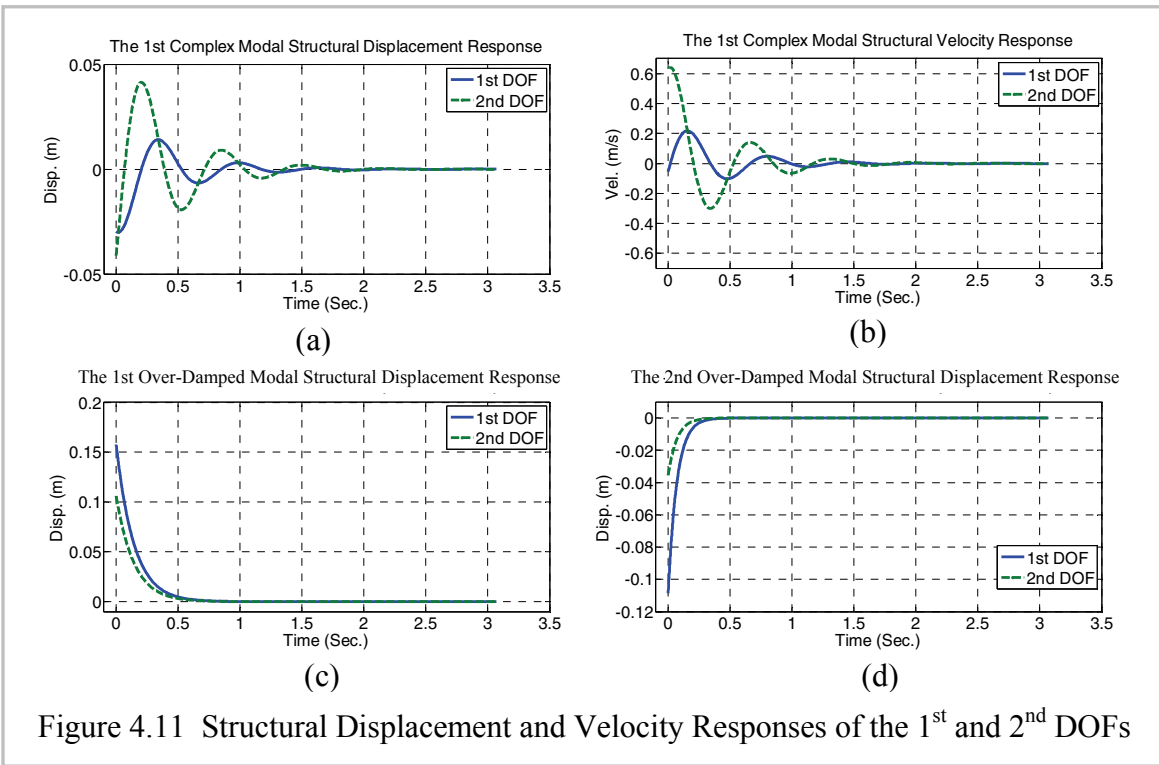
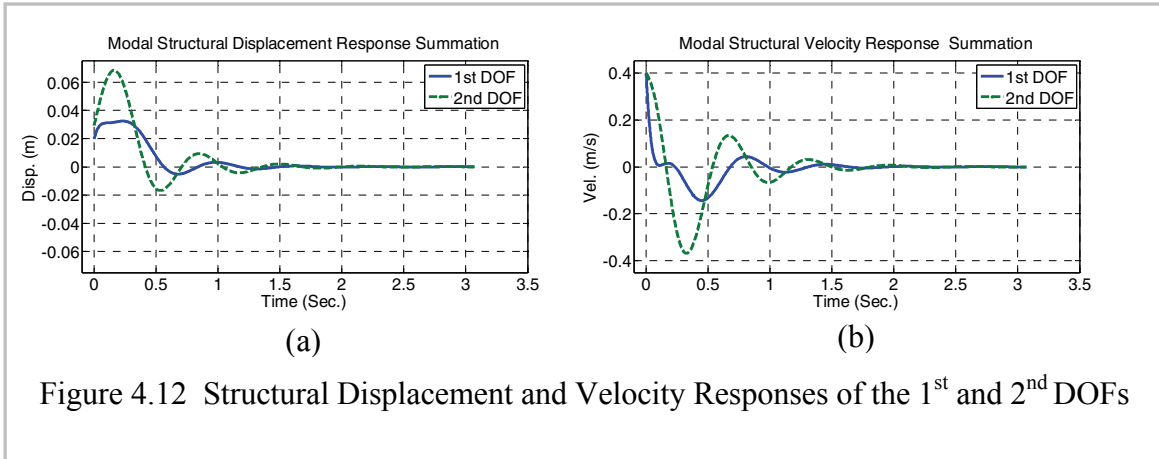


Figure 4.11 Structural Displacement and Velocity Responses of the 1<sup>st</sup> and 2<sup>nd</sup> DOFs



## 4.7 General Modal Energy

### 4.7.1 Energy Integral for Arbitrary Ground Motion Excitation

For convenience, the governing differential motion Equation (2.1) for a linear structure is rewritten here again:

$$\mathbf{M}\ddot{\mathbf{x}}(t) + \mathbf{C}\dot{\mathbf{x}}(t) + \mathbf{K}\mathbf{x}(t) = \mathbf{f}(t) \quad (4.94)$$

For earthquake ground motion excitation, let  $\mathbf{f}(t) = -\mathbf{M}\mathbf{J}\ddot{x}_g(t)$  and substitute it into the above equation, we have

$$\mathbf{M}\ddot{\mathbf{x}}(t) + \mathbf{C}\dot{\mathbf{x}}(t) + \mathbf{K}\mathbf{x}(t) = -\mathbf{M}\mathbf{J}\ddot{x}_g(t) \quad (4.95)$$

Pre-multiplying vector  $(\dot{\mathbf{x}})^T dt$  to the both sides of Equation (4.95) and taking integral operation with respect to time from zero to  $t$  results in the following system energy integration equation:

$$\int_0^t (\dot{\mathbf{x}}^T \mathbf{M} \ddot{\mathbf{x}}) dt + \int_0^t (\dot{\mathbf{x}}^T \mathbf{C} \dot{\mathbf{x}}) dt + \int_0^t (\dot{\mathbf{x}}^T \mathbf{K} \mathbf{x}) dt = -\int_0^t \dot{\mathbf{x}}^T (\mathbf{M}\mathbf{J}) \ddot{x}_g(t) dt \in \mathbb{R} \quad (4.96)$$

that is

$$\int_0^t \ddot{\mathbf{x}}^T \mathbf{M} \dot{\mathbf{x}} dt + \int_0^t \dot{\mathbf{x}}^T \mathbf{C} \dot{\mathbf{x}} dt + \int_0^t \mathbf{x}^T \mathbf{K} \dot{\mathbf{x}} dt = -\int_0^t \ddot{x}_g \dot{\mathbf{x}}^T (\mathbf{M}\mathbf{J}) dt \quad (4.97)$$

Supplementing an identical equation

$$\int_0^t \ddot{\mathbf{x}}^T \mathbf{M} \dot{\mathbf{x}} dt - \int_0^t \dot{\mathbf{x}}^T \mathbf{M} \dot{\mathbf{x}} dt = 0 \quad \in \mathbb{R} \quad (4.98)$$

where  $\int_0^t \dot{\mathbf{x}}^T \mathbf{M} \dot{\mathbf{x}} dt = \int_0^t \dot{\mathbf{x}}^T \mathbf{M} (d\mathbf{x})$  is work done by structural inertia force and combining the above two equations

$$\begin{cases} \int_0^t (\ddot{\mathbf{x}}^T \mathbf{M} \dot{\mathbf{x}} - \dot{\mathbf{x}}^T \mathbf{M} \dot{\mathbf{x}}) dt = 0 \\ \int_0^t (\ddot{\mathbf{x}}^T \mathbf{M} \dot{\mathbf{x}} + \dot{\mathbf{x}}^T \mathbf{C} \dot{\mathbf{x}} + \mathbf{x}^T \mathbf{K} \dot{\mathbf{x}}) dt = -\int_0^t (\mathbf{M}\mathbf{J})^T \dot{\mathbf{x}}(t) \ddot{x}_g dt \end{cases} \quad (4.99)$$

$$\int_0^t \begin{bmatrix} \ddot{\mathbf{x}} \\ \dot{\mathbf{x}} \end{bmatrix}^T \begin{pmatrix} \mathbf{0} & \mathbf{M} \\ \mathbf{M} & \mathbf{C} \end{pmatrix} \begin{bmatrix} \ddot{\mathbf{x}} \\ \dot{\mathbf{x}} \end{bmatrix} + \begin{bmatrix} \ddot{\mathbf{x}} \\ \dot{\mathbf{x}} \end{bmatrix}^T \begin{pmatrix} -\mathbf{M} & \mathbf{0} \\ \mathbf{0} & \mathbf{K} \end{pmatrix} \begin{bmatrix} \dot{\mathbf{x}} \\ \mathbf{x} \end{bmatrix} dt = -\int_0^t \begin{bmatrix} \ddot{\mathbf{x}} \\ \dot{\mathbf{x}} \end{bmatrix}^T \begin{pmatrix} \mathbf{0} \\ \mathbf{M}\mathbf{J} \end{pmatrix} \ddot{x}_g dt \quad (4.100)$$

Notice that

$$\begin{aligned} & \left[ \begin{bmatrix} \ddot{\mathbf{x}} \\ \dot{\mathbf{x}} \end{bmatrix}^T \begin{pmatrix} \mathbf{0} & \mathbf{M} \\ \mathbf{M} & \mathbf{C} \end{pmatrix} \begin{bmatrix} \ddot{\mathbf{x}} \\ \dot{\mathbf{x}} \end{bmatrix} + \begin{bmatrix} \ddot{\mathbf{x}} \\ \dot{\mathbf{x}} \end{bmatrix}^T \begin{pmatrix} -\mathbf{M} & \mathbf{0} \\ \mathbf{0} & \mathbf{K} \end{pmatrix} \begin{bmatrix} \dot{\mathbf{x}} \\ \mathbf{x} \end{bmatrix} \right] \\ &= (\dot{\mathbf{x}}^T \mathbf{M}, \ddot{\mathbf{x}}^T \mathbf{M} + \dot{\mathbf{x}}^T \mathbf{C}) \begin{bmatrix} \ddot{\mathbf{x}} \\ \dot{\mathbf{x}} \end{bmatrix} + (-\ddot{\mathbf{x}}^T \mathbf{M}, \dot{\mathbf{x}}^T \mathbf{K}) \begin{bmatrix} \dot{\mathbf{x}} \\ \mathbf{x} \end{bmatrix} \\ &= \dot{\mathbf{x}}^T \mathbf{M} \ddot{\mathbf{x}} + \ddot{\mathbf{x}}^T \mathbf{M} \dot{\mathbf{x}} + \dot{\mathbf{x}}^T \mathbf{C} \dot{\mathbf{x}} - \ddot{\mathbf{x}}^T \mathbf{M} \dot{\mathbf{x}} + \dot{\mathbf{x}}^T \mathbf{K} \mathbf{x} \\ &= \ddot{\mathbf{x}}^T \mathbf{M} \dot{\mathbf{x}} + \dot{\mathbf{x}}^T \mathbf{C} \dot{\mathbf{x}} + \mathbf{x}^T \mathbf{K} \dot{\mathbf{x}} \end{aligned} \quad (4.101)$$



and

$$\begin{pmatrix} \left\{ \begin{matrix} \ddot{\mathbf{x}} \\ \dot{\mathbf{x}} \end{matrix} \right\}^T \\ \left\{ \begin{matrix} \mathbf{0} \\ \mathbf{MJ} \end{matrix} \right\} \end{pmatrix} = \dot{\mathbf{x}}^T (\mathbf{MJ}) \quad (4.102)$$

Thus, Equations (4.97) and (4.100) are completely identical.

Utilizing Equations (2.3) and (4.11), Equation (4.100) becomes

$$\int_0^t \left[ \dot{\mathbf{u}}_S (\mathbf{A}_{ST}^T \mathbf{A} \mathbf{A}_{ST}) \dot{\mathbf{u}}_S + \dot{\mathbf{u}}_S (\mathbf{A}_{ST}^T \mathbf{B} \mathbf{A}_{ST}) \mathbf{u}_S \right] dt = \int_0^t \left( \dot{\mathbf{u}}_S^T \mathbf{A}_{ST}^T \begin{pmatrix} \mathbf{0} \\ \mathbf{MJ} \end{pmatrix} \right) \ddot{\mathbf{x}}_g dt \quad (4.103)$$

Substituting Equations (4.27) to (4.29) and simplifying the consequent expressions, we have following results:

$$\sum_{i=1}^{N_C} E_{C_i} + \sum_{i=1}^{N_P} E_{P_i} = \sum_{i=1}^{N_C} E_{C_i}^{\text{In}} + \sum_{i=1}^{N_P} E_{P_i}^{\text{In}} \in \mathbb{R} \quad (4.103a)$$

where  $E_{C_i}$  and  $E_{P_i}$  denote the distributed energy to the  $i$ th complex mode and  $i$ th over-damped mode, respectively, while  $E_{C_i}^{\text{In}}$  and  $E_{P_i}^{\text{In}}$  are the work done by general modal forces input to the  $i$ th complex mode and by the  $i$ th over-damped mode, respectively.

For each complex mode,

$$\begin{aligned} E_{C_i} &= \int_0^t \left[ \begin{pmatrix} \ddot{q}_i \\ \dot{q}_i \end{pmatrix}^T \mathbf{\Gamma}_{C_i}^T \begin{pmatrix} a_i & 0 \\ 0 & a_i^* \end{pmatrix} \mathbf{\Gamma}_{C_i} \begin{pmatrix} \ddot{q}_i \\ \dot{q}_i \end{pmatrix} + \begin{pmatrix} \ddot{q}_i \\ \dot{q}_i \end{pmatrix}^T \mathbf{\Gamma}_{C_i}^T \begin{pmatrix} b_i & 0 \\ 0 & b_i^* \end{pmatrix} \mathbf{\Gamma}_{C_i} \begin{pmatrix} \dot{q}_i \\ q_i \end{pmatrix} \right] dt \\ &= \text{Re} \left[ \frac{2(\boldsymbol{\phi}_i^T \mathbf{MJ})^2}{a_i} \int_0^t (\ddot{q}_i + 2\xi_i \omega_i \dot{q}_i + \omega_i^2 q_i) \ddot{q}_i dt \right. \\ &\quad \left. + \text{Re} \left[ \frac{-2\lambda_i^* (\boldsymbol{\phi}_i^T \mathbf{MJ})^2}{a_i} \int_0^t (\ddot{q}_i + 2\xi_i \omega_i \dot{q}_i + \omega_i^2 q_i) \dot{q}_i dt \right] \right] \\ &= \int_0^t (\ddot{q}_i + 2\xi_i \omega_i \dot{q}_i + \omega_i^2 q_i) \left( \text{Re} \left[ \frac{2(\boldsymbol{\phi}_i^T \mathbf{MJ})^2}{a_i} \right] \ddot{q}_i + \text{Re} \left[ \frac{-2\lambda_i^* (\boldsymbol{\phi}_i^T \mathbf{MJ})^2}{a_i} \right] \dot{q}_i \right) dt \quad (4.104) \end{aligned}$$

$$\begin{aligned}
E_{Ci}^{\text{In}} &= -\int_0^t \left\{ \begin{matrix} \ddot{q}_i \\ \dot{q}_i \end{matrix} \right\}^T \left( 2 \operatorname{Re} \left[ \frac{(\boldsymbol{\varphi}_i^T \mathbf{M} \mathbf{J})^2}{a_i} \right], -\operatorname{Re} \left[ \frac{\lambda_2^* (\boldsymbol{\varphi}_i^T \mathbf{M} \mathbf{J})^2}{a_i} \right] \right)^T \ddot{x}_g dt \\
&= -\int_0^t \operatorname{Re} \left[ \frac{2(\boldsymbol{\varphi}_i^T \mathbf{M} \mathbf{J})^2}{a_i} \right] \ddot{x}_g \dot{q}_i dt - \int_0^t \operatorname{Re} \left[ \frac{-2\lambda_2^* (\boldsymbol{\varphi}_i^T \mathbf{M} \mathbf{J})^2}{a_i} \right] \ddot{x}_g \dot{q}_i dt \quad (4.105)
\end{aligned}$$

For each  $i$ th over-damped mode,

$$E_{Pi} = \int_0^t \frac{(\boldsymbol{\varphi}_i^p \mathbf{M} \mathbf{J})^2}{a_i^p} (\dot{q}_i^p + \omega_i^p q_i^p) \dot{q}_i^p dt \quad (4.106)$$

$$E_{Pi}^{\text{In}} = -\int_0^t \frac{(\boldsymbol{\varphi}_i^p \mathbf{M} \mathbf{J})^2}{a_i^p} \dot{q}_i^p \ddot{x}_g(t) dt \quad (4.107)$$

Substituting (4.36a) and (4.38) into (4.104) and (4.106), and comparing the resulting equations with (4.105) and (4.107), respectively, it can be observed that

$$E_{Ci} = E_{Ci}^{\text{In}} \quad (4.108)$$

and

$$E_{Pi} = E_{Pi}^{\text{In}} \quad (4.109)$$

Actually, the identities shown in Equations (4.108) and (4.109) are obvious if we refer to the decoupled modal Equations (4.35), (4.36) and (4.37), which indicate that the work done by input ground motion excitation for each mode for initial instant to time  $t$  equals to the energy possessed (accumulated and dissipated) by the equivalent SDOF systems. For a complex mode, from Equation (4.105), we can see that the first term corresponds to Equation (4.35), while the second one corresponds to (4.36). The latter one can be expressed as (with zero initial conditions)

$$-\int_0^t \operatorname{Re} \left[ \frac{-2\lambda_2^* (\boldsymbol{\varphi}_i^T \mathbf{M} \mathbf{J})^2}{a_i} \right] \ddot{x}_g \dot{q}_i dt = \operatorname{Re} \left[ \frac{-2\lambda_2^* (\boldsymbol{\varphi}_i^T \mathbf{M} \mathbf{J})^2}{a_i} \right] \int_0^t (\dot{q}_i + 2\xi_i \omega_i \dot{q}_i + \omega_i^2 q_i) \dot{q}_i dt$$

$$= \operatorname{Re} \left[ \frac{-2\lambda_i^* (\boldsymbol{\varphi}_i^T \mathbf{M} \mathbf{J})^2}{a_i} \right] \left[ \frac{1}{2} \dot{q}_i^2 + 2\xi_i \omega_i \int_0^t \dot{q}_i^2 dt + \omega_i^2 \frac{1}{2} q_i^2 \right] \quad (4.110)$$

has clear physical meaning, that is, the work done by the input to a pure SDOF system with mass  $\operatorname{Re} \left[ \frac{-2\lambda_i^* (\boldsymbol{\varphi}_i^T \mathbf{M} \mathbf{J})^2}{a_i} \right]$  equals to summation of current instant kinetic and potential energy and dissipated energy in the time period zero to  $t$ . However, it is difficult to provide a clear physical interpretation for the first term of (4.105) other than the fact is certainly caused by the phenomena of complex modes.

Regarding to an over-damped mode with zero over-damped modal initial conditions, from Equation (4.106), we further have

$$E_{pi} = \frac{(\boldsymbol{\varphi}_i^p \mathbf{M} \mathbf{J})^2}{a_i^p} \int_0^t (\dot{q}_i^p)^2 dt + \frac{1}{2} \frac{(\boldsymbol{\varphi}_i^p \mathbf{M} \mathbf{J})^2}{a_i^p} \omega_i^p (q_i^p)^2 \quad (4.111)$$

in which, the first term is dissipated energy by the system energy dissipation unit, while the second is the energy accumulated by energy storage unit of the system in the instant  $t$ .

#### 4.7.2 Energy Integral for Sinusoidal Ground Motion Excitation

In order to further uncover the nature of general modal energy distribution, transfer and dissipation within a generally damped linear system, it is assumed that the system is excited by sinusoidal ground motion acceleration, which can be expressed as

$$\ddot{x}_g = -G \sin(\omega t) \quad (4.112)$$

where  $G$  is the amplitude of sinusoidal wave and  $\omega$  is circular excitation frequency (rad/s) When  $\ddot{x}_g$  applies to equations (4.35) or (4.36) and (4.39), the following steady modal responses can be derived. For complex modes,

$$q_i = Q_i \sin(\omega t + \alpha_i) \quad (4.113)$$

$$\dot{q}_i = \omega Q_i \cos(\omega t + \alpha_i) \quad (4.114)$$

$$\ddot{q}_i = -\omega^2 Q_i \sin(\omega t + \alpha_i) \quad (4.115)$$

where  $Q_i$  and  $\alpha_i$  are the amplitude and phase difference of steady complex modal displacement response, respectively. For over-damped modes

$$q_i^p = Q_i^p \sin(\omega t + \alpha_i^p) \quad (4.116)$$

$$\dot{q}_i^p = \omega Q_i^p \cos(\omega t + \alpha_i^p) \quad (4.117)$$

where  $Q_i^p$  and  $\alpha_i^p$  are the amplitude and phase difference of steady over-damped modal displacement response, respectively. According to linear system vibration theory (Chopra 2001), the expressions for  $Q_i$ ,  $\alpha_i$ ,  $Q_i^p$  and  $\alpha_i^p$  are

$$Q_i = \frac{G}{\sqrt{(\omega^2 - \omega_i^2)^2 + (2\xi_i \omega_i \omega)^2}} \quad (4.118)$$

$$\alpha_i = \tan^{-1} \frac{2\xi_i \omega_i \omega}{\omega^2 - \omega_i^2} \quad (4.119)$$

$$Q_i^p = \frac{G}{\sqrt{\omega^2 + (\omega_i^p)^2}} \quad (4.120)$$

$$\alpha_i^p = \tan^{-1} \frac{(-\omega)}{\omega_i^p} \quad (4.121)$$

Substituting Equations (4.114) and (4.115) into (4.105) brings up

$$\begin{aligned}
E_{Ci}^{\text{In}} = & \omega^2 Q_i G \operatorname{Re} \left[ \frac{2(\boldsymbol{\varphi}_i^T \mathbf{M} \mathbf{J})^2}{a_i} \right] \int_0^t \sin(\omega t + \alpha_i) \sin(\omega t) dt \\
& - \omega Q_i G \operatorname{Re} \left[ \frac{-2\lambda_i^* (\boldsymbol{\varphi}_i^T \mathbf{M} \mathbf{J})^2}{a_i} \right] \int_0^t \cos(\omega t + \alpha_i) \sin(\omega t) dt
\end{aligned} \tag{4.122}$$

in which

$$\int_0^t \sin(\omega t + \alpha_i) \sin(\omega t) dt = \left[ \frac{\cos(\alpha_i)}{2} t + \frac{\sin(\alpha_i)}{4\omega} \right] - \frac{1}{4\omega} \sin(2\omega t + \alpha_i) \tag{4.123}$$

and

$$\int_0^t \cos(\omega t + \alpha_i) \sin(\omega t) dt = \left[ -\frac{\sin(\alpha_i)}{2} t + \frac{\cos(\alpha_i)}{4\omega} \right] - \frac{1}{4\omega} \cos(2\omega t + \alpha_i) \tag{4.124}$$

After substituting Equations (4.123) and (4.124) into (4.122), (4.122) becomes

$$\begin{aligned}
E_{Ci}^{\text{In}} = & \omega^2 Q_i G \operatorname{Re} \left[ \frac{2(\boldsymbol{\varphi}_i^T \mathbf{M} \mathbf{J})^2}{a_i} \right] \left\{ \left[ \frac{\cos(\alpha_i)}{2} t + \frac{\sin(\alpha_i)}{4\omega} \right] - \frac{1}{4\omega} \sin(2\omega t + \alpha_i) \right\} \\
& - \omega Q_i G \operatorname{Re} \left[ \frac{-2\lambda_i^* (\boldsymbol{\varphi}_i^T \mathbf{M} \mathbf{J})^2}{a_i} \right] \left\{ \left[ -\frac{\sin(\alpha_i)}{2} t + \frac{\cos(\alpha_i)}{4\omega} \right] - \frac{1}{4\omega} \cos(2\omega t + \alpha_i) \right\}
\end{aligned} \tag{4.125}$$

When  $t = T = \frac{2\pi}{\omega}$ , that is, the interval of energy integral is in a complete oscillation cycle

with the excitation frequency of  $\omega$ , Equation (4.125) can be simplified as

$$\begin{aligned}
 E_{Ci}^{\text{In}} &= \pi Q_i G \omega \text{Re} \left[ \frac{2(\boldsymbol{\varphi}_i^T \mathbf{M} \mathbf{J})^2}{a_i} \right] \cos(\alpha_i) + \pi Q_i G \text{Re} \left[ \frac{-2\lambda_i^* (\boldsymbol{\varphi}_i^T \mathbf{M} \mathbf{J})^2}{a_i} \right] \sin(\alpha_i) \\
 &= \pi Q_i G \left\{ \omega \text{Re} \left[ \frac{2(\boldsymbol{\varphi}_i^T \mathbf{M} \mathbf{J})^2}{a_i} \right] \cos(\alpha_i) + \text{Re} \left[ \frac{-2\lambda_i^* (\boldsymbol{\varphi}_i^T \mathbf{M} \mathbf{J})^2}{a_i} \right] \sin(\alpha_i) \right\}
 \end{aligned} \tag{4.126}$$

Since  $\omega_i > 0$  and  $\omega > 0$ , and after further using (4.119), we have

$$\sin(\alpha_i) = \left( \frac{2\xi_i \omega_i \omega}{|\omega^2 - \omega_i^2|} \right) / \sqrt{1 + \left( \frac{2\xi_i \omega_i \omega}{\omega^2 - \omega_i^2} \right)^2} = \frac{(2\xi_i \omega_i \omega)}{\sqrt{(\omega^2 - \omega_i^2)^2 + (2\xi_i \omega_i \omega)^2}} \tag{4.127}$$

$$\cos(\alpha_i) = \text{sign}(\omega^2 - \omega_i^2) / \sqrt{1 + \left( \frac{2\xi_i \omega_i \omega}{\omega^2 - \omega_i^2} \right)^2} = \frac{(\omega^2 - \omega_i^2)}{\sqrt{(\omega^2 - \omega_i^2)^2 + (2\xi_i \omega_i \omega)^2}} \tag{4.128}$$

Substituting (4.118), (4.127) and (4.128) into (4.126) leads

$$E_{Ci}^{\text{In}} = \frac{\pi G^2}{(\omega^2 - \omega_i^2)^2 + (2\xi_i \omega_i \omega)^2} \left\{ \omega(\omega^2 - \omega_i^2) \text{Re} \left[ \frac{2(\boldsymbol{\varphi}_i^T \mathbf{M} \mathbf{J})^2}{a_i} \right] + (2\xi_i \omega_i \omega) \text{Re} \left[ \frac{-2\lambda_i^* (\boldsymbol{\varphi}_i^T \mathbf{M} \mathbf{J})^2}{a_i} \right] \right\} \tag{4.129}$$

Furthermore, if  $\omega = \omega_i$ , the first term in the notation “{}” equals to zero, which indicates that under current circumstance, the summarized amount of energy introduced by Equation (4.35) does not restore or dissipate any energy in one complete oscillation cycle. This part of energy is gained from the input and completely returned back to the input. The second term in Equation (4.129), which corresponds to Equation (4.36), can be simplified as

$$\begin{aligned} E_{Ci}^{\text{In}} &= \frac{\pi G^2}{2\xi_i \omega_i^2} \text{Re} \left[ \frac{-2\lambda_i^* (\boldsymbol{\varphi}_i^T \mathbf{M} \mathbf{J})^2}{a_i} \right] = \pi Q_i G \text{Re} \left[ \frac{-2\lambda_i^* (\boldsymbol{\varphi}_i^T \mathbf{M} \mathbf{J})^2}{a_i} \right] \\ &= 2\pi \xi_i \omega_i^2 Q_i^2 \text{Re} \left[ \frac{-2\lambda_i^* (\boldsymbol{\varphi}_i^T \mathbf{M} \mathbf{J})^2}{a_i} \right] \end{aligned} \quad (4.130)$$

Equation (4.130) is exactly same as the result of energy integral for a pure SDOF system with same excitation condition and with same system parameters (such as natural frequency, damping ratio and mass) as the  $i$ th complex mode, which indicates that the work done by the input in one cycle are totally dissipated by system damping (Chopra

2001). Notice that the term,  $\text{Re} \left[ \frac{-2\lambda_i^* (\boldsymbol{\varphi}_i^T \mathbf{M} \mathbf{J})^2}{a_i} \right]$  has mass dimension and is determined

only by the system’s modal parameters, mass and its distribution, which has been shown to have an important role as an equivalent complex modal mass in several places in this report. Its other physical interpretation and application for modal truncation will be further detailed in the next section.

For an over-damped mode, substituting Equations (4.116) and (4.117) into (4.111) and letting  $t = T = \frac{2\pi}{\omega}$ ,

$$E_{Pi} = \frac{(\boldsymbol{\varphi}_i^p \mathbf{M} \mathbf{J})^2}{a_i^p} (Q_i^p)^2 \left\{ \omega^2 \int_0^t \cos^2(\omega t + \alpha_i^p) dt + \frac{1}{2} \omega_i^p \sin^2(\omega t + \alpha_i^p) \right\}_{t=\frac{2\pi}{\omega}}$$

$$= \frac{(\boldsymbol{\varphi}_i^p \mathbf{M} \mathbf{J})^2}{a_i^p} \frac{1}{2} (Q_i^p)^2 \left\{ \omega \left[ (2\pi + \alpha_i^p) + \sin(\alpha_i^p) \cos(\alpha_i^p) \right] + \omega_i^p \sin^2(\alpha_i^p) \right\} \quad (4.131)$$

Based on Equation (4.121), we have

$$\sin(\alpha_i^p) = \frac{-\omega}{\sqrt{\omega^2 + (\omega_i^p)^2}} \quad (4.132)$$

and

$$\cos(\alpha_i^p) = \frac{\omega_i^p}{\sqrt{\omega^2 + (\omega_i^p)^2}} \quad (4.133)$$

Thus, Equation (4.131) becomes

$$E_{pi} = \frac{1}{2} \frac{(\boldsymbol{\varphi}_i^p \mathbf{M} \mathbf{J})^2}{a_i^p} (Q_i^p)^2 (2\pi + \alpha_i^p) \omega \quad (4.134)$$

If  $\omega = \omega_i^p$ ,  $\alpha_i^p = -\frac{\pi}{4}$  and Equation (4.134) is simplified as

$$E_{pi} = \frac{7\pi\omega_i^p}{8} \frac{(\boldsymbol{\varphi}_i^p \mathbf{M} \mathbf{J})^2}{a_i^p} (Q_i^p)^2 \quad (4.135)$$

## 4.8 Reduction to Classically Damped System

As mentioned in Chapter 3, when a system satisfies the Caughey Criterion, its modal shapes are real-valued and the system is a special case of generally damped system. As a consequence, corresponding expressions developed in this section can be reduced and simplified, which will be introduced in the followings.

### 4.8.1 Reduction of Modal Transformation Matrix

Since Equations (2.71a) and (3.63) exist, it can be shown that  $\mathbf{A}_{Di} = \mathbf{0}$  and  $\mathbf{B}_{Di} = \Gamma_i \boldsymbol{\varphi}_i$  (referred to Equations (3.64) and (3.65)). However, due to the nature of over-



damped modes, both  $\mathbf{R}_i^p$  and  $\mathbf{A}_{D_i}^p$  remain the same format. Furthermore, after substituting Equations (2.71a) into (3.42), we have

$$\mathbf{A}_{V_i} = \Gamma_i \boldsymbol{\varphi}_i \in \mathbb{R}^N \quad (4.136)$$

$$\mathbf{B}_{V_i} = \mathbf{0} \in \mathbb{R}^N \quad (4.137)$$

$$\mathbf{A}_{V_i}^p = -\omega_i^p \Gamma_i^p \boldsymbol{\varphi}_i^p = -\omega_i^p \mathbf{A}_{D_i}^p \in \mathbb{R}^N \quad (4.138)$$

Substituting Equations (3.64), (3.65) and (4.136) to (4.138) into Equation (4.3), we have

$$\mathbf{A}_T = \begin{pmatrix} \mathbf{A}_V & \mathbf{0} & \mathbf{A}_V^p \\ \mathbf{0} & \mathbf{B}_D & \mathbf{A}_D^p \end{pmatrix} \in \mathbb{R}^{2N \times 2N} \quad (4.139)$$

The above equation implies that the modal velocity terms and displacement terms in  $\mathbf{A}_T$  for all complex modes are decoupled, that is,

$$\mathbf{x}(t) = \sum_{i=1}^{N_C} \Gamma_i \boldsymbol{\varphi}_i q_i(t) + \sum_{i=1}^{N_P} \Gamma_i^p \boldsymbol{\varphi}_i^p q_i^p(t) \quad (4.140)$$

$$\dot{\mathbf{x}}(t) = \sum_{i=1}^{N_C} \Gamma_i \boldsymbol{\varphi}_i \dot{q}_i(t) + \sum_{i=1}^{N_P} (-\omega_i^p) \Gamma_i^p \boldsymbol{\varphi}_i^p q_i^p(t) \quad (4.141)$$

It is clear that the original differential motion equations can be decoupled into Equations (4.35), (4.36) and (4.37) by using the transformation matrix  $\mathbf{A}_T$  shown in (4.139). However, considering the Equation (2.71a), we have

$$\operatorname{Re} \left[ \frac{2(\boldsymbol{\varphi}_i^T \mathbf{M} \mathbf{J})^2}{a_i} \right] = 0 \in \mathbb{R} \quad (4.142)$$

$$\operatorname{Re} \left[ \frac{2\lambda_i^* (\boldsymbol{\varphi}_i^T \mathbf{M} \mathbf{J})^2}{a_i} \right] = \frac{(\boldsymbol{\varphi}_i^T \mathbf{M} \mathbf{J})^2}{m_i} \in \mathbb{R} \quad (4.143)$$

Thus, after the transformation, Equation (4.35) disappears and the Equation (4.36) becomes

$$\frac{(\boldsymbol{\varphi}_i^T \mathbf{M} \mathbf{J})^2}{m_i} [\ddot{q}_i + 2\xi_i \omega_i \dot{q}_i + \omega_i^2 q_i] = \frac{(\boldsymbol{\varphi}_i^T \mathbf{M} \mathbf{J})^2}{m_i} [-\ddot{x}_g(t)] \quad (4.144)$$

or

$$m_i^{\text{eff}} [\ddot{q}_i + 2\xi_i \omega_i \dot{q}_i + \omega_i^2 q_i] = m_i^{\text{eff}} [-\ddot{x}_g(t)] \quad (4.145)$$

where

$$m_i^{\text{eff}} = \frac{(\boldsymbol{\varphi}_i^T \mathbf{M} \mathbf{J})^2}{m_i} \geq 0 \in \mathbb{R} \quad (4.146)$$

is well known as effective real modal mass. Notice that Equation (4.145) differs from conventional format in which the modal participation factor is involved (Clough and Penzien 1993 and Chopra 2001). It is exactly identical to the governing differential equation for a pure SDOF system with mass  $m_i^{\text{eff}}$  and excited by the ground motion acceleration  $\ddot{x}_g(t)$ , and the excitation acceleration magnitude to each mode is same. Figure (4.13) intuitively shows the physical interpretation for  $m_i^{\text{eff}}$  (assuming that no over-damped modes exist.)

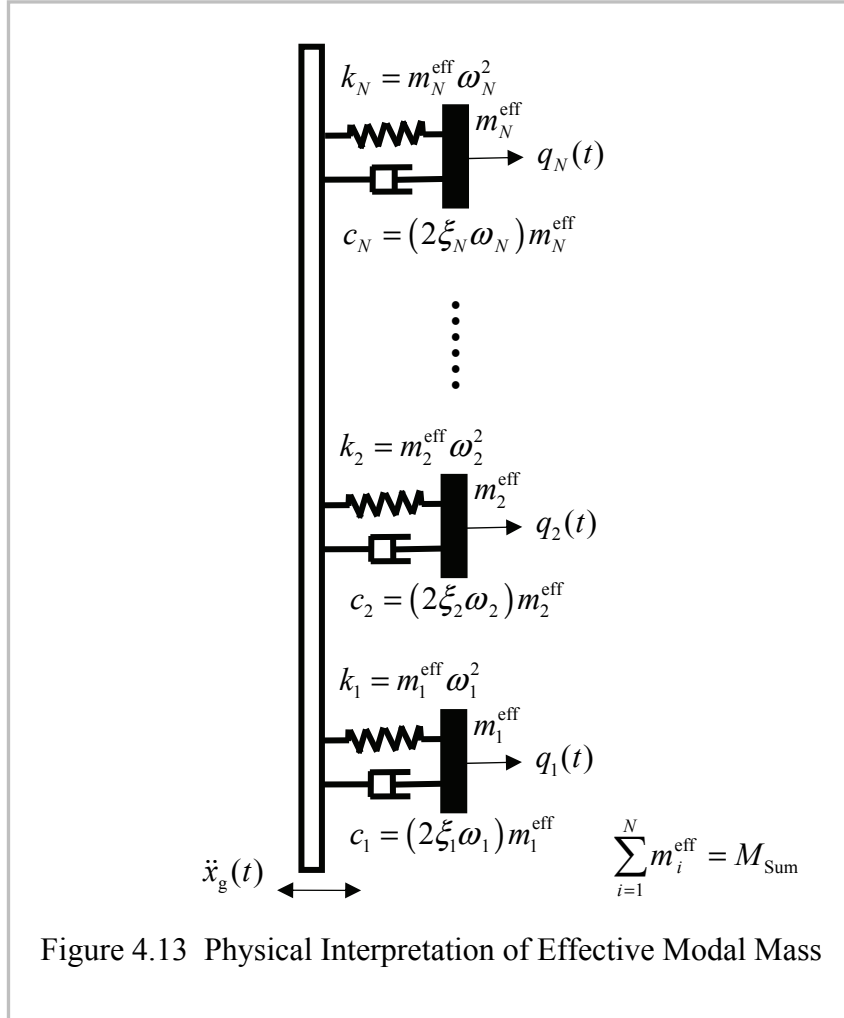


Figure 4.13 Physical Interpretation of Effective Modal Mass

In earthquake engineering,  $m_i^{\text{eff}}$  (or effective modal weight  $W_i^{\text{eff}} = m_i^{\text{eff}} g$ ) is used by many codes for evaluating the significance and importance of each real mode to structural base shear estimation (Clough and Penzien 1993, BSSC 2003 and Ramirez et al. 2000). It has also been noticed in these literatures that  $m_i^{\text{eff}}$  has mass dimension and the summation for all modes (under-damped system without over-damped modes) equals to the total structural mass. From Equation (4.145), which is developed based on current general coordinate transformation matrix and modal coordinates definition proposed, it is much easier to understand the role of  $m_i^{\text{eff}}$  which is used as a criterion for modal significance.  $m_i^{\text{eff}}$  is not only useful for structural base shear estimation, but is also important to other type of structural responses in earthquake engineering. This concept of effective modal mass has been studied and applied in other fields for dynamic analysis and design for

classically damped linear structural systems subjected by base excitations (Sedaghati et al. 2003 and Girard and Imbert 1991). However, no one has used the approach that is same as that proposed in this report to clarify the relationships among coordinates transformation, modal response analysis and physical interpretation.

#### 4.8.2 Reduction of Modal Responses to Initial Conditions

When the modal shapes are real vectors, the terms in Equations (4.69) and (4.70) can be simplified as

$$\text{Im}\left(\frac{\lambda_i \boldsymbol{\varphi}_i^T \mathbf{M}}{\boldsymbol{\varphi}_i^T \mathbf{M} \mathbf{J}}\right) = \omega_{di} \frac{\boldsymbol{\varphi}_i^T \mathbf{M}}{\boldsymbol{\varphi}_i^T \mathbf{M} \mathbf{J}} \in \mathbb{R}^N \quad (4.147)$$

$$\text{Im}\left(\frac{\boldsymbol{\varphi}_i^T \mathbf{K}}{\boldsymbol{\varphi}_i^T \mathbf{M} \mathbf{J}}\right) = \mathbf{0} \in \mathbb{R}^N \quad (4.148)$$

$$\text{Im}\left(\frac{\boldsymbol{\varphi}_i^T \mathbf{M}}{\boldsymbol{\varphi}_i^T \mathbf{M} \mathbf{J}}\right) = \mathbf{0} \in \mathbb{R}^N \quad (4.149)$$

$$\text{Im}\left(\frac{\boldsymbol{\varphi}_i^T \mathbf{K}}{\lambda_i \boldsymbol{\varphi}_i^T \mathbf{M} \mathbf{J}}\right) = -\frac{\sqrt{1-\xi_i^2} \boldsymbol{\varphi}_i^T \mathbf{K}}{\omega_i (\boldsymbol{\varphi}_i^T \mathbf{M} \mathbf{J})} \in \mathbb{R}^N \quad (4.150)$$

Thus, Equations (4.69) and (4.70) become

$$\dot{q}_{0i} = \left(\frac{\boldsymbol{\varphi}_i^T \mathbf{M}}{\boldsymbol{\varphi}_i^T \mathbf{M} \mathbf{J}}\right) \dot{\mathbf{x}}_0 \in \mathbb{R} \quad (4.151)$$

and

$$q_{0i} = \left(\frac{\boldsymbol{\varphi}_i^T \mathbf{K}}{\omega_i^2 (\boldsymbol{\varphi}_i^T \mathbf{M} \mathbf{J})}\right) \mathbf{x}_0 \in \mathbb{R} \quad (4.152)$$

The above results show that, for a real mode, the initial modal velocity only depends on  $\dot{\mathbf{x}}_0$  and initial modal displacement only depends on  $\mathbf{x}_0$  regardless of the formats of initial condition vectors  $\dot{\mathbf{x}}_0$  and  $\mathbf{x}_0$ . Equation (4.71) for calculating the initial over-

damped modal displacement remains the same. In addition, the formulas for evaluating the modal responses subjected to initial modal conditions for each mode remain the same as Equations (4.88), (4.89) and (4.92) for real under-damped modes and over-damped modes, respectively. If  $\mathbf{x}_0$  and  $\dot{\mathbf{x}}_0$  are determined by Equations (4.77) and (4.81) for a classically-damped system, the formats of Equations (4.85) to (4.87) as well as Equations (4.90), (4.91) and (4.93) will also remain the same.

### 4.8.3 Reduction of Energy Integral

Considering Equations (4.142) and (4.143) for classically damped systems, the energy integral shown in Equations (4.104) and (4.105) as (with non-zero initial modal conditions)

$$\begin{aligned} E_{Ci} &= m_i^{\text{eff}} \int_0^t (\ddot{q}_i + 2\xi_i \omega_i \dot{q}_i + \omega_i^2 q_i) \dot{q}_i dt \\ &= m_i^{\text{eff}} \left[ \frac{1}{2} \dot{q}_i^2(t) + \omega_i^2 \frac{1}{2} q_i^2(t) - \frac{1}{2} \dot{q}_{0i}^2 - \omega_i^2 \frac{1}{2} q_{0i}^2 + 2\xi_i \omega_i \int_0^t \dot{q}_i^2 dt \right] \in \mathbb{R} \end{aligned} \quad (4.153)$$

$$\begin{aligned} E_{Ci}^{\text{In}} &= -m_i^{\text{eff}} \int_0^t \ddot{x}_g \dot{q}_i dt \\ &= m_i^{\text{eff}} \left[ \frac{1}{2} \dot{q}_i^2(t) + \omega_i^2 \frac{1}{2} q_i^2(t) - \frac{1}{2} \dot{q}_{0i}^2 - \omega_i^2 \frac{1}{2} q_{0i}^2 + 2\xi_i \omega_i \int_0^t \dot{q}_i^2 dt \right] \in \mathbb{R} \end{aligned} \quad (4.154)$$

For over-damped modes, Equations (4.106) and (4.107) remain the same format, in which, if the initial modal conditions are not zero,

$$E_{Pi} = \frac{(\boldsymbol{\Phi}_i^p \mathbf{M} \mathbf{J})^2}{a_i^p} \int_0^t (\dot{q}_i^p)^2 dt + \frac{1}{2} \frac{(\boldsymbol{\Phi}_i^p \mathbf{M} \mathbf{J})^2}{a_i^p} \omega_i^p [q_i^p(t)]^2 - \frac{1}{2} \frac{(\boldsymbol{\Phi}_i^p \mathbf{M} \mathbf{J})^2}{a_i^p} \omega_i^p (q_{0i}^p)^2 \in \mathbb{R} \quad (4.155)$$

In Equation (4.154), the terms  $\frac{1}{2} m_i^{\text{eff}} \dot{q}_i^2(t)$ ,  $\frac{1}{2} m_i^{\text{eff}} \omega_i^2 q_i^2(t)$ ,  $\frac{1}{2} m_i^{\text{eff}} \dot{q}_{0i}^2$ ,  $\frac{1}{2} m_i^{\text{eff}} \omega_i^2 q_{0i}^2$  and  $2\xi_i \omega_i m_i^{\text{eff}} \int_0^t \dot{q}_i^2(t) dt$  have clear physical meanings. They are real modal instant kinetic energy, instant potential energy, initial kinetic energy, initial potential energy and dissipated energy in the duration from 0 to  $t$ . From these terms, it is observed the

individual modal energy of a system can be fully represented by an equivalent SDOF system with the effective modal mass  $m_i^{\text{eff}}$ , which justifies the use of effective modal mass to determine the contribution of each mode through the energy analysis. The term  $\frac{1}{2} \frac{(\boldsymbol{\phi}_i^p \mathbf{M} \mathbf{J})^2}{\alpha_i^p} \omega_i^p (q_{0i}^p)^2$  in Equation (4.155) is initial stored energy in the energy storage unit of the first order system.

If we further assume that there are no over-damped modes in the system, utilizing Equations (3.68) and (3.69), we can simplify the expressions for system total instant kinetic energy  $E_K(t)$  and potential energy  $E_p(t)$  at time  $t$  (that are stored in all structural masses and elastic elements) and accumulated energy dissipation  $E_D(t)$  from time 0 to  $t$ ,

$$\begin{aligned} E_K(t) &= \frac{1}{2} \dot{\mathbf{x}}^T(t) \mathbf{M} \dot{\mathbf{x}}(t) = \frac{1}{2} \left[ \sum_{i=1}^N \Gamma_i \boldsymbol{\phi}_i \dot{q}_i(t) \right]^T \mathbf{M} \left[ \sum_{i=1}^N \Gamma_i \boldsymbol{\phi}_i \dot{q}_i(t) \right] \\ &= \frac{1}{2} \sum_{i=1}^N \frac{(\boldsymbol{\phi}_i \mathbf{M} \mathbf{J})^2}{m_i^2} m_i \dot{q}_i^2(t) = \sum_{i=1}^N \frac{1}{2} m_i^{\text{eff}} \dot{q}_i^2(t) = \sum_{i=1}^N E_{K_i}(t) \in \mathbb{R} \end{aligned} \quad (4.156)$$

$$\begin{aligned} E_p(t) &= \frac{1}{2} \mathbf{x}^T(t) \mathbf{K} \mathbf{x}(t) = \frac{1}{2} \left[ \sum_{i=1}^N \Gamma_i \boldsymbol{\phi}_i q_i(t) \right]^T \mathbf{K} \left[ \sum_{i=1}^N \Gamma_i \boldsymbol{\phi}_i q_i(t) \right] \\ &= \frac{1}{2} \sum_{i=1}^N \frac{\omega_i^2 (\boldsymbol{\phi}_i \mathbf{M} \mathbf{J})^2}{m_i^2} m_i q_i^2(t) = \sum_{i=1}^N \frac{1}{2} m_i^{\text{eff}} \omega_i^2 q_i^2(t) = \sum_{i=1}^N E_{p_i}(t) \in \mathbb{R} \end{aligned} \quad (4.157)$$

$$\begin{aligned} E_D(t) &= \int_0^t \dot{\mathbf{x}}^T(t) \mathbf{C} \dot{\mathbf{x}}(t) dt = \int_0^t \left[ \sum_{i=1}^N \Gamma_i \boldsymbol{\phi}_i \dot{q}_i(t) \right]^T \mathbf{C} \left[ \sum_{i=1}^N \Gamma_i \boldsymbol{\phi}_i \dot{q}_i(t) \right] dt \\ &= \int_0^t \sum_{i=1}^N \left[ 2\xi_i \omega_i m_i \frac{(\boldsymbol{\phi}_i \mathbf{M} \mathbf{J})^2}{m_i^2} \dot{q}_i^2(t) \right] dt = \sum_{i=1}^N (2\xi_i \omega_i m_i^{\text{eff}}) \int_0^t \dot{q}_i^2(t) dt \\ &= \sum_{i=1}^N E_{D_i}(t) \in \mathbb{R} \end{aligned} \quad (4.158)$$

Equations (4.156) to (4.158) show that for a classically under-damped structural system, the total kinetic energy, potential energy and energy dissipated by dampers can be decoupled. In other words, the summation of all modal kinetic energy equals to structural total kinetic energy; the summation of all modal potential energy equals to

structural total potential energy and the summation of all modal dissipated energy by equivalent modal damper equals to structural total dissipated energy by the dampers. Based on this conclusion, the intuitive physical interpretation shown in Figure 4.13 is further enhanced.

In addition, the following formulas can be easily developed. For initial kinetic energy and potential energy, we have

$$E_{0K} = \frac{1}{2} \dot{\mathbf{x}}_0^T \mathbf{M} \dot{\mathbf{x}}_0 = \sum_{i=1}^N \frac{1}{2} m_i^{\text{eff}} \dot{q}_{0i}^2 = \sum_{i=1}^N E_{0Ki} \in \mathbb{R} \quad (4.159)$$

$$E_{0P} = \frac{1}{2} \mathbf{x}_0^T \mathbf{K} \mathbf{x}_0 = \sum_{i=1}^N \frac{1}{2} m_i^{\text{eff}} \omega_i^2 q_{0i}^2 = \sum_{i=1}^N E_{0Pi} \in \mathbb{R} \quad (4.160)$$

For each mode,

$$E_{Ki}(t) + E_{Pi}(t) + E_{Di}(t) - E_{0Ki} - E_{0Pi} = -m_i^{\text{eff}} \int_0^t \ddot{x}_g \dot{q}_i dt \in \mathbb{R} \quad (4.161)$$

and the summation of energy over all modes can be expressed as

$$\begin{aligned} & \sum_{i=1}^N E_{Ki}(t) + \sum_{i=1}^N E_{Pi}(t) + \sum_{i=1}^N E_{Di}(t) - \sum_{i=1}^N E_{0Ki} - \sum_{i=1}^N E_{0Pi} \\ & = -\sum_{i=1}^N m_i^{\text{eff}} \int_0^t \ddot{x}_g(t) \dot{q}_i(t) dt = -\int_0^t \dot{\mathbf{x}}^T(t) (\mathbf{M}\mathbf{J}) \ddot{x}_g(t) dt \in \mathbb{R} \end{aligned} \quad (4.162)$$

## 4.9 Dual Modal Space Approach and Structural DOFs Reduction

### 4.9.1 Formulas Development

A structural system without supplemental dampers can still dissipate certain amount of energy either in a free vibration or in a forced vibration. The dissipated energy is commonly treated as or equivalent to linear viscous damping in earthquake engineering theoretical analysis and practical applications. In other words, before the structure is enhanced with supplemental dampers, it has certain quantity of damping. Based on practical engineering experience,  $\leq 2\%$  critical damping ratio for steel frame structures

and  $\leq 5\%$  critical damping ratios for RC structures are used for structural fundamental mode. The modal damping ratios are directly specified for the uncoupled equations of motion after real modal decomposition approach is utilized. Following this way, evaluating the original structural damping coefficient matrix  $\mathbf{C}_0$ , which is often very difficult to be determined, can be avoided. This directly assigned damping is usually termed as Wilson's damping (Bathe 1995) since which was first proposed and suggested by Wilson.

In damping design of an aseismic structure, we may need to take into consideration of Wilson's damping when calculating the total damping of the structural system in order to increase the accuracy of the structural dynamic modeling and simulation accuracy.

In addition, in damping design for new or existing building/bridge structures we usually need to first establish their dynamic models. Some popular commercially available finite element programs, such as SAP2000, ETABS and Adina, may be used for modeling the original structure without dampers added. These programs can carry out eigen-analysis (real modal analysis, ignoring damping) after the system's mass and stiffness matrices are established internally in the programs, and can further output mass matrix as well as a limited number of lower orders natural frequencies or periods and modal shapes (eigenvectors or Ritz vectors). However, the structural stiffness matrix for a complex structure is difficult to be presented and manipulated, because it could be a huge matrix for a complex structure with large DOFs. As matter of fact, the dynamic responses of a structure subjected earthquake ground motion are dominated by a few lower order modes (real, complex or over-damped modes). Thus, directly utilizing a limited number of modal analysis results, we may significantly reduce the scale of modeling and computation burden for a structure with supplemental damping.

In the following, a two-steps modal decomposition approach, which can be termed as dual modal space approach, is adopted to deal with the aforementioned issues.

First, ignoring the structural damping in the structure, we can simplify Equation (2.1) as

$$\mathbf{M}\ddot{\mathbf{x}}(t) + \mathbf{K}\mathbf{x}(t) = \mathbf{f}(t) \quad (4.163)$$



Its corresponding eigen-equation is given by

$$-\lambda_0 \mathbf{M} \boldsymbol{\varphi}_0 + \mathbf{K} \boldsymbol{\varphi}_0 = \mathbf{0} \quad (4.164)$$

where subscript “0” indicates that the eigenvalue  $\lambda_0 (= \omega_0^2 \in \mathbb{R})$  and eigenvector  $\boldsymbol{\varphi}_0 \in \mathbb{R}^N$  will be calculated for the non-damped structure. In order to solve Equation (4.164), the subspace iteration approach may be implemented for a system with large number of DOFs  $N$  (Wilson 2004 and Clough and Penzien 1993). Assuming that  $N_0 (< N$  and maybe  $\ll N$  for large  $N$ ) pairs of eigen-solutions have been obtained, the spectrum matrix  $\boldsymbol{\Lambda}_0$  and modal shape matrix  $\boldsymbol{\Phi}_0$  can be denoted as, respectively,

$$\boldsymbol{\Lambda}_0 = \text{diag}(\lambda_{01}, \lambda_{02} \cdots \lambda_{0N_0}) = \text{diag}(\omega_{01}^2, \omega_{02}^2 \cdots \omega_{0N_0}^2) \in \mathbb{R}^{N_0 \times N_0} \quad (4.165)$$

$$\boldsymbol{\Phi}_0 = [\boldsymbol{\varphi}_{01}, \boldsymbol{\varphi}_{02} \cdots \boldsymbol{\varphi}_{0N_0}] \in \mathbb{R}^{N \times N_0} \quad (4.166)$$

Since the structural mass matrix is easier to be acquired, each modal shape can be normalized with respect to its unitary modal mass, that is

$$\boldsymbol{\varphi}_{0i}^T \mathbf{M} \boldsymbol{\varphi}_{0i} = m_{0i} = 1 \quad (i = 1, 2 \cdots N_0) \quad (4.167)$$

which brings out

$$\boldsymbol{\Phi}_0^T \mathbf{M} \boldsymbol{\Phi}_0 = \mathbf{I} \in \mathbb{R}^{N_0 \times N_0} \quad (4.168)$$

and

$$\boldsymbol{\Phi}_0^T \mathbf{K} \boldsymbol{\Phi}_0 = \boldsymbol{\Lambda}_0 = \text{diag}(\omega_{01}^2, \omega_{02}^2 \cdots \omega_{0N_0}^2) \in \mathbb{R}^{N_0 \times N_0} \quad (4.169)$$

Denote  $\mathbf{C}_0$  as the inherent damping coefficient matrix of the original structure.  $\mathbf{C}_0$  may not be expressed explicitly. However, it must generate small damping ratios that can be assumed as classical damping. This means that modal shape matrix  $\Phi_0$  can be used to decouple  $\mathbf{C}_0$ . Thus,

$$\begin{aligned}
\Phi_0^T \mathbf{C}_0 \Phi_0 &= \tilde{\mathbf{C}}_0 \\
&= \text{diag} \left( 2\xi_{01} \omega_{01} m_{01}, 2\xi_{02} \omega_{02} m_{02} \cdots 2\xi_{0N_0} \omega_{0N_0} m_{0N_0} \right) \\
&= \text{diag} \left( 2\xi_{01} \omega_{01}, 2\xi_{02} \omega_{02} \cdots 2\xi_{0N_0} \omega_{0N_0} \right) \in \mathbb{R}^{N_0 \times N_0}
\end{aligned} \tag{4.170}$$

where  $\xi_{0i}$  ( $i = 1, 2 \cdots N_0$ ) is the  $i$ th modal damping ratio that the original structure holds inherently. As mentioned earlier, the values of  $\xi_{0i}$  ( $i = 1, 2 \cdots N_0$ ) can be directly specified as Wilson's damping.

Now supposing supplemental linear viscous dampers are added to the structure, we can easily establish the corresponding damping coefficient matrix  $\mathbf{C}_s$  based on the predetermined damper configurations (related to installation locations and angles with respect to the DOFs) in the structure. For the sake of simplicity in introducing the principle of the proposed theory, no extra DOFs and masses as well as stiffness changes are further assumed. Thus, matrix  $\mathbf{M}$  and  $\mathbf{K}$  remain the same, while the complete damping matrix is given by

$$\mathbf{C} = \mathbf{C}_0 + \mathbf{C}_s \tag{4.171}$$

where  $\mathbf{C}$  may or may not satisfy the Caughey criterion and may or may not bring out the over-damped modes.

Taking first step of modal coordinates transformation,

$$\mathbf{x}(t) = \Phi_0 \tilde{\mathbf{x}}(t) \in \mathbb{R}^N \tag{4.172}$$

where  $\tilde{\mathbf{x}}(t)$  is the modal response vector in the original structural real modal space (the first modal space) and

$$\tilde{\mathbf{x}}(t) = (\tilde{x}_1, \tilde{x}_2 \cdots \tilde{x}_{N_0})^T \in \mathbb{R}^{N_0} \quad (4.173)$$

Note that  $\Phi_0$  is a  $N \times N_0$  dimension matrix. Thus Equation (4.172) is an incomplete and approximate linear space transformation when  $N_0 < N$ , which will transform a time-variable vector from  $N$ -dimensions complete physical space to  $N_0$ -dimensions incomplete (truncated) modal sub-space. However, the simulation results carried out by authors indicate that, if the value of  $N_0$  is set to a sufficiently large number and make sure that the summation of real modal mass ratios for modal orders from one to  $N_0$  is larger than 99.5%, the final analysis results could be accurate enough for applications from the practical point of view in earthquake engineering. The analysis results may include eigen-solutions, time history responses of interests and peak response estimations based on response spectrum analysis. Furthermore, it has been determined by the authors that this incomplete real modal transformation can even be used in nonlinear structural systems enhanced with non-linear dampers with satisfied results.

Substituting Equation (4.172) into Equation (2.1) and pre-multiplying  $\Phi_0^T$  to the both sides of the resulting equation, we have

$$\Phi_0^T \mathbf{M} \Phi_0 \ddot{\tilde{\mathbf{x}}}(t) + \Phi_0^T \mathbf{C} \Phi_0 \dot{\tilde{\mathbf{x}}}(t) + \Phi_0^T \mathbf{K} \Phi_0 \tilde{\mathbf{x}}(t) = \Phi_0^T \mathbf{f}(t) \in \mathbb{R}^{N_0} \quad (4.173)$$

Further utilizing Equations (4.168) to (4.171), Equation (4.173) becomes

$$\ddot{\tilde{\mathbf{x}}}(t) + \tilde{\mathbf{C}}(t) \dot{\tilde{\mathbf{x}}}(t) + \Lambda_0 \tilde{\mathbf{x}}(t) = \tilde{\mathbf{f}}(t) \in \mathbb{R}^{N_0} \quad (4.174)$$

where  $\tilde{\mathbf{C}}$  is the damping matrix expressed in the first modal space and

$$\tilde{\mathbf{C}} = \tilde{\mathbf{C}}_0 + \Phi_0^T \mathbf{C}_s \Phi_0 \in \mathbb{R}^{N_0 \times N_0} \quad (4.175)$$

$\tilde{\mathbf{f}}(t)$  is a general force vector and  $\tilde{\mathbf{f}}(t) = \Phi_0^T \mathbf{f}(t)$ . If  $\mathbf{f}(t)$  is introduced by seismic motion,  $\tilde{\mathbf{f}}(t)$  can be rewritten as

$$\tilde{\mathbf{f}}(t) = -(\Phi_0^T \mathbf{M} \mathbf{J}) \ddot{\mathbf{x}}_g(t) \in \mathbb{R}^{N_0} \quad (4.176)$$

From the above formation and Equation (4.174), we can see that the matrices  $\mathbf{K}$  and  $\mathbf{C}_0$  for the original structure are not directly involved.

The format of Equations (4.174) and (2.1) are similar with a few differences, such as, (a) the scale of Equation (4.174) is reduced. If  $N_0 \ll N$ , the reduction may be significant; (b) the mass and stiffness matrix is normalized as a unitary matrix and a diagonalized spectrum matrix, respectively; (c)  $\tilde{\mathbf{C}}$ ,  $\tilde{\mathbf{x}}(t)$ ,  $\dot{\tilde{\mathbf{x}}}(t)$ ,  $\ddot{\tilde{\mathbf{x}}}(t)$  and  $\tilde{\mathbf{f}}(t)$  are general damping matrix, modal displacement response, velocity response and acceleration response vectors as well as general applied force vector, which do not have explicit meaning in the original physical space. However, mathematically speaking, for both equations, the consequent complex modal (over-damped modes may appear) analysis procedure and related formulas that will be used for further dynamic solutions remain the same. For example, in parallel to Equations (2.3), the consequent coefficient matrices and vectors in the corresponding state space will be

$$\tilde{\mathbf{A}} = \begin{pmatrix} \mathbf{0} & \mathbf{I} \\ \mathbf{I} & \tilde{\mathbf{C}} \end{pmatrix} \in \mathbb{R}^{2N_0 \times 2N_0} \quad (4.177)$$

$$\tilde{\mathbf{B}} = \begin{pmatrix} -\mathbf{I} & \mathbf{0} \\ \mathbf{0} & \Lambda_0 \end{pmatrix} \in \mathbb{R}^{2N_0 \times 2N_0} \quad (4.178)$$

$$\tilde{\mathbf{y}}(t) = \begin{Bmatrix} \dot{\tilde{\mathbf{x}}}(t) \\ \tilde{\mathbf{x}}(t) \end{Bmatrix} \in \mathbb{R}^{2N_0} \quad (4.179)$$

$$\tilde{\mathbf{f}}_s(t) = \begin{Bmatrix} \mathbf{0} \\ \tilde{\mathbf{f}}(t) \end{Bmatrix} \in \mathbb{R}^{2N_0} \quad (4.180)$$

After solving the corresponding eigen-problem, we have the following second modal space transformation

$$\tilde{\mathbf{y}}(t) = \begin{Bmatrix} \dot{\tilde{\mathbf{x}}}(t) \\ \tilde{\mathbf{x}}(t) \end{Bmatrix} = \tilde{\Psi} \tilde{\mathbf{z}}(t) = \begin{pmatrix} \tilde{\Phi} \tilde{\Lambda} \\ \tilde{\Phi} \end{pmatrix} \tilde{\mathbf{z}}(t) \quad (4.181)$$

where  $\tilde{\Psi} \in \mathbb{C}^{2N_0 \times 2N_0}$ ,  $\tilde{\Phi} \in \mathbb{C}^{N_0 \times 2N_0}$ ,  $\tilde{\Lambda} \in \mathbb{C}^{2N_0 \times 2N_0}$  and  $\tilde{\mathbf{z}}(t) \in \mathbb{C}^{2N_0}$  are complex eigenvector matrix, complex modal shape matrix, complex diagonalized spectrum matrix and complex modal response vector in the second modal space. Equation (4.181) can be used to further decouple the Equation (4.174). As one of the results, we can obtain structural relative displacement response vector in original physical space, after  $\tilde{\mathbf{z}}(t)$  has been solved and Equations (4.172) and (4.181) are used,

$$\mathbf{x}(t) = \tilde{\Phi}_0 \tilde{\mathbf{x}}(t) = \tilde{\Phi}_0 \tilde{\Phi} \tilde{\mathbf{z}}(t) \in \mathbb{R}^N \quad (4.182)$$

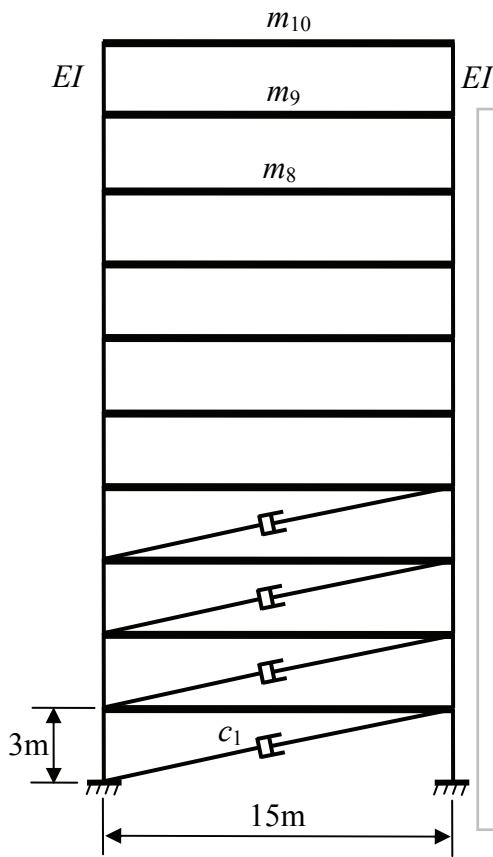
Note that the complex modal responses in the second modal space can be expressed in other format with real numbers, instead of complex numbers, whose method and further analysis procedure is exactly the same as what are introduced in Chapter 2 and Chapter 3.

#### 4.9.2 Numerical Example

Figure 4.14 shows a 10-story planar shear frame structure model (10 DOFs) and major structural parameters. For simplicity, the original structural inherent damping is assumed as proportional damping instead of directly assigning Wilson's damping to each mode. The inherent damping coefficient matrix is given by  $\mathbf{C}_0 = 0.2002\mathbf{M} + 0.0019\mathbf{K}$ . Based on these structural parameters, the original structural modal parameters can be obtained and are listed in Table 4.2

Table 4.2 Original Structural Modal Parameters

Mode #	1	2	3	4	5	6	7	8	9	10
Period (Sec.)	0.7672	0.2577	0.1569	0.1147	0.0920	0.0782	0.0694	0.0636	0.0600	0.0580
Natural Freq.(Hz)	1.3034	3.8812	6.3723	8.7210	10.875	12.786	14.411	15.715	16.667	17.247
Damping (100%)	2.0000	2.7272	4.0537	5.3883	6.6378	7.7566	8.7127	9.4816	10.044	10.387



**Main Structural Parameters:**

Number of Stories: 10

Number of Bays: 1

Story Height:  $H = 3$  (m)

Bay Width:  $L = 15$  (m)

Column: I Beam -- W36X300

Material: Steel,  $E = 1.999E+11$  (N/m<sup>2</sup>)

Inertial Moment of Section:  $I = 8.449E-3$  (m<sup>4</sup>)

Lumped Mass for Each Floor:  $m_i = 5.0E+05$  (Kg)

Inter-story Stiffness:  $k = 2 \frac{12EI}{L^3} = \frac{24EI}{L^3}$  (N/m)

Figure 4.14, 10-Story Shear Frame Structure Model (10 DOFs)

Now four supplemental linear viscous dampers are added to the structure, as shown in Figure 4.14, and the damper parameters are  $c_1 = c_2 = c_3 = c_4 = c$ , where  $c = 2.74\text{E}+07$  (N.s/m). Considering damper installation configuration, all effective damping coefficients for supplemental dampers become  $c \cos^2 [\text{tg}^{-1}(H/L)] = 0.9615c$ . After carrying out eigen-analysis for structural system supplemented with four dampers, we can obtain complete and exact complex modal parameters (without over-damped modes developed), which will be compared with those estimated by using dual modal space approach.

Tables 4.3 lists estimated modal period results and error comparison, while Table 4.4 lists the results and error comparison for damping ratios. In the tables, reserved modal number means that the real lower order modes (calculated only from  $\mathbf{M}$  and  $\mathbf{K}$ ) less than or equal to this number ( $N_0 \leq N = 10$ ) are used to establish the first modal space. From Table 4.3, we can see that, when  $N_0$  changes from 1 to 10, the period for each complex mode, except the mode #  $N_0$  for partial cases (when  $N_0 = 3, 4, 5, 6$  and  $8$ ) is estimated with good accuracy. Observed from the results listed in Table 4.4, we can find that the estimation accuracy for damping ratios is not as good as for periods. However, the results for the complex modes with orders much less than  $N_0$  still have acceptable estimation accuracy. Preliminary numerical simulation experience learned by the authors shows that when using dual modal space approach, if we want to obtain sufficiently accurate estimation results for the lower orders of modal parameters, say, the orders up to  $N'$ , the real modal orders have to be satisfy  $N_0 \geq 1.5N'$ . Based on this criterion and when we further use the estimated modal parameters (including modal shapes either for complex modes or over-damped modes) for generally damped system to evaluate the structural responses to seismic acceleration excitations, the result accurate may be ensured. The issue about how to determine  $N'$  will be introduced in details in the next chapter.

Table 4.3 Modal Periods Estimation Results and Error Comparison

Reserved Mode Number		1		2		3		4		5	
Mode #	Exact Value (Sec.)	Est. (Sec.)	Error (100%)	Est. (Sec.)	Error (100%)	Est. (Sec.)	Error (100%)	Est. (Sec.)	Error (100%)	Est. (Sec.)	Error (100%)
1	0.7653	0.7672	0.2502	0.7657	0.0554	0.7657	0.0514	0.7655	0.0328	0.7654	0.0211
2	0.2564			0.2582	0.7014	0.2564	0.0295	0.2563	0.0030	0.2564	0.0072
3	0.1477			0.1580	6.9843	0.1475	0.1447	0.1490	0.9131		
4	0.1101			0.1229	11.640	0.1095	0.5663				
5	0.0965			0.1022	5.9100						
6	0.0749										
7	0.0740										
8	0.0642										
9	0.0609										
10	0.0589										

– Continued

Reserved Mode Number		6		7		8		9		10	
Mode #	Exact Value (Sec.)	Est. (Sec.)	Error (100%)	Est. (Sec.)	Error (100%)	Est. (Sec.)	Error (100%)	Est. (Sec.)	Error (100%)	Est. (Sec.)	Error (100%)
1	0.7653	0.7654	0.0204	0.7654	0.0107	0.7654	0.0091	0.7653	0.0059	0.7653	0.0000
2	0.2564	0.2563	0.0088	0.2563	0.0034	0.2563	0.0023	0.2563	0.0035	0.2564	0.0000
3	0.1477	0.1482	0.3620	0.1479	0.1450	0.1481	0.2700	0.1477	0.0328	0.1477	0.0000
4	0.1101	0.1088	1.1989	0.1103	0.1482	0.1075	2.3260	0.1099	0.1676	0.1101	0.0000
5	0.0965	0.0922	4.4245	0.0961	0.3614	0.0958	0.6733	0.0958	0.6771	0.0965	0.0000
6	0.0749	0.0877	17.108	0.0766	2.3165	0.0727	2.8974	0.0743	0.7798	0.0749	0.0000
7	0.0740			0.0753	1.7572	0.0725	2.0782	0.0708	4.3127	0.0740	0.0000
8	0.0642			0.0716	11.512	0.0663	3.2440	0.0642	0.0000		
9	0.0609			0.0637	4.5347	0.0609	0.0000				
10	0.0589			0.0589	0.0000						



Table 4.4 Damping Ratio Estimation Results and Error Comparison

Reserved Mode Number		1		2		3		4		5	
Mode #	Exact Value (100%)	Est. (100%)	Error (100%)	Est. (100%)	Error (100%)	Est. (100%)	Error (100%)	Est. (100%)	Error (100%)	Est. (100%)	Error (100%)
1	6.8781	6.8751	0.0436	6.8773	0.0113	6.8754	0.0389	6.8779	0.0036	6.8770	0.0162
2	9.6827			9.8737	1.9730	9.8075	1.2893	9.7029	0.2090	9.7138	0.3207
3	12.1020			16.826	39.032	13.906	14.903	13.095	8.2026		
4	40.0778			29.412	26.613	40.646	1.4167				
5	12.4341			16.747	34.686						
6	10.6576										
7	79.2850										
8	10.3708										
9	99.8543										
10	10.4459										

– Continued

Reserved Mode Number		6		7		8		9		10	
Mode #	Exact Value (100%)	Est. (100%)	Error (100%)	Est. (100%)	Error (100%)	Est. (100%)	Error (100%)	Est. (100%)	Error (100%)	Est. (100%)	Error (100%)
1	6.8781	6.8775	0.0093	6.8779	0.0027	6.8776	0.0082	6.8781	0.0003	6.8781	0.0000
2	9.6827	9.7049	0.2296	9.6922	0.0986	9.6943	0.1198	9.6880	0.0549	9.6827	0.0000
3	12.102	13.279	9.7252	12.560	3.7801	12.559	3.7739	12.387	2.3540	12.102	0.0000
4	40.078	31.118	22.357	38.070	5.0106	38.624	3.6286	38.493	3.9538	40.078	0.0000
5	12.434	13.883	11.654	13.482	8.4269	14.646	17.790	12.903	3.7693	12.434	0.0000
6	10.658	49.439	363.88	70.989	566.09	80.217	652.67	10.839	1.7042	10.658	0.0000
7	79.285			12.326	84.453	12.727	83.948	69.858	11.891	79.285	0.0000
8	10.371			27.765	167.72	84.753	717.23	10.371	0.0000		
9	99.854			10.406	89.579	99.854	0.0000				
10	10.446			10.446	0.0000						



## CHAPTER 5

### TRUNCATION OF MODES

#### 5.1 Introduction

When using the modal superposition method, the response contributions of all modes should be included to achieve the exact result. However, experience suggests that a limited amount of modes can usually provide sufficiently accurate results. The number of modes required is well defined in the case of classical damping using of the cumulative effective modal mass. The most common criterion used is the “90% rule for participating mass” specified in many design codes (IBC 2003). For the generally damped systems with or without over-damped modes, similar criteria have not been well addressed. This issue is considered in this chapter. First, the formulation of the effective modal mass and its physical interpretation in classically damped systems is briefly reviewed. Then, a general effective modal mass is formulated in a manner which has a parallel physical interpretation as in the classically damped systems. In addition, examples are given to demonstrate the applicability of the newly formulated general effective modal mass for the determination of the number of modes required in the modal superposition.

#### 5.2 Effective Modal Mass for Classically Damped Systems w/o Over-Damped Modes

The definition of the effective modal mass discussed in this section mainly follows the work given in Chopra (2001). It is briefly reviewed to facilitate the subsequent formulation of the general effective modal mass. The equation of motion governing the response of a planar  $N$ -DOFs multistory frame as shown in Figure 5.1 due to earthquake induced ground motion,  $\ddot{x}_g(t)$ , is shown in Equation (4.95). For a classically damped system, it possesses normal modes, which are re-denoted as  $\phi_i \in \mathbb{R}^N$  in order to distinguish them from complex modes in the discussion. The spatial distribution of the effective earthquake force is defined by  $\mathbf{s} = \mathbf{M}\mathbf{J}$  and it is loosely referred to as force vector although it has a unit of mass or can be considered as force vector produced by

unitary ground motion acceleration by letting  $\ddot{x}_g(t) = 1$ . Further, it can be expanded as a summation of the modal inertia force distribution  $\mathbf{s}_i$

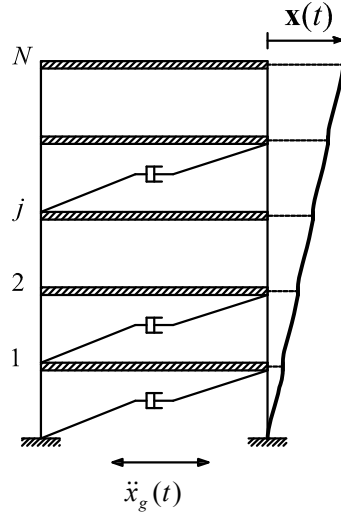


Figure 5.1 A planar  $N$ -DOFs multistory frame

$$\mathbf{s} = \mathbf{M}\mathbf{J} = \sum_{i=1}^N \mathbf{s}_i = \sum_{i=1}^N \mathbf{M}\boldsymbol{\phi}_i \Gamma_i \quad (5.1)$$

where

$$\Gamma_i = \frac{\boldsymbol{\phi}_i^T \mathbf{M}\mathbf{J}}{\boldsymbol{\phi}_i^T \mathbf{M}\boldsymbol{\phi}_i} \quad (5.2)$$

is the  $i$ th modal participation factor defined for classically damped systems. As a result, the contribution of the  $i$ th mode to the structural displacement vector  $\mathbf{x}(t)$  can be expressed by

$$\mathbf{x}_i(t) = \Gamma_i \boldsymbol{\phi}_i \frac{A_i(t)}{\omega_i^2} \quad (5.3)$$

where  $A_i(t)$  is the over-damped acceleration response of a SDOF system with the  $i$ th modal damping ratio and the  $i$ th circular frequency subjected to  $\ddot{x}_g(t)$ . Consequently, the  $i$ th modal response contribution  $r_i(t)$  to any response quantity  $r(t)$  can be determined by the static analysis of the structure combined with the dynamic response,  $A_i(t)$ , of the corresponding SDOF. That is,

$$r_i(t) = r_i^{\text{st}} A_i(t) \quad (5.4)$$

where  $r_i^{\text{st}}$  denotes the modal static response due to external force  $\mathbf{s}_i$ . This is explained schematically in Figure 5.2. The base shear due to the  $i$ th mode is obtained by specializing Equation (5.4) for  $V_{bi}$ :

$$V_{bi}(t) = V_{bi}^{\text{st}} A_i(t) \quad (5.5)$$

in which  $V_{bi}^{\text{st}}$  is the base shear force due to the applied force  $\mathbf{s}_i$  as shown in Figure 5.2 and it can be expressed as

$$V_{bi}^{\text{st}} = \sum_{j=1}^N s_{ji} = \mathbf{J}^T \mathbf{s}_i = \frac{(\boldsymbol{\phi}_i^T \mathbf{M} \mathbf{J})^2}{\boldsymbol{\phi}_i^T \mathbf{M} \boldsymbol{\phi}_i} \quad (5.6)$$

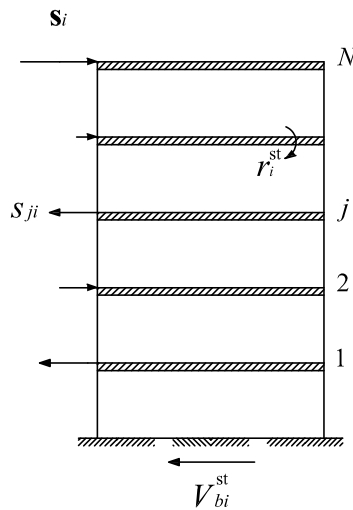


Figure 5.2 Illustration of the static structural response subjected to  $\mathbf{s}_i$

where  $s_{ji}$  is the  $j$ th component of the  $i$ th external force  $\mathbf{s}_i$ . Equation (5.6) is also recognized as the base shear effective modal mass for a classically damped system or, for brevity, effective modal mass, which can be re-denoted as

$$m_i^{\text{eff}} = \frac{(\boldsymbol{\phi}_i^T \mathbf{M} \mathbf{J})^2}{\boldsymbol{\phi}_i^T \mathbf{M} \boldsymbol{\phi}_i} \geq 0 \quad \in \mathbb{R} \quad (5.6a)$$

Equation (5.6a) is exactly identical to Equation (4.146). In Chapter 4, the effective mass has been introduced by using modal coordinate transformation approach and its complete physical interpretation has also been given in details.

It can be proved that the sum of all effective modal masses is equal to the total mass of the system (Chopra 2001 pp.524 and Clough and Penzien 1993 pp.627).

As a result, Equation (5.5) can be written as nature

$$V_{br}(t) = m_i^{\text{eff}} A_i(t) \in \mathbb{R} \quad (5.7)$$

Equation (5.7) indicates that only the portion  $m_i^{\text{eff}}$  of the total mass of the system is responding to the earthquake in each mode. Therefore, the effective modal mass  $m_i^{\text{eff}}$  is commonly used as a criterion to determine how many modes should be included in the modal superposition, e.g. the 90% rule of the participating mass specified in most seismic design codes. The preceding formulation states that the effective modal mass for mode  $i$  is equivalent to the static base shear force due to the external force  $\mathbf{s}_i$ . This implies that the 90% rule used to determine the number of modes required in the analysis can only guarantee the base shear force under static external force is less than 10% error. For other response quantity, the error may exceed 10%. In addition, the modal response is also affected by the dynamic response term  $A_i(t)$ , which means that even a sufficient number of modes are included to achieve the 90% of the total static response, the error in the dynamic response may exceed 10%. Nevertheless, the effective modal mass is still accepted in engineering practice as a reasonable modal truncation index for its simplicity. Especially, to improve the response analysis accuracy under the condition that no extra

significant computation burden is added, the summation of effective modal mass ratio should be reached as high as possible, say, up to 99%.

### 5.3 Effective Modal Mass for Generally Damped Systems

The section presents two manners to derive the effective modal mass for a generally damped linear system. Manner 1 follows a similar concept in the derivation of the effective modal mass in the classically damped systems. Manner 2 is formulated based on the modal expansion of the inverse of the mass matrix, which can be referred to Section 2.7.1.

#### *Manner 1*

In light of the preceding explanation, we only consider the portion of the static response as a manner to define the effective modal mass. Thus, the central idea here is to expand the inertia force distribution  $\mathbf{s} = \mathbf{M}\mathbf{J}$  in terms of the complex modal shapes possessed by the generally damped systems for each mode as represented by  $\mathbf{s}_i$ . This expanded  $\mathbf{s}_i$  is therefore applied to the structure and the resulting static base shear force will be regarded as the effective modal mass of the  $i$ th mode. To do so, let us calculate the static displacement vector, denoted as  $\mathbf{x}_0$ , of the systems subjected to the inertia force distribution  $\mathbf{s} = \mathbf{M}\mathbf{J}$ . Consequently, the static displacement vector  $\mathbf{x}_0$  is

$$\mathbf{x}_0 = \mathbf{K}^{-1}\mathbf{M}\mathbf{J} \in \mathbb{R}^N \quad (5.8)$$

Substituting the expansion of  $\mathbf{K}^{-1}$  shown in Equation (2.67) into Equation (5.8) gives

$$\mathbf{x}_0 = -2 \sum_{i=1}^{N_c} \text{Re} \left( \frac{\boldsymbol{\varphi}_i \boldsymbol{\varphi}_i^T \mathbf{M}\mathbf{J}}{\lambda_i a_i} \right) - \sum_{i=1}^{N_p} \frac{\boldsymbol{\varphi}_i^p (\boldsymbol{\varphi}_i^p)^T \mathbf{M}\mathbf{J}}{\lambda_i^p a_i^p} \quad (5.9)$$

Equation (5.9) states that the static displacement contributed from the  $i$ th complex mode (including its conjugate part),  $\mathbf{x}_{0i}$ , can be written as

$$\mathbf{x}_{0i} = -2 \operatorname{Re} \left( \frac{\boldsymbol{\varphi}_i \boldsymbol{\varphi}_i^T \mathbf{M} \mathbf{J}}{\lambda_i a_i} \right) \in \mathbb{R}^N \quad (5.10)$$

Also, the static displacement contributed from the  $i$ th over-damped mode,  $\mathbf{x}_{0i}^p$ , can be expressed as

$$\mathbf{x}_{0i}^p = -\frac{\boldsymbol{\varphi}_i^p (\boldsymbol{\varphi}_i^p)^T \mathbf{M} \mathbf{J}}{\lambda_i^p a_i^p} \in \mathbb{R}^N \quad (5.11)$$

Therefore, the contribution of the  $i$ th complex mode to the vector  $\mathbf{s} = \mathbf{M} \mathbf{J}$  is

$$\mathbf{s}_i = \mathbf{K} \mathbf{x}_{0i} = -2 \operatorname{Re} \left( \frac{\mathbf{K} \boldsymbol{\varphi}_i \boldsymbol{\varphi}_i^T \mathbf{M} \mathbf{J}}{\lambda_i a_i} \right) \in \mathbb{R}^N \quad (5.12)$$

and the contribution of the  $i$ th over-damped mode to the vector  $\mathbf{s} = \mathbf{M} \mathbf{J}$  is

$$\mathbf{s}_i^p = \mathbf{K} \mathbf{x}_{0i}^p = -\frac{\mathbf{K} \boldsymbol{\varphi}_i^p (\boldsymbol{\varphi}_i^p)^T \mathbf{M} \mathbf{J}}{\lambda_i^p a_i^p} \in \mathbb{R}^N \quad (5.13)$$

Summation of Equations (5.12) and (5.13) over modes gives the expansion of the  $\mathbf{s} = \mathbf{M} \mathbf{J}$ . The concept of this expansion is illustrated schematically in Figure 5.3. As a result, the resulting base shear force due to the static inertia force  $\mathbf{s}_i$  is

$$\begin{aligned} V_{bi}^{\text{st}} &= \sum_{j=1}^{N_c} s_{ji} = \mathbf{J}^T \mathbf{s}_i \\ &= -2 \operatorname{Re} \left( \frac{\mathbf{J}^T \mathbf{K} \boldsymbol{\varphi}_i \boldsymbol{\varphi}_i^T \mathbf{M} \mathbf{J}}{\lambda_i a_i} \right) \\ &= -2 \operatorname{Re} \left( \frac{\boldsymbol{\varphi}_i^T \mathbf{K} \mathbf{J} \boldsymbol{\varphi}_i^T \mathbf{M} \mathbf{J}}{\lambda_i a_i} \right) \in \mathbb{R} \end{aligned} \quad (5.14)$$

The resulting base shear force due to the static inertia force  $\mathbf{s}_i^p$  is



$$\begin{aligned}
V_{bi}^{\text{Pst}} &= \sum_{j=1}^{N_p} s_{ji}^{\text{P}} = \mathbf{J}^{\text{T}} \mathbf{s}_i^{\text{P}} \\
&= - \frac{\mathbf{J}^{\text{T}} \mathbf{K} \boldsymbol{\varphi}_i^{\text{P}} (\boldsymbol{\varphi}_i^{\text{P}})^{\text{T}} \mathbf{M} \mathbf{J}}{\lambda_i^{\text{P}} a_i^{\text{P}}} \\
&= - \frac{(\boldsymbol{\varphi}_i^{\text{P}})^{\text{T}} \mathbf{K} \mathbf{J} (\boldsymbol{\varphi}_i^{\text{P}})^{\text{T}} \mathbf{M} \mathbf{J}}{\lambda_i^{\text{P}} a_i^{\text{P}}} \in \mathbb{R}
\end{aligned} \tag{5.15}$$

Thus, in parallel to the definition of the effective modal mass defined in the classically damped systems, Equation (5.14) is then defined as the general effective modal mass,  $\hat{m}_i^{\text{eff}}$ , associated with the  $i$ th complex mode (including its conjugate counterpart) and Equation (5.15) is defined as the general effective modal mass,  $\hat{m}_i^{\text{Peff}}$ , for the  $i$ th overdamped mode. These effective modal masses  $\hat{m}_i^{\text{eff}}$  and  $\hat{m}_i^{\text{Peff}}$  are then sequenced in an ascending order according to the absolute value of their corresponding eigenvalues ( $\lambda_i$  and  $\lambda_i^{\text{P}}$ ). The cumulative mass based on this sequence is used to determine how many modes will be required to reach the prescribed participation mass ratio (e.g. the 90% rule).

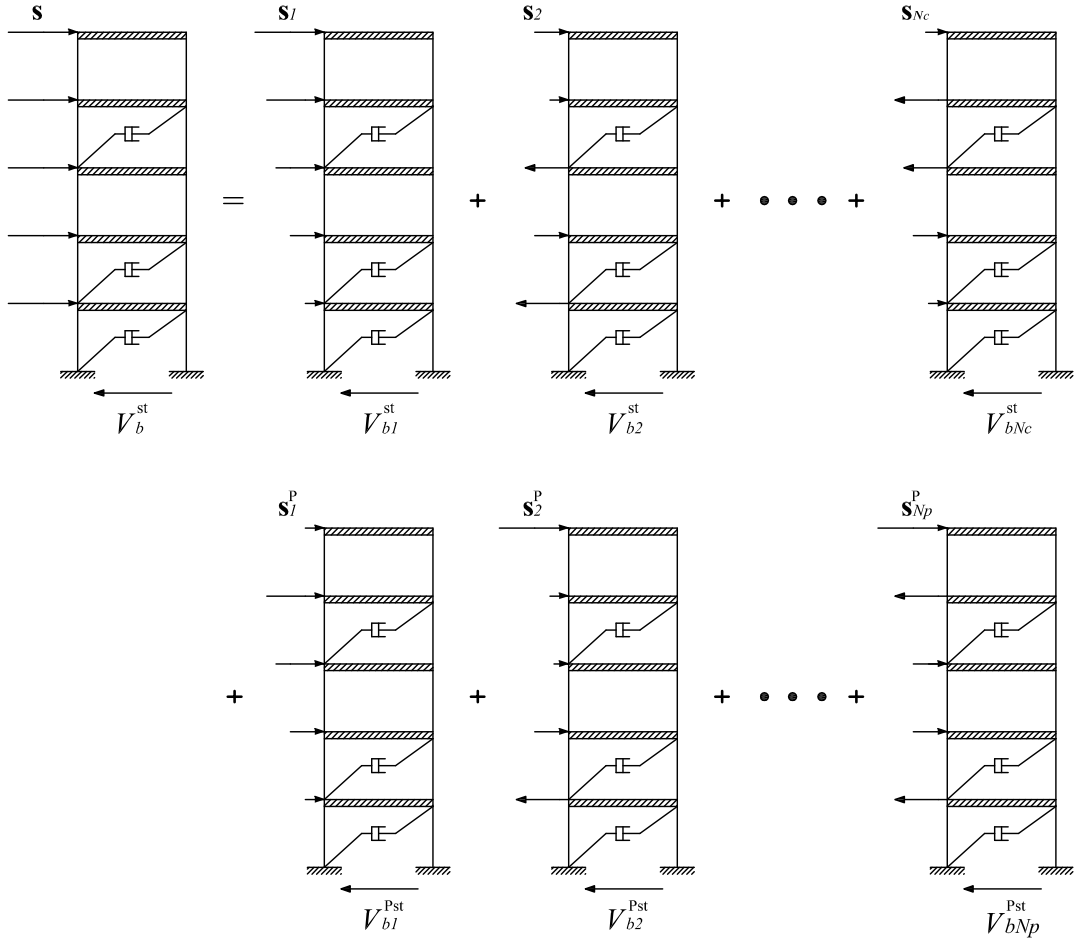


Figure 5.3 Conceptual explanation of the expansion of  $\mathbf{s} = \mathbf{MJ}$  and the resulting base shear forces

Similar to the case of classically damped systems, the sum of all general effective modal masses is equal to the total mass of the system by expressing the total mass  $M_{\Sigma}$  as

$$\sum_{i=1}^{N_c} \hat{m}_i^{\text{eff}} + \sum_{i=1}^{N_p} \hat{m}_i^{\text{Peff}} = M_{\Sigma} = \mathbf{J}^T \mathbf{M} \mathbf{J} \in \mathbb{R} \quad (5.16)$$

Equation (5.16) can be proven by recognizing that  $\hat{m}_i^{\text{eff}} = \mathbf{J}^T \mathbf{s}_i$  [Equation. (5.14)] and  $\hat{m}_i^{\text{Peff}} = \mathbf{J}^T \mathbf{s}_i^p$  [Equation.(5.15)], which implies that the sum of all effective modal mass equals to  $\mathbf{J}^T \left( \sum_{i=1}^{N_c} \mathbf{s}_i + \sum_{i=1}^{N_p} \mathbf{s}_i^p \right) = \mathbf{J}^T \mathbf{M} \mathbf{J}$ . This gives the desired result.

### Manner 2

Alternatively, the inertia force distribution  $\mathbf{s} = \mathbf{M}\mathbf{J}$  can also be expanded in another pattern different from the one derived in manner 1. First, the expansion of the inverse of the mass matrix  $\mathbf{M}^{-1}$  shown in Equation (2.50) is repeated here.

$$\begin{aligned}\mathbf{M}^{-1} &= \mathbf{\Phi} \hat{\mathbf{a}}^{-1} \mathbf{\Lambda} \mathbf{\Phi}^T \\ &= 2 \sum_{i=1}^{N_c} \text{Re} \left( \frac{\lambda_i \boldsymbol{\varphi}_i \boldsymbol{\varphi}_i^T}{a_i} \right) + \sum_{i=1}^{N_p} \frac{\lambda_i^p \boldsymbol{\varphi}_i^p (\boldsymbol{\varphi}_i^p)^T}{a_i^p} \in \mathbb{R}^{N \times N}\end{aligned}\quad (5.17)$$

Post-multiplying by  $\mathbf{M}\mathbf{J}$  in Equation (5.17) results in

$$\begin{aligned}\mathbf{J} &= \mathbf{\Phi} \hat{\mathbf{a}}^{-1} \mathbf{\Lambda} \mathbf{\Phi}^T \mathbf{M}\mathbf{J} \\ &= 2 \sum_{i=1}^{N_c} \text{Re} \left( \frac{\lambda_i \boldsymbol{\varphi}_i \boldsymbol{\varphi}_i^T \mathbf{M}\mathbf{J}}{a_i} \right) + \sum_{i=1}^{N_p} \frac{\lambda_i^p \boldsymbol{\varphi}_i^p (\boldsymbol{\varphi}_i^p)^T \mathbf{M}\mathbf{J}}{a_i^p} \in \mathbb{R}^N\end{aligned}\quad (5.18)$$

Thus the inertia force distribution  $\mathbf{s} = \mathbf{M}\mathbf{J} \in \mathbb{R}^N$  can be expanded as

$$\mathbf{s} = \mathbf{M}\mathbf{J} = \sum_{i=1}^{N_c} \mathbf{s}_i + \sum_{i=1}^{N_p} \mathbf{s}_i^p = 2 \sum_{i=1}^{N_c} \text{Re} \left( \frac{\lambda_i \mathbf{M} \boldsymbol{\varphi}_i \boldsymbol{\varphi}_i^T \mathbf{M}\mathbf{J}}{a_i} \right) + \sum_{i=1}^{N_p} \frac{\lambda_i^p \mathbf{M} \boldsymbol{\varphi}_i^p (\boldsymbol{\varphi}_i^p)^T \mathbf{M}\mathbf{J}}{a_i^p} \quad (5.19)$$

The concept illustration of this expansion is identical the one addressed in the manner 1 (see Figure 5.3). Therefore, the contribution of the  $i$ th complex mode to the vector  $\mathbf{s} = \mathbf{M}\mathbf{J}$  is

$$\mathbf{s}_i = 2 \text{Re} \left( \frac{\lambda_i \mathbf{M} \boldsymbol{\varphi}_i \boldsymbol{\varphi}_i^T \mathbf{M}\mathbf{J}}{a_i} \right) \in \mathbb{R}^N \quad (5.20)$$

and the contribution of the  $i$ th over-damped mode to the vector  $\mathbf{s} = \mathbf{M}\mathbf{J}$  is

$$\mathbf{s}_i^p = \frac{\lambda_i^p \mathbf{M} \boldsymbol{\varphi}_i^p (\boldsymbol{\varphi}_i^p)^T \mathbf{M}\mathbf{J}}{a_i^p} \in \mathbb{R}^N \quad (5.21)$$

The resulting static base shear force due to  $\mathbf{s}_i$  is defined as the  $i$ th general effective modal mass,  $\hat{m}_i^{\text{eff}}$ , associated with the  $i$ th complex mode (including its conjugate counterpart).

That is,

$$\begin{aligned}
 V_{bi}^{\text{st}} &= \hat{m}_i^{\text{eff}} \\
 &= \sum_{j=1}^N s_{ji} = \mathbf{J}^T \mathbf{s}_i \\
 &= 2 \operatorname{Re} \left( \frac{\lambda_i (\boldsymbol{\phi}_i^T \mathbf{M} \mathbf{J})^2}{a_i} \right) \in \mathbb{R}
 \end{aligned} \tag{5.22}$$

Also, the resulting static base shear force due to  $\mathbf{s}_i^{\text{p}}$  is defined as the  $i$ th general effective modal mass,  $\hat{m}_i^{\text{Peff}}$ , associated with the  $i$ th over-damped mode

$$\begin{aligned}
 V_{bi}^{\text{Pst}} &= \hat{m}_i^{\text{Peff}} \\
 &= \sum_{j=1}^N s_{ji}^{\text{p}} = \mathbf{J}^T \mathbf{s}_i^{\text{p}} \\
 &= \frac{\lambda_i^{\text{p}} [(\boldsymbol{\phi}_i^{\text{p}})^T \mathbf{M} \mathbf{J}]^2}{a_i^{\text{p}}} \in \mathbb{R}
 \end{aligned} \tag{5.23}$$

Similarly, the sum of all general effective modal masses is equal to the total mass of the system by expressing the total mass  $M_{\Sigma}$  as

$$M_{\Sigma} = \mathbf{J}^T \mathbf{M} \mathbf{J} \tag{5.24}$$

Substituting Equation (5.19) into Equation (5.24) gives

$$\begin{aligned}
 M_{\Sigma} &= \sum_{i=1}^{N_c} \mathbf{J}^T \mathbf{s}_i + \sum_{i=1}^{N_p} \mathbf{J}^T \mathbf{s}_i^{\text{p}} \\
 &= \sum_{i=1}^{N_c} \hat{m}_i^{\text{eff}} + \sum_{i=1}^{N_p} \hat{m}_i^{\text{Peff}}
 \end{aligned} \tag{5.25}$$

This completes the proof. Another alternative to prove this property shown in Equation (5.25) is to use the expansion of the total mass shown in Equation (2.70), in which the  $i$ th

term in the complex mode and the  $i$ th term in the over-damped mode are equivalent to the definition of the effective modal mass shown in Equation (5.22) and Equation (5.23), respectively. This also shows that the sum of the all general effective modal masses is equal to the total mass of the system.

It is noted that the  $\hat{m}_i^{\text{eff}}$  and  $\hat{m}_i^{\text{Peff}}$ , formulated in manner 1 and manner 2, may be positive or negative and are independent of how the mode shapes are normalized. This indicates that the summation of the general effective modal mass over modes may or may not be monotonic, although the summation contributed from all modes converges to the total mass of the system. In this study, the effective modal mass expressions derived in both manners are considered as an indicator to determine the number of modes required in the superposition. The participating mass percentage rule used in the classically damped systems still applies in the generally damped linear MDOF systems. Moreover, manner 2 is preferred and suggested because in manner 2 the structural mass matrix  $\mathbf{M}$  is used, which is much easier to be obtained in engineering practice, rather than the stiffness matrix  $\mathbf{K}$ . Table 5.1 gives a summary of the expressions of the general effective modal mass derived by manner 1 and manner 2, including the special case in which classical damping is seen.

Parallel to the definition for classically damped system, we can define effective modal mass ratios for generally damped system,  $R_{mi}$  and  $R_{mi}^{\text{P}}$ , and

$$R_{mi} = \hat{m}_i^{\text{eff}} / M_{\Sigma} \quad (5.26)$$

$$R_{mi}^{\text{P}} = \hat{m}_i^{\text{Peff}} / M_{\Sigma} \quad (5.27)$$

Based on Equations (5.16) and (5.25), following equation can be easily derived.

$$\sum_{i=1}^{N_c} R_{mi} + \sum_{i=1}^{N_p} R_{mi}^{\text{P}} = 1 \quad (5.28)$$

Table 5.1 Summary of the expressions of the effective modal mass

Effective Modal Mass	Generally Damped Systems		Classically Damped Systems
	Manner 1	Manner 2	
$\hat{m}_i^{\text{eff}}$ , Complex Mode	$-2 \operatorname{Re} \left( \frac{(\boldsymbol{\phi}_i^T \mathbf{K} \mathbf{J})(\boldsymbol{\phi}_i^T \mathbf{M} \mathbf{J})}{\lambda_i a_i} \right)$	$2 \operatorname{Re} \left( \frac{\lambda_i (\boldsymbol{\phi}_i^T \mathbf{M} \mathbf{J})^2}{a_i} \right)$	$\frac{(\boldsymbol{\phi}_i^T \mathbf{M} \mathbf{J})^2}{\boldsymbol{\phi}_i^T \mathbf{M} \boldsymbol{\phi}_i}$
$\hat{m}_i^{\text{Peff}}$ , over-damped Mode	$-\frac{[(\boldsymbol{\phi}_i^{\text{P}})^T \mathbf{K} \mathbf{J}][(\boldsymbol{\phi}_i^{\text{P}})^T \mathbf{M} \mathbf{J}]}{\lambda_i^{\text{P}} a_i^{\text{P}}}$	$\frac{\lambda_i^{\text{P}} [(\boldsymbol{\phi}_i^{\text{P}})^T \mathbf{M} \mathbf{J}]^2}{a_i^{\text{P}}}$	

When the generally damped system is reduced to classically damped system, all modal shapes become real number vector, which can be expressed as  $\boldsymbol{\phi}_i = \boldsymbol{\phi}_r \in \mathbb{R}^N$  and  $\boldsymbol{\phi}_j^{\text{P}} = \boldsymbol{\phi}_s \in \mathbb{R}^N$ , where  $i = 1, 2, \dots, N_C$  and  $j = 1, 2, \dots, N_p$  denoted for under-damped modes and over-damped modes, respectively, while  $r$  and  $s$  are denoted as one of the modes that are calculated only based on matrices  $\mathbf{M}$  and  $\mathbf{K}$ ,  $r, s \in (1, 2, \dots, N)$  (referring to Appendix B). Considering Equation (2.71a) and regarding to the manner 1, the effective modal mass defined in Equation (5.14) can be simplified as

$$\begin{aligned} \hat{m}_i^{\text{eff}} &= -2 \operatorname{Re} \left( \frac{(\mathbf{K} \boldsymbol{\phi}_r)^T \mathbf{J} \boldsymbol{\phi}_r^T \mathbf{M} \mathbf{J}}{\lambda_i a_i} \right) = -2 \operatorname{Re} \left( \frac{(\omega_i^2 \mathbf{M} \boldsymbol{\phi}_r)^T \mathbf{J} \boldsymbol{\phi}_r^T \mathbf{M} \mathbf{J}}{(-\xi_i \omega_i + j \omega_{di})(j 2 m_i \omega_{di})} \right) \\ &= \frac{(\boldsymbol{\phi}_r^T \mathbf{M} \mathbf{J})^2}{m_i} = \frac{(\boldsymbol{\phi}_r^T \mathbf{M} \mathbf{J})^2}{\boldsymbol{\phi}_r^T \mathbf{M} \boldsymbol{\phi}_r} \geq 0 \end{aligned} \quad (5.29)$$

For over-damped modes, considering Equations (2.9), (2.31) and (5.15), we have

$$\begin{aligned} \hat{m}_j^{\text{Peff}} &= \frac{(\mathbf{K} \boldsymbol{\phi}_s)^T \mathbf{J} \boldsymbol{\phi}_s^T \mathbf{M} \mathbf{J}}{\omega_j^{\text{P}} a_j^{\text{P}}} = \frac{(\omega_s^2 \mathbf{M} \boldsymbol{\phi}_s)^T \mathbf{J} \boldsymbol{\phi}_s^T \mathbf{M} \mathbf{J}}{\omega_j^{\text{P}} a_j^{\text{P}}} \\ &= \frac{\omega_s^2 (\boldsymbol{\phi}_s^T \mathbf{M} \mathbf{J})^2}{\omega_j^{\text{P}} \boldsymbol{\phi}_s^T (-\omega_j^{\text{P}} \mathbf{M} + \mathbf{C}) \boldsymbol{\phi}_s} \geq 0 \end{aligned} \quad (5.30)$$

Regarding to the manner 2, following similar way, we have

$$\hat{m}_i^{\text{eff}} = 2 \operatorname{Re} \left( \frac{(-\zeta_i \omega_i + j \omega_{di}) (\boldsymbol{\phi}_r^T \mathbf{M} \mathbf{J})^2}{a_i} \right) = \frac{(\boldsymbol{\phi}_r^T \mathbf{M} \mathbf{J})^2}{\boldsymbol{\phi}_r^T \mathbf{M} \boldsymbol{\phi}_r} \geq 0 \quad (5.31)$$

and

$$\hat{m}_j^{\text{peff}} = -\frac{\omega_j^p [(\boldsymbol{\phi}_s^T \mathbf{M} \mathbf{J})^2]}{\boldsymbol{\phi}_s^T (-\omega_j^p \mathbf{M} + \mathbf{C}) \boldsymbol{\phi}_s} \leq 0 \quad (5.32)$$

It can be easily found that Equations (5.29) and (5.31) for the real modes are identical. However, for the over-damped modes, the simplified equations shown by Equation (5.30) and (5.32) are different.

If we further assume that no over-damped modes exist in the system, all effective modal masses obtained from two manners are exactly same as those for classically under-damped system.

#### 5.4 Example

To demonstrate the applicability of the newly developed general effective mass either by manner 1 or manner 2, the 10-story building example (Figure 4.14, without over-damped modes existing) in Section 4.9 is considered. Figure 5.4 shows the cumulative effective modal mass ratios calculated by Manner 1 and Manner 2 as well as conventional cumulative effective modal mass ratio defined in classical damping cases. It is observed that, unlike the conventional cumulative effective modal mass, the newly developed general cumulative effective modal mass (either by Manner 1 or Manner 2) does not increase monotonically; however, the fluctuation ranges of the curves decrease gradually when the modal order increases. It can be predicted that for a structure with large DOFs, the fluctuation phenomena caused by using both new methods will fall into a very small range and can be ignored, as long as participating lower modal order reaches sufficient high number, say, truncated mode order  $N' = 30 (\ll N)$ . And it may be also anticipated that the higher order modes larger than  $N'$  have small contributions to the whole structural responses. This prediction may be able to be interpreted from mathematical

point of view. Regarding to a higher mode, the elements in the modal shape fluctuate significantly and, as a result, the vector inner-products  $\boldsymbol{\phi}_i^T(\mathbf{KJ})$ ,  $\boldsymbol{\phi}_i^T(\mathbf{MJ})$ ,  $(\boldsymbol{\phi}_i^p)^T(\mathbf{KJ})$  and  $(\boldsymbol{\phi}_i^p)^T(\mathbf{MJ})$ , which are used to calculate effective modal masses as major terms shown in Table 5.1, end up with very small absolute values.

When all modes are included, all curves will converge to 100% eventually.

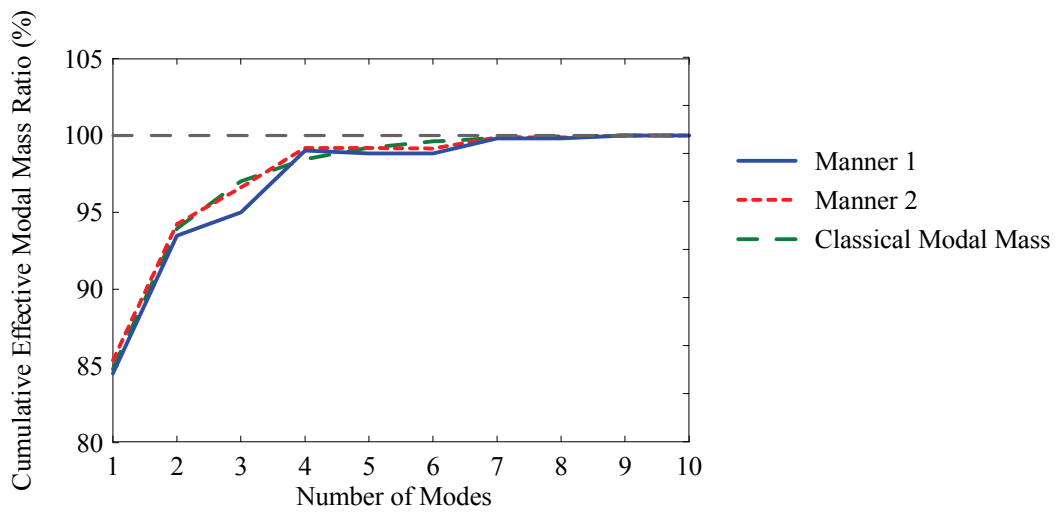


Figure 5.4 Cumulative effective modal mass



## CHAPTER 6

### RESPONSE SPECTRUM METHOD

#### 6.1 Introduction

This chapter develops a response-spectrum-based analysis procedure for the seismic responses of a generally damped linear structure. This development is in parallel with the development of the CQC rule with an extension to the consideration of the responses resulted from the over-damped modes, in which an over-damped mode response spectrum concept is introduced. For the purposes of structural design, a procedure to convert the site response spectrum to the corresponding over-damped mode response spectrum is established.

#### 6.2 Analytical Formulation

The analytical formulation of the general modal combination rule (GCQC) considering the effect of non-classical damping and over-damped modes is presented in this section. According to the general modal response analysis method formulated in Chapter 3, the responses of a generally damped linear structure subjected to single directional seismic excitation are expressed as

$$\mathbf{x}_0(t) = \sum_{i=1}^{N_C} [\mathbf{A}_{0i} \dot{q}_i(t) + \mathbf{B}_{0i} q_i(t)] + \sum_{i=1}^{N_P} [\mathbf{A}_{0i}^P q_i^P(t)] \in \mathbb{R}^N \quad (6.1)$$

where  $\mathbf{x}_0(t) = [x_{01}(t), x_{02}(t), \dots, x_{0N}(t)]^T$  represents a response vector for any response quantity of interest;  $\dot{q}_i(t)$ ,  $q_i(t)$  and  $q_i^P(t)$  are the modal displacement, velocity and over-damped mode responses, respectively.  $\mathbf{A}_{0i} \in \mathbb{R}^N$ ,  $\mathbf{B}_{0i} \in \mathbb{R}^N$  and  $\mathbf{A}_{0i}^P \in \mathbb{R}^N$  are the coefficient vectors associated with  $\dot{q}_i(t)$ ,  $q_i(t)$  and  $q_i^P(t)$ , respectively. Note that these coefficient vectors are only dependent on the structural modal parameters and they are time invariant. The expressions of these coefficient vectors for most response quantities are given in Chapter 3.

## 6.2.1 Definition of Vector Operation Symbols

Before starting the formulation, it is useful to define a number of vector operators for convenience. They are:

• : Vector multiplication. For example, assuming that  $\mathbf{a}$ ,  $\mathbf{b}$  and  $\mathbf{c}$  have the same dimension,  $\mathbf{c} = \mathbf{a} \bullet \mathbf{b}$  means that each element in vector  $\mathbf{c}$  is the product of the corresponding element in  $\mathbf{a}$  and  $\mathbf{b}$ .

$\{\}^{\bullet 1/2}$  or  $\sqrt{\{\}}$  : Taking the square root of each element in the vector  $\{\}$  individually.

$\{\}^{\bullet 2}$  : Taking the square of the element in the vector  $\{\}$  individually.

$\{\}_{\max}$  : Representing the peak response of each response history in the vector  $\{\}$ .

## 6.2.2 Covariance of Responses to Stationary Excitation

Consider the input ground acceleration  $\ddot{x}_g(t)$  as a wide-band stationary process. Based on the theory of random vibration, the responses of a linear system subjected to a stationary process are also stationary and the covariance or mean squares of the response  $\mathbf{x}_0(t)$  from Equation (6.1) is in the form of

$$\begin{aligned}
 E[\mathbf{x}_0^{\bullet 2}(t)] &= E\left[\left\{\sum_{i=1}^{N_c} [\mathbf{A}_{0i} \dot{q}_i(t) + \mathbf{B}_{0i} q_i(t)] + \sum_{i=1}^{N_p} [\mathbf{A}_{0i}^p q_i^p(t)]\right\}^{\bullet 2}\right] \\
 &= \sum_{i=1}^{N_c} \sum_{j=1}^{N_c} \left\{ \mathbf{A}_{0i} \bullet \mathbf{A}_{0j} E[\dot{q}_i(t) \dot{q}_j(t)] + \mathbf{B}_{0i} \bullet \mathbf{B}_{0j} E[q_i(t) q_j(t)] + 2\mathbf{A}_{0i} \bullet \mathbf{B}_{0j} E[\dot{q}_i(t) q_j(t)] \right\} \\
 &\quad + 2 \sum_{i=1}^{N_c} \sum_{j=1}^{N_p} \left\{ \mathbf{A}_{0i} \bullet \mathbf{A}_{0j}^p E[\dot{q}_i(t) q_j^p(t)] + \mathbf{B}_{0i} \bullet \mathbf{A}_{0j}^p E[q_i(t) q_j^p(t)] \right\} \\
 &\quad + \sum_{i=1}^{N_p} \sum_{j=1}^{N_p} \left\{ \mathbf{A}_{0i}^p \bullet \mathbf{A}_{0j}^p E[q_i^p(t) q_j^p(t)] \right\} \in \mathbb{R}^N
 \end{aligned} \tag{6.2}$$

Equation (6.2) shows that it is necessary to compute the covariance of the response produced by two modes (e.g.  $E[q_i(t)q_j(t)]$ ) in order to obtain the variance of  $\mathbf{x}_0(t)$ . Before proceeding to calculate the covariance produced by two modes, a number of expressions derived in Chapter 3 are required in the following formulation. They are repeated as follows.

$$q_i(t) = \int_0^t h_i(t-\tau)\ddot{x}_g(\tau)d\tau \quad (6.3)$$

$$q_i^p(t) = \int_0^t h_i^p(t-\tau)\ddot{x}_g(\tau)d\tau \quad (6.4)$$

$$H_i(j\omega) = \int_{-\infty}^{+\infty} h_i(t)e^{-j\omega t} dt = -\frac{1}{-\omega^2 + j2\xi_i\omega + \omega_i^2} \in \mathbb{C} \quad (6.5)$$

$$H_{v_i}(j\omega) = -\frac{j\omega}{-\omega^2 + j2\xi_i\omega + \omega_i^2} \in \mathbb{C} \quad (6.6)$$

$$H_i^p(j\omega) = -\frac{1}{j\omega + \omega_i^p} \in \mathbb{C} \quad (6.7)$$

The displacement response covariance term  $E[q_i(t)q_j(t)]$  in Equation (6.2) is first examined. According to Equation (6.3), this term may be written as

$$E[q_i(t)q_j(t)] = \int_0^t \int_0^t h_i(\tau_1)h_j(\tau_2)E[\ddot{x}_g(t-\tau_1)\ddot{x}_g(t-\tau_2)]d\tau_1d\tau_2 \in \mathbb{R} \quad (6.8)$$

Knowing that ground excitation  $\ddot{x}_g(t)$  commences from zero at the time instant  $t=0$  (i.e.  $\ddot{x}_g(t)=0$  when  $t \leq 0$ ), it is reasonable to extend the lower limit of the integration in Equation (6.8) to negative infinity as

$$E[q_i(t)q_j(t)] = \int_{-\infty}^t \int_{-\infty}^t h_i(\tau_1)h_j(\tau_2)E[\ddot{x}_g(t-\tau_1)\ddot{x}_g(t-\tau_2)]d\tau_1d\tau_2 \quad (6.9)$$

Now, suppose that the ground excitation  $\ddot{x}_g(t)$  is further considered a white noise process with zero mean, described by a constant power spectral density  $S_0$ , it follows that the term  $E[\ddot{x}_g(t-\tau_1)\ddot{x}_g(t-\tau_2)]$  in Equation (6.9) becomes

$$E[\ddot{x}_g(t-\tau_1)\ddot{x}_g(t-\tau_2)] = 2\pi S_0 \delta(\tau_1 - \tau_2) \quad (6.10)$$

where  $\delta(\tau)$  is the Dirac function and is defined as follows.

$$\delta(\tau) = \begin{cases} +\infty & \tau = 0 \\ 0 & \tau \neq 0 \end{cases} \quad (6.11)$$

and

$$\int_{-\infty}^{+\infty} \delta(\tau) d\tau = 1 \quad (6.12)$$

In light of the inverse of Fourier transform, the Dirac function also can be expressed as

$$\delta(\tau) = \frac{1}{2\pi} \int_{-\infty}^{+\infty} e^{j\omega\tau} d\omega \quad (6.13)$$

or

$$\delta(\tau_1 - \tau_2) = \frac{1}{2\pi} \int_{-\infty}^{+\infty} e^{j\omega(\tau_1 - \tau_2)} d\omega \quad (6.14)$$

Substituting Equations (6.10) and (6.14) in Equation (6.9) and setting the upper integral limit to infinity to retain the steady state response, Equation (6.9) becomes

$$\begin{aligned} E[q_i(+\infty)q_j(+\infty)] &= S_0 \int_{-\infty}^{+\infty} \int_{-\infty}^{+\infty} \int_{-\infty}^{+\infty} h_i(\tau_1)h_j(\tau_2)e^{j\omega(\tau_1 - \tau_2)} d\tau_1 d\tau_2 d\omega \\ &= S_0 \int_{-\infty}^{+\infty} \left( \int_{-\infty}^{+\infty} h_i(\tau_1)e^{j\omega\tau_1} d\tau_1 \int_{-\infty}^{+\infty} h_j(\tau_2)e^{-j\omega\tau_2} d\tau_2 \right) d\omega \end{aligned} \quad (6.15)$$

Making use of Equation (6.5), Equation (6.15) may be written as

$$R_{ij}^{DD} = E[q_i(+\infty)q_j(+\infty)] = S_0 \int_{-\infty}^{+\infty} H_i(-j\omega)H_j(j\omega)d\omega \quad (6.16)$$

Substituting Equation (6.5) into Equation (6.16) and using contour integration in the complex plane, it yields

$$R_{ij}^{DD} = \frac{\pi S_0}{2\omega_i \omega_j \sqrt{\omega_i \omega_j \xi_i \xi_j}} \rho_{ij}^{DD} \quad (6.17)$$

where

$$\rho_{ij}^{DD} = \frac{8\sqrt{\xi_i \xi_j} (\gamma_{ij} \xi_i + \xi_j) \gamma_{ij}^{3/2}}{(1 - \gamma_{ij}^2)^2 + 4\xi_i \xi_j \gamma_{ij} (1 + \gamma_{ij}^2) + 4(\xi_i^2 + \xi_j^2) \gamma_{ij}^2}, \quad (\gamma_{ij} = \omega_i / \omega_j, \quad i, j = 1, 2, \dots, N_C) \quad (6.18)$$

is the well-known complex modal displacement correlation coefficient originally derived for the CQC rule (Der Kiureghian 1981). Let  $i = j$  in Equation (6.17), the complex modal displacement variance can be obtained as

$$R_{ii}^{DD} = \frac{\pi S_0}{2\xi_i \omega_i^3} \quad (6.19)$$

Consequently, Equation (6.17) can be entirely expressed in the complex modal displacement variance terms. That is,

$$R_{ij}^{DD} = \sqrt{R_{ii}^{DD} R_{jj}^{DD}} \rho_{ij}^{DD}, \quad (i, j = 1, 2, \dots, N_C) \quad (6.20)$$

Following the similar procedures of the derivation of the complex modal displacement response covariance  $R_{ij}^{DD}$ , the complex modal velocity response covariance  $R_{ij}^{VV}$  and the covariance of the  $i$ th complex modal velocity and the  $j$ th complex modal displacement  $R_{ij}^{VD}$  can also be derived as

$$\begin{aligned} R_{ij}^{VV} &= E[\dot{q}_i(+\infty)\dot{q}_j(+\infty)] = S_0 \int_{-\infty}^{\infty} \omega^2 H_i(-j\omega) H_j(j\omega) d\omega \\ &= \frac{\pi S_0}{2\sqrt{\omega_i \omega_j \xi_i \xi_j}} \rho_{ij}^{VV} \\ &= \omega_i \omega_j \sqrt{R_{ii}^{DD} R_{jj}^{DD}} \rho_{ij}^{VV}, \quad (i, j = 1, 2, \dots, N_C) \end{aligned} \quad (6.21)$$

where

$$\rho_{ij}^{VV} = \frac{8\sqrt{\xi_i \xi_j} (\xi_i + \gamma_{ij} \xi_j) \gamma_{ij}^{3/2}}{(1 - \gamma_{ij}^2)^2 + 4\xi_i \xi_j \gamma_{ij} (1 + \gamma_{ij}^2) + 4(\xi_i^2 + \xi_j^2) \gamma_{ij}^2}, \quad (\gamma_{ij} = \omega_i / \omega_j, \quad i, j = 1, 2, \dots, N_C) \quad (6.22)$$

is the complex modal velocity correlation coefficient and

$$\begin{aligned} R_{ij}^{VD} &= E[\dot{q}_i(+\infty)q_j(+\infty)] = S_0 \int_{-\infty}^{+\infty} j\omega H_i(-j\omega)H_j(j\omega)d\omega \\ &= \frac{\pi S_0}{2\omega_j \sqrt{\omega_i \omega_j \xi_i \xi_j}} \rho_{ij}^{VD} \\ &= \omega_i \sqrt{R_{ii}^{DD} R_{jj}^{DD}} \rho_{ij}^{VD}, \quad (i, j = 1, 2, \dots, N_C) \end{aligned} \quad (6.23)$$

where

$$\rho_{ij}^{VD} = \frac{4\sqrt{\xi_i \xi_j} (1 - \gamma_{ij}^2) \gamma_{ij}^{1/2}}{(1 - \gamma_{ij}^2)^2 + 4\xi_i \xi_j \gamma_{ij} (1 + \gamma_{ij}^2) + 4(\xi_i^2 + \xi_j^2) \gamma_{ij}^2}, \quad (\gamma_{ij} = \omega_i / \omega_j, \quad i, j = 1, 2, \dots, N_C) \quad (6.24)$$

is the complex modal velocity-displacement correlation coefficient. It is noted that when  $i = j$ , the variance of the velocity response  $R_{ii}^{VV}$  and the covariance of the velocity and displacement response  $R_{ij}^{VD}$  becomes

$$R_{ii}^{VV} = \frac{\pi S_0}{2\omega_i \xi_i} = \omega_i^2 R_{ii}^{DD} \quad (6.25)$$

$$\text{and} \quad R_{ii}^{VD} = 0 \quad (6.26)$$

It should be clear from Equations (6.25) and (6.26) that the velocity variance and the displacement variance of a SDOF system is related by the squares of its natural circular frequency, and the modal displacement and velocity responses of a SDOF system are orthogonal with each other under the white noise excitation assumption. It is also noted from Equations (6.21) and (6.23) that the velocity covariance  $R_{ij}^{VV}$  and the velocity-displacement covariance  $R_{ij}^{VD}$  can simply be expressed in terms of the modal displacement variances  $R_{ii}^{DD}$  and  $R_{jj}^{DD}$ . They are connected by the two correlation

coefficients  $\rho_{ij}^{VV}$  and  $\rho_{ij}^{VD}$ . The presence of  $R_{ij}^{VV}$  and  $R_{ij}^{VD}$  is due to the non-classical damping effect.

To examine the covariance terms associated with over-damped modes (i.e. over-damped mode response), let us consider the over-damped mode response covariance term  $E[q_i^p(t)q_j^p(t)]$  in Equation (6.2).

$$\begin{aligned} R_{ii}^{PP} &= E[q_i^p(t)q_j^p(t)] \\ &= S_0 \int_{-\infty}^{+\infty} H_i^p(-j\omega)H_j^p(j\omega)d\omega, \quad (i, j = 1, 2, \dots, N_p) \end{aligned} \quad (6.27)$$

Substitution of Equation (6.7) into Equation (6.27) and manipulation with contour integration in the complex plane leads to

$$R_{ij}^{PP} = \frac{2\pi S_0}{\omega_i^p + \omega_j^p}, \quad (i, j = 1, 2, \dots, N_p) \quad (6.28)$$

Similarly, considering the  $i$ th over-damped mode response variance by letting  $i = j$  leads to

$$R_{ii}^{PP} = \frac{\pi S_0}{\omega_i^p}, \quad (i = 1, 2, \dots, N_p) \quad (6.29)$$

Thus, Equation (6.27) can be rewritten as

$$R_{ij}^{PP} = \sqrt{R_{ii}^{PP} R_{jj}^{PP}} \rho_{ij}^{PP}, \quad (i, j = 1, 2, \dots, N_p) \quad (6.30)$$

in which

$$\rho_{ij}^{PP} = \frac{2\sqrt{\omega_i^p \omega_j^p}}{\omega_i^p + \omega_j^p}, \quad (i, j = 1, 2, \dots, N_p) \quad (6.31)$$

is a newly derived correlation coefficient that accounts for the relationship among all over-damped mode responses.

Similarly, the complex modal displacement and over-damped mode response covariance term  $E[q_i(t)q_j^p(t)]$  in Equation (6.2) can be written in the form of

$$\begin{aligned}
R_{ij}^{DP} &= E[q_i(+\infty)q_j^p(+\infty)] \\
&= S_0 \int_{-\infty}^{+\infty} H_i(-j\omega)H_j^p(j\omega)d\omega \\
&= \frac{2\pi S_0}{\omega_i^2 + 2\xi_i\omega_i\omega_j^p + (\omega_j^p)^2} \\
&= \sqrt{R_{ii}^{DD}R_{jj}^{PP}\rho_{ij}^{DP}}, \quad (i=1,2,\dots,N_c, j=1,2,\dots,N_p)
\end{aligned} \tag{6.32}$$

By analogy, the complex modal velocity and over-damped mode response covariance term  $E[\dot{q}_i(t)q_j^p(t)]$  in Equation (6.2) becomes

$$\begin{aligned}
R_{ij}^{VP} &= E[\dot{q}_i(+\infty)q_j^p(+\infty)] \\
&= S_0 \int_{-\infty}^{+\infty} H_{vi}(j\omega)H_j^p(-j\omega)d\omega \\
&= \frac{2\pi\omega_j^p S_0}{\omega_i^2 + 2\xi_i\omega_i\omega_j^p + (\omega_j^p)^2} \\
&= \sqrt{R_{ii}^{DD}R_{jj}^{PP}\omega_j^p\rho_{ij}^{DP}}, \quad (i=1,2,\dots,N_c, j=1,2,\dots,N_p)
\end{aligned} \tag{6.33}$$

where

$$\rho_{ij}^{DP} = \frac{2\omega_i\sqrt{2\xi_i\omega_i\omega_j^p}}{\omega_i^2 + 2\xi_i\omega_i\omega_j^p + (\omega_j^p)^2}, \quad (i=1,2,\dots,N_c, j=1,2,\dots,N_p) \tag{6.34}$$

is the correlation coefficient which accounts for the correlation between the complex modal displacements and the over-damped mode response. Equations (6.27) to (6.34) are new relationships established in this study to consider the presence of over-damped modes.

Upon substitution of the above derived covariance given by Equations (6.20), (6.21), (6.23), (6.30), (6.32) and (6.33) into Equation (6.2), Equation (6.2) can be written as



$$\begin{aligned}
E[\mathbf{x}_0^2(t)] = & \sum_{i=1}^{N_C} \sum_{j=1}^{N_C} \left[ \rho_{ij}^{VV} \omega_i \omega_j \mathbf{A}_{0i} \cdot \mathbf{A}_{0j} + \rho_{ij}^{DD} \mathbf{B}_{0i} \cdot \mathbf{B}_{0j} + 2\rho_{ij}^{VD} \omega_i \mathbf{A}_{0i} \cdot \mathbf{B}_{0j} \right] \sqrt{R_{ii}^{DD} R_{jj}^{DD}} \\
& + 2 \sum_{i=1}^{N_C} \sum_{j=1}^{N_P} \rho_{ij}^{DP} \left[ \omega_j^P \mathbf{A}_{0i} \cdot \mathbf{A}_{0j}^P + \mathbf{B}_{0i} \cdot \mathbf{A}_{0j}^P \right] \sqrt{R_{ii}^{DD} R_{jj}^{PP}} \\
& + \sum_{i=1}^{N_P} \sum_{j=1}^{N_P} \left[ \rho_{ij}^{PP} \mathbf{A}_{0i} \cdot \mathbf{A}_{0j}^P \right] \sqrt{R_{ii}^{PP} R_{jj}^{PP}}
\end{aligned} \tag{6.35}$$

### 6.2.3 Development of Response Spectrum Method

It has been shown in (Davenport 1964 and Vanmarcke 1972) that the mean maximum modal response of a linear system over a specified duration to a stationary excitation is proportional to its root mean square, i.e.,

$$|q_i(t)|_{\max} = S_i = p_i \sqrt{R_{ii}^{DD}} \quad (i=1, 2 \dots N_C) \tag{6.36}$$

$$|q_i^P(t)|_{\max} = S_i^P = p_i \sqrt{R_{ii}^{PP}} \quad (i=1, 2 \dots N_P) \tag{6.37}$$

where the  $S_i$  is the ordinate of the mean displacement response spectrum and  $S_i^P$  is the mean over-damped mode response spectrum. The definition of the over-damped mode response spectrum will be addressed in a later section. The numerical value of  $p_i$ , in general, does not differ greatly in magnitude from mode to mode. Thus, for practical applications, it is reasonable to assign the same value to  $p_i$  for each mode, even for the combined responses. As a result, the relationship between the maximum response of interest and all modal displacement response maxima can be expressed as

$$|\mathbf{x}_0(t)|_{\max} = \left\{ \begin{aligned} & \sum_{i=1}^{N_C} \sum_{j=1}^{N_C} \rho_{ij}^{DD} \left[ \mu_{ij} \omega_i \omega_j \mathbf{A}_{0i} \cdot \mathbf{A}_{0j} + \mathbf{B}_{0i} \cdot \mathbf{B}_{0j} + 2\nu_{ij} \omega_i \mathbf{A}_{0i} \cdot \mathbf{B}_{0j} \right] |q_i(t)|_{\max} |q_j(t)|_{\max} \\ & + 2 \sum_{i=1}^{N_C} \sum_{j=1}^{N_P} \rho_{ij}^{DP} \left[ \omega_j^P \mathbf{A}_{0i} \cdot \mathbf{A}_{0j}^P + \mathbf{B}_{0i} \cdot \mathbf{A}_{0j}^P \right] |q_i(t)|_{\max} |q_j^P(t)|_{\max} \\ & + \sum_{i=1}^{N_P} \sum_{j=1}^{N_P} \left[ \rho_{ij}^{PP} \mathbf{A}_{0i} \cdot \mathbf{A}_{0j}^P \right] |q_i^P(t)|_{\max} |q_j^P(t)|_{\max} \end{aligned} \right\}^{1/2} \tag{6.38}$$

where

$$\mu_{ij} = \frac{\rho_{ij}^{VV}}{\rho_{ij}^{DD}} = \frac{\xi_i + \xi_j \gamma_{ij}}{\xi_j + \xi_i \gamma_{ij}}, \quad (i, j = 1, 2, \dots, N_C) \quad (6.39)$$

$$\nu_{ij} = \frac{\rho_{ij}^{VD}}{\rho_{ij}^{DD}} = \frac{1 - \gamma_{ij}^2}{2\gamma_{ij}(\xi_j + \xi_i \gamma_{ij})}, \quad (i, j = 1, 2, \dots, N_C) \quad (6.40)$$

Equation (6.38), termed as the General Complete Quadratic Combination rule (GCQC rule), gives the peak response of a generally damped linear structure when the input excitations are described in terms of response spectra.

If the correlations between each mode are ignored; that is, when  $i \neq j$   $\rho_{ij}^{DD} = 0$ ,  $\rho_{ij}^{PP} = 0$  as well as  $\nu_{ij} = 0$  and  $\rho_{ij}^{DP} = 0$  for all  $i$  and  $j$ , Equation (6.38) is further reduced to

$$|\mathbf{x}_0(t)|_{\max} = \sqrt{\sum_{i=1}^{N_C} (\omega_i^2 \mathbf{A}_{0i}^* \mathbf{A}_{0i} + \mathbf{B}_{0i}^* \mathbf{B}_{0i}) |q_i(t)|_{\max}^2 + \sum_{i=1}^{N_p} (\mathbf{A}_{0i}^P)^* \mathbf{A}_{0i}^P |q_i^P(t)|_{\max}^2} \quad (6.41)$$

Equation (6.41) is termed as General Square-Root-of-Sum-of-Square combination (GSRSS) rule.

#### 6.2.4 Investigation of the Correlation Factors

The correlation coefficients  $\rho_{ij}^{DD}$ ,  $\rho_{ij}^{VV}$ ,  $\rho_{ij}^{VD}$ ,  $\rho_{ij}^{DP}$  and  $\rho_{ij}^{PP}$  for responses to the white noise input are presented in Figure 6.1 to Figure 6.5, respectively. Each correlation coefficient was plotted against the ratio  $\omega_i/\omega_j$  for certain representative damping levels. Figure 6.1(a) compares the  $\rho_{ij}^{DD}$  variations for different level of damping, in which the complex modal damping ratios of  $i$ th and  $j$ th mode are the same; whereas Figure 6.1(b) compares the  $\rho_{ij}^{DD}$  variations when the  $i$ th and  $j$ th complex modal damping ratio are not equal. It is observed that the  $\rho_{ij}^{DD}$  becomes smaller as the two modal frequencies  $\omega_i$  and  $\omega_j$  move apart. This is particularly true for cases of small damping. However, the  $\rho_{ij}^{DD}$  does not diminish rapidly when one of the modal damping is significantly large. This

implies that heavily damped modes may have strong interaction with other modes. Similar results can also be found for the velocity correlation coefficient  $\rho_{ij}^{VV}$  as shown in Figure 6.2. Figure 6.3 shows the variations of the velocity-displacement correlation coefficient  $\rho_{ij}^{VD}$ . It can be seen that the variation of  $\rho_{ij}^{VD}$  is quite different from the displacement correlation coefficient  $\rho_{ij}^{DD}$ . It has negative values when the ratio  $\omega_i/\omega_j$  is greater than unity. This means negative correlations exist between complex modal displacement and complex modal velocity. When  $\omega_i/\omega_j$  is equal to unity,  $\rho_{ij}^{VD}$  is zero. This result is reasonable as the complex modal displacement and velocity belonging to the same mode are independent under the white noise input assumption. The value of  $\rho_{ij}^{VD}$  is significant when  $\omega_i/\omega_j$  is less than unity, indicating that the correlation between complex modal velocity and displacement may not be neglected. Figure 6.4 shows the variation of  $\rho_{ij}^{DP}$  with respect to the ratio  $\omega_i/\omega_j^p$ . It is found that the values of  $\rho_{ij}^{DP}$  are significant, especially true at large damping levels. Also,  $\rho_{ij}^{DP}$  grows as the ratio  $\omega_i/\omega_j^p$  approaches two and decreases slowly beyond that value. The variation of  $\rho_{ij}^{PP}$  versus  $\omega_i^p/\omega_j^p$  is shown in Figure 6.5, from which it is observed that the value of  $\rho_{ij}^{PP}$  remains to be a significant component across the range of the ratios of  $\omega_i^p/\omega_j^p$  considered. The results from Figure 6.4 and Figure 6.5 suggest that over-damped mode may have strong contributions to the structural responses and should be considered in the combination rule appropriately.

### 6.2.5 Reduction to Classically under-Damped Structures

Consider a classically damped MDOF structure which is under-damped ( $N_C = N$ ,  $N_p = 0$ ), the peak displacement response  $|\mathbf{x}(t)|_{\max}$  and the absolute acceleration response  $|\ddot{\mathbf{x}}_A(t)|_{\max}$  can be estimated from Equation (6.38) as

$$|\mathbf{x}(t)|_{\max} = \sqrt{\sum_{i=1}^N \sum_{j=1}^N \rho_{ij}^{DD} \boldsymbol{\phi}_i \cdot \boldsymbol{\phi}_j \Gamma_i \Gamma_j |q_i(t)|_{\max} |q_j(t)|_{\max}} \quad (6.42)$$

and

$$\begin{aligned}
|\ddot{\mathbf{x}}_A(t)|_{\max} &= \left\{ \sum_{i=1}^N \sum_{j=1}^N \rho_{ij}^{\text{DD}} \left[ \omega_i^2 \omega_j^2 \Gamma_i \Gamma_j \boldsymbol{\phi}_i \cdot \boldsymbol{\phi}_j + 4\mu_{ij} \xi_i \xi_j \omega_i^2 \omega_j^2 \Gamma_i \Gamma_j \boldsymbol{\phi}_i \cdot \boldsymbol{\phi}_j \right. \right. \\
&\quad \left. \left. + 4\nu_{ij} \xi_i \omega_i^2 \omega_j^2 \Gamma_i \Gamma_j \boldsymbol{\phi}_i \cdot \boldsymbol{\phi}_j \right] |q_i(t)|_{\max} |q_j(t)|_{\max} \right\}^{1/2} \\
&= \left\{ \sum_{i=1}^N \sum_{j=1}^N \rho_{ij}^{\text{DD}} \left[ 1 + 4\mu_{ij} \xi_i \xi_j + 4\nu_{ij} \xi_i \right] \omega_i^2 \omega_j^2 \Gamma_i \Gamma_j \boldsymbol{\phi}_i \cdot \boldsymbol{\phi}_j |q_i(t)|_{\max} |q_j(t)|_{\max} \right\}^{1/2} \\
&= \left\{ \sum_{i=1}^N \sum_{j=1}^N \rho_{ij}^{\text{DD}} \sigma_{ij} \omega_i^2 \omega_j^2 \Gamma_i \Gamma_j \boldsymbol{\phi}_i \cdot \boldsymbol{\phi}_j |q_i(t)|_{\max} |q_j(t)|_{\max} \right\}^{1/2}
\end{aligned} \tag{6.43}$$

where

$$\sigma_{ij} = \frac{\xi_j \gamma_{ij} + 4\xi_i \xi_j \gamma_{ij} (\xi_i + \xi_j \gamma_{ij}) + \xi_i (2 - \gamma_{ij}^2)}{\gamma_{ij} (\xi_j + \xi_i \gamma_{ij})}, \quad (i, j = 1, 2, \dots, N) \tag{6.44}$$

In Equation (6.43)  $\boldsymbol{\phi}_i$  is the  $i$ th undamped mode shape, and  $\Gamma_i = \boldsymbol{\phi}_i^T \mathbf{M} \mathbf{J} / \boldsymbol{\phi}_i^T \mathbf{M} \boldsymbol{\phi}_i$  is the  $i$ th modal participation factor. Note that Equation (6.42) coincides with the conventional CQC rule, as expected. Equation (6.43) is a newly established formula to evaluate the peak absolute acceleration of classically damped structures using response spectrum method. As well known, the pseudo-acceleration spectra  $S_{\text{PA}}$  can be written as  $S_{\text{PA}}(\omega_i, \xi_i) = \omega_i^2 |q_i(t)|_{\max}$ . Thus, Equation (6.43) may be expressed as

$$|\ddot{\mathbf{x}}_A(t)|_{\max} = \left\{ \sum_{i=1}^N \sum_{j=1}^N \rho_{ij}^{\text{DD}} \sigma_{ij} \Gamma_i \Gamma_j \boldsymbol{\phi}_i \cdot \boldsymbol{\phi}_j S_{\text{PA}}(\omega_i, \xi_i) S_{\text{PA}}(\omega_j, \xi_j) \right\}^{1/2} \tag{6.45}$$

Examining Equation (6.45), it is seen that, when using the pseudo-acceleration spectra to estimate the peak absolute acceleration, the results should be modified by the factor  $\sigma_{ij}$  in the combination rule. This important feature offers improved estimates on the absolute acceleration of classically damped structures and should be very useful in the earthquake engineering applications. Now if the correlations between every mode are ignored, Equation (6.45) can be further simplified in the SRSS form as

$$|\ddot{\mathbf{x}}_A(t)|_{\max} = \left\{ \sum_{i=1}^N (1 + 4\xi_i^2) \omega_i^4 \Gamma_i^2 \Phi_i^2 |q_i|_{\max}^2 \right\}^{1/2} \quad (6.46)$$

Further, if the system is a SDOF system, Equation (6.46) becomes

$$|\ddot{x}_A(t)|_{\max} = \sqrt{1 + 4\xi^2} S_{pA}(\omega_n, \xi) \quad (6.47)$$

This formulation provides an efficient and reasonable transformation between the pseudo-acceleration and peak absolute acceleration. This relationship was also earlier derived by (Song et al. 2007). The applicability and accuracy of Equation (6.47) was also examined in their study. The results indicated that when the damping ratio is less than, say 40%, Equation (6.47) provides excellent estimates. As a matter of fact, Equation (6.47) is equivalent to the formula proposed by Tsopelas et al. (1997), which predicts the maximum acceleration based on the given pseudo-acceleration. It was developed under the assumption that during the cycle of maximum response the SDOF system undergoes a harmonic motion with the natural frequency of the SDOF. The equation of this method takes the form of

$$S_A = (f_1 + 2\xi f_2) S_{pA}(\omega_n, \xi) \quad (6.48)$$

where  $f_1 = \cos[\tan^{-1}(2\xi)]$  and  $f_2 = \sin[\tan^{-1}(2\xi)]$ . It is further found that Equation (6.48) is valid not only for sinusoidal excitation but also for strong phase earthquake excitation with white noise assumption (Song et al. 2007).

### 6.3 Over-Damped Mode Response Spectrum

Because the peak over-damped mode responses are not available when performing response spectrum analysis in engineering practice, it is necessary to predict the associated peak over-damped mode responses from the prescribed 5% pseudo-acceleration response spectrum. Thus, a new ‘over-damped mode’ response spectrum is introduced in this study. The over-damped mode response spectrum follows a similar definition as the conventional response spectrum used in earthquake engineering. The objective of the over-damped mode response spectrum is to account for the peak over-

damped mode response of structures that have over-damped modes. The interpretation of the over-damped mode response spectrum and an approach that is able to construct an over-damped mode response spectrum from the given conventional response spectrum are described in this section. Validation of the adequacy of the proposed over-damped mode response spectrum construction approach is also given.

### 6.3.1 The Concept

Before discussing the over-damped mode response spectrum, it is helpful to briefly review the concept of conventional response spectrum. Consider a SDOF under-damped system subjected to a ground motion  $\ddot{x}_g(t)$ , the equation of motion can be written as

$$\ddot{q}(t) + 2\xi\omega_n\dot{q}(t) + \omega_n^2q(t) = -\ddot{x}_g(t) \quad (6.49)$$

where  $q(t)$ ,  $\dot{q}(t)$  and  $\ddot{q}(t)$  are the relative displacement, velocity and acceleration, respectively;  $\xi$  is the damping ratio and  $\omega_n$  is the natural circular frequency of the SDOF system. The conventional response spectrum is constructed by performing a series of linear response-history analysis to a SDOF system under a given ground acceleration  $\ddot{x}_g(t)$ . The response spectrum is a plot of the peak values of a response quantity as a function of natural vibration period  $T_n$  (or corresponding natural circular frequency  $\omega_n$ ). Each plot is for a SDOF system having a fixed damping ratio  $\xi$ , and a number of such plots for different values of  $\xi$  are included to account for the effect of viscous damping encountered in real structures (Chopra 2005).

Recalling the over-damped mode term defined Chapter 3, the response of a over-damped mode can be characterized by the following linear first order differential equation

$$\dot{q}^p(t) + \omega^p q^p(t) = -\ddot{x}_g(t) \quad (6.50)$$

where  $q^p(t)$  is the over-damped mode response and  $\dot{q}^p(t)$  is the time derivative of, and  $\omega^p$  is the “over-damped modal natural frequency” (rad/sec). Similar to the concept of

conventional response spectrum, the over-damped mode response spectrum is defined as a plot of the peak over-damped mode responses  $q^p(t)$ , as a function of the over-damped modal frequency  $\omega^p$  or the over-damped modal period  $T^p = 2\pi/\omega^p$  under a given ground acceleration via Equation (6.50). Unlike the conventional response spectrum, there is only one parameter,  $\omega^p$ , influencing the response. The procedure to construct the over-damped mode response spectrum is illustrated in Figure 6.6, and it consists of the following three steps: (1) Select the ground motion to be considered (as seen in Figure 6.6(a)); (2) Determine the peak over-damped mode responses represented by Equation (6.50) using the selected ground motion for different over-damped modal frequencies (see Figure 6.6(b)); and (3) The peak over-damped mode response obtained offers a point on the over-damped mode response spectrum as shown in Figure 6.6(c).

### **6.3.2 Construction of Over-Damped Mode Response Spectrum Consistent with 5% Displacement Response Spectrum**

The construction of over-damped mode response spectrum relies on the availability of the ground acceleration history. However, when using the response spectrum approach, site design response spectrum specified in design provisions is used rather than the ground acceleration histories. Therefore, the over-damped mode response spectrum that is compatible with the site design response spectrum cannot be directly generated due to the unavailability of ground acceleration records. In this study, an approach based on the theory of random vibration is developed to address this issue, by assuming that the ground excitation can be considered as a wide-banded stationary Gaussian process. In this approach, the input excitation and responses are represented in terms of their respective power spectral density (PSD) function. For a linear system, the PSD of a response is the product of the response transmittancy function and the PSD of the input process. Further, most structural responses can be characterized by their corresponding response PSD functions. For example, the standard deviation or root mean square (RMS) of a response process is the area under its PSD (Der Kiureghian 1980). In addition, it has been shown in (Davenport 1964 and Vanmarcke 1972) that the peak value of a response process can be related to its root mean square by a proportional factor. From the above considerations,

the following procedure is established. First, the ground motion PSD mapped from given 5% damping displacement spectrum can be established, which is independent of the characteristics of the SDOF systems. Second, this ground motion PSD is used as a base to predict the over-damped mode response spectrum. This proposed approach is based on the work by (Song et al. 2007) to construct the real velocity spectrum from the given 5% response spectrum.

### 6.3.2.1 Response Spectrum Consistent PSD $G_{\dot{x}_g}(\omega)$

A reasonable estimate of ground motion PSD,  $G_{\dot{x}_g}(\omega)$ , consistent with pre-determined 5% displacement spectrum was proposed by (Song et al. 2007) as follows.

$$G_{\dot{x}_g}(\omega) = \frac{0.1S_d^2(\omega, 5\%)\omega^3}{\alpha^2(\omega, 5\%)\pi} \quad (6.51)$$

where  $S_d(\omega, 5\%)$  represents the given 5% displacement response spectrum as a function of  $\omega$ .  $\alpha(\omega, 5\%)$  is a factor that relates the standard deviation or root mean square (RMS)  $\sigma(\omega)$  of its response process to its peak response as

$$S_d(\omega, 5\%) = \alpha(\omega, 5\%) \times \sigma(\omega) \quad (6.52)$$

Values of  $\alpha(\omega, 5\%)$  determined numerically by using a group of artificial white noise processes can be found in Song et al. (2007). The applicability of Equation (6.51) along with the white-noise-determined  $\alpha(\omega, 5\%)$  has been shown to be appropriate when used in estimating the real spectral velocities Song et al. (2007). This response spectrum consistent PSD  $G_{\dot{x}_g}(\omega)$  will serve as a foundation to develop the over-damped mode response spectrum described next.

### 6.3.2.2 Procedures

From the over-damped mode equation of motion given by Equation (6.50), it is easy to obtain the over-damped mode frequency response function,  $H^p(j\omega) = -1/(\omega^p + j\omega)$ .



Under the wide-band stationary input process assumption, the PSD,  $G_{q^p}$ , of the over-damped mode response can be related to ground motion PSD  $G_{\ddot{x}_g}(\omega)$  via frequency response function,  $H^p(\omega)$ , as

$$G_{q^p} = |H^p(j\omega)|^2 \times G_{\ddot{x}_g}(\omega) \quad (6.53)$$

Then, the standard deviation or RMS,  $\sigma_{q^p}$ , of the over-damped response may be obtained through

$$\begin{aligned} \sigma_{q^p}^2 &= \int_0^\infty G_{q^p} d\omega \\ &= \int_0^\infty |H^p(j\omega)|^2 G_{\ddot{x}_g} d\omega \end{aligned} \quad (6.54)$$

Further, the peak value of over-damped mode response  $q^p(t)$  can also be related to its RMS  $\sigma_{q^p}$  by a different proportional factor  $\eta(\omega^p)$

$$|q^p(t)|_{\max} = \eta(\omega^p) \times \sigma_{q^p}(\omega^p) \quad (6.55)$$

where  $\eta(\omega^p)$  is a proportional factor by which the standard deviation must be multiplied to account for the expected peak over-damped mode response. The derivation of  $\eta(\omega^p)$  is provided in the following section.

### 6.3.2.3 $\eta$ Factor Determination

Based on the definition of  $\eta$ , it may be determined numerically by investigating the ratio between the peak value and the RMS of the response solved from Equation (6.50) while considering the excitation  $\ddot{x}_g(t)$  as an artificially generated white noise process for every over-damped modal frequency  $\omega^p$  of interest. The generated white noise has a duration of eleven seconds and a 0.005 sec time step. A total of 15,000 response-history analyses via Equation (6.50) were performed (corresponding to 150 over-damped modal frequencies  $\omega^p$  logarithmically spaced between 0.1 Hz and 30 Hz and 100 artificially

generated white noise inputs). Mean peak over-damped mode response and its RMS were obtained for each over-damped modal frequencies  $\omega^p$ . The  $\eta$  factor was then determined based on the ratio of these two values accordingly. The resulting  $\eta$  factors are tabulated in Table 6.1 while Figure 6.7 shows the plot of  $\eta$  as a function of the over-damped modal frequency  $\omega^p$  and the over-damped modal period  $T^p$ . The so determined  $\eta$  factors are termed as white-noise-determined  $\eta$  factors. It should be noted that  $\eta$  factors are readily available in advance of the construction of over-damped mode response spectrum and do not favor any ground motion records. Finally, the procedure to construct the over-damped mode response spectrum is illustrated schematically in Figure 6.8.

### 6.3.3 Validation of the Over-Damped Mode Response Spectrum

In order to demonstrate the accuracy and applicability of the formulation to construct the over-damped mode response spectrum from a given response spectrum, the exact mean over-damped mode response spectrum and the estimated over-damped mode response spectrum constructed by the proposed procedures were compared via real earthquake events. Two far-field ground motion ensembles are used in this study. The first, termed ensemble A, is the ensemble used by Vamvatsikos and Cornell (2004). The detailed information of the records is tabulated in Table 6.2. These records are selected to have large magnitudes of 6.5 to 6.9 and moderate distances from the fault recorded on firm soil. Near-fault data are excluded. The second, termed ensemble B, is a set containing 50 far-field ground motions used by ATC (2007) to study the earthquake ground motion records scaling method targeted at performance-based design. The detailed information of the records of this ensemble is tabulated in Table 6.3. In this second set of records, the records are selected based on the magnitudes between 6.3 and 7.3, distances from the fault between 21Km to 50Km, and site conditions characterized by soil C and D. To be consistent with the amount of records used in ensemble A, only the first 20 records from ensemble B are used. In this study, all records are scaled to have PGA equal to 0.4g. Figure 6.9 shows the mean 5% displacement response spectra for both ensembles. The mean exact over-damped modal spectra were constructed by performing a series of response-history analysis per over-damped mode equation of

motion shown in Equation (6.50) for each record. The over-damped modal period are chosen to be identical to those used in the determination of  $\eta$ . The resulting mean peak over-damped mode response is plotted against over-damped modal period  $T^P$  shown as a solid line in Figure 6.10. The construction of the over-damped mode response follows the proposed procedures mentioned above. The resulting over-damped mode response spectra estimated from the 5% displacement spectra are indicated by the dotted line in Figure 6.10. It is observed that the over-damped mode response spectrum constructed by the proposed procedures is in close agreement with the exact values. This consistency indicates the applicability of the proposed procedures.

Table 6.1 White-noise-determined  $\eta$  factor for over-damped mode response

$\omega^p$	$\eta$	$\omega^p$	$\eta$	$\omega^p$	$\eta$	$\omega^p$	$\eta$	$\omega^p$	$\eta$	$\omega^p$	$\eta$	$\omega^p$	$\eta$
0.63	2.55	1.46	2.81	3.39	3.04	7.86	3.28	18.25	3.41	42.36	3.50	98.33	3.43
0.65	2.56	1.52	2.82	3.52	3.05	8.17	3.28	18.96	3.41	44.01	3.50	102.1	3.42
0.68	2.57	1.57	2.83	3.66	3.07	8.49	3.29	19.70	3.42	45.73	3.50	106.1	3.41
0.70	2.59	1.64	2.84	3.80	3.08	8.82	3.30	20.47	3.43	47.51	3.51	110.2	3.41
0.73	2.60	1.70	2.85	3.95	3.10	9.16	3.31	21.27	3.43	49.37	3.51	114.6	3.40
0.76	2.61	1.77	2.86	4.10	3.11	9.52	3.32	22.10	3.44	51.29	3.51	119.0	3.39
0.79	2.62	1.84	2.87	4.26	3.13	9.89	3.32	22.96	3.44	53.29	3.51	123.7	3.38
0.82	2.64	1.91	2.88	4.43	3.14	10.28	3.33	23.85	3.44	55.37	3.51	128.5	3.36
0.85	2.65	1.98	2.89	4.60	3.15	10.68	3.34	24.78	3.44	57.53	3.51	133.5	3.35
0.89	2.66	2.06	2.90	4.78	3.16	11.09	3.34	25.75	3.44	59.78	3.51	138.7	3.34
0.92	2.67	2.14	2.91	4.97	3.17	11.53	3.35	26.76	3.45	62.11	3.51	144.1	3.32
0.96	2.69	2.22	2.92	5.16	3.18	11.98	3.36	27.80	3.45	64.54	3.51	149.8	3.31
0.99	2.70	2.31	2.93	5.36	3.19	12.44	3.36	28.89	3.46	67.05	3.50	155.6	3.29
1.03	2.71	2.40	2.94	5.57	3.20	12.93	3.37	30.01	3.46	69.67	3.50	161.7	3.28
1.07	2.72	2.49	2.95	5.79	3.21	13.43	3.37	31.18	3.47	72.39	3.49	168.0	3.27
1.12	2.73	2.59	2.96	6.01	3.22	13.96	3.38	32.40	3.47	75.22	3.49	174.6	3.25
1.16	2.74	2.69	2.97	6.25	3.23	14.50	3.38	33.67	3.47	78.15	3.48	181.4	3.24
1.20	2.75	2.80	2.99	6.49	3.24	15.07	3.39	34.98	3.48	81.20	3.48	188.5	3.22
1.25	2.76	2.91	2.99	6.74	3.25	15.66	3.39	36.34	3.48	84.37	3.47		
1.30	2.77	3.02	3.00	7.01	3.25	16.27	3.39	37.76	3.48	87.66	3.46		
1.35	2.78	3.14	3.01	7.28	3.26	16.90	3.40	39.24	3.49	91.08	3.45		
1.40	2.79	3.26	3.03	7.56	3.27	17.56	3.40	40.77	3.49	94.64	3.44		

$\omega^p$  = over-damped modal frequency (rad/sec)

Table 6.2 Far-field ground motions used in ATC-58

Designation	Event	Station	$M^1$	$r^1$
FF1, FF2	Cape Mendocino 04/25/92 18:06	89509 Eureka—Myrtle & West	7.1	44.6
FF3, FF4	Cape Mendocino 04/25/92 18:06	89486 Fortuna—Fortuna Blvd	7.1	23.6
FF5, FF6	Coalinga 1983/05/02 23:42	36410 Parkfield—Cholame 3W	6.4	43.9
FF7, FF8	Coalinga 1983/05/02 23:42	36444 Parkfield—Fault Zone 10	6.4	30.4
FF9, FF10	Coalinga 1983/05/02 23:42	36408 Parkfield—Fault Zone 3	6.4	36.4
FF11, FF12	Coalinga 1983/05/02 23:42	36439 Parkfield—Gold Hill 3E	6.4	29.2
FF13, FF14	Imperial Valley 10/15/79 23:16	5052 Plaster City	6.5	31.7
FF15, FF16	Imperial Valley 10/15/79 23:16	724 Niland Fire Station	6.5	35.9
FF17, FF18	Imperial Valley 10/15/79 23:16	6605 Delta	6.5	43.6
FF19, FF20	Imperial Valley 10/15/79 23:16	5066 Coachella Canal #4	6.5	49.3
FF21, FF22	Landers 06/28/92 11:58	22074 Yermo Fire Station	7.3	24.9
FF23, FF24	Landers 06/28/92 11:58	12025 Palm Springs Airport	7.3	37.5
FF25, FF26	Landers 06/28/92 11:58	12149 Desert Hot Springs	7.3	23.2
FF27, FF28	Loma Prieta 10/18/89 00:05	47524 Hollister—South & Pine	6.9	28.8
FF29, FF30	Loma Prieta 10/18/89 00:05	47179 Salinas—John & Work	6.9	32.6
FF31, FF32	Loma Prieta 10/18/89 00:05	1002 APEEL 2—Redwood City	6.9	47.9
FF33, FF34	Northridge 01/17/94 12:31	14368 Downey—Co Maint Bldg	6.7	47.6
FF35, FF36	Northridge 01/17/94 12:31	24271 Lake Hughes #1	6.7	36.3
FF37, FF38	Northridge 01/17/94 12:31	14403 LA—116th St School	6.7	41.9
FF39, FF40	San Fernando 02/09/71 14:00	125 Lake Hughes #1	6.6	25.8
FF41, FF42	San Fernando 02/09/71 14:00	262 Palmdale Fire Station	6.6	25.4
FF43, FF44	San Fernando 02/09/71 14:00	289 Whittier Narrows Dam	6.6	45.1
FF45, FF46	San Fernando 02/09/71 14:00	135 LA—Hollywood Stor Lot	6.6	21.2
FF47, FF48	Superstition Hills (A) 11/24/87 05:14	5210 Wildlife Liquef. Array	6.3	24.7
FF49, FF50	Superstition Hills (B) 11/24/87 13:16	5210 Wildlife Liquef. Array	6.7	24.4

1.  $M$  = moment magnitude;  $r$  = closest site-to-fault-rupture distance

(Courtesy of Y.N.Huang)

Table 6.3 Far-field ground motions used by Vamvatsikos and Cornell 2004

No	Event	Station	$\phi^{\circ 1}$
1	Loma Prieta, 1989	Agnews State Hospital	090
2	Imperial Valley, 1979	Plaster City	135
3	Loma Prieta, 1989	Hollister Diff. Array	255
4	Loma Prieta, 1989	Anderson Dam Downstrm	270
5	Loma Prieta, 1989	Coyote Lake Dam Downstrm	285
6	Imperial Valley, 1979	Cucapah	085
7	Loma Prieta, 1989	Sunnyvale Colton Ave	270
8	Imperial Valley, 1979	El Centro Array #13	140
9	Imperial Valley, 1979	Westmoreland Fire Station	090
10	Loma Prieta, 1989	Hollister South & Pine	000
11	Loma Prieta, 1989	Sunnyvale Colton Ave	360
12	Superstition Hills, 1987	Wildlife Liquefaction Array	090
13	Imperial Valley, 1979	Chihuahua	282
14	Imperial Valley, 1979	El Centro Array #13	230
15	Imperial Valley, 1979	Westmoreland Fire Station	180
16	Loma Prieta, 1989	WAHO	000
17	Superstition Hills, 1987	Wildlife Liquefaction Array	360
18	Imperial Valley, 1979	Plaster City	045
19	Loma Prieta, 1989	Hollister Diff. Array	165
20	Loma Prieta, 1989	WAHO	090

1. component

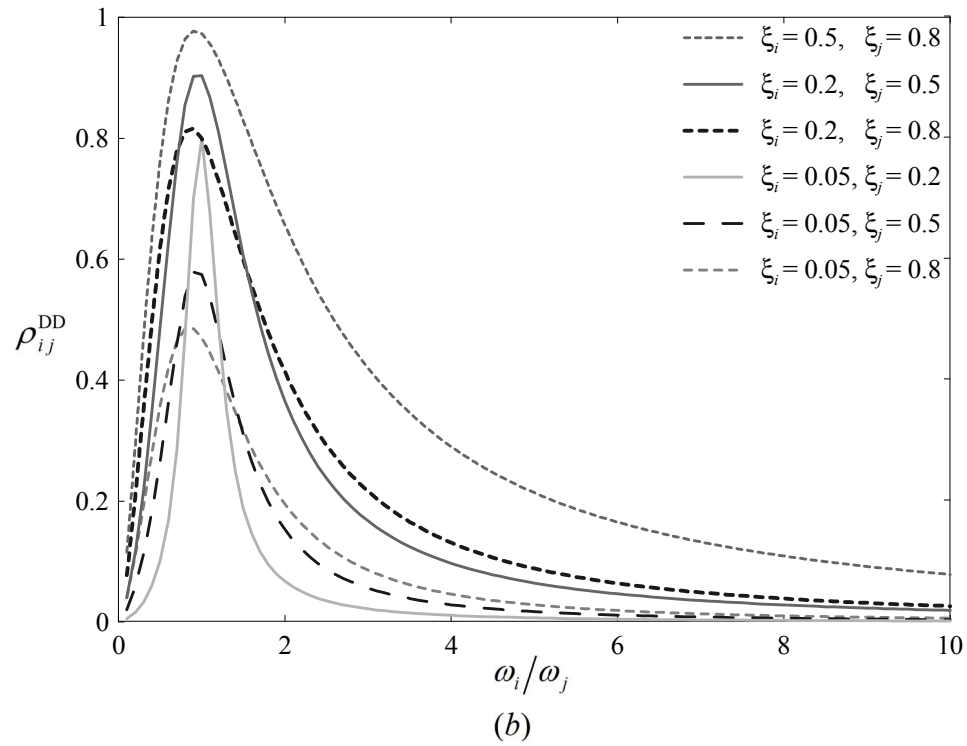
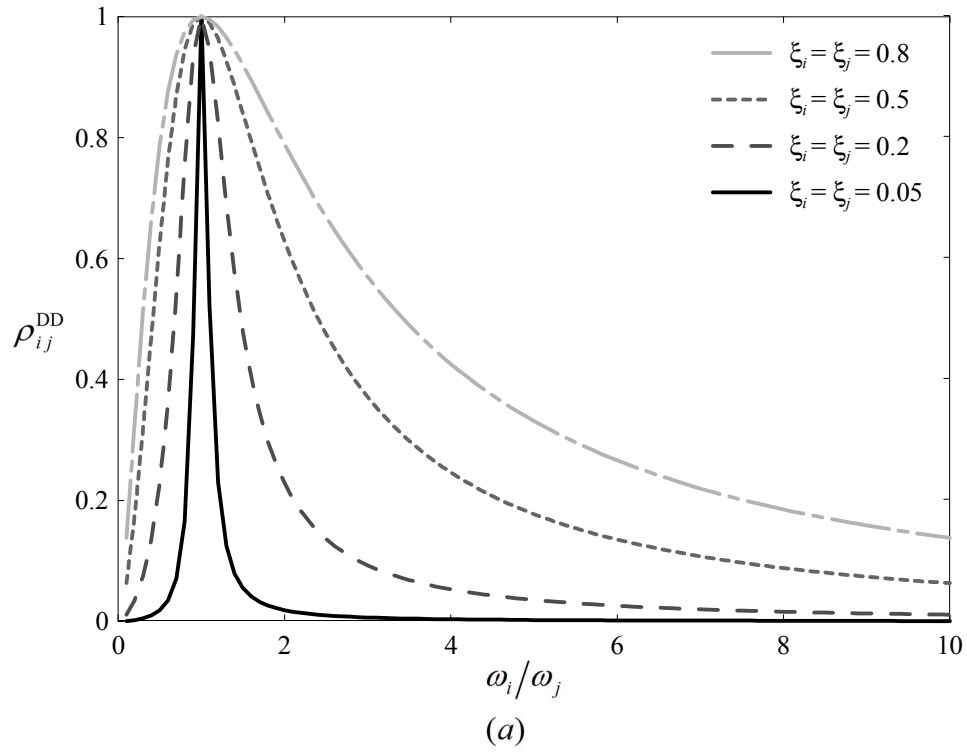


Figure 6.1 Correlation coefficient  $\rho_{ij}^{\text{DD}}$  for responses to white noise excitations

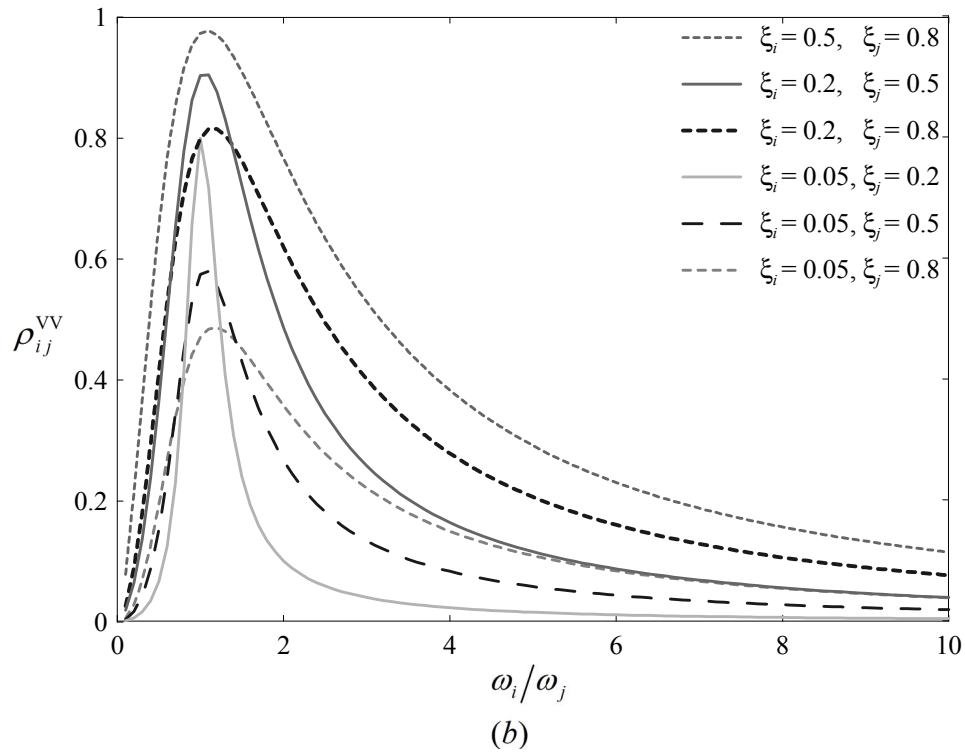
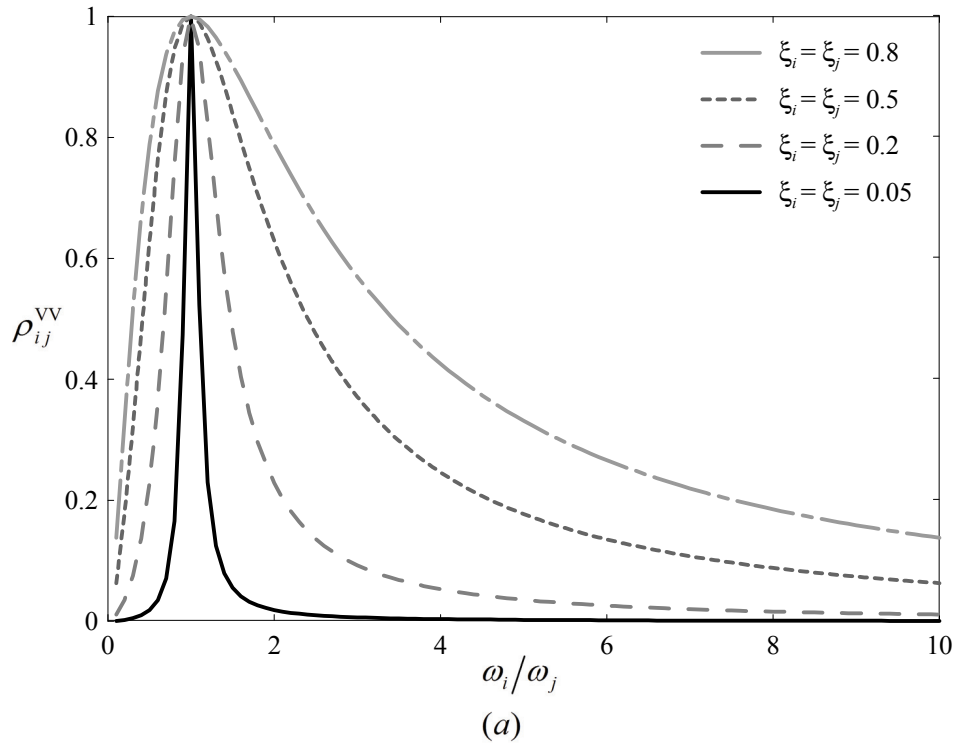


Figure 6.2 Correlation coefficient  $\rho_{ij}^{VV}$  for responses to white noise excitations



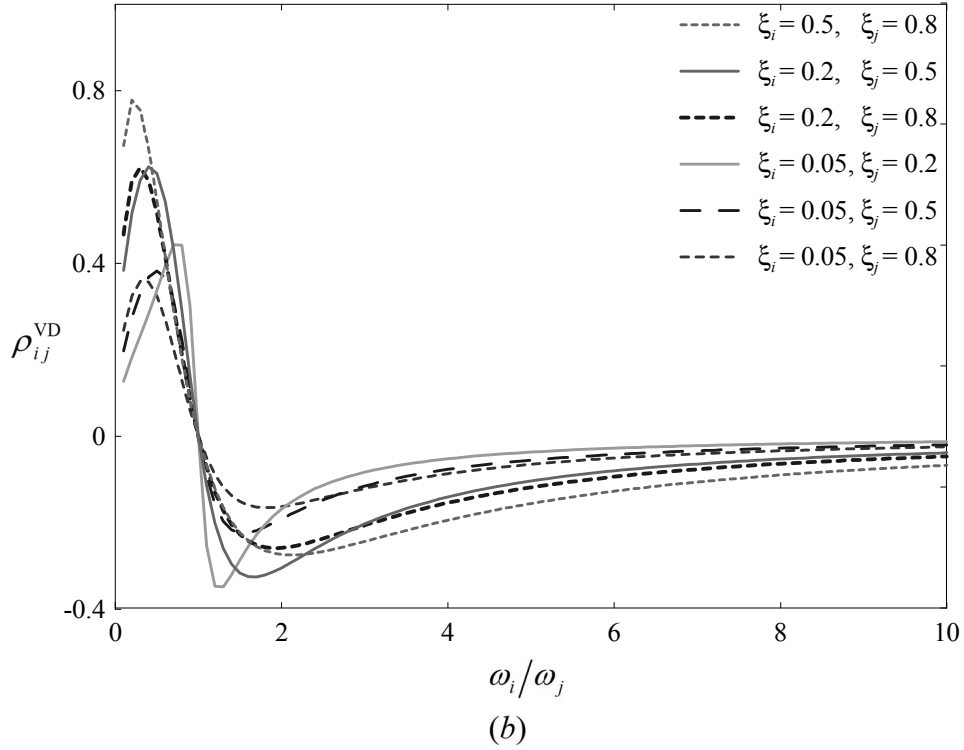
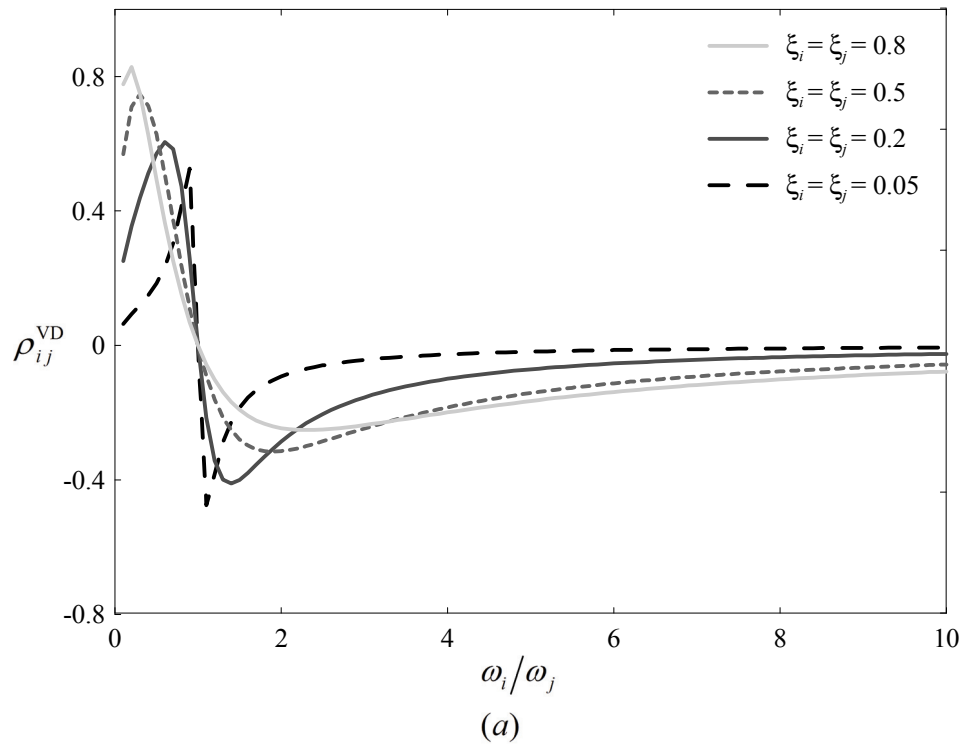


Figure 6.3 Correlation coefficient  $\rho_{ij}^{\text{VD}}$  for responses to white noise excitations

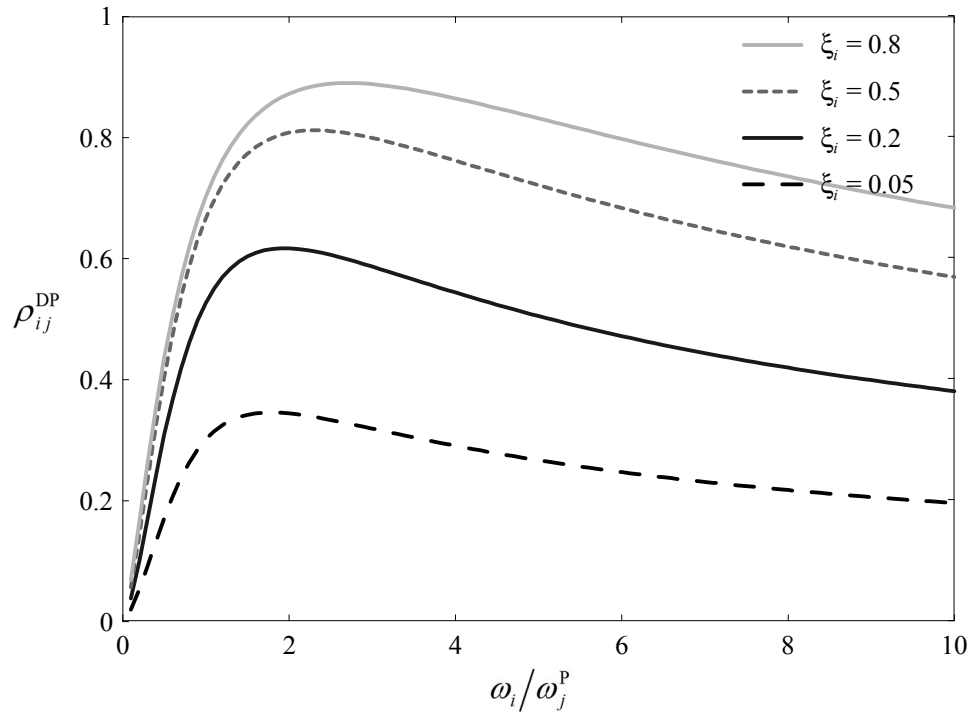


Figure 6.4 Correlation coefficient  $\rho_{ij}^{DP}$  for responses to white noise excitations

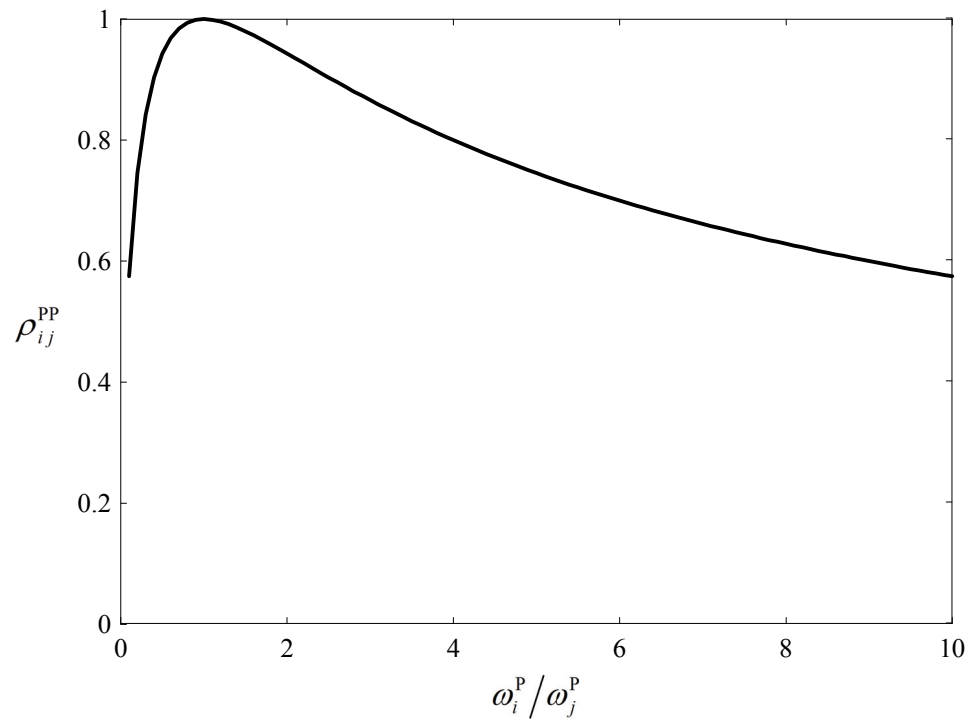


Figure 6.5 Correlation coefficient  $\rho_{ij}^{PP}$  for responses to white noise excitations

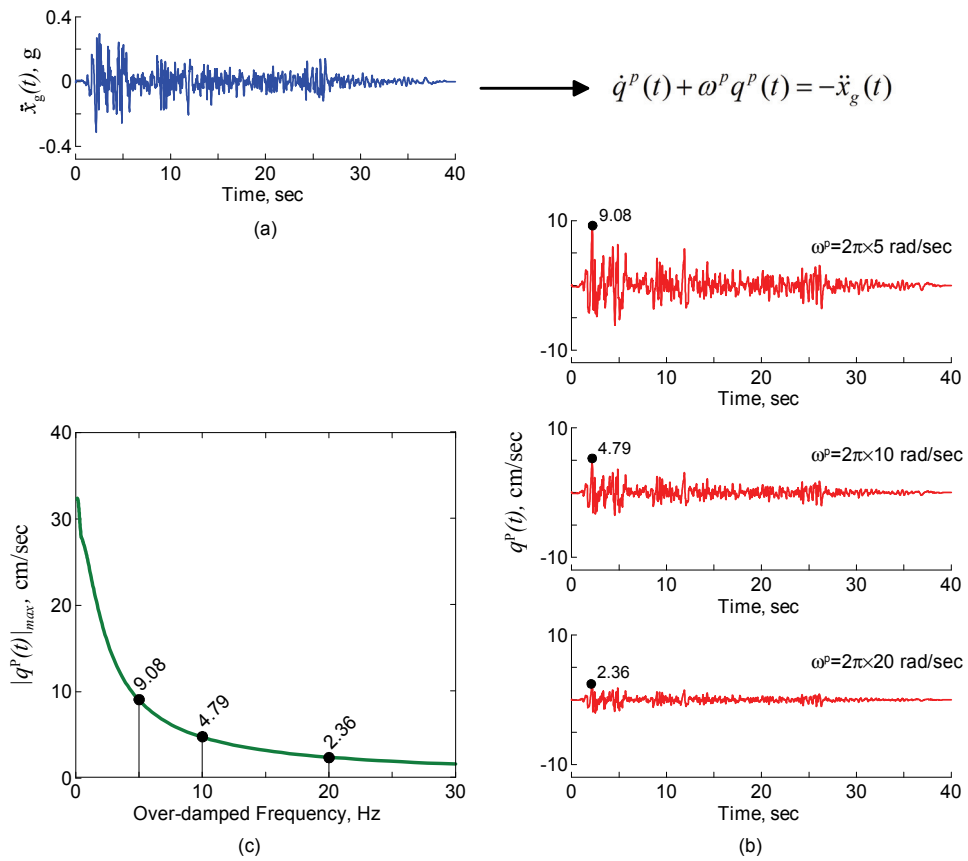


Figure 6.6 Generation of over-damped mode response spectrum

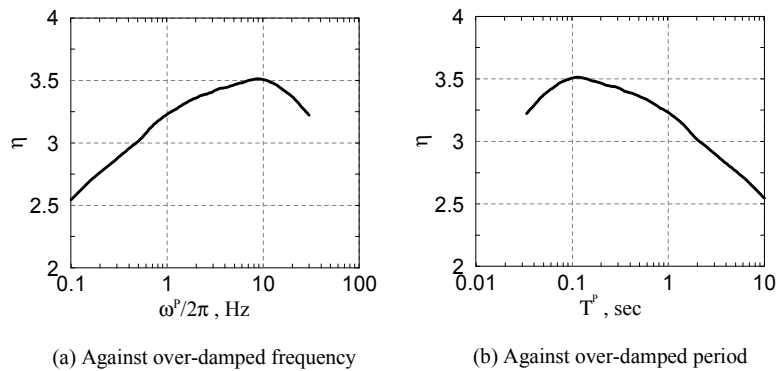


Figure 6.7 Variation of  $\eta$  factor for over-damped mode response

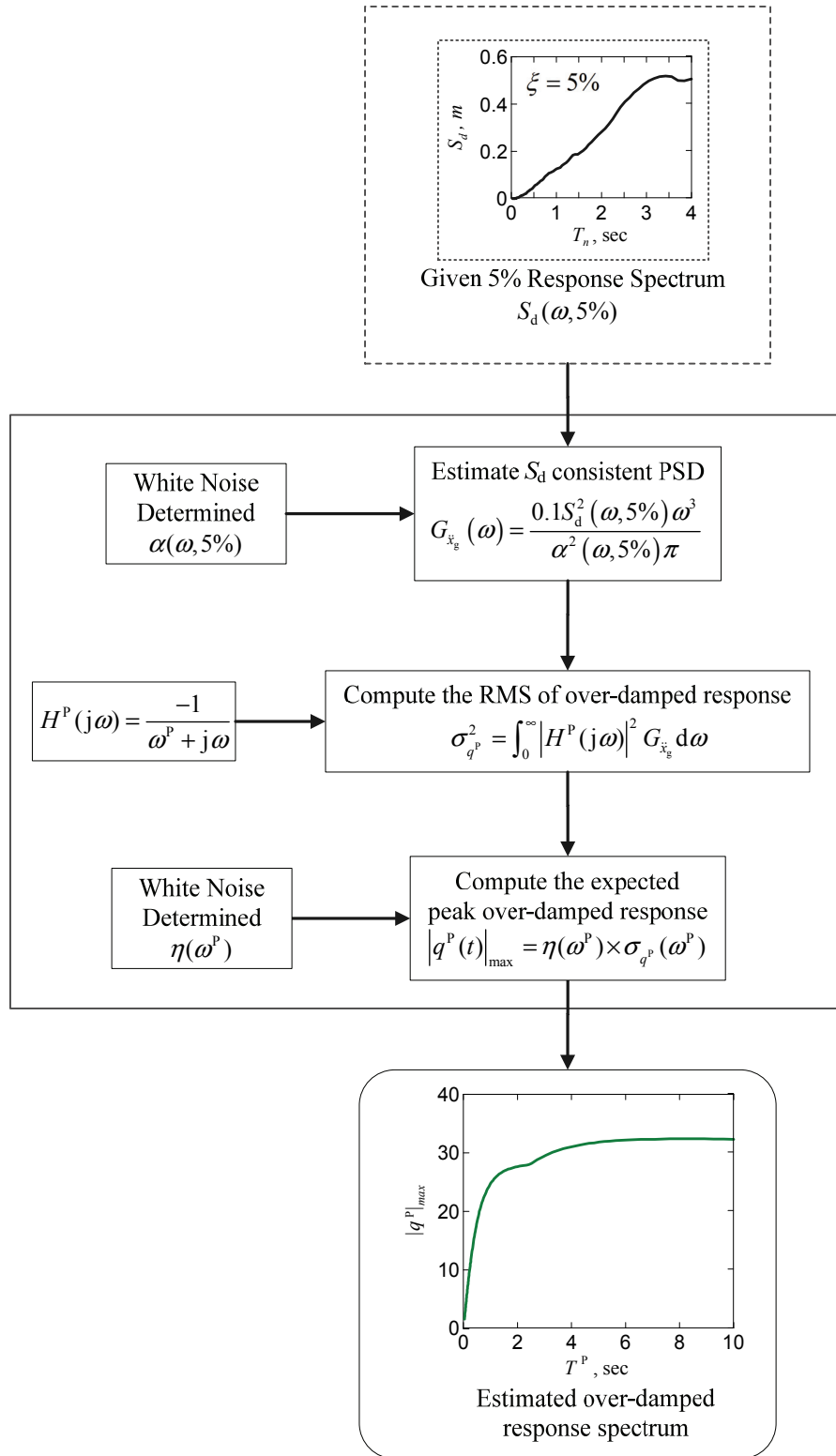


Figure 6.8 over-damped mode response spectrum construction procedures

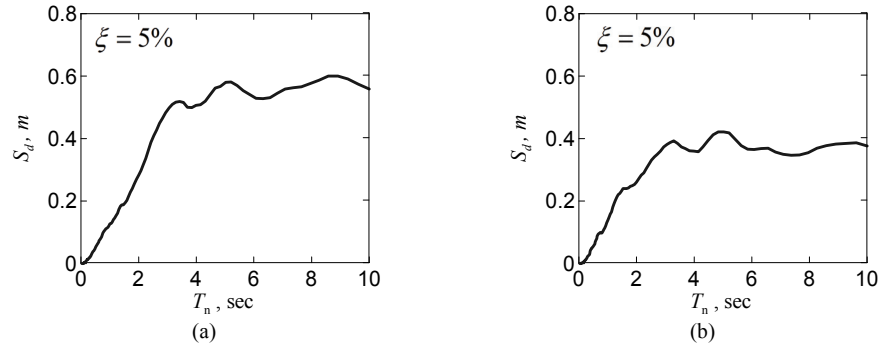


Figure 6.9 Mean 5% damping displacement response spectrum (a) ensemble A (b) ensemble B

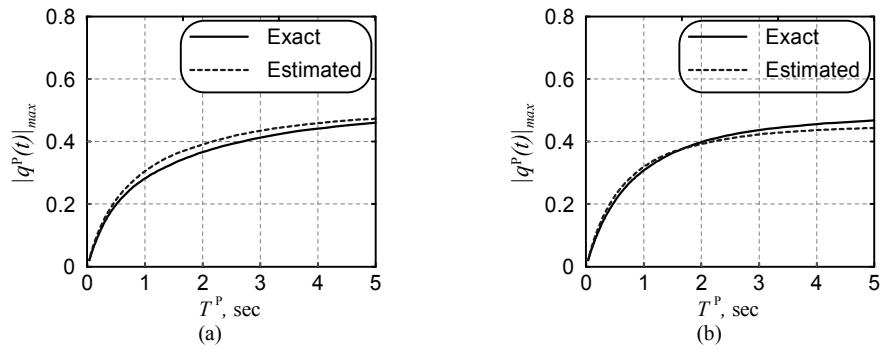


Figure 6.10 Comparisons of exact and estimated over-damped mode response spectrum (a) ensemble A (b) ensemble B



## CHAPTER 7

### ANALYSIS APPLICATION EXAMPLES

#### 7.1 Introduction

In Chapters 3 and 6 using the ground motion history and the response spectrum as input excitations in the modal analysis procedures is given. In this chapter, we demonstrate the applications of these two methods and examine the effects of using the classical damping assumption and ignoring the over-damped modes on the analysis results. This is achieved by using three example buildings which share the same reference frame but with different damper configurations. We first describe the configurations of the three example building frames, followed by the evaluations of the two analysis procedures. It is noted that the procedure developed in Chapter 5 for the response spectrum method is based on the random vibration theory and with the assumptions involving the peak proportional factors. The ground motion is assumed to have a strong stationary phase with broad frequency content and a duration several times longer than the fundamental period of the structure. These assumptions will affect the accuracy of the response spectrum method dealing with real earthquakes.

#### 7.2 Example Building Frames

Three steel frame buildings used in this study are referred to as examples A, B and C (see Figure 7.1). The reference frame for these three examples is adopted from a 5-story shear building used in Hanson and Soong (2001), which has a constant story mass for each floor given as  $m = 408,233$  (kg) and a constant story stiffness for all floors given as  $k = 1.75127 \times 10^6$  (N/m). Each example structure differs in the configuration of damper installation. All the dampers used in these examples are assumed to be linear viscous dampers. Example A has one linear viscous damper added in the first floor of the reference frame, which results in a damping coefficient  $C_A = 2.4 \times 10^7$  (N·sec/m). This example is aimed to represent a highly non-classically damped structure. For example B, each story of the reference frame was equipped with a linear viscous damper. The

resulting damping coefficient for each floor is  $C_B = 1.08 \times 10^7 \text{ N} \cdot \text{sec}/\text{m}$ . This example represents a classically damped structure but some of its modes are over-damped. For example C, the stiffness of the first story was reduced to be 10% of the stiffness of the reference frame and a damper with damping coefficient  $C_C = 3 \times 10^6 \text{ N} \cdot \text{sec}/\text{m}$  is equipped in the first floor to represent an isolated-structure. The inherent damping ratios for the three examples are assumed to be 2% for the first two modes characterized by proportional damping. The resulting mass, damping and stiffness matrices for each example are listed as bellow.

$$\mathbf{M}_A = \mathbf{M}_B = \mathbf{M}_C = 408233 \times \begin{bmatrix} 1 & 0 & 0 & 0 & 0 \\ 0 & 1 & 0 & 0 & 0 \\ 0 & 0 & 1 & 0 & 0 \\ 0 & 0 & 0 & 1 & 0 \\ 0 & 0 & 0 & 0 & 1 \end{bmatrix} \text{ kg} \quad (7.1)$$

$$\mathbf{K}_A = \mathbf{K}_B = 175127 \times \begin{bmatrix} 2 & -1 & 0 & 0 & 0 \\ -1 & 2 & -1 & 0 & 0 \\ 0 & -1 & 2 & -1 & 0 \\ 0 & 0 & -1 & 2 & -1 \\ 0 & 0 & 0 & -1 & 1 \end{bmatrix} \text{ kN}/\text{m} \quad (7.2)$$

$$\mathbf{K}_C = 175127 \times \begin{bmatrix} 1.1 & -1 & 0 & 0 & 0 \\ -1 & 2 & -1 & 0 & 0 \\ 0 & -1 & 2 & -1 & 0 \\ 0 & 0 & -1 & 2 & -1 \\ 0 & 0 & 0 & -1 & 1 \end{bmatrix} \text{ kN}/\text{m} \quad (7.3)$$

$$\mathbf{C}_A = \begin{bmatrix} 24678 & -303 & 0 & 0 & 0 \\ -303 & 678 & -303 & 0 & 0 \\ 0 & -303 & 678 & -303 & 0 \\ 0 & 0 & -303 & 678 & -303 \\ 0 & 0 & 0 & -303 & 375 \end{bmatrix} \text{ kN} \cdot \text{sec}/\text{m} \quad (7.4)$$

$$\mathbf{C}_B = \begin{bmatrix} 22278 & -11103 & 0 & 0 & 0 \\ -11103 & 22278 & -11103 & 0 & 0 \\ 0 & -11103 & 22278 & -11103 & 0 \\ 0 & 0 & -11103 & 22278 & -11103 \\ 0 & 0 & 0 & -11103 & 11175 \end{bmatrix} \text{ kN} \cdot \text{sec}/\text{m} \quad (7.5)$$



$$\mathbf{C}_c = \begin{bmatrix} 3405 & -303 & 0 & 0 & 0 \\ -303 & 678 & -303 & 0 & 0 \\ 0 & -303 & 678 & -303 & 0 \\ 0 & 0 & -303 & 678 & -303 \\ 0 & 0 & 0 & -303 & 375 \end{bmatrix} \text{ kN} \cdot \text{sec}/\text{m} \quad (7.6)$$

The modal properties of each example are determined by eigenvalue analysis programmed in MATLAB by using both forced classical damping assumption and state space approach.

Table 7.1 and Table 7.2 summarize the modal periods and damping ratios for the three examples, respectively. The data listed in these two tables are sorted in an ascending order in terms of the modal period. Data in Table 7.1 and Table 7.2 show that there are two over-damped modes in example A and four over-damped modes in example B even example B is a classically damped structure. For example C, all modes are under-damped and it has a long period in its first mode.

For example A, the damping ratios obtained by using the forced classical damping assumption are significantly different from those exact damping ratios determined from the state space approach. In particular, using the forced classical damping assumption overestimates the damping ratios and the presence of two over-damped modes cannot be observed. In example B, the first modal damping ratio obtained under forced classical damping assumption is 20.2%, which is a reasonable value used in seismic design of structures with added dampers. It should be noted that four modes are over-damped in this case. This reveals the possibility that certain modes could be over-damped in classically damped structures even when the first mode is not heavily damped.

### 7.3 Response History Analysis using Modal Superposition Method

The three example structures, shown in Figure 7.1, demonstrated the application of the proposed general modal response analysis approach presented in Chapter 3. The following approaches are used to compare the analytical assumptions from the view point of structural responses: (1) Using the general modal analysis of Equation (3.61), (2) Using the classical damping assumption while excluding the over-damped modes of

Equation (3.67) as appropriate, and (3) Ignoring the contribution of over-damped modes in the analysis (i.e., considering the first two terms in Equation (3.61) only).

### **7.3.1 Ground Motions**

The ground motion ensemble A used in Section 6.3.3 to verify the accuracy of the transformed over-damped mode response spectrum is adopted again. It consists of a total of 20 far-field ground motions (Vamvatsikos and Cornell 2004). In this study, all records are scaled to have PGA equal to 0.4g and the mean peak responses are presented for comparisons.

### **7.3.2 Comparison of the Analysis Results**

Peak response quantities were then obtained for each history. Their mean values are presented in Table 7.3 to Table 7.5. Five response quantities are included in Table 7.3 to Table 7.5, which are: (a) peak inter-story drift, (b) peak inter-story velocity, (c) story-shear force at maximum drift, (d) maximum general story-shear force (which includes the damping forces as appropriate), and (e) peak floor absolute acceleration. The mean results obtained from the general modal analysis are considered to be the exact values. Figure 7.2 and Figure 7.3 present the mean values of the estimated error arising from the classical damping assumption as well as by ignoring the over-damped modes for the five response quantities.

For example A (see Figure 7.2), using the forced classical damping assumption results in inaccurate results for all the responses considered. And most results determined from the forced classical damping assumption are underestimated and for some response quantities, the errors can be as high as 30% to 40%. The error becomes large as the level of story increases. In addition, the maximum base shear is underestimated by approximately 20%, which may lead to inappropriate design for the foundation systems. The source of errors can be attributed to the inaccurate calculation of damping ratios and modal periods determined under the classical damping assumption. Further, most response quantities are slightly overestimated when over-damped modes are ignored in the response calculations. Exceptions are the peak floor acceleration of the first floor was

underestimated by 48% while the peak inter story velocity of the first floor was overestimated by 40%. This may result in considerable error for the seismic demand estimation of nonstructural components. For example B (see Figure 7.3), the results obtained from using the forced classical damping assumption and excluding the over-damped modes are identical since the over-damped modes are also neglected when adopting classical damping assumption in this study. Apparently these two methods both underestimated the floor acceleration of the first floor and overestimated the floor acceleration of the second floor. For the rest of the structural responses, the effect of ignoring over-damped modes is not significant in this example. For example C, the results from the exact general modal analysis and ignoring over-damped modes effect are the same since there is no over-damped modes being present in this case. Similar to example A, the using forced classical damping assumption cannot conclude the structural responses accurately for those above second story and most of which are underestimated. This implies that for a base-isolated structure the structural responses should be carefully examined when adopting forced classical damping assumption.

From the above comparisons, it may be observed that over-damped modes should be considered appropriately in order to obtain more accurate structural responses more accurately. This is particularly true for structures with non-uniform damper configurations (which may result in highly non-classically damped systems as illustrated in example A). Further, using the forced classical damping assumption may lead to large inaccuracies when the structures are non-classically damped.

#### **7.4 Response Spectrum Analysis**

Having established the applicability of the proposed general modal response analysis procedures, examined the effect of classical damping assumption and illustrated the effect of the over-damped modes, we now proceed to assesses the ability of the improved response spectrum method (GCQC rule) in predicting the peak responses and examine the effect of the classical assumption and over-damped modes when using the response spectrum method. The accuracy and applicability of the proposed GCQC rule is evaluated by conducting response analyses of the same three examples described earlier

numerically. The response quantities calculated are identical to those used in the modal response analysis procedure.

#### **7.4.1 Ground Motions**

The ground motion ensemble used is identical to the one used in the evaluation of the modal analysis procedure presented in Section 7.3.1.

#### **7.4.2 Comparison of the Analysis Results**

Each example building frame was analyzed by using linear response history analysis subjected to each ground motion record listed in the ensemble. The mean linear response analysis results were then used to examine the accuracy of the GCQC rule, including a comparison of the effect of: (1) using the forced classical damping assumption, and (2) ignoring the over-damped modes when they are present. Three sets of results are obtained and compared with the exact values. These three sets are obtained under the following conditions:

1. Results of the first set are obtained based on the proposed GCQC rule, defined by in Equation (6.38). The state space approach was used to derive the mode shapes, modal periods and modal damping ratios. These modal properties were then used to generate the correlation coefficients and peak modal responses required in the GCQC rule. The contributions from over-damped modes are considered when they are present.
2. Results of the second set are based on the modal properties obtained under the forced classical damping assumption. Similar to the GCQC rule, these properties were used to generate the data required in the modal combination rule. The over-damped modes are ignored when they are present. This process is conventionally used for the design and analysis of structures with added damping devices. This rule is referred to as the forced CDA (forced classical damping assumption).
3. Results of the third set are identical to the GCQC rule except that it does not consider the over-damped modes in the modal combination process. This

consideration is aimed to examine the effects of over-damped modes in terms of response quantities. This rule is referred to as the EOM (exclude over-damped modes).

The exact peak modal responses required in each modal combination rule above were obtained by performing response history analysis using the respective modal properties. Comparisons of the results for each example are given in Table 7.6. As seen, the GCQC provides excellent estimates overall. Figure 7.5 shows the estimation errors of each combination rule for example A. It is shown that the GCQC provided excellent results except it overestimated the first floor acceleration by about 35% where the damper is added. The CDA, however, considerably underestimated the peak responses with one exception (overestimated the peak inter-story velocity of the first floor by 25%). The error increases as the level of story increases. This overestimation is more profound for inter-story velocity and floor acceleration. EOM overestimated the inter-story velocity while it underestimated the floor acceleration at the first floor. In this case (Example A), the EOM provided conservative estimates for the rest of the response quantities. Figure 7.6 shows the estimation errors for example B. It is found that the results from CDA and EOM are the same since the structure is classically damped and the over-damped modes are ignored in both cases. Results from these three sets provide acceptable estimates except that they slightly overestimated the floor acceleration of the second floor. The effect of over-damped modes is not significant in this case. This may be attributed to their presence in the higher modes. Figure 7.7 shows the estimation errors for example C, the results estimated by GCQC and EOM are the same since all modes are under-damped in this example. The GCQC again provided good estimates in this example. The results given by CDA are greatly underestimated, particular true for the inter-story velocity.

In general, these results show that the GCQC, which is able to consider the over-damped modes, if exist, can estimate the peak responses accurately. It is found that the inter-story velocity and floor acceleration, as an instance, are significantly influenced by the over-damped modes in these example studies. This is particularly true for the floors at which dampers are installed (Example A). The responses estimated by using the forced classical damping assumption deviate substantially from the exact values (see Figure 7.5).

Most of the responses were underestimated. This is understandable because the modal properties calculated by using the forced classical damping assumption are different from the exact values computed by the state space approach. This implies that the utility of the forced classical damping assumption should be further examined in the design and analysis of structures with added damping devices.

Table 7.1 Modal periods of example buildings A, B and C

Mode	Period (sec)								
	Example A <sup>1,2,3,*</sup>			Example B			Example C		
	Bare frame	Damped frame		Bare frame	Damped frame		Bare frame	Damped frame	
Exact		CDA	Exact		CDA	Exact		CDA	
1	1.07	1.00	1.08	1.07	1.09	1.09	2.28	2.32	2.35
2	0.37	<b>0.46</b>	0.39	0.37	0.44	0.44	0.47	0.47	0.47
3	0.23	0.31	0.25	0.23	0.46	0.46	0.26	0.26	0.26
4	0.18	0.20	0.19	0.18	<b>0.32</b>	NA	0.19	0.19	0.19
5	0.16	0.16	0.16	0.16	<b>0.29</b>	NA	0.16	0.16	0.16
6	NA	<b>0.15</b>	NA	NA	<b>0.11</b>	NA	NA	NA	NA
7	NA	NA	NA	NA	<b>0.08</b>	NA	NA	NA	NA

\*Bold face corresponds to over-damped modes

Table 7.2 Modal damping ratios of example buildings A, B and C

Mode	Damping ratio (%)								
	Example A <sup>1,2,3</sup>			Example B			Example C		
	Bare frame	Damped frame		Bare frame	Damped frame		Bare frame	Damped frame	
Exact		CDA	Exact		CDA	Exact		CDA	
1	2.0	12.9	16.4	2.0	20.2	20.2	3.4	24.6	24.4
2	2.0	NA	37.5	2.0	55.1	55.1	1.8	12.2	12.0
3	2.7	8.3	41.3	2.7	86.3	86.3	2.5	6.7	6.7
4	3.3	5.2	28.7	3.3	NA	110.7	3.2	4.8	4.8
5	3.7	4.1	11.5	3.7	NA	126.2	3.6	4.0	4.0
6	NA	NA	NA	NA	NA	NA	NA	NA	NA
7	NA	NA	NA	NA	NA	NA	NA	NA	NA

1. NA=Not Available
2. Exact=2N dimensional eigenvalue analysis
3. CDA= Classical damping assumption

Table 7.3 Results of mean peak responses of example A via modal superposition methods

Level of story	Response quantities														
	Story drift (mm) <sup>1,2,3</sup>		Inter-story velocity (mm/sec)		Story Shear at Max. Drift (KN)		Max. Story Shear (KN)		Floor Acceleration (g)						
	Exact	CDA	EOM	Exact	CDA	EOM	Exact	CDA	EOM	Exact	CDA	EOM			
1	30	31	30	173	203	237	5194	5471	5292	6765	5885	7097	0.36	0.33	0.19
2	35	28	38	263	182	278	6160	4951	6622	6194	5216	6673	0.43	0.29	0.49
3	30	23	31	233	152	217	5311	4093	5463	5335	4327	5496	0.47	0.32	0.50
4	23	17	24	209	115	205	4093	2953	4142	4104	3126	4161	0.50	0.37	0.51
5	14	9	14	187	63	185	2465	1552	2469	2466	1650	2475	0.62	0.41	0.62

Table 7.4 Results of mean peak responses of example B via modal superposition methods

Level of story	Response quantities														
	Story drift (mm) <sup>1,2,3</sup>		Inter-story velocity (mm/sec)		Story Shear at Max. Drift (KN)		Max. Story Shear (KN)		Floor Acceleration (g)						
	Exact	CDA	EOM	Exact	CDA	EOM	Exact	CDA	EOM	Exact	CDA	EOM			
1	29	29	29	185	184	184	5062	5049	5049	5554	5532	5532	0.30	0.26	0.26
2	26	26	26	160	159	159	4494	4506	4506	4903	4910	4910	0.28	0.31	0.31
3	21	21	21	134	137	137	3683	3682	3682	4035	4044	4044	0.30	0.30	0.30
4	15	15	15	100	101	101	2629	2630	2630	2893	2899	2899	0.35	0.35	0.35
5	8	8	8	54	52	52	1372	1369	1369	1513	1505	1505	0.38	0.38	0.38

Table 7.5 Results of response history analysis of example C via modal superposition methods

Level of story	Response quantities														
	Story drift (mm) <sup>1,2,3</sup>		Inter-story velocity (mm/sec)		Story Shear at Max. Drift (KN)		Max. Story Shear (KN)		Floor Acceleration (g)						
	Exact	CDA	EOM	Exact	CDA	EOM	Exact	CDA	EOM	Exact	CDA	EOM			
1	167	167	167	525	531	525	2927	2928	2927	3482	3395	3482	0.22	0.18	0.22
2	16	14	16	81	48	81	2827	2443	2827	2897	2760	2897	0.22	0.18	0.22
3	13	11	13	80	43	80	2335	1913	2335	2377	2116	2377	0.21	0.17	0.21
4	10	8	10	73	35	73	1734	1339	1734	1760	1464	1760	0.22	0.18	0.22
5	6	4	6	62	22	62	969	698	969	982	754	982	0.25	0.19	0.25

1. Exact=General modal analysis including effects of over-damped modes
2. CDA= Classical damping assumption while over-damped modes excluded
3. EOM= General modal analysis excluding over-damped modes



Table 7.6 Comparisons of results by GCQC, CDA and EOM to mean results of response history analysis for examples A, B and C

Response Quantity	Story	Example A				Example B				Example C			
		Exact	GCQC	CDA	EOM	Exact	GCQC	CDA	EOM	Exact	GCQC	CDA	EOM
Story Drift (mm)	1	30	30	32	30	29	29	29	29	167	168	167	168
	2	35	36	28	38	26	26	26	26	16	16	14	16
	3	30	30	23	31	21	21	21	21	13	13	11	13
	4	23	23	16	23	15	15	15	15	10	9	7	9
	5	14	13	9	13	8	8	8	8	6	5	4	5
Inter-Story Velocity (mm/sec)	1	173	165	216	230	185	192	192	192	525	461	465	461
	2	263	280	173	288	160	156	153	153	81	70	41	70
	3	233	216	145	200	134	127	130	130	80	73	37	73
	4	209	196	108	192	100	94	95	95	73	71	31	71
	5	187	170	59	170	54	50	49	49	62	59	20	59
Story Shear at Max. Drift (KN)	1	5194	5316	5556	5207	5062	5152	5134	5134	2927	2943	2933	2943
	2	6160	6222	4937	6632	4494	4494	4517	4517	2827	2721	2413	2721
	3	5311	5258	4027	5432	3683	3625	3618	3618	2335	2196	1865	2196
	4	4093	3968	2871	4029	2629	2559	2557	2557	1734	1613	1283	1613
	5	2465	2320	1500	2339	1372	1328	1332	1332	969	912	660	912
Max. General Story Shear (KN)	1	6765	6659	7755	7113	5554	5643	5624	5624	3482	3334	3269	3334
	2	6194	6255	4940	6683	4903	4864	4875	4875	2897	2778	2658	2778
	3	5335	5281	4022	5465	4035	3920	3924	3924	2377	2236	2032	2236
	4	4104	3982	2864	4047	2893	2782	2785	2785	1760	1637	1384	1637
	5	2466	2326	1495	2347	1513	1449	1451	1451	982	922	707	922
Floor Acceleration (g)	1	0.36	0.48	1.44	0.19	0.30	0.30	0.30	0.30	0.22	0.22	0.16	0.22
	2	0.43	0.47	0.28	0.46	0.28	0.34	0.33	0.33	0.22	0.19	0.17	0.19
	3	0.47	0.49	0.30	0.48	0.30	0.30	0.30	0.30	0.21	0.19	0.17	0.19
	4	0.50	0.50	0.34	0.50	0.35	0.34	0.34	0.34	0.22	0.20	0.17	0.20
	5	0.62	0.59	0.37	0.59	0.38	0.36	0.36	0.36	0.25	0.23	0.18	0.23

Exact: mean results from the response-history analysis

GCQC: General complete quadratic combination rule

CDA: Complete quadratic combination rule using forced classical damping assumption

EOM: General complete quadratic combination rule excluding over-damped modes

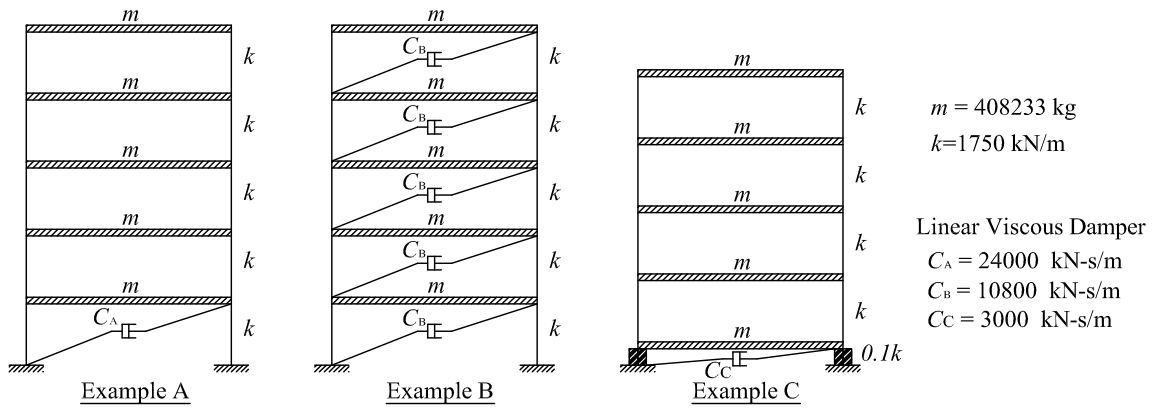


Figure 7.1 Configurations of example building frames A, B and C

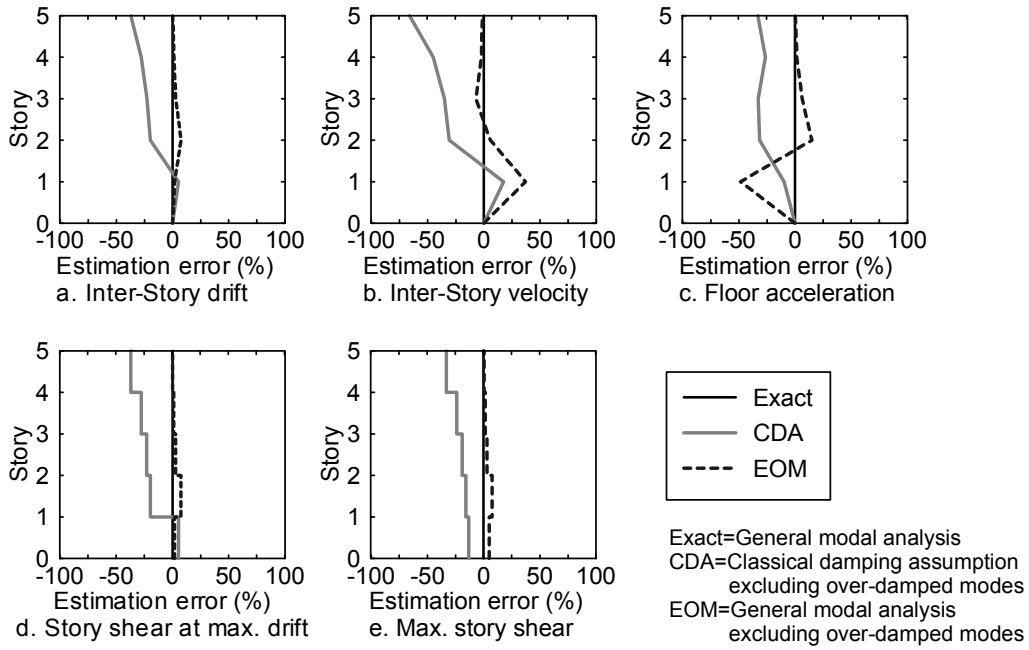


Figure 7.2 Estimated errors of forced classical damping assumption and exclusion of over-damped modes in example A

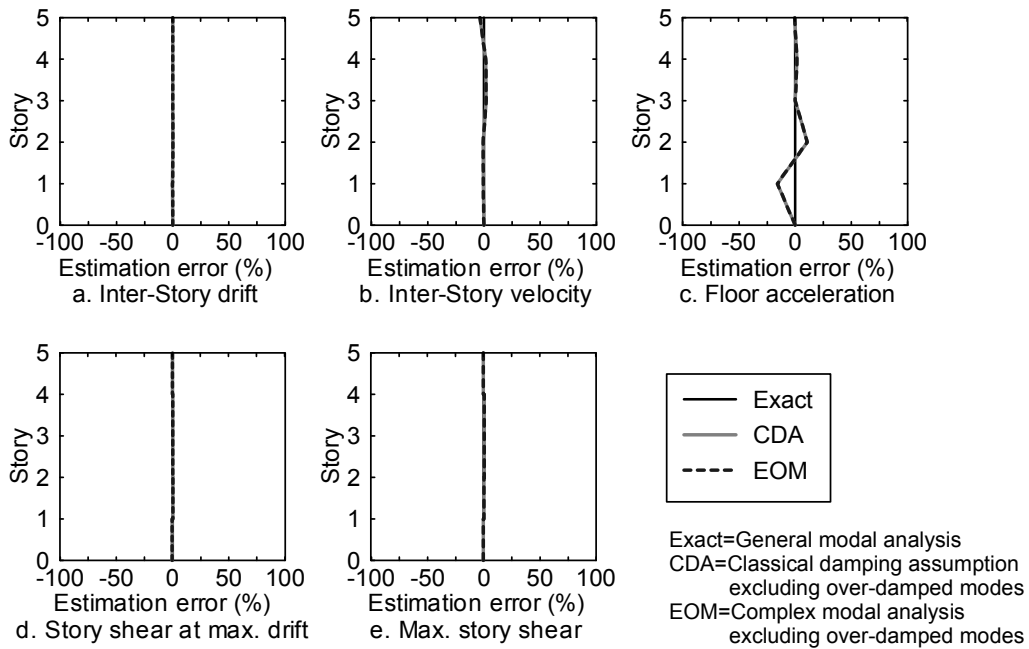


Figure 7.3 Estimated errors of forced classical damping assumption and exclusion of over-damped modes in example B

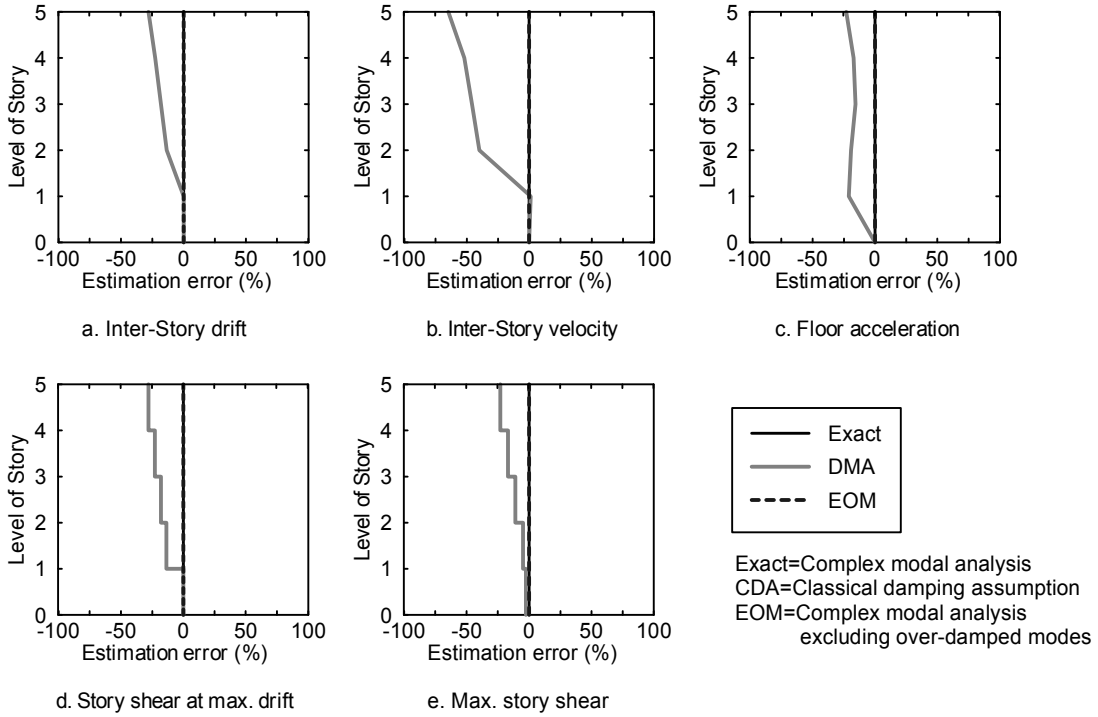


Figure 7.4 Estimated errors of forced classical damping assumption and exclusion of over-damped modes in example C

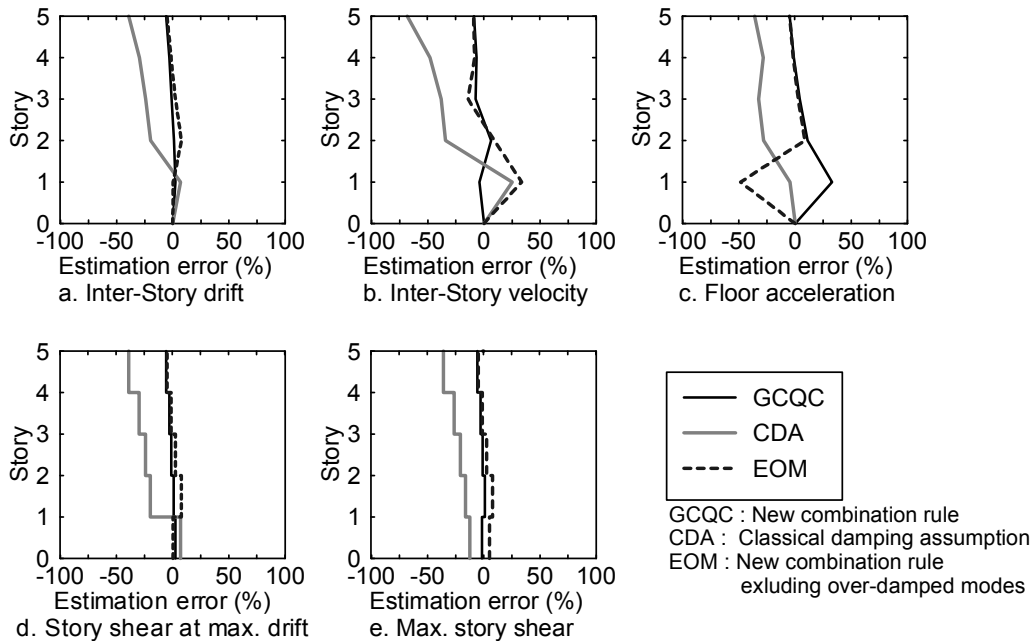


Figure 7.5 Estimated errors due to GCQC, CDA and EOM in example A

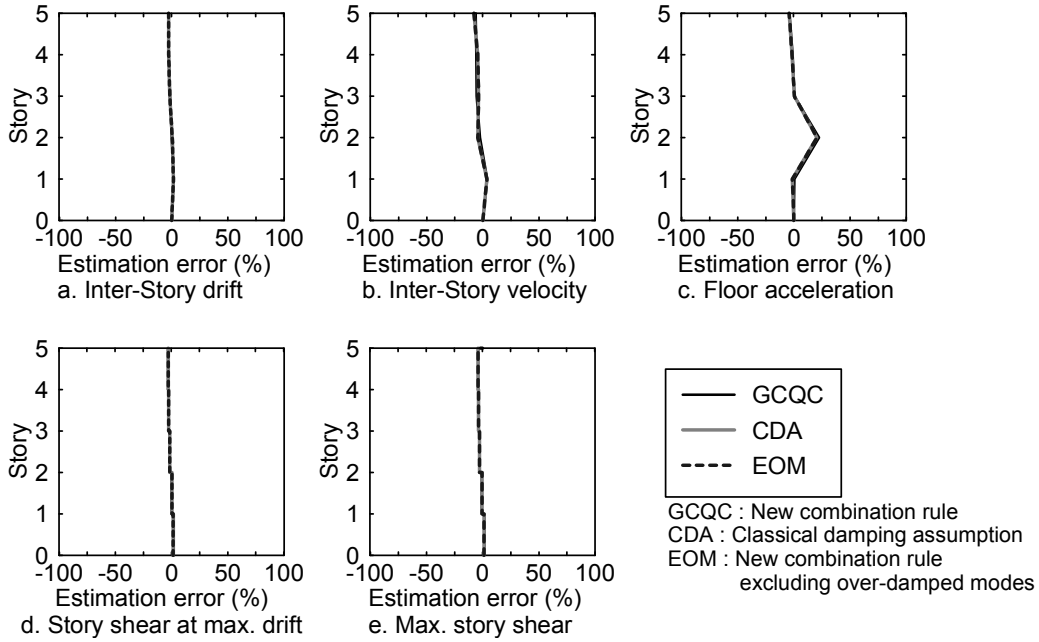


Figure 7.6 Estimated errors due to GCQC,CDA and EOM in example B

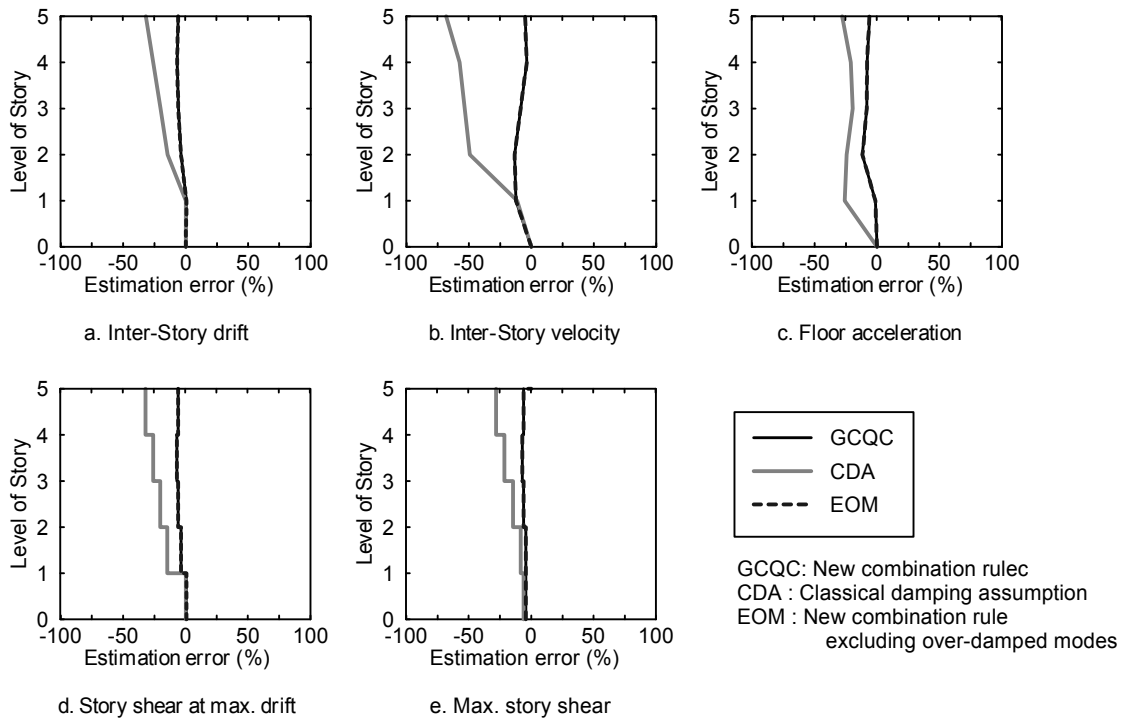


Figure 7.7 Estimated errors due to GCQC,CDA and EOM in example C



## CHAPTER 8

### SUMMARY, CONCLUSIONS AND FUTURE RESEARCH

#### 8.1 Summary

A modal analysis approach for generally damped linear MDOF systems is presented, in which a new ‘over-damped mode’ term is introduced to handle the real eigenvalues and their corresponding eigenvectors when they arise. The central idea to deal with over-damped mode is to consider the associated eigenvalues and eigenvectors individually as a one-order linear system instead of grouping them in pairs. The velocity response vectors and absolute acceleration response vectors expressed in a modal superposition form with the identical modal response quantities required for nodal displacement vectors are derived. These two response vectors are obtained based on the important structural modal properties developed in Chapter 2 of the report. In addition, a unified response form, which is capable of describing most response quantities with interest, is also established. This unified form involves only the modal relative displacement and modal relative velocity of a SDOF system as well as the over-damped mode response of a one order linear system. Also, a general real-valued transformation matrix is established based on the formulations for structural response analysis. This transformation matrix can be used to decouple the equations of motion of a generally damped structure in terms of real-valued modal coordinates, which has been rigorously proved. Furthermore, non-singularity of this matrix and other properties related to general modal transformation, such as modal responses to initial conditions and modal energy distribution, are discussed in details in the report to expose the dynamic nature of the generally damped structural system. When the structural damping matrix satisfies Caughey criterion, the general modal transformation matrix as well as the related formulas and properties can be reduced. Especially, the effective modal mass is brought out consequently by the reduced modal transformation, whose roles in the governing motion equation of the system, structural responses and modal energy distribution are clarified from physical point of view. Based on these properties, a criterion on determining the number of modes that

should be included in the modal analysis for the generally damped linear MDOF system is given in the report

The modal decomposition based on system eigen-analysis and the modal response combination method using design response spectrum to evaluate structural peak response values with interests is one of the most commonly adopted approaches. However, when damping devices are added, the structures are, in general, heavily non-classically damped and some over-damped modes may present. In such circumstances, the conventional CQC or SRSS for the response spectrum method, assuming the structures are classically-damped, is no longer applicable. A new modal combination rule for the response spectrum method, denoted as GCQC, is developed in this report to accommodate the presence of non-classical damping and over-damped modes. This GCQC rule retains the conceptual simplicity of the CQC rule and offers an efficient and accurate estimation of the peak responses of structures with added damping devices. In addition, a procedure to construct the over-damped mode response spectrum from the given design spectrum is also developed. This ensures the applicability of the GCQC rule in engineering practice. Examples show that MDOF systems with added dampers should be modeled as non-classically damped systems and the over-damped modes should be included in the analysis to achieve more reliable estimates.

## 8.2 Conclusions

Major conclusions of this research are:

- (1) An ‘over-damped mode’ is introduced to handle the presence of over-damped modes. This concept treats the real eigenvalues and real eigenvectors individually instead of grouping them in pairs. It can be easily included in dynamics analysis and in control theory.
- (2) Most response quantities of interest can be represented by the unified form given by Equation (3.63) or Equation (3.63). This unified form involves only the three sets of modal responses  $q_i(t)$ ,  $\dot{q}_i(t)$  and  $q_i^p(t)$ .



- (3) When computing the absolute acceleration  $\ddot{\mathbf{x}}_A(t)$ , the modal acceleration  $\ddot{q}(t)$  and ground acceleration  $\ddot{x}_g(t)$  are not required. This is an attractive feature.
- (4) The modal mass of a classically-damped system brought out by the reduced general modal coordinates transformation proposed in this study has clear physical meanings, which is not only useful for structural base shear estimation, but is also important to other type of structural responses in earthquake engineering.
- (5) Two manners to calculate the effective modal mass of generally damped system are proposed in this study, providing a reasonable index for the modal truncation to save computation burden while the accurate response estimates still can be reached.
- (6) When a structural system has a large number of DOFs and Wilson's damping is assumed for the system, the dual modal space approach proposed in the report can be adopted to include the inherent damping of the structure and reduce the scale of the modeling and computation effort for structural response analysis and damping design.
- (7) The conventional combination rules for response spectrum method can be expanded for its application to a generally damped linear MDOF system with the non-classical damping and over-damped modes, and are termed as GCQC and GSRSS. For non-classically damped systems, two additional terms are introduced into the conventional CQC rule, in which two correlation coefficients,  $\rho_{ij}^{VD}$  and  $\rho_{ij}^{VV}$ , are used to consider the correlation between the modal displacement and the modal velocity. When the over-damped modes do exist, they are considered by the over-damped mode response term. The interrelationships between the modal displacement, modal velocity and over-damped mode response are related by another three correlation coefficients,  $\rho_{ij}^{DP}$ ,  $\rho_{ij}^{VP}$  and  $\rho_{ij}^{PP}$ .
- (8) The over-damped mode response spectrum needed in the new combination rule can be easily converted directly from the 5% damping pseudo acceleration

spectrum, which may vary site by site. This construction process is easy and can be well incorporated into the current available analysis programs.

### **8.3 Future Research**

It should be noted that the general modal analysis approach presented in this study is formulated based on a two dimensional structure subjected to single directional excitation and the examples examined are assumed to be a planar shear-type buildings. Neither the three-dimensional systems nor the multiple directional excitations have been considered. Furthermore, the current response analysis method is basically appropriate to estimate the maximum value of a single response quantity along the predefined coordinate system (e.g. the peak inter-story velocity along the predefined X-direction). For those response quantities which are the combination of the several individual response quantities (e.g. the peak damper force or the maximum traveling distance of the isolators in the three dimensional space), the direction of the combined vectors along which the response reaches its maxima may not coincide with any of the predefined directions of the coordinate system. As a matter of fact, the direction is an unknown. For such cases, it is desirable to develop a method, either for time history analysis or response spectrum analysis, to determine the peak value of the spatially combined responses. Of course, this method should be applicable to any generally damped linear MDOF systems, in which the uncertainty of the seismic incidence is also considered. The authors are presently pursuing the following tasks:

- (1) Formulations presented in this study are extended for the application of any three dimensional structures excited by multi-component inputs, including the uncertainty of the seismic incident angles.
- (2) Based on the extended formulation work being established in (1), developing a response-history-based procedure and a response-spectrum-based procedure to predict the peak value of the spatially combined response vector. These procedures will consider the uncertainty of the seismic incidence.

- (3) Development of computer software system which incorporates all the proposed procedures to handle the non-classical damping effect and the over-damped modes when modal analysis approach is employed.
- (4) Research on the nonlinear behavior of structures which are supplemented with nonlinear damping devices and subjected to 3D earthquake excitations. Based on this research result, a linear equivalent MDOF model that can more accurately represent 3D nonlinear structures for response spectrum analysis will be developed. With this equivalent method, new design principles and guidelines based on the developed linear modal analysis for the structure-damper system may be established.



## CHAPTER 9 REFERENCES

- Applied Technology Council (ATC). (2007) “*Guidelines for seismic performance assessment of buildings. ATC-58 35% Draft*”, Applied Technology Council, Redwood city, CA.
- Bathe, K.J. (1995) *Finite Element Procedures in Engineering Analysis*, Prentice-Hall, Englewood Cliffs, NJ.
- Building Seismic Safety Council (BSSC). (2003) “*NEHRP Recommended Provisions for Seismic Regulation for New Buildings and Other Structures, 2003 Edition*”, Report Nos. FEMA 450, Federal Emergency Management Agency, Washington, DC.
- Caughey, T.K. and O’Kelly, M.E.J. (1965) “Classical normal modes in damped linear dynamic systems”, *Journal of Applied Mechanics, ASME*, 32, 583-588.
- Chopra, A.K. (2001). *Dynamics of Structures: Theory and Applications to Earthquake Engineering* (Second Edition), Prentice-Hal: Englewood Cliffs, NJ, USA.
- Chopra, A.K. (2005). *Earthquake dynamics of structures, A Primer*. EERI MNO-11, Oakland, CA.
- Clough, R.W. and Mojtahedi, S. (1976) “Earthquake response analysis considering non-proportional damping”, *Earthquake Engineering and Structural Dynamics*, 4, 489-496.
- Clough, R.W. and Penzien, J. (1993). “*Dynamics of Structures*”, Second Edition, McGraw-Hill, New York, NY.
- Davenport, A.G. (1964). “Note on the distribution of the largest value of a random function with application to gust loading”, *Proceedings, Institution of Civil Engineers*, 28, 187-196.
- Der Kiureghian, A. (1980). “Structural response to stationary excitation”, *Journal of the Engineering Mechanics Division, ASCE*, 106, 1195-1213.
- Der Kiureghian, A. (1981). “A response spectrum method for random vibration analysis of MDF systems”, *Earthquake Engineering and Structural Dynamics*, 9, 419-435.

- Foss, F.K. (1958). "Co-ordinates which uncouple the linear dynamic systems", *Journal of Applied Mechanics, ASME*, 24, 361-364.
- Girard, A. and Imbert, J.F. (1991). "Modal Effective Mass Models in Structural Dynamic". *Proceeding of 9<sup>th</sup> International Modal Analysis Conference*, Florence, Italy, 15-18, April, Society for Experimental Mechanics, New York.
- Greenberg, M. D. (1998) "Advanced Engineering Mathematics", Second Edition, Prentice Hall, Upper Saddle River, N.J.
- Gupta, A.K. and Jaw, J.-W. (1986). "Response spectrum method for nonclassically damped systems", *Nuclear Engineering and Design*, 91, 161-169.
- Hanson, R.D. and Soong T.T. (2001). "Seismic design with supplemental energy dissipation devices", EERI, MNO-8, Oakland, CA.
- Hart, G.C. and Wong, K. (1999). *Structural Dynamics for Structural Engineers*, Wiley & Sons, Inc., New York, USA.
- Inman, D.J. and Andry, Jr. A.N. (1980). "Some results on the nature of eigenvalues of discrete damped linear systems", *Journal of Applied Mechanics, ASME*, 47, 927-930.
- International Code Council, (2003). "2003 International Building Code", ICBO, Whittier, CA.
- Igusa, T., Der Kiurghian, A. and Sackman, J.L. (1984). "Modal decomposition method for stationary response of non-classically damped systems", *Earthquake Engineering and Structural Dynamics*, 12, 121-136.
- Lancaster, P. (1966). *Lambda-matrices and vibrating systems*, Pergamon Press, Oxford, New York.
- Lin, W. H. and Chopra A. K., (2003) "Earthquake response of symmetric and asymmetric one-story elastic systems with nonlinear fluid viscous dampers or nonlinear viscoelastic dampers." *EERC Report*, No. EERC-2003-02, Berkeley, CA, USA
- Maldonado, G.O. and Singh, M.P. (1991). "An improved response spectrum method for calculating seismic design response. Part 2: Non-classically damped structures", *Earthquake Engineering and Structural Dynamics*, 20(7): 637-649.

- Ramirez, O. M., Constantinou, M. C., Kircher, C. A., Whittaker, A. S., Johnson, M. W., Gomez, J. D. and Chrysostomou, C. Z. (2000) *Development and evaluation of simplified procedures for analysis and design of buildings with passive energy dissipation systems*, MCEER Report 00-0010 Revision 1, MCEER, University at Buffalo, Buffalo, NY, USA.
- Rosenblueth, E. (1951). *A basis for aseismic design. Ph.D. Thesis*, University of Illinois, Urbana, USA.
- Sedaghati, R., Scoucy, Y and Etienne, N. (2003). "Efficient Estimation of Effective Mass for Complex Structures under Base Excitations". *Canadian Aeronautics and Space Journal*, Vol. 49, No. 3, 135-143.
- Singh, M.P. (1980). "Seismic response by SRSS for nonproportional damping", *Journal of the Engineering Mechanics Division, ASCE*, 106(6), 1405-1419.
- Singh, M.P. and Ghafory-Ashtiany, M. (1986). "Modal time-history analysis of non-classically damped structures for seismic motions", *Earthquake Engineering and Structural Dynamics*, 1986, 14, 133-146.
- Sinha, R. and Igusa, T. (1995). "CQC and SRSS methods for non-classically damped structures", *Earthquake Engineering and Structural Dynamics*, 24, 615-619.
- Song, JW., Chu, Y.-L., Liang, Z. and Lee, G.C. (2007). "Estimation of peak relative velocity and peak absolute acceleration of linear SDOF systems", *Earthquake Engineering and Engineering Vibration*, 6(1), 1-10.
- Takewaki, I. (2004). "Frequency domain modal analysis of earthquake input energy to highly damped passive control structures", *Earthquake Engineering and Structural Dynamics*, 33, 575-590.
- Traill-Nash, R.W. (1981). "Modal methods in the dynamics of systems with non-classical damping", *Earthquake Engineering and Structural Dynamics*, 9, 153-169.
- Tsopelas, P., Constantinou, M. C., Kircher, C. A. and Whittaker, A S. (1997) *Evaluation of Simplified Methods of Analysis for Yielding Structures*, NCEER Report 97-0012 NCEER, University at Buffalo, Buffalo, NY, USA.

- Vamvatsikos, D. and Cornell, C.A. (2004). Applied Incremental dynamic analysis. *Earthquake Spectra*, 20(2), 523-553.
- Vanmarcke, E.H. (1972). “Properties of spectral moments with applications to random vibration”, *Journal of the Engineering Mechanics Division*, ASCE, 98, 425-446.
- Veletsos, A.S. and Ventura, C.E. (1986). “Modal analysis of non-classically damped linear systems”, *Earthquake Engineering and Structural Dynamics*, 14, 217-243.
- Ventura, C.E. (1985). “Dynamic analysis of nonclassically damped systems”, *Ph.D. Thesis*. Rice University, Houston, Texas, USA.
- Villaverde, R. (1988). “Rosenblueth’s modal combination rule for systems with non-classical damping”, *Earthquake Engineering and Structural Dynamics*, 16, 315-328.
- Warburton, G.B. and Soni, S.R. (1977). “Errors in response calculations of non-classically damped structures”, *Earthquake Engineering and Structural Dynamics*, 5, 365-376.
- Wilkinson, J.H. (1965). *“The algebraic eigenvalue problem”*, Oxford University Press, UK
- Wilson, E.L. (2004). *Static & Dynamic Analysis of Structures* (Fourth Edition), Computers and Structures, Inc., Berkeley, California, USA.
- Yang, J.N., Sarkani, S. and Long, F.X. (1987). “Modal Analysis of Nonclassically Damped Structural Systems Using Canonical Transformation”, Technical Report NCEER-87-0019, National Center for Earthquake Engineering Research, State University of New York at Buffalo, Buffalo, NY, USA.
- Yang, J.N., Sarkani, S. and Long, F.X. (1988). “A Response Spectrum Approach for Analysis of Nonclassically Damped Structures”, Technical Report NCEER-88-0020, National Center for Earthquake Engineering Research, State University of New York at Buffalo, Buffalo, NY, USA.
- Zhou, X.Y., Yu, R. and Dong, D. (2004). “Complex mode superposition algorithm for seismic responses of non-classically damped linear MDOF system”, *Journal of Earthquake Engineering*, 8(4), 597-641.



## APPENDIX A

### NON-SINGULARITY OF MATRICES $\mathbf{A}$ , $\mathbf{B}$ , $\hat{\mathbf{a}}$ AND $\hat{\mathbf{b}}$

#### A.1 Non-Singularity of $\mathbf{A}$ and $\mathbf{B}$

Assuming that the studied structural system is completely constrained and has no zero-valued mass for all considered DOFs, it is followed that  $\det(\mathbf{M}) \neq 0$ ,  $\det(\mathbf{K}) \neq 0$  and no zero eigenvalues exist in the eigen-system expressed by equation (4). Here  $\det(\bullet)$  is a determinant operator for a square matrix. Based on these conditions, the following results can be deduced.

$$\begin{aligned} \det(\mathbf{A}) &= \det \begin{pmatrix} \mathbf{0} & \mathbf{M} \\ \mathbf{M} & \mathbf{C} \end{pmatrix} = \det \left[ \begin{pmatrix} \mathbf{0} & \mathbf{I} \\ \mathbf{I} & \mathbf{CM}^{-1} \end{pmatrix} \begin{pmatrix} \mathbf{M} & \mathbf{0} \\ \mathbf{0} & \mathbf{M} \end{pmatrix} \right] \\ &= \det \begin{pmatrix} \mathbf{0} & \mathbf{I} \\ \mathbf{I} & \mathbf{CM}^{-1} \end{pmatrix} \cdot \det \begin{pmatrix} \mathbf{M} & \mathbf{0} \\ \mathbf{0} & \mathbf{M} \end{pmatrix} = (-1)^N \det(\mathbf{M}^2) \neq 0 \end{aligned} \quad (\text{A.1})$$

and

$$\det(\mathbf{B}) = \det \begin{pmatrix} -\mathbf{M} & \mathbf{0} \\ \mathbf{0} & \mathbf{K} \end{pmatrix} = \det(-\mathbf{MK}) = (-1)^N \det(\mathbf{M}) \cdot \det(\mathbf{K}) \neq 0 \quad (\text{A.2})$$

which means that  $\mathbf{A}$  and  $\mathbf{B}$  are non-singular matrices, and further,  $\mathbf{A}^{-1}\mathbf{B}$  exists and is also a non-singular matrix.

#### A.2 Non-Singularity of $\hat{\mathbf{a}}$ and $\hat{\mathbf{b}}$

Since  $\mathbf{A}^{-1} = \begin{pmatrix} -\mathbf{M}^{-1}\mathbf{C}\mathbf{M}^{-1} & \mathbf{M}^{-1} \\ \mathbf{M}^{-1} & \mathbf{0} \end{pmatrix}$ , the following equation can be derived

$$\mathbf{A}^{-1}\mathbf{B} = \begin{pmatrix} -\mathbf{M}^{-1}\mathbf{C}\mathbf{M}^{-1} & \mathbf{M}^{-1} \\ \mathbf{M}^{-1} & \mathbf{0} \end{pmatrix} \begin{pmatrix} -\mathbf{M} & \mathbf{0} \\ \mathbf{0} & \mathbf{K} \end{pmatrix} = \begin{pmatrix} \mathbf{M}^{-1}\mathbf{C} & \mathbf{M}^{-1}\mathbf{K} \\ -\mathbf{I} & \mathbf{0} \end{pmatrix} = -\mathbf{A}_s \quad (\text{A.3})$$

where

$$\mathbf{A}_S = -\mathbf{A}^{-1}\mathbf{B} = \begin{pmatrix} -\mathbf{M}^{-1}\mathbf{C} & -\mathbf{M}^{-1}\mathbf{K} \\ \mathbf{I} & \mathbf{0} \end{pmatrix} \in \mathbb{R}^{2N \times 2N} \quad (\text{A.4})$$

is a well-known the state coefficient matrix of a linear vibratory system.

From Equation (A.4), the general eigen-equation associated with it can be changed into an equivalent standard eigen-equation:

$$\mathbf{A}_S \boldsymbol{\psi} = \lambda \boldsymbol{\psi} \quad (\text{A.5})$$

If there are no repeated eigenvalues in the system, all eigenvector solved from (A.4) or (A.5) are independent with respect to each other, implying that the eigenvector matrix  $\boldsymbol{\Psi}$  will be a non-singular matrix, that is,  $\boldsymbol{\Psi}^{-1}$  exists (Wilkinson 1965) and satisfies following relationship:

$$\boldsymbol{\Psi}^{-1} \mathbf{A}_S \boldsymbol{\Psi} = \boldsymbol{\Lambda} \in \mathbb{C}^{2N \times 2N} \quad (\text{A.6})$$

where  $\boldsymbol{\Lambda} = \text{diag}(\lambda_1, \lambda_2 \dots \lambda_{N_c}, \lambda_1^*, \lambda_2^* \dots \lambda_{N_c}^*, \lambda_1^p, \lambda_2^p \dots \lambda_{N_p}^p)$  is well known as the system spectrum matrix. With the assumption of non-zero eigenvalues,  $\det(\boldsymbol{\Lambda}) \neq 0$  follows.

According to the orthogonality shown in Equations (2.27) and (2.28), following results can be obtained, that are

$$\det(\hat{\mathbf{a}}) = \prod_{i=1}^{N_c} a_i \prod_{i=1}^{N_c} a_i^* \prod_{i=1}^{N_p} a_i^p = \det(\boldsymbol{\Psi}^T \mathbf{A} \boldsymbol{\Psi}) = \det(\boldsymbol{\Psi}^T) \cdot \det(\mathbf{A}) \cdot \det(\boldsymbol{\Psi}) \neq 0 \quad (\text{A.7})$$

$$\det(\hat{\mathbf{b}}) = \prod_{i=1}^{N_c} b_i \prod_{i=1}^{N_c} b_i^* \prod_{i=1}^{N_p} b_i^p = \det(\boldsymbol{\Psi}^T \mathbf{B} \boldsymbol{\Psi}) = \det(\boldsymbol{\Psi}^T) \cdot \det(\mathbf{B}) \cdot \det(\boldsymbol{\Psi}) \neq 0 \quad (\text{A.8})$$

Therefore,  $\hat{\mathbf{a}}$  and  $\hat{\mathbf{b}}$  are non-singular and diagonal matrices. And it can be observed that

$$\hat{\mathbf{b}} = -\hat{\mathbf{a}} \boldsymbol{\Lambda} = -\boldsymbol{\Lambda} \hat{\mathbf{a}} \quad (\text{A.9})$$

$$\boldsymbol{\Lambda} = -\hat{\mathbf{b}} \hat{\mathbf{a}}^{-1} = -\hat{\mathbf{a}}^{-1} \hat{\mathbf{b}} \quad (\text{A.10})$$

## APPENDIX B

### PROOF OF CAUGHEY CRITERION

**Theorem** : There exists a real matrix which diagonalizes matrices  $\mathbf{M}$ ,  $\mathbf{C}$  and  $\mathbf{K}$  simultaneously if, and only if, the following condition holds true.

$$\mathbf{C}\mathbf{M}^{-1}\mathbf{K} = \mathbf{K}\mathbf{M}^{-1}\mathbf{C} \in \mathbb{R}^{N \times N} \quad (\text{B.1})$$

*Proof:*

Let  $\Phi_0 \in \mathbb{R}^{N \times N}$  denote the eigenvector matrix that is solved from eigen-equation  $-\lambda_0 \mathbf{M}\Phi_0 + \mathbf{K}\Phi_0 = \mathbf{0}$  and has been normalized with respect to the mass matrix  $\mathbf{M}$  and  $\Lambda_0 = \text{diag}(\lambda_{0i}) = \text{diag}(\omega_{0i}^2) \in \mathbb{R}^{N \times N}$  denote the eigenvalue matrix determined from the eigenvalue problem of the associated undamped system. It is well known that

$$\Phi_0^T \mathbf{M} \Phi_0 = \mathbf{I} \quad (\text{B.2})$$

$$\Phi_0^T \mathbf{K} \Phi_0 = \Lambda_0 \quad (\text{B.3})$$

where  $\mathbf{I}$  is an  $N \times N$  identity matrix. From Equation (B.2), it can be shown that

$$\mathbf{M}^{-1} = \Phi_0 \Phi_0^T \quad (\text{B.4})$$

Further, using Equation (B.4) in Equation (B.3), it can be shown that

$$\mathbf{M}^{-1}\mathbf{K} = \Phi_0 \Lambda_0 \Phi_0^{-1} \in \mathbb{R}^{N \times N} \quad (\text{B.5})$$

Note that the mass matrix  $\mathbf{M}$  and the stiffness matrix  $\mathbf{K}$  can be diagonalized by the eigenvector matrix  $\Phi_0$ . Thus one only needs to prove that (1) whether the eigenvector matrix  $\Phi_0$  can diagonalize the damping matrix  $\mathbf{C}$  when  $\mathbf{C}\mathbf{M}^{-1}\mathbf{K} = \mathbf{K}\mathbf{M}^{-1}\mathbf{C}$  holds and, (2) whether the  $\mathbf{C}\mathbf{M}^{-1}\mathbf{K} = \mathbf{K}\mathbf{M}^{-1}\mathbf{C}$  holds when the eigenvector matrix  $\Phi_0$  is able to diagonalize the damping matrix  $\mathbf{C}$ .

(a) When  $\mathbf{C}\mathbf{M}^{-1}\mathbf{K} = \mathbf{K}\mathbf{M}^{-1}\mathbf{C}$  holds true

Suppose that damping matrix  $\mathbf{C}$  meets the criterion shown in Equation (B.1). Let us rewrite Equation (B.1) as

$$\mathbf{C}(\mathbf{M}^{-1}\mathbf{K}) = (\mathbf{M}^{-1}\mathbf{K})^T \mathbf{C} \quad (\text{B.6})$$

Substituting Equation (B.5) into Equation (B.6) leads to

$$\begin{aligned} \mathbf{C}\Phi_0\Lambda_0\Phi_0^{-1} &= (\Phi_0\Lambda_0\Phi_0^{-1})^T \mathbf{C} \\ &= \Phi_0^{-T}\Lambda_0\Phi_0^T \mathbf{C} \end{aligned} \quad (\text{B.7})$$

Pre-multiply  $\Phi_0^T$  and post-multiply  $\Phi_0$  to both sides of Equation (B.7), we can obtain

$$\Phi_0^T \mathbf{C} \Phi_0 \Lambda_0 = \Lambda_0 \Phi_0^T \mathbf{C} \Phi_0 \quad (\text{B.8})$$

Assume that

$$\mathbf{Q} = \Phi_0^T \mathbf{C} \Phi_0 = \begin{bmatrix} q_{11} & q_{12} & \cdots & q_{1N} \\ q_{21} & q_{22} & \cdots & q_{2N} \\ \cdots & \cdots & \cdots & \cdots \\ q_{N1} & q_{N2} & \cdots & q_{NN} \end{bmatrix} \in \mathbb{R}^{N \times N} \quad (\text{B.9})$$

Note that  $\mathbf{Q}$  is a symmetric matrix. Consequently, Equation (B.8) becomes

$$\mathbf{Q}\Lambda_0 = \Lambda_0\mathbf{Q} \in \mathbb{R}^{N \times N} \quad (\text{B.10})$$

Equation (B.10) can also be expressed as

$$\begin{bmatrix} q_{11}\lambda_1 & q_{12}\lambda_2 & \cdots & q_{1N}\lambda_N \\ q_{21}\lambda_1 & q_{22}\lambda_2 & \cdots & q_{2N}\lambda_N \\ \cdots & \cdots & \cdots & \cdots \\ q_{N1}\lambda_1 & q_{N2}\lambda_2 & \cdots & q_{NN}\lambda_N \end{bmatrix} = \begin{bmatrix} q_{11}\lambda_1 & q_{12}\lambda_1 & \cdots & q_{1N}\lambda_1 \\ q_{21}\lambda_2 & q_{22}\lambda_2 & \cdots & q_{2N}\lambda_2 \\ \cdots & \cdots & \cdots & \cdots \\ q_{N1}\lambda_N & q_{N2}\lambda_N & \cdots & q_{NN}\lambda_N \end{bmatrix} \quad (\text{B.11})$$

It is known that when two matrices are equal, their corresponding elements must be identical. Thus, one has

$$q_{ij}\lambda_j = q_{ij}\lambda_i \in \mathbb{R} \quad (\text{B.12})$$

Equation (B.12) is rearranged as

$$(\lambda_j - \lambda_i)q_{ij} = 0 \in \mathbb{R} \quad (\text{B.13})$$

in which  $i, j=1, 2, \dots, N$ .

As the aforementioned, we assume that there are no repeated eigenvalues in the studied vibration system. Therefore, when  $i \neq j$ , i.e.,  $(\lambda_i - \lambda_j) \neq 0$ , the off-diagonal terms  $q_{ij}$  must be equal to zero. This means that  $\mathbf{Q}$  is a diagonal matrix, showing that the eigenvector matrix  $\mathbf{\Lambda}_0$  is able to diagonalize the damping matrix  $\mathbf{C}$ .

**(b)** When  $\mathbf{\Phi}_0$  diagonalizes  $\mathbf{C}$

Suppose that  $\mathbf{\Phi}$  is able to diagonalize the damping matrix  $\mathbf{C}$  as

$$\mathbf{\Phi}_0^T \mathbf{C} \mathbf{\Phi}_0 = \hat{\mathbf{C}} = \begin{bmatrix} c_1 & & 0 \\ & c_1 & \ddots \\ & 0 & & c_N \end{bmatrix} \quad (\text{B.14})$$

Let us rewrite Equation (B.14) in the following form

$$\mathbf{C} = \mathbf{\Phi}_0^{-T} \hat{\mathbf{C}} \mathbf{\Phi}_0^{-1} \quad (\text{B.15})$$

Assembling Equations (B.5) and (B.15), it can be found that the terms  $\mathbf{C}(\mathbf{M}^{-1}\mathbf{K})$  and  $(\mathbf{M}^{-1}\mathbf{K})^T \mathbf{C}$  can be represented as

$$\begin{aligned} \mathbf{C}(\mathbf{M}^{-1}\mathbf{K}) &= \mathbf{\Phi}_0^{-T} \hat{\mathbf{C}} \mathbf{\Phi}_0^{-1} \mathbf{\Phi}_0 \mathbf{\Lambda}_0 \mathbf{\Phi}_0^{-1} \\ &= \mathbf{\Phi}_0^{-T} \hat{\mathbf{C}} \mathbf{\Lambda}_0 \mathbf{\Phi}_0^{-1} \end{aligned} \quad (\text{B.16})$$

$$\begin{aligned} (\mathbf{M}^{-1}\mathbf{K})^T \mathbf{C} &= (\mathbf{\Phi}_0 \mathbf{\Lambda}_0 \mathbf{\Phi}_0^{-1})^T \mathbf{\Phi}_0^{-T} \hat{\mathbf{C}} \mathbf{\Phi}_0^{-1} \\ &= \mathbf{\Phi}_0^{-T} \mathbf{\Lambda}_0 \mathbf{\Phi}_0^T \mathbf{\Phi}_0^{-T} \hat{\mathbf{C}} \mathbf{\Phi}_0^{-1} \\ &= \mathbf{\Phi}_0^{-T} \mathbf{\Lambda}_0 \hat{\mathbf{C}} \mathbf{\Phi}_0^{-1} \end{aligned} \quad (\text{B.17})$$

Note that both  $\mathbf{\Lambda}_0$  and  $\hat{\mathbf{C}}$  are diagonal matrices. Thus, the following identity holds.

$$\Lambda_0 \hat{\mathbf{C}} = \hat{\mathbf{C}} \Lambda_0 \quad (\text{B.18})$$

Equation (B.18) suggests that the identity

$$\begin{aligned} \mathbf{C}(\mathbf{M}^{-1}\mathbf{K}) &= (\mathbf{M}^{-1}\mathbf{K})^T \mathbf{C} \\ &= \mathbf{K}\mathbf{M}^{-1}\mathbf{C} \end{aligned} \quad (\text{B.19})$$

holds true.

It is observed from the proof that there is no specific constraint applied to the form of the damping matrix  $\mathbf{C}$ , implying that a system developing over-damped modes is also categorized as a classically damped system as long as it satisfies the Caughey criterion.

When damping matrix  $\mathbf{C}$  satisfies Caughey criterion, let

$$\boldsymbol{\varphi} = \boldsymbol{\Phi}_0 \tilde{\boldsymbol{\varphi}} \quad (\text{B.20})$$

Substituting Equation (B.20) into the original format of Equation (2.4) for coordinate transformation, which is expressed as

$$(\lambda^2 \mathbf{M} + \lambda \mathbf{C} + \mathbf{K}) \boldsymbol{\varphi} = \mathbf{0} \in \mathbb{R}^N \quad (\text{B.21})$$

we have,

$$(\lambda^2 \mathbf{M} + \lambda \mathbf{C} + \mathbf{K}) \boldsymbol{\Phi}_0 \tilde{\boldsymbol{\varphi}} = \mathbf{0} \in \mathbb{R}^N \quad (\text{B.22})$$

Pre-multiplying  $\boldsymbol{\Phi}_0^T$  to the above equations and further using Equations (B.2), (B.3) and (B.14) yields

$$(\lambda^2 \mathbf{I} + \lambda \hat{\mathbf{C}} + \Lambda_0) \tilde{\boldsymbol{\varphi}} = \mathbf{0} \in \mathbb{R}^N \quad (\text{B.23})$$

Since  $\mathbf{I}$ ,  $\hat{\mathbf{C}}$  and  $\Lambda_0$  are all diagonal matrix, Equation (B.23) can be divided as a  $N$  decoupled eigen-equations, in which the  $i$ th equation is given by

$$(\lambda^2 + \lambda c_i + \omega_{0i}^2) \tilde{\varphi}_i = 0 \in \mathbb{R} \quad (\text{B.24})$$

where  $\tilde{\varphi}_i$  ( $i=1,2,\dots,N$ ) can be any non zero number and

$$\lambda^2 + \lambda c_i + \omega_{0i}^2 = 0 \in \mathbb{R} \quad (\text{B.25})$$

The eigen-value solved for Equation (B.25) is easily expressed as

$$\lambda_r = \frac{1}{2} \left( -c_i \pm \sqrt{c_i^2 - 4\omega_{0i}^2} \right) \in \mathbb{C} \quad (\text{B.26})$$

In the following, we will discuss Equation (B.26) for three cases with different damping levels.

**(a)** When  $c_i < 2\omega_{0i}$ , the corresponding mode belongs to a under-damped subsystem and Equation (B.26) becomes

$$\lambda_r = \frac{1}{2} \left( -c_i \pm j\sqrt{4\omega_{0i}^2 - c_i^2} \right) = -\xi_i \omega_{0i} \pm j\sqrt{1 - \xi_i^2} \omega_{0i} \in \mathbb{C} \quad (r=1,2,\dots,N_c) \quad (\text{B.27})$$

where  $\xi_r = \xi_i = \frac{c_i}{2\omega_{0i}} = \frac{\boldsymbol{\varphi}_i^T \mathbf{C} \boldsymbol{\varphi}_i}{2\omega_{0i} \boldsymbol{\varphi}_i^T \mathbf{M} \boldsymbol{\varphi}_i} < 1$  is well known as the  $r$ th modal damping ratio. To

all under-damped modes, the modal properties and responses solution method are exactly same as those for classically under-damped modes. Note that Equation (B.27) includes two conjugate eigenvalues, corresponding to one real mode with circular natural frequency  $\omega_r = \omega_{0i}$ . When obtaining the eigen-solutions based on the state space approach, any eigen-values for an under-damped real mode always appear in a conjugate pair, even for a non-damping mode. And the conjugate pairs of eigenvalues and corresponding eigenvectors belong to different eigen-solutions, even though they are considered as one mode. Regarding to the modal shape, for simplicity, we can set  $\tilde{\varphi}_i = 1$  (similar to a normalization factor) and further have  $\boldsymbol{\varphi}_r = \tilde{\varphi}_i \boldsymbol{\varphi}_{0i} = \boldsymbol{\varphi}_{0i} \in \mathbb{R}^N$  after considering Equation (B.20).

(b) When  $c_i > 2\omega_{0i}$ , the corresponding mode belongs to a over-damped subsystem and Equation (B.26) becomes

$$\lambda_r = -\zeta_i \omega_{0i} \pm \sqrt{\zeta_i^2 - 1} \omega_{0i} \in \mathbb{R} \quad (r = 1, 2 \dots N_p / 2) \quad (\text{B.28})$$

that is,

$$\omega_{r1}^p = \zeta_i \omega_{0i} - \sqrt{\zeta_i^2 - 1} \omega_{0i} > 0 \in \mathbb{R} \quad (\text{B.29})$$

$$\omega_{r2}^p = \zeta_i \omega_{0i} + \sqrt{\zeta_i^2 - 1} \omega_{0i} > 0 \in \mathbb{R} \quad (\text{B.30})$$

where  $\zeta_i = \frac{c_i}{2\omega_{0i}} = \frac{\boldsymbol{\varphi}_i^T \mathbf{C} \boldsymbol{\varphi}_i}{2\omega_{0i} \boldsymbol{\varphi}_i^T \mathbf{M} \boldsymbol{\varphi}_i} > 1$ , and  $\omega_{r1}^p$  and  $\omega_{r2}^p$  are two over-damped modal circular frequencies. The corresponding over-damped modal shapes are given by  $\boldsymbol{\varphi}_{r1}^p = \boldsymbol{\varphi}_{r2}^p = \boldsymbol{\varphi}_{0i} \in \mathbb{R}^N$ , ( $r = 1, 2 \dots N_p / 2$ ) after letting  $\tilde{\varphi}_i = 1$ , which shows that in this case, one original mode (a mode without damping involved in eigen-solutions) is divided into two over-damped modes. In other words, two over-damped modes share one modal shape. Thus, it can be concluded that for a classically damped system, if an over-damped mode appears, there must be second over-damped mode in the system that has the same modal shape as the first one. Based on this point, the two over-damped modes that have the same modal shape may be paired in the analysis. However, this conclusion cannot be further extended to non-classically damped system. Therefore, for a general case, all over-damped modes should be processed independently one by one.

(c) When  $c_i = 2\omega_{0i}$ , we have a critically damped system. From Equations (B.29) and

(B.30), we have  $\zeta_i = \frac{c_i}{2\omega_{0i}} = \frac{\boldsymbol{\varphi}_i^T \mathbf{C} \boldsymbol{\varphi}_i}{2\omega_{0i} \boldsymbol{\varphi}_i^T \mathbf{M} \boldsymbol{\varphi}_i} = 1$  and

$$\omega_{r1}^p = \omega_{r2}^p = \omega_{0i} \in \mathbb{R} \quad (\text{B.31})$$

Based on the point of view stemmed from the state space approach, the system has a repeated eigenvalue. In this case, special efforts are need to be addressed, such as to



establish an extra modal sub-space within the complete modal space for these repeated eigenvalues and to further ensure the orthogonal property for all modes. However, these related contents are beyond the scope of this report. The readers with interests can find detailed discussions about the repeated eigenvalues from references such as Wilkinson (1965) and Lancaster (1966).



## MCEER Technical Reports

MCEER publishes technical reports on a variety of subjects written by authors funded through MCEER. These reports are available from both MCEER Publications and the National Technical Information Service (NTIS). Requests for reports should be directed to MCEER Publications, MCEER, University at Buffalo, State University of New York, Red Jacket Quadrangle, Buffalo, New York 14261. Reports can also be requested through NTIS, 5285 Port Royal Road, Springfield, Virginia 22161. NTIS accession numbers are shown in parenthesis, if available.

- NCEER-87-0001 "First-Year Program in Research, Education and Technology Transfer," 3/5/87, (PB88-134275, A04, MF-A01).
- NCEER-87-0002 "Experimental Evaluation of Instantaneous Optimal Algorithms for Structural Control," by R.C. Lin, T.T. Soong and A.M. Reinhorn, 4/20/87, (PB88-134341, A04, MF-A01).
- NCEER-87-0003 "Experimentation Using the Earthquake Simulation Facilities at University at Buffalo," by A.M. Reinhorn and R.L. Ketter, to be published.
- NCEER-87-0004 "The System Characteristics and Performance of a Shaking Table," by J.S. Hwang, K.C. Chang and G.C. Lee, 6/1/87, (PB88-134259, A03, MF-A01). This report is available only through NTIS (see address given above).
- NCEER-87-0005 "A Finite Element Formulation for Nonlinear Viscoplastic Material Using a Q Model," by O. Gyebe and G. Dasgupta, 11/2/87, (PB88-213764, A08, MF-A01).
- NCEER-87-0006 "Symbolic Manipulation Program (SMP) - Algebraic Codes for Two and Three Dimensional Finite Element Formulations," by X. Lee and G. Dasgupta, 11/9/87, (PB88-218522, A05, MF-A01).
- NCEER-87-0007 "Instantaneous Optimal Control Laws for Tall Buildings Under Seismic Excitations," by J.N. Yang, A. Akbarpour and P. Ghaemmaghami, 6/10/87, (PB88-134333, A06, MF-A01). This report is only available through NTIS (see address given above).
- NCEER-87-0008 "IDARC: Inelastic Damage Analysis of Reinforced Concrete Frame - Shear-Wall Structures," by Y.J. Park, A.M. Reinhorn and S.K. Kunnath, 7/20/87, (PB88-134325, A09, MF-A01). This report is only available through NTIS (see address given above).
- NCEER-87-0009 "Liquefaction Potential for New York State: A Preliminary Report on Sites in Manhattan and Buffalo," by M. Budhu, V. Vijayakumar, R.F. Giese and L. Baumgras, 8/31/87, (PB88-163704, A03, MF-A01). This report is available only through NTIS (see address given above).
- NCEER-87-0010 "Vertical and Torsional Vibration of Foundations in Inhomogeneous Media," by A.S. Veletsos and K.W. Dotson, 6/1/87, (PB88-134291, A03, MF-A01). This report is only available through NTIS (see address given above).
- NCEER-87-0011 "Seismic Probabilistic Risk Assessment and Seismic Margins Studies for Nuclear Power Plants," by Howard H.M. Hwang, 6/15/87, (PB88-134267, A03, MF-A01). This report is only available through NTIS (see address given above).
- NCEER-87-0012 "Parametric Studies of Frequency Response of Secondary Systems Under Ground-Acceleration Excitations," by Y. Yong and Y.K. Lin, 6/10/87, (PB88-134309, A03, MF-A01). This report is only available through NTIS (see address given above).
- NCEER-87-0013 "Frequency Response of Secondary Systems Under Seismic Excitation," by J.A. HoLung, J. Cai and Y.K. Lin, 7/31/87, (PB88-134317, A05, MF-A01). This report is only available through NTIS (see address given above).
- NCEER-87-0014 "Modelling Earthquake Ground Motions in Seismically Active Regions Using Parametric Time Series Methods," by G.W. Ellis and A.S. Cakmak, 8/25/87, (PB88-134283, A08, MF-A01). This report is only available through NTIS (see address given above).
- NCEER-87-0015 "Detection and Assessment of Seismic Structural Damage," by E. DiPasquale and A.S. Cakmak, 8/25/87, (PB88-163712, A05, MF-A01). This report is only available through NTIS (see address given above).

- NCEER-87-0016 "Pipeline Experiment at Parkfield, California," by J. Isenberg and E. Richardson, 9/15/87, (PB88-163720, A03, MF-A01). This report is available only through NTIS (see address given above).
- NCEER-87-0017 "Digital Simulation of Seismic Ground Motion," by M. Shinozuka, G. Deodatis and T. Harada, 8/31/87, (PB88-155197, A04, MF-A01). This report is available only through NTIS (see address given above).
- NCEER-87-0018 "Practical Considerations for Structural Control: System Uncertainty, System Time Delay and Truncation of Small Control Forces," J.N. Yang and A. Akbarpour, 8/10/87, (PB88-163738, A08, MF-A01). This report is only available through NTIS (see address given above).
- NCEER-87-0019 "Modal Analysis of Nonclassically Damped Structural Systems Using Canonical Transformation," by J.N. Yang, S. Sarkani and F.X. Long, 9/27/87, (PB88-187851, A04, MF-A01).
- NCEER-87-0020 "A Nonstationary Solution in Random Vibration Theory," by J.R. Red-Horse and P.D. Spanos, 11/3/87, (PB88-163746, A03, MF-A01).
- NCEER-87-0021 "Horizontal Impedances for Radially Inhomogeneous Viscoelastic Soil Layers," by A.S. Veletsos and K.W. Dotson, 10/15/87, (PB88-150859, A04, MF-A01).
- NCEER-87-0022 "Seismic Damage Assessment of Reinforced Concrete Members," by Y.S. Chung, C. Meyer and M. Shinozuka, 10/9/87, (PB88-150867, A05, MF-A01). This report is available only through NTIS (see address given above).
- NCEER-87-0023 "Active Structural Control in Civil Engineering," by T.T. Soong, 11/11/87, (PB88-187778, A03, MF-A01).
- NCEER-87-0024 "Vertical and Torsional Impedances for Radially Inhomogeneous Viscoelastic Soil Layers," by K.W. Dotson and A.S. Veletsos, 12/87, (PB88-187786, A03, MF-A01).
- NCEER-87-0025 "Proceedings from the Symposium on Seismic Hazards, Ground Motions, Soil-Liquefaction and Engineering Practice in Eastern North America," October 20-22, 1987, edited by K.H. Jacob, 12/87, (PB88-188115, A23, MF-A01). This report is available only through NTIS (see address given above).
- NCEER-87-0026 "Report on the Whittier-Narrows, California, Earthquake of October 1, 1987," by J. Pantelic and A. Reinhorn, 11/87, (PB88-187752, A03, MF-A01). This report is available only through NTIS (see address given above).
- NCEER-87-0027 "Design of a Modular Program for Transient Nonlinear Analysis of Large 3-D Building Structures," by S. Srivastav and J.F. Abel, 12/30/87, (PB88-187950, A05, MF-A01). This report is only available through NTIS (see address given above).
- NCEER-87-0028 "Second-Year Program in Research, Education and Technology Transfer," 3/8/88, (PB88-219480, A04, MF-A01).
- NCEER-88-0001 "Workshop on Seismic Computer Analysis and Design of Buildings With Interactive Graphics," by W. McGuire, J.F. Abel and C.H. Conley, 1/18/88, (PB88-187760, A03, MF-A01). This report is only available through NTIS (see address given above).
- NCEER-88-0002 "Optimal Control of Nonlinear Flexible Structures," by J.N. Yang, F.X. Long and D. Wong, 1/22/88, (PB88-213772, A06, MF-A01).
- NCEER-88-0003 "Substructuring Techniques in the Time Domain for Primary-Secondary Structural Systems," by G.D. Manolis and G. Juhn, 2/10/88, (PB88-213780, A04, MF-A01).
- NCEER-88-0004 "Iterative Seismic Analysis of Primary-Secondary Systems," by A. Singhal, L.D. Lutes and P.D. Spanos, 2/23/88, (PB88-213798, A04, MF-A01).
- NCEER-88-0005 "Stochastic Finite Element Expansion for Random Media," by P.D. Spanos and R. Ghanem, 3/14/88, (PB88-213806, A03, MF-A01).

- NCEER-88-0006 "Combining Structural Optimization and Structural Control," by F.Y. Cheng and C.P. Pantelides, 1/10/88, (PB88-213814, A05, MF-A01).
- NCEER-88-0007 "Seismic Performance Assessment of Code-Designed Structures," by H.H-M. Hwang, J-W. Jaw and H-J. Shau, 3/20/88, (PB88-219423, A04, MF-A01). This report is only available through NTIS (see address given above).
- NCEER-88-0008 "Reliability Analysis of Code-Designed Structures Under Natural Hazards," by H.H-M. Hwang, H. Ushiba and M. Shinozuka, 2/29/88, (PB88-229471, A07, MF-A01). This report is only available through NTIS (see address given above).
- NCEER-88-0009 "Seismic Fragility Analysis of Shear Wall Structures," by J-W Jaw and H.H-M. Hwang, 4/30/88, (PB89-102867, A04, MF-A01).
- NCEER-88-0010 "Base Isolation of a Multi-Story Building Under a Harmonic Ground Motion - A Comparison of Performances of Various Systems," by F-G Fan, G. Ahmadi and I.G. Tadjbakhsh, 5/18/88, (PB89-122238, A06, MF-A01). This report is only available through NTIS (see address given above).
- NCEER-88-0011 "Seismic Floor Response Spectra for a Combined System by Green's Functions," by F.M. Lavelle, L.A. Bergman and P.D. Spanos, 5/1/88, (PB89-102875, A03, MF-A01).
- NCEER-88-0012 "A New Solution Technique for Randomly Excited Hysteretic Structures," by G.Q. Cai and Y.K. Lin, 5/16/88, (PB89-102883, A03, MF-A01).
- NCEER-88-0013 "A Study of Radiation Damping and Soil-Structure Interaction Effects in the Centrifuge," by K. Weissman, supervised by J.H. Prevost, 5/24/88, (PB89-144703, A06, MF-A01).
- NCEER-88-0014 "Parameter Identification and Implementation of a Kinematic Plasticity Model for Frictional Soils," by J.H. Prevost and D.V. Griffiths, to be published.
- NCEER-88-0015 "Two- and Three- Dimensional Dynamic Finite Element Analyses of the Long Valley Dam," by D.V. Griffiths and J.H. Prevost, 6/17/88, (PB89-144711, A04, MF-A01).
- NCEER-88-0016 "Damage Assessment of Reinforced Concrete Structures in Eastern United States," by A.M. Reinhorn, M.J. Seidel, S.K. Kunnath and Y.J. Park, 6/15/88, (PB89-122220, A04, MF-A01). This report is only available through NTIS (see address given above).
- NCEER-88-0017 "Dynamic Compliance of Vertically Loaded Strip Foundations in Multilayered Viscoelastic Soils," by S. Ahmad and A.S.M. Israil, 6/17/88, (PB89-102891, A04, MF-A01).
- NCEER-88-0018 "An Experimental Study of Seismic Structural Response With Added Viscoelastic Dampers," by R.C. Lin, Z. Liang, T.T. Soong and R.H. Zhang, 6/30/88, (PB89-122212, A05, MF-A01). This report is available only through NTIS (see address given above).
- NCEER-88-0019 "Experimental Investigation of Primary - Secondary System Interaction," by G.D. Manolis, G. Juhn and A.M. Reinhorn, 5/27/88, (PB89-122204, A04, MF-A01).
- NCEER-88-0020 "A Response Spectrum Approach For Analysis of Nonclassically Damped Structures," by J.N. Yang, S. Sarkani and F.X. Long, 4/22/88, (PB89-102909, A04, MF-A01).
- NCEER-88-0021 "Seismic Interaction of Structures and Soils: Stochastic Approach," by A.S. Veletsos and A.M. Prasad, 7/21/88, (PB89-122196, A04, MF-A01). This report is only available through NTIS (see address given above).
- NCEER-88-0022 "Identification of the Serviceability Limit State and Detection of Seismic Structural Damage," by E. DiPasquale and A.S. Cakmak, 6/15/88, (PB89-122188, A05, MF-A01). This report is available only through NTIS (see address given above).
- NCEER-88-0023 "Multi-Hazard Risk Analysis: Case of a Simple Offshore Structure," by B.K. Bhartia and E.H. Vanmarcke, 7/21/88, (PB89-145213, A05, MF-A01).

- NCEER-88-0024 "Automated Seismic Design of Reinforced Concrete Buildings," by Y.S. Chung, C. Meyer and M. Shinozuka, 7/5/88, (PB89-122170, A06, MF-A01). This report is available only through NTIS (see address given above).
- NCEER-88-0025 "Experimental Study of Active Control of MDOF Structures Under Seismic Excitations," by L.L. Chung, R.C. Lin, T.T. Soong and A.M. Reinhorn, 7/10/88, (PB89-122600, A04, MF-A01).
- NCEER-88-0026 "Earthquake Simulation Tests of a Low-Rise Metal Structure," by J.S. Hwang, K.C. Chang, G.C. Lee and R.L. Ketter, 8/1/88, (PB89-102917, A04, MF-A01).
- NCEER-88-0027 "Systems Study of Urban Response and Reconstruction Due to Catastrophic Earthquakes," by F. Kozin and H.K. Zhou, 9/22/88, (PB90-162348, A04, MF-A01).
- NCEER-88-0028 "Seismic Fragility Analysis of Plane Frame Structures," by H.H-M. Hwang and Y.K. Low, 7/31/88, (PB89-131445, A06, MF-A01).
- NCEER-88-0029 "Response Analysis of Stochastic Structures," by A. Kardara, C. Bucher and M. Shinozuka, 9/22/88, (PB89-174429, A04, MF-A01).
- NCEER-88-0030 "Nonnormal Accelerations Due to Yielding in a Primary Structure," by D.C.K. Chen and L.D. Lutes, 9/19/88, (PB89-131437, A04, MF-A01).
- NCEER-88-0031 "Design Approaches for Soil-Structure Interaction," by A.S. Veletsos, A.M. Prasad and Y. Tang, 12/30/88, (PB89-174437, A03, MF-A01). This report is available only through NTIS (see address given above).
- NCEER-88-0032 "A Re-evaluation of Design Spectra for Seismic Damage Control," by C.J. Turkstra and A.G. Tallin, 11/7/88, (PB89-145221, A05, MF-A01).
- NCEER-88-0033 "The Behavior and Design of Noncontact Lap Splices Subjected to Repeated Inelastic Tensile Loading," by V.E. Sagan, P. Gergely and R.N. White, 12/8/88, (PB89-163737, A08, MF-A01).
- NCEER-88-0034 "Seismic Response of Pile Foundations," by S.M. Mamoon, P.K. Banerjee and S. Ahmad, 11/1/88, (PB89-145239, A04, MF-A01).
- NCEER-88-0035 "Modeling of R/C Building Structures With Flexible Floor Diaphragms (IDARC2)," by A.M. Reinhorn, S.K. Kunnath and N. Panahshahi, 9/7/88, (PB89-207153, A07, MF-A01).
- NCEER-88-0036 "Solution of the Dam-Reservoir Interaction Problem Using a Combination of FEM, BEM with Particular Integrals, Modal Analysis, and Substructuring," by C-S. Tsai, G.C. Lee and R.L. Ketter, 12/31/88, (PB89-207146, A04, MF-A01).
- NCEER-88-0037 "Optimal Placement of Actuators for Structural Control," by F.Y. Cheng and C.P. Pantelides, 8/15/88, (PB89-162846, A05, MF-A01).
- NCEER-88-0038 "Teflon Bearings in Aseismic Base Isolation: Experimental Studies and Mathematical Modeling," by A. Mokha, M.C. Constantinou and A.M. Reinhorn, 12/5/88, (PB89-218457, A10, MF-A01). This report is available only through NTIS (see address given above).
- NCEER-88-0039 "Seismic Behavior of Flat Slab High-Rise Buildings in the New York City Area," by P. Weidlinger and M. Ettouney, 10/15/88, (PB90-145681, A04, MF-A01).
- NCEER-88-0040 "Evaluation of the Earthquake Resistance of Existing Buildings in New York City," by P. Weidlinger and M. Ettouney, 10/15/88, to be published.
- NCEER-88-0041 "Small-Scale Modeling Techniques for Reinforced Concrete Structures Subjected to Seismic Loads," by W. Kim, A. El-Attar and R.N. White, 11/22/88, (PB89-189625, A05, MF-A01).
- NCEER-88-0042 "Modeling Strong Ground Motion from Multiple Event Earthquakes," by G.W. Ellis and A.S. Cakmak, 10/15/88, (PB89-174445, A03, MF-A01).

- NCEER-88-0043 "Nonstationary Models of Seismic Ground Acceleration," by M. Grigoriu, S.E. Ruiz and E. Rosenblueth, 7/15/88, (PB89-189617, A04, MF-A01).
- NCEER-88-0044 "SARCF User's Guide: Seismic Analysis of Reinforced Concrete Frames," by Y.S. Chung, C. Meyer and M. Shinozuka, 11/9/88, (PB89-174452, A08, MF-A01).
- NCEER-88-0045 "First Expert Panel Meeting on Disaster Research and Planning," edited by J. Pantelic and J. Stoyle, 9/15/88, (PB89-174460, A05, MF-A01).
- NCEER-88-0046 "Preliminary Studies of the Effect of Degrading Infill Walls on the Nonlinear Seismic Response of Steel Frames," by C.Z. Chrysostomou, P. Gergely and J.F. Abel, 12/19/88, (PB89-208383, A05, MF-A01).
- NCEER-88-0047 "Reinforced Concrete Frame Component Testing Facility - Design, Construction, Instrumentation and Operation," by S.P. Pessiki, C. Conley, T. Bond, P. Gergely and R.N. White, 12/16/88, (PB89-174478, A04, MF-A01).
- NCEER-89-0001 "Effects of Protective Cushion and Soil Compliancy on the Response of Equipment Within a Seismically Excited Building," by J.A. HoLung, 2/16/89, (PB89-207179, A04, MF-A01).
- NCEER-89-0002 "Statistical Evaluation of Response Modification Factors for Reinforced Concrete Structures," by H.H-M. Hwang and J-W. Jaw, 2/17/89, (PB89-207187, A05, MF-A01).
- NCEER-89-0003 "Hysteretic Columns Under Random Excitation," by G-Q. Cai and Y.K. Lin, 1/9/89, (PB89-196513, A03, MF-A01).
- NCEER-89-0004 "Experimental Study of 'Elephant Foot Bulge' Instability of Thin-Walled Metal Tanks," by Z-H. Jia and R.L. Ketter, 2/22/89, (PB89-207195, A03, MF-A01).
- NCEER-89-0005 "Experiment on Performance of Buried Pipelines Across San Andreas Fault," by J. Isenberg, E. Richardson and T.D. O'Rourke, 3/10/89, (PB89-218440, A04, MF-A01). This report is available only through NTIS (see address given above).
- NCEER-89-0006 "A Knowledge-Based Approach to Structural Design of Earthquake-Resistant Buildings," by M. Subramani, P. Gergely, C.H. Conley, J.F. Abel and A.H. Zaghaw, 1/15/89, (PB89-218465, A06, MF-A01).
- NCEER-89-0007 "Liquefaction Hazards and Their Effects on Buried Pipelines," by T.D. O'Rourke and P.A. Lane, 2/1/89, (PB89-218481, A09, MF-A01).
- NCEER-89-0008 "Fundamentals of System Identification in Structural Dynamics," by H. Imai, C-B. Yun, O. Maruyama and M. Shinozuka, 1/26/89, (PB89-207211, A04, MF-A01).
- NCEER-89-0009 "Effects of the 1985 Michoacan Earthquake on Water Systems and Other Buried Lifelines in Mexico," by A.G. Ayala and M.J. O'Rourke, 3/8/89, (PB89-207229, A06, MF-A01).
- NCEER-89-R010 "NCEER Bibliography of Earthquake Education Materials," by K.E.K. Ross, Second Revision, 9/1/89, (PB90-125352, A05, MF-A01). This report is replaced by NCEER-92-0018.
- NCEER-89-0011 "Inelastic Three-Dimensional Response Analysis of Reinforced Concrete Building Structures (IDARC-3D), Part I - Modeling," by S.K. Kunnath and A.M. Reinhorn, 4/17/89, (PB90-114612, A07, MF-A01). This report is available only through NTIS (see address given above).
- NCEER-89-0012 "Recommended Modifications to ATC-14," by C.D. Poland and J.O. Malley, 4/12/89, (PB90-108648, A15, MF-A01).
- NCEER-89-0013 "Repair and Strengthening of Beam-to-Column Connections Subjected to Earthquake Loading," by M. Corazao and A.J. Durrani, 2/28/89, (PB90-109885, A06, MF-A01).
- NCEER-89-0014 "Program EXKAL2 for Identification of Structural Dynamic Systems," by O. Maruyama, C-B. Yun, M. Hoshiya and M. Shinozuka, 5/19/89, (PB90-109877, A09, MF-A01).

- NCEER-89-0015 "Response of Frames With Bolted Semi-Rigid Connections, Part I - Experimental Study and Analytical Predictions," by P.J. DiCorso, A.M. Reinhorn, J.R. Dickerson, J.B. Radzinski and W.L. Harper, 6/1/89, to be published.
- NCEER-89-0016 "ARMA Monte Carlo Simulation in Probabilistic Structural Analysis," by P.D. Spanos and M.P. Mignolet, 7/10/89, (PB90-109893, A03, MF-A01).
- NCEER-89-P017 "Preliminary Proceedings from the Conference on Disaster Preparedness - The Place of Earthquake Education in Our Schools," Edited by K.E.K. Ross, 6/23/89, (PB90-108606, A03, MF-A01).
- NCEER-89-0017 "Proceedings from the Conference on Disaster Preparedness - The Place of Earthquake Education in Our Schools," Edited by K.E.K. Ross, 12/31/89, (PB90-207895, A012, MF-A02). This report is available only through NTIS (see address given above).
- NCEER-89-0018 "Multidimensional Models of Hysteretic Material Behavior for Vibration Analysis of Shape Memory Energy Absorbing Devices, by E.J. Graesser and F.A. Cozzarelli, 6/7/89, (PB90-164146, A04, MF-A01).
- NCEER-89-0019 "Nonlinear Dynamic Analysis of Three-Dimensional Base Isolated Structures (3D-BASIS)," by S. Nagarajaiah, A.M. Reinhorn and M.C. Constantinou, 8/3/89, (PB90-161936, A06, MF-A01). This report has been replaced by NCEER-93-0011.
- NCEER-89-0020 "Structural Control Considering Time-Rate of Control Forces and Control Rate Constraints," by F.Y. Cheng and C.P. Pantelides, 8/3/89, (PB90-120445, A04, MF-A01).
- NCEER-89-0021 "Subsurface Conditions of Memphis and Shelby County," by K.W. Ng, T-S. Chang and H-H.M. Hwang, 7/26/89, (PB90-120437, A03, MF-A01).
- NCEER-89-0022 "Seismic Wave Propagation Effects on Straight Jointed Buried Pipelines," by K. Elhadi and M.J. O'Rourke, 8/24/89, (PB90-162322, A10, MF-A02).
- NCEER-89-0023 "Workshop on Serviceability Analysis of Water Delivery Systems," edited by M. Grigoriu, 3/6/89, (PB90-127424, A03, MF-A01).
- NCEER-89-0024 "Shaking Table Study of a 1/5 Scale Steel Frame Composed of Tapered Members," by K.C. Chang, J.S. Hwang and G.C. Lee, 9/18/89, (PB90-160169, A04, MF-A01).
- NCEER-89-0025 "DYNA1D: A Computer Program for Nonlinear Seismic Site Response Analysis - Technical Documentation," by Jean H. Prevost, 9/14/89, (PB90-161944, A07, MF-A01). This report is available only through NTIS (see address given above).
- NCEER-89-0026 "1:4 Scale Model Studies of Active Tendon Systems and Active Mass Dampers for Aseismic Protection," by A.M. Reinhorn, T.T. Soong, R.C. Lin, Y.P. Yang, Y. Fukao, H. Abe and M. Nakai, 9/15/89, (PB90-173246, A10, MF-A02). This report is available only through NTIS (see address given above).
- NCEER-89-0027 "Scattering of Waves by Inclusions in a Nonhomogeneous Elastic Half Space Solved by Boundary Element Methods," by P.K. Hadley, A. Askar and A.S. Cakmak, 6/15/89, (PB90-145699, A07, MF-A01).
- NCEER-89-0028 "Statistical Evaluation of Deflection Amplification Factors for Reinforced Concrete Structures," by H.H.M. Hwang, J-W. Jaw and A.L. Ch'ng, 8/31/89, (PB90-164633, A05, MF-A01).
- NCEER-89-0029 "Bedrock Accelerations in Memphis Area Due to Large New Madrid Earthquakes," by H.H.M. Hwang, C.H.S. Chen and G. Yu, 11/7/89, (PB90-162330, A04, MF-A01).
- NCEER-89-0030 "Seismic Behavior and Response Sensitivity of Secondary Structural Systems," by Y.Q. Chen and T.T. Soong, 10/23/89, (PB90-164658, A08, MF-A01).
- NCEER-89-0031 "Random Vibration and Reliability Analysis of Primary-Secondary Structural Systems," by Y. Ibrahim, M. Grigoriu and T.T. Soong, 11/10/89, (PB90-161951, A04, MF-A01).



- NCEER-89-0032 "Proceedings from the Second U.S. - Japan Workshop on Liquefaction, Large Ground Deformation and Their Effects on Lifelines, September 26-29, 1989," Edited by T.D. O'Rourke and M. Hamada, 12/1/89, (PB90-209388, A22, MF-A03).
- NCEER-89-0033 "Deterministic Model for Seismic Damage Evaluation of Reinforced Concrete Structures," by J.M. Bracci, A.M. Reinhorn, J.B. Mander and S.K. Kunnath, 9/27/89, (PB91-108803, A06, MF-A01).
- NCEER-89-0034 "On the Relation Between Local and Global Damage Indices," by E. DiPasquale and A.S. Cakmak, 8/15/89, (PB90-173865, A05, MF-A01).
- NCEER-89-0035 "Cyclic Undrained Behavior of Nonplastic and Low Plasticity Silts," by A.J. Walker and H.E. Stewart, 7/26/89, (PB90-183518, A10, MF-A01).
- NCEER-89-0036 "Liquefaction Potential of Surficial Deposits in the City of Buffalo, New York," by M. Budhu, R. Giese and L. Baumgrass, 1/17/89, (PB90-208455, A04, MF-A01).
- NCEER-89-0037 "A Deterministic Assessment of Effects of Ground Motion Incoherence," by A.S. Veletsos and Y. Tang, 7/15/89, (PB90-164294, A03, MF-A01).
- NCEER-89-0038 "Workshop on Ground Motion Parameters for Seismic Hazard Mapping," July 17-18, 1989, edited by R.V. Whitman, 12/1/89, (PB90-173923, A04, MF-A01).
- NCEER-89-0039 "Seismic Effects on Elevated Transit Lines of the New York City Transit Authority," by C.J. Costantino, C.A. Miller and E. Heymsfield, 12/26/89, (PB90-207887, A06, MF-A01).
- NCEER-89-0040 "Centrifugal Modeling of Dynamic Soil-Structure Interaction," by K. Weissman, Supervised by J.H. Prevost, 5/10/89, (PB90-207879, A07, MF-A01).
- NCEER-89-0041 "Linearized Identification of Buildings With Cores for Seismic Vulnerability Assessment," by I-K. Ho and A.E. Aktan, 11/1/89, (PB90-251943, A07, MF-A01).
- NCEER-90-0001 "Geotechnical and Lifeline Aspects of the October 17, 1989 Loma Prieta Earthquake in San Francisco," by T.D. O'Rourke, H.E. Stewart, F.T. Blackburn and T.S. Dickerman, 1/90, (PB90-208596, A05, MF-A01).
- NCEER-90-0002 "Nonnormal Secondary Response Due to Yielding in a Primary Structure," by D.C.K. Chen and L.D. Lutes, 2/28/90, (PB90-251976, A07, MF-A01).
- NCEER-90-0003 "Earthquake Education Materials for Grades K-12," by K.E.K. Ross, 4/16/90, (PB91-251984, A05, MF-A05). This report has been replaced by NCEER-92-0018.
- NCEER-90-0004 "Catalog of Strong Motion Stations in Eastern North America," by R.W. Busby, 4/3/90, (PB90-251984, A05, MF-A01).
- NCEER-90-0005 "NCEER Strong-Motion Data Base: A User Manual for the GeoBase Release (Version 1.0 for the Sun3)," by P. Friberg and K. Jacob, 3/31/90 (PB90-258062, A04, MF-A01).
- NCEER-90-0006 "Seismic Hazard Along a Crude Oil Pipeline in the Event of an 1811-1812 Type New Madrid Earthquake," by H.H.M. Hwang and C-H.S. Chen, 4/16/90, (PB90-258054, A04, MF-A01).
- NCEER-90-0007 "Site-Specific Response Spectra for Memphis Sheahan Pumping Station," by H.H.M. Hwang and C.S. Lee, 5/15/90, (PB91-108811, A05, MF-A01).
- NCEER-90-0008 "Pilot Study on Seismic Vulnerability of Crude Oil Transmission Systems," by T. Ariman, R. Dobry, M. Grigoriu, F. Kozin, M. O'Rourke, T. O'Rourke and M. Shinozuka, 5/25/90, (PB91-108837, A06, MF-A01).
- NCEER-90-0009 "A Program to Generate Site Dependent Time Histories: EQGEN," by G.W. Ellis, M. Srinivasan and A.S. Cakmak, 1/30/90, (PB91-108829, A04, MF-A01).
- NCEER-90-0010 "Active Isolation for Seismic Protection of Operating Rooms," by M.E. Talbott, Supervised by M. Shinozuka, 6/8/9, (PB91-110205, A05, MF-A01).

- NCEER-90-0011 "Program LINEARID for Identification of Linear Structural Dynamic Systems," by C-B. Yun and M. Shinozuka, 6/25/90, (PB91-110312, A08, MF-A01).
- NCEER-90-0012 "Two-Dimensional Two-Phase Elasto-Plastic Seismic Response of Earth Dams," by A.N. Yiagos, Supervised by J.H. Prevost, 6/20/90, (PB91-110197, A13, MF-A02).
- NCEER-90-0013 "Secondary Systems in Base-Isolated Structures: Experimental Investigation, Stochastic Response and Stochastic Sensitivity," by G.D. Manolis, G. Juhn, M.C. Constantinou and A.M. Reinhorn, 7/1/90, (PB91-110320, A08, MF-A01).
- NCEER-90-0014 "Seismic Behavior of Lightly-Reinforced Concrete Column and Beam-Column Joint Details," by S.P. Pessiki, C.H. Conley, P. Gergely and R.N. White, 8/22/90, (PB91-108795, A11, MF-A02).
- NCEER-90-0015 "Two Hybrid Control Systems for Building Structures Under Strong Earthquakes," by J.N. Yang and A. Daniellians, 6/29/90, (PB91-125393, A04, MF-A01).
- NCEER-90-0016 "Instantaneous Optimal Control with Acceleration and Velocity Feedback," by J.N. Yang and Z. Li, 6/29/90, (PB91-125401, A03, MF-A01).
- NCEER-90-0017 "Reconnaissance Report on the Northern Iran Earthquake of June 21, 1990," by M. Mehrain, 10/4/90, (PB91-125377, A03, MF-A01).
- NCEER-90-0018 "Evaluation of Liquefaction Potential in Memphis and Shelby County," by T.S. Chang, P.S. Tang, C.S. Lee and H. Hwang, 8/10/90, (PB91-125427, A09, MF-A01).
- NCEER-90-0019 "Experimental and Analytical Study of a Combined Sliding Disc Bearing and Helical Steel Spring Isolation System," by M.C. Constantinou, A.S. Mokha and A.M. Reinhorn, 10/4/90, (PB91-125385, A06, MF-A01). This report is available only through NTIS (see address given above).
- NCEER-90-0020 "Experimental Study and Analytical Prediction of Earthquake Response of a Sliding Isolation System with a Spherical Surface," by A.S. Mokha, M.C. Constantinou and A.M. Reinhorn, 10/11/90, (PB91-125419, A05, MF-A01).
- NCEER-90-0021 "Dynamic Interaction Factors for Floating Pile Groups," by G. Gazetas, K. Fan, A. Kaynia and E. Kausel, 9/10/90, (PB91-170381, A05, MF-A01).
- NCEER-90-0022 "Evaluation of Seismic Damage Indices for Reinforced Concrete Structures," by S. Rodriguez-Gomez and A.S. Cakmak, 9/30/90, PB91-171322, A06, MF-A01).
- NCEER-90-0023 "Study of Site Response at a Selected Memphis Site," by H. Desai, S. Ahmad, E.S. Gazetas and M.R. Oh, 10/11/90, (PB91-196857, A03, MF-A01).
- NCEER-90-0024 "A User's Guide to Strongmo: Version 1.0 of NCEER's Strong-Motion Data Access Tool for PCs and Terminals," by P.A. Friberg and C.A.T. Susch, 11/15/90, (PB91-171272, A03, MF-A01).
- NCEER-90-0025 "A Three-Dimensional Analytical Study of Spatial Variability of Seismic Ground Motions," by L-L. Hong and A.H.-S. Ang, 10/30/90, (PB91-170399, A09, MF-A01).
- NCEER-90-0026 "MUMOID User's Guide - A Program for the Identification of Modal Parameters," by S. Rodriguez-Gomez and E. DiPasquale, 9/30/90, (PB91-171298, A04, MF-A01).
- NCEER-90-0027 "SARCF-II User's Guide - Seismic Analysis of Reinforced Concrete Frames," by S. Rodriguez-Gomez, Y.S. Chung and C. Meyer, 9/30/90, (PB91-171280, A05, MF-A01).
- NCEER-90-0028 "Viscous Dampers: Testing, Modeling and Application in Vibration and Seismic Isolation," by N. Makris and M.C. Constantinou, 12/20/90 (PB91-190561, A06, MF-A01).
- NCEER-90-0029 "Soil Effects on Earthquake Ground Motions in the Memphis Area," by H. Hwang, C.S. Lee, K.W. Ng and T.S. Chang, 8/2/90, (PB91-190751, A05, MF-A01).

- NCEER-91-0001 "Proceedings from the Third Japan-U.S. Workshop on Earthquake Resistant Design of Lifeline Facilities and Countermeasures for Soil Liquefaction, December 17-19, 1990," edited by T.D. O'Rourke and M. Hamada, 2/1/91, (PB91-179259, A99, MF-A04).
- NCEER-91-0002 "Physical Space Solutions of Non-Proportionally Damped Systems," by M. Tong, Z. Liang and G.C. Lee, 1/15/91, (PB91-179242, A04, MF-A01).
- NCEER-91-0003 "Seismic Response of Single Piles and Pile Groups," by K. Fan and G. Gazetas, 1/10/91, (PB92-174994, A04, MF-A01).
- NCEER-91-0004 "Damping of Structures: Part 1 - Theory of Complex Damping," by Z. Liang and G. Lee, 10/10/91, (PB92-197235, A12, MF-A03).
- NCEER-91-0005 "3D-BASIS - Nonlinear Dynamic Analysis of Three Dimensional Base Isolated Structures: Part II," by S. Nagarajaiah, A.M. Reinhorn and M.C. Constantinou, 2/28/91, (PB91-190553, A07, MF-A01). This report has been replaced by NCEER-93-0011.
- NCEER-91-0006 "A Multidimensional Hysteretic Model for Plasticity Deforming Metals in Energy Absorbing Devices," by E.J. Graesser and F.A. Cozzarelli, 4/9/91, (PB92-108364, A04, MF-A01).
- NCEER-91-0007 "A Framework for Customizable Knowledge-Based Expert Systems with an Application to a KBES for Evaluating the Seismic Resistance of Existing Buildings," by E.G. Ibarra-Anaya and S.J. Fennes, 4/9/91, (PB91-210930, A08, MF-A01).
- NCEER-91-0008 "Nonlinear Analysis of Steel Frames with Semi-Rigid Connections Using the Capacity Spectrum Method," by G.G. Deierlein, S-H. Hsieh, Y-J. Shen and J.F. Abel, 7/2/91, (PB92-113828, A05, MF-A01).
- NCEER-91-0009 "Earthquake Education Materials for Grades K-12," by K.E.K. Ross, 4/30/91, (PB91-212142, A06, MF-A01). This report has been replaced by NCEER-92-0018.
- NCEER-91-0010 "Phase Wave Velocities and Displacement Phase Differences in a Harmonically Oscillating Pile," by N. Makris and G. Gazetas, 7/8/91, (PB92-108356, A04, MF-A01).
- NCEER-91-0011 "Dynamic Characteristics of a Full-Size Five-Story Steel Structure and a 2/5 Scale Model," by K.C. Chang, G.C. Yao, G.C. Lee, D.S. Hao and Y.C. Yeh," 7/2/91, (PB93-116648, A06, MF-A02).
- NCEER-91-0012 "Seismic Response of a 2/5 Scale Steel Structure with Added Viscoelastic Dampers," by K.C. Chang, T.T. Soong, S-T. Oh and M.L. Lai, 5/17/91, (PB92-110816, A05, MF-A01).
- NCEER-91-0013 "Earthquake Response of Retaining Walls; Full-Scale Testing and Computational Modeling," by S. Alampalli and A-W.M. Elgamal, 6/20/91, to be published.
- NCEER-91-0014 "3D-BASIS-M: Nonlinear Dynamic Analysis of Multiple Building Base Isolated Structures," by P.C. Tsopelas, S. Nagarajaiah, M.C. Constantinou and A.M. Reinhorn, 5/28/91, (PB92-113885, A09, MF-A02).
- NCEER-91-0015 "Evaluation of SEAOC Design Requirements for Sliding Isolated Structures," by D. Theodossiou and M.C. Constantinou, 6/10/91, (PB92-114602, A11, MF-A03).
- NCEER-91-0016 "Closed-Loop Modal Testing of a 27-Story Reinforced Concrete Flat Plate-Core Building," by H.R. Somaprasad, T. Toksoy, H. Yoshiyuki and A.E. Aktan, 7/15/91, (PB92-129980, A07, MF-A02).
- NCEER-91-0017 "Shake Table Test of a 1/6 Scale Two-Story Lightly Reinforced Concrete Building," by A.G. El-Attar, R.N. White and P. Gergely, 2/28/91, (PB92-222447, A06, MF-A02).
- NCEER-91-0018 "Shake Table Test of a 1/8 Scale Three-Story Lightly Reinforced Concrete Building," by A.G. El-Attar, R.N. White and P. Gergely, 2/28/91, (PB93-116630, A08, MF-A02).
- NCEER-91-0019 "Transfer Functions for Rigid Rectangular Foundations," by A.S. Veletsos, A.M. Prasad and W.H. Wu, 7/31/91, to be published.

- NCEER-91-0020 "Hybrid Control of Seismic-Excited Nonlinear and Inelastic Structural Systems," by J.N. Yang, Z. Li and A. Daniellians, 8/1/91, (PB92-143171, A06, MF-A02).
- NCEER-91-0021 "The NCEER-91 Earthquake Catalog: Improved Intensity-Based Magnitudes and Recurrence Relations for U.S. Earthquakes East of New Madrid," by L. Seeber and J.G. Armbruster, 8/28/91, (PB92-176742, A06, MF-A02).
- NCEER-91-0022 "Proceedings from the Implementation of Earthquake Planning and Education in Schools: The Need for Change - The Roles of the Changemakers," by K.E.K. Ross and F. Winslow, 7/23/91, (PB92-129998, A12, MF-A03).
- NCEER-91-0023 "A Study of Reliability-Based Criteria for Seismic Design of Reinforced Concrete Frame Buildings," by H.H.M. Hwang and H-M. Hsu, 8/10/91, (PB92-140235, A09, MF-A02).
- NCEER-91-0024 "Experimental Verification of a Number of Structural System Identification Algorithms," by R.G. Ghanem, H. Gavin and M. Shinozuka, 9/18/91, (PB92-176577, A18, MF-A04).
- NCEER-91-0025 "Probabilistic Evaluation of Liquefaction Potential," by H.H.M. Hwang and C.S. Lee, 11/25/91, (PB92-143429, A05, MF-A01).
- NCEER-91-0026 "Instantaneous Optimal Control for Linear, Nonlinear and Hysteretic Structures - Stable Controllers," by J.N. Yang and Z. Li, 11/15/91, (PB92-163807, A04, MF-A01).
- NCEER-91-0027 "Experimental and Theoretical Study of a Sliding Isolation System for Bridges," by M.C. Constantinou, A. Kartoum, A.M. Reinhorn and P. Bradford, 11/15/91, (PB92-176973, A10, MF-A03).
- NCEER-92-0001 "Case Studies of Liquefaction and Lifeline Performance During Past Earthquakes, Volume 1: Japanese Case Studies," Edited by M. Hamada and T. O'Rourke, 2/17/92, (PB92-197243, A18, MF-A04).
- NCEER-92-0002 "Case Studies of Liquefaction and Lifeline Performance During Past Earthquakes, Volume 2: United States Case Studies," Edited by T. O'Rourke and M. Hamada, 2/17/92, (PB92-197250, A20, MF-A04).
- NCEER-92-0003 "Issues in Earthquake Education," Edited by K. Ross, 2/3/92, (PB92-222389, A07, MF-A02).
- NCEER-92-0004 "Proceedings from the First U.S. - Japan Workshop on Earthquake Protective Systems for Bridges," Edited by I.G. Buckle, 2/4/92, (PB94-142239, A99, MF-A06).
- NCEER-92-0005 "Seismic Ground Motion from a Haskell-Type Source in a Multiple-Layered Half-Space," A.P. Theoharis, G. Deodatis and M. Shinozuka, 1/2/92, to be published.
- NCEER-92-0006 "Proceedings from the Site Effects Workshop," Edited by R. Whitman, 2/29/92, (PB92-197201, A04, MF-A01).
- NCEER-92-0007 "Engineering Evaluation of Permanent Ground Deformations Due to Seismically-Induced Liquefaction," by M.H. Baziar, R. Dobry and A-W.M. Elgamel, 3/24/92, (PB92-222421, A13, MF-A03).
- NCEER-92-0008 "A Procedure for the Seismic Evaluation of Buildings in the Central and Eastern United States," by C.D. Poland and J.O. Malley, 4/2/92, (PB92-222439, A20, MF-A04).
- NCEER-92-0009 "Experimental and Analytical Study of a Hybrid Isolation System Using Friction Controllable Sliding Bearings," by M.Q. Feng, S. Fujii and M. Shinozuka, 5/15/92, (PB93-150282, A06, MF-A02).
- NCEER-92-0010 "Seismic Resistance of Slab-Column Connections in Existing Non-Ductile Flat-Plate Buildings," by A.J. Durrani and Y. Du, 5/18/92, (PB93-116812, A06, MF-A02).
- NCEER-92-0011 "The Hysteretic and Dynamic Behavior of Brick Masonry Walls Upgraded by Ferrocement Coatings Under Cyclic Loading and Strong Simulated Ground Motion," by H. Lee and S.P. Prawel, 5/11/92, to be published.
- NCEER-92-0012 "Study of Wire Rope Systems for Seismic Protection of Equipment in Buildings," by G.F. Demetriades, M.C. Constantinou and A.M. Reinhorn, 5/20/92, (PB93-116655, A08, MF-A02).

- NCEER-92-0013 "Shape Memory Structural Dampers: Material Properties, Design and Seismic Testing," by P.R. Witting and F.A. Cozzarelli, 5/26/92, (PB93-116663, A05, MF-A01).
- NCEER-92-0014 "Longitudinal Permanent Ground Deformation Effects on Buried Continuous Pipelines," by M.J. O'Rourke, and C. Nordberg, 6/15/92, (PB93-116671, A08, MF-A02).
- NCEER-92-0015 "A Simulation Method for Stationary Gaussian Random Functions Based on the Sampling Theorem," by M. Grigoriu and S. Balopoulou, 6/11/92, (PB93-127496, A05, MF-A01).
- NCEER-92-0016 "Gravity-Load-Designed Reinforced Concrete Buildings: Seismic Evaluation of Existing Construction and Detailing Strategies for Improved Seismic Resistance," by G.W. Hoffmann, S.K. Kunnath, A.M. Reinhorn and J.B. Mander, 7/15/92, (PB94-142007, A08, MF-A02).
- NCEER-92-0017 "Observations on Water System and Pipeline Performance in the Limón Area of Costa Rica Due to the April 22, 1991 Earthquake," by M. O'Rourke and D. Ballantyne, 6/30/92, (PB93-126811, A06, MF-A02).
- NCEER-92-0018 "Fourth Edition of Earthquake Education Materials for Grades K-12," Edited by K.E.K. Ross, 8/10/92, (PB93-114023, A07, MF-A02).
- NCEER-92-0019 "Proceedings from the Fourth Japan-U.S. Workshop on Earthquake Resistant Design of Lifeline Facilities and Countermeasures for Soil Liquefaction," Edited by M. Hamada and T.D. O'Rourke, 8/12/92, (PB93-163939, A99, MF-E11).
- NCEER-92-0020 "Active Bracing System: A Full Scale Implementation of Active Control," by A.M. Reinhorn, T.T. Soong, R.C. Lin, M.A. Riley, Y.P. Wang, S. Aizawa and M. Higashino, 8/14/92, (PB93-127512, A06, MF-A02).
- NCEER-92-0021 "Empirical Analysis of Horizontal Ground Displacement Generated by Liquefaction-Induced Lateral Spreads," by S.F. Bartlett and T.L. Youd, 8/17/92, (PB93-188241, A06, MF-A02).
- NCEER-92-0022 "IDARC Version 3.0: Inelastic Damage Analysis of Reinforced Concrete Structures," by S.K. Kunnath, A.M. Reinhorn and R.F. Lobo, 8/31/92, (PB93-227502, A07, MF-A02).
- NCEER-92-0023 "A Semi-Empirical Analysis of Strong-Motion Peaks in Terms of Seismic Source, Propagation Path and Local Site Conditions, by M. Kamiyama, M.J. O'Rourke and R. Flores-Berrones, 9/9/92, (PB93-150266, A08, MF-A02).
- NCEER-92-0024 "Seismic Behavior of Reinforced Concrete Frame Structures with Nonductile Details, Part I: Summary of Experimental Findings of Full Scale Beam-Column Joint Tests," by A. Beres, R.N. White and P. Gergely, 9/30/92, (PB93-227783, A05, MF-A01).
- NCEER-92-0025 "Experimental Results of Repaired and Retrofitted Beam-Column Joint Tests in Lightly Reinforced Concrete Frame Buildings," by A. Beres, S. El-Borgi, R.N. White and P. Gergely, 10/29/92, (PB93-227791, A05, MF-A01).
- NCEER-92-0026 "A Generalization of Optimal Control Theory: Linear and Nonlinear Structures," by J.N. Yang, Z. Li and S. Vongchavalitkul, 11/2/92, (PB93-188621, A05, MF-A01).
- NCEER-92-0027 "Seismic Resistance of Reinforced Concrete Frame Structures Designed Only for Gravity Loads: Part I - Design and Properties of a One-Third Scale Model Structure," by J.M. Bracci, A.M. Reinhorn and J.B. Mander, 12/1/92, (PB94-104502, A08, MF-A02).
- NCEER-92-0028 "Seismic Resistance of Reinforced Concrete Frame Structures Designed Only for Gravity Loads: Part II - Experimental Performance of Subassemblages," by L.E. Aycaardi, J.B. Mander and A.M. Reinhorn, 12/1/92, (PB94-104510, A08, MF-A02).
- NCEER-92-0029 "Seismic Resistance of Reinforced Concrete Frame Structures Designed Only for Gravity Loads: Part III - Experimental Performance and Analytical Study of a Structural Model," by J.M. Bracci, A.M. Reinhorn and J.B. Mander, 12/1/92, (PB93-227528, A09, MF-A01).

- NCEER-92-0030 "Evaluation of Seismic Retrofit of Reinforced Concrete Frame Structures: Part I - Experimental Performance of Retrofitted Subassemblages," by D. Choudhuri, J.B. Mander and A.M. Reinhorn, 12/8/92, (PB93-198307, A07, MF-A02).
- NCEER-92-0031 "Evaluation of Seismic Retrofit of Reinforced Concrete Frame Structures: Part II - Experimental Performance and Analytical Study of a Retrofitted Structural Model," by J.M. Bracci, A.M. Reinhorn and J.B. Mander, 12/8/92, (PB93-198315, A09, MF-A03).
- NCEER-92-0032 "Experimental and Analytical Investigation of Seismic Response of Structures with Supplemental Fluid Viscous Dampers," by M.C. Constantinou and M.D. Symans, 12/21/92, (PB93-191435, A10, MF-A03). This report is available only through NTIS (see address given above).
- NCEER-92-0033 "Reconnaissance Report on the Cairo, Egypt Earthquake of October 12, 1992," by M. Khater, 12/23/92, (PB93-188621, A03, MF-A01).
- NCEER-92-0034 "Low-Level Dynamic Characteristics of Four Tall Flat-Plate Buildings in New York City," by H. Gavin, S. Yuan, J. Grossman, E. Pekelis and K. Jacob, 12/28/92, (PB93-188217, A07, MF-A02).
- NCEER-93-0001 "An Experimental Study on the Seismic Performance of Brick-Infilled Steel Frames With and Without Retrofit," by J.B. Mander, B. Nair, K. Wojtkowski and J. Ma, 1/29/93, (PB93-227510, A07, MF-A02).
- NCEER-93-0002 "Social Accounting for Disaster Preparedness and Recovery Planning," by S. Cole, E. Pantoja and V. Razak, 2/22/93, (PB94-142114, A12, MF-A03).
- NCEER-93-0003 "Assessment of 1991 NEHRP Provisions for Nonstructural Components and Recommended Revisions," by T.T. Soong, G. Chen, Z. Wu, R-H. Zhang and M. Grigoriu, 3/1/93, (PB93-188639, A06, MF-A02).
- NCEER-93-0004 "Evaluation of Static and Response Spectrum Analysis Procedures of SEAOC/UBC for Seismic Isolated Structures," by C.W. Winters and M.C. Constantinou, 3/23/93, (PB93-198299, A10, MF-A03).
- NCEER-93-0005 "Earthquakes in the Northeast - Are We Ignoring the Hazard? A Workshop on Earthquake Science and Safety for Educators," edited by K.E.K. Ross, 4/2/93, (PB94-103066, A09, MF-A02).
- NCEER-93-0006 "Inelastic Response of Reinforced Concrete Structures with Viscoelastic Braces," by R.F. Lobo, J.M. Bracci, K.L. Shen, A.M. Reinhorn and T.T. Soong, 4/5/93, (PB93-227486, A05, MF-A02).
- NCEER-93-0007 "Seismic Testing of Installation Methods for Computers and Data Processing Equipment," by K. Kosar, T.T. Soong, K.L. Shen, J.A. HoLung and Y.K. Lin, 4/12/93, (PB93-198299, A07, MF-A02).
- NCEER-93-0008 "Retrofit of Reinforced Concrete Frames Using Added Dampers," by A. Reinhorn, M. Constantinou and C. Li, to be published.
- NCEER-93-0009 "Seismic Behavior and Design Guidelines for Steel Frame Structures with Added Viscoelastic Dampers," by K.C. Chang, M.L. Lai, T.T. Soong, D.S. Hao and Y.C. Yeh, 5/1/93, (PB94-141959, A07, MF-A02).
- NCEER-93-0010 "Seismic Performance of Shear-Critical Reinforced Concrete Bridge Piers," by J.B. Mander, S.M. Waheed, M.T.A. Chaudhary and S.S. Chen, 5/12/93, (PB93-227494, A08, MF-A02).
- NCEER-93-0011 "3D-BASIS-TABS: Computer Program for Nonlinear Dynamic Analysis of Three Dimensional Base Isolated Structures," by S. Nagarajaiah, C. Li, A.M. Reinhorn and M.C. Constantinou, 8/2/93, (PB94-141819, A09, MF-A02).
- NCEER-93-0012 "Effects of Hydrocarbon Spills from an Oil Pipeline Break on Ground Water," by O.J. Helweg and H.H.M. Hwang, 8/3/93, (PB94-141942, A06, MF-A02).
- NCEER-93-0013 "Simplified Procedures for Seismic Design of Nonstructural Components and Assessment of Current Code Provisions," by M.P. Singh, L.E. Suarez, E.E. Matheu and G.O. Maldonado, 8/4/93, (PB94-141827, A09, MF-A02).
- NCEER-93-0014 "An Energy Approach to Seismic Analysis and Design of Secondary Systems," by G. Chen and T.T. Soong, 8/6/93, (PB94-142767, A11, MF-A03).

- NCEER-93-0015 "Proceedings from School Sites: Becoming Prepared for Earthquakes - Commemorating the Third Anniversary of the Loma Prieta Earthquake," Edited by F.E. Winslow and K.E.K. Ross, 8/16/93, (PB94-154275, A16, MF-A02).
- NCEER-93-0016 "Reconnaissance Report of Damage to Historic Monuments in Cairo, Egypt Following the October 12, 1992 Dahshur Earthquake," by D. Sykora, D. Look, G. Croci, E. Karaesmen and E. Karaesmen, 8/19/93, (PB94-142221, A08, MF-A02).
- NCEER-93-0017 "The Island of Guam Earthquake of August 8, 1993," by S.W. Swan and S.K. Harris, 9/30/93, (PB94-141843, A04, MF-A01).
- NCEER-93-0018 "Engineering Aspects of the October 12, 1992 Egyptian Earthquake," by A.W. Elgamal, M. Amer, K. Adalier and A. Abul-Fadl, 10/7/93, (PB94-141983, A05, MF-A01).
- NCEER-93-0019 "Development of an Earthquake Motion Simulator and its Application in Dynamic Centrifuge Testing," by I. Krstelj, Supervised by J.H. Prevost, 10/23/93, (PB94-181773, A-10, MF-A03).
- NCEER-93-0020 "NCEER-Taisei Corporation Research Program on Sliding Seismic Isolation Systems for Bridges: Experimental and Analytical Study of a Friction Pendulum System (FPS)," by M.C. Constantinou, P. Tsopelas, Y-S. Kim and S. Okamoto, 11/1/93, (PB94-142775, A08, MF-A02).
- NCEER-93-0021 "Finite Element Modeling of Elastomeric Seismic Isolation Bearings," by L.J. Billings, Supervised by R. Shepherd, 11/8/93, to be published.
- NCEER-93-0022 "Seismic Vulnerability of Equipment in Critical Facilities: Life-Safety and Operational Consequences," by K. Porter, G.S. Johnson, M.M. Zadeh, C. Scawthorn and S. Eder, 11/24/93, (PB94-181765, A16, MF-A03).
- NCEER-93-0023 "Hokkaido Nansei-oki, Japan Earthquake of July 12, 1993, by P.I. Yanev and C.R. Scawthorn, 12/23/93, (PB94-181500, A07, MF-A01).
- NCEER-94-0001 "An Evaluation of Seismic Serviceability of Water Supply Networks with Application to the San Francisco Auxiliary Water Supply System," by I. Markov, Supervised by M. Grigoriu and T. O'Rourke, 1/21/94, (PB94-204013, A07, MF-A02).
- NCEER-94-0002 "NCEER-Taisei Corporation Research Program on Sliding Seismic Isolation Systems for Bridges: Experimental and Analytical Study of Systems Consisting of Sliding Bearings, Rubber Restoring Force Devices and Fluid Dampers," Volumes I and II, by P. Tsopelas, S. Okamoto, M.C. Constantinou, D. Ozaki and S. Fujii, 2/4/94, (PB94-181740, A09, MF-A02 and PB94-181757, A12, MF-A03).
- NCEER-94-0003 "A Markov Model for Local and Global Damage Indices in Seismic Analysis," by S. Rahman and M. Grigoriu, 2/18/94, (PB94-206000, A12, MF-A03).
- NCEER-94-0004 "Proceedings from the NCEER Workshop on Seismic Response of Masonry Infills," edited by D.P. Abrams, 3/1/94, (PB94-180783, A07, MF-A02).
- NCEER-94-0005 "The Northridge, California Earthquake of January 17, 1994: General Reconnaissance Report," edited by J.D. Goltz, 3/11/94, (PB94-193943, A10, MF-A03).
- NCEER-94-0006 "Seismic Energy Based Fatigue Damage Analysis of Bridge Columns: Part I - Evaluation of Seismic Capacity," by G.A. Chang and J.B. Mander, 3/14/94, (PB94-219185, A11, MF-A03).
- NCEER-94-0007 "Seismic Isolation of Multi-Story Frame Structures Using Spherical Sliding Isolation Systems," by T.M. Al-Hussaini, V.A. Zayas and M.C. Constantinou, 3/17/94, (PB94-193745, A09, MF-A02).
- NCEER-94-0008 "The Northridge, California Earthquake of January 17, 1994: Performance of Highway Bridges," edited by I.G. Buckle, 3/24/94, (PB94-193851, A06, MF-A02).
- NCEER-94-0009 "Proceedings of the Third U.S.-Japan Workshop on Earthquake Protective Systems for Bridges," edited by I.G. Buckle and I. Friedland, 3/31/94, (PB94-195815, A99, MF-A06).

- NCEER-94-0010 "3D-BASIS-ME: Computer Program for Nonlinear Dynamic Analysis of Seismically Isolated Single and Multiple Structures and Liquid Storage Tanks," by P.C. Tsopelas, M.C. Constantinou and A.M. Reinhorn, 4/12/94, (PB94-204922, A09, MF-A02).
- NCEER-94-0011 "The Northridge, California Earthquake of January 17, 1994: Performance of Gas Transmission Pipelines," by T.D. O'Rourke and M.C. Palmer, 5/16/94, (PB94-204989, A05, MF-A01).
- NCEER-94-0012 "Feasibility Study of Replacement Procedures and Earthquake Performance Related to Gas Transmission Pipelines," by T.D. O'Rourke and M.C. Palmer, 5/25/94, (PB94-206638, A09, MF-A02).
- NCEER-94-0013 "Seismic Energy Based Fatigue Damage Analysis of Bridge Columns: Part II - Evaluation of Seismic Demand," by G.A. Chang and J.B. Mander, 6/1/94, (PB95-18106, A08, MF-A02).
- NCEER-94-0014 "NCEER-Taisei Corporation Research Program on Sliding Seismic Isolation Systems for Bridges: Experimental and Analytical Study of a System Consisting of Sliding Bearings and Fluid Restoring Force/Damping Devices," by P. Tsopelas and M.C. Constantinou, 6/13/94, (PB94-219144, A10, MF-A03).
- NCEER-94-0015 "Generation of Hazard-Consistent Fragility Curves for Seismic Loss Estimation Studies," by H. Hwang and J-R. Huo, 6/14/94, (PB95-181996, A09, MF-A02).
- NCEER-94-0016 "Seismic Study of Building Frames with Added Energy-Absorbing Devices," by W.S. Pong, C.S. Tsai and G.C. Lee, 6/20/94, (PB94-219136, A10, A03).
- NCEER-94-0017 "Sliding Mode Control for Seismic-Excited Linear and Nonlinear Civil Engineering Structures," by J. Yang, J. Wu, A. Agrawal and Z. Li, 6/21/94, (PB95-138483, A06, MF-A02).
- NCEER-94-0018 "3D-BASIS-TABS Version 2.0: Computer Program for Nonlinear Dynamic Analysis of Three Dimensional Base Isolated Structures," by A.M. Reinhorn, S. Nagarajaiah, M.C. Constantinou, P. Tsopelas and R. Li, 6/22/94, (PB95-182176, A08, MF-A02).
- NCEER-94-0019 "Proceedings of the International Workshop on Civil Infrastructure Systems: Application of Intelligent Systems and Advanced Materials on Bridge Systems," Edited by G.C. Lee and K.C. Chang, 7/18/94, (PB95-252474, A20, MF-A04).
- NCEER-94-0020 "Study of Seismic Isolation Systems for Computer Floors," by V. Lambrou and M.C. Constantinou, 7/19/94, (PB95-138533, A10, MF-A03).
- NCEER-94-0021 "Proceedings of the U.S.-Italian Workshop on Guidelines for Seismic Evaluation and Rehabilitation of Unreinforced Masonry Buildings," Edited by D.P. Abrams and G.M. Calvi, 7/20/94, (PB95-138749, A13, MF-A03).
- NCEER-94-0022 "NCEER-Taisei Corporation Research Program on Sliding Seismic Isolation Systems for Bridges: Experimental and Analytical Study of a System Consisting of Lubricated PTFE Sliding Bearings and Mild Steel Dampers," by P. Tsopelas and M.C. Constantinou, 7/22/94, (PB95-182184, A08, MF-A02).
- NCEER-94-0023 "Development of Reliability-Based Design Criteria for Buildings Under Seismic Load," by Y.K. Wen, H. Hwang and M. Shinozuka, 8/1/94, (PB95-211934, A08, MF-A02).
- NCEER-94-0024 "Experimental Verification of Acceleration Feedback Control Strategies for an Active Tendon System," by S.J. Dyke, B.F. Spencer, Jr., P. Quast, M.K. Sain, D.C. Kaspari, Jr. and T.T. Soong, 8/29/94, (PB95-212320, A05, MF-A01).
- NCEER-94-0025 "Seismic Retrofitting Manual for Highway Bridges," Edited by I.G. Buckle and I.F. Friedland, published by the Federal Highway Administration (PB95-212676, A15, MF-A03).
- NCEER-94-0026 "Proceedings from the Fifth U.S.-Japan Workshop on Earthquake Resistant Design of Lifeline Facilities and Countermeasures Against Soil Liquefaction," Edited by T.D. O'Rourke and M. Hamada, 11/7/94, (PB95-220802, A99, MF-E08).



- NCEER-95-0001 “Experimental and Analytical Investigation of Seismic Retrofit of Structures with Supplemental Damping: Part 1 - Fluid Viscous Damping Devices,” by A.M. Reinhorn, C. Li and M.C. Constantinou, 1/3/95, (PB95-266599, A09, MF-A02).
- NCEER-95-0002 “Experimental and Analytical Study of Low-Cycle Fatigue Behavior of Semi-Rigid Top-And-Seat Angle Connections,” by G. Pekcan, J.B. Mander and S.S. Chen, 1/5/95, (PB95-220042, A07, MF-A02).
- NCEER-95-0003 “NCEER-ATC Joint Study on Fragility of Buildings,” by T. Anagnos, C. Rojahn and A.S. Kiremidjian, 1/20/95, (PB95-220026, A06, MF-A02).
- NCEER-95-0004 “Nonlinear Control Algorithms for Peak Response Reduction,” by Z. Wu, T.T. Soong, V. Gattulli and R.C. Lin, 2/16/95, (PB95-220349, A05, MF-A01).
- NCEER-95-0005 “Pipeline Replacement Feasibility Study: A Methodology for Minimizing Seismic and Corrosion Risks to Underground Natural Gas Pipelines,” by R.T. Eguchi, H.A. Seligson and D.G. Honegger, 3/2/95, (PB95-252326, A06, MF-A02).
- NCEER-95-0006 “Evaluation of Seismic Performance of an 11-Story Frame Building During the 1994 Northridge Earthquake,” by F. Naeim, R. DiSulio, K. Benuska, A. Reinhorn and C. Li, to be published.
- NCEER-95-0007 “Prioritization of Bridges for Seismic Retrofitting,” by N. Basöz and A.S. Kiremidjian, 4/24/95, (PB95-252300, A08, MF-A02).
- NCEER-95-0008 “Method for Developing Motion Damage Relationships for Reinforced Concrete Frames,” by A. Singhal and A.S. Kiremidjian, 5/11/95, (PB95-266607, A06, MF-A02).
- NCEER-95-0009 “Experimental and Analytical Investigation of Seismic Retrofit of Structures with Supplemental Damping: Part II - Friction Devices,” by C. Li and A.M. Reinhorn, 7/6/95, (PB96-128087, A11, MF-A03).
- NCEER-95-0010 “Experimental Performance and Analytical Study of a Non-Ductile Reinforced Concrete Frame Structure Retrofitted with Elastomeric Spring Dampers,” by G. Pekcan, J.B. Mander and S.S. Chen, 7/14/95, (PB96-137161, A08, MF-A02).
- NCEER-95-0011 “Development and Experimental Study of Semi-Active Fluid Damping Devices for Seismic Protection of Structures,” by M.D. Symans and M.C. Constantinou, 8/3/95, (PB96-136940, A23, MF-A04).
- NCEER-95-0012 “Real-Time Structural Parameter Modification (RSPM): Development of Innervated Structures,” by Z. Liang, M. Tong and G.C. Lee, 4/11/95, (PB96-137153, A06, MF-A01).
- NCEER-95-0013 “Experimental and Analytical Investigation of Seismic Retrofit of Structures with Supplemental Damping: Part III - Viscous Damping Walls,” by A.M. Reinhorn and C. Li, 10/1/95, (PB96-176409, A11, MF-A03).
- NCEER-95-0014 “Seismic Fragility Analysis of Equipment and Structures in a Memphis Electric Substation,” by J-R. Huo and H.H.M. Hwang, 8/10/95, (PB96-128087, A09, MF-A02).
- NCEER-95-0015 “The Hanshin-Awaji Earthquake of January 17, 1995: Performance of Lifelines,” Edited by M. Shinozuka, 11/3/95, (PB96-176383, A15, MF-A03).
- NCEER-95-0016 “Highway Culvert Performance During Earthquakes,” by T.L. Youd and C.J. Beckman, available as NCEER-96-0015.
- NCEER-95-0017 “The Hanshin-Awaji Earthquake of January 17, 1995: Performance of Highway Bridges,” Edited by I.G. Buckle, 12/1/95, to be published.
- NCEER-95-0018 “Modeling of Masonry Infill Panels for Structural Analysis,” by A.M. Reinhorn, A. Madan, R.E. Valles, Y. Reichmann and J.B. Mander, 12/8/95, (PB97-110886, MF-A01, A06).
- NCEER-95-0019 “Optimal Polynomial Control for Linear and Nonlinear Structures,” by A.K. Agrawal and J.N. Yang, 12/11/95, (PB96-168737, A07, MF-A02).

- NCEER-95-0020 "Retrofit of Non-Ductile Reinforced Concrete Frames Using Friction Dampers," by R.S. Rao, P. Gergely and R.N. White, 12/22/95, (PB97-133508, A10, MF-A02).
- NCEER-95-0021 "Parametric Results for Seismic Response of Pile-Supported Bridge Bents," by G. Mylonakis, A. Nikolaou and G. Gazetas, 12/22/95, (PB97-100242, A12, MF-A03).
- NCEER-95-0022 "Kinematic Bending Moments in Seismically Stressed Piles," by A. Nikolaou, G. Mylonakis and G. Gazetas, 12/23/95, (PB97-113914, MF-A03, A13).
- NCEER-96-0001 "Dynamic Response of Unreinforced Masonry Buildings with Flexible Diaphragms," by A.C. Costley and D.P. Abrams, 10/10/96, (PB97-133573, MF-A03, A15).
- NCEER-96-0002 "State of the Art Review: Foundations and Retaining Structures," by I. Po Lam, to be published.
- NCEER-96-0003 "Ductility of Rectangular Reinforced Concrete Bridge Columns with Moderate Confinement," by N. Wehbe, M. Saiidi, D. Sanders and B. Douglas, 11/7/96, (PB97-133557, A06, MF-A02).
- NCEER-96-0004 "Proceedings of the Long-Span Bridge Seismic Research Workshop," edited by I.G. Buckle and I.M. Friedland, to be published.
- NCEER-96-0005 "Establish Representative Pier Types for Comprehensive Study: Eastern United States," by J. Kulicki and Z. Prucz, 5/28/96, (PB98-119217, A07, MF-A02).
- NCEER-96-0006 "Establish Representative Pier Types for Comprehensive Study: Western United States," by R. Imbsen, R.A. Schamber and T.A. Osterkamp, 5/28/96, (PB98-118607, A07, MF-A02).
- NCEER-96-0007 "Nonlinear Control Techniques for Dynamical Systems with Uncertain Parameters," by R.G. Ghanem and M.I. Bujakov, 5/27/96, (PB97-100259, A17, MF-A03).
- NCEER-96-0008 "Seismic Evaluation of a 30-Year Old Non-Ductile Highway Bridge Pier and Its Retrofit," by J.B. Mander, B. Mahmoodzadegan, S. Bhadra and S.S. Chen, 5/31/96, (PB97-110902, MF-A03, A10).
- NCEER-96-0009 "Seismic Performance of a Model Reinforced Concrete Bridge Pier Before and After Retrofit," by J.B. Mander, J.H. Kim and C.A. Ligozio, 5/31/96, (PB97-110910, MF-A02, A10).
- NCEER-96-0010 "IDARC2D Version 4.0: A Computer Program for the Inelastic Damage Analysis of Buildings," by R.E. Valles, A.M. Reinhorn, S.K. Kunnath, C. Li and A. Madan, 6/3/96, (PB97-100234, A17, MF-A03).
- NCEER-96-0011 "Estimation of the Economic Impact of Multiple Lifeline Disruption: Memphis Light, Gas and Water Division Case Study," by S.E. Chang, H.A. Seligson and R.T. Eguchi, 8/16/96, (PB97-133490, A11, MF-A03).
- NCEER-96-0012 "Proceedings from the Sixth Japan-U.S. Workshop on Earthquake Resistant Design of Lifeline Facilities and Countermeasures Against Soil Liquefaction, Edited by M. Hamada and T. O'Rourke, 9/11/96, (PB97-133581, A99, MF-A06).
- NCEER-96-0013 "Chemical Hazards, Mitigation and Preparedness in Areas of High Seismic Risk: A Methodology for Estimating the Risk of Post-Earthquake Hazardous Materials Release," by H.A. Seligson, R.T. Eguchi, K.J. Tierney and K. Richmond, 11/7/96, (PB97-133565, MF-A02, A08).
- NCEER-96-0014 "Response of Steel Bridge Bearings to Reversed Cyclic Loading," by J.B. Mander, D-K. Kim, S.S. Chen and G.J. Premus, 11/13/96, (PB97-140735, A12, MF-A03).
- NCEER-96-0015 "Highway Culvert Performance During Past Earthquakes," by T.L. Youd and C.J. Beckman, 11/25/96, (PB97-133532, A06, MF-A01).
- NCEER-97-0001 "Evaluation, Prevention and Mitigation of Pounding Effects in Building Structures," by R.E. Valles and A.M. Reinhorn, 2/20/97, (PB97-159552, A14, MF-A03).
- NCEER-97-0002 "Seismic Design Criteria for Bridges and Other Highway Structures," by C. Rojahn, R. Mayes, D.G. Anderson, J. Clark, J.H. Hom, R.V. Nutt and M.J. O'Rourke, 4/30/97, (PB97-194658, A06, MF-A03).

- NCEER-97-0003 "Proceedings of the U.S.-Italian Workshop on Seismic Evaluation and Retrofit," Edited by D.P. Abrams and G.M. Calvi, 3/19/97, (PB97-194666, A13, MF-A03).
- NCEER-97-0004 "Investigation of Seismic Response of Buildings with Linear and Nonlinear Fluid Viscous Dampers," by A.A. Seleemah and M.C. Constantinou, 5/21/97, (PB98-109002, A15, MF-A03).
- NCEER-97-0005 "Proceedings of the Workshop on Earthquake Engineering Frontiers in Transportation Facilities," edited by G.C. Lee and I.M. Friedland, 8/29/97, (PB98-128911, A25, MR-A04).
- NCEER-97-0006 "Cumulative Seismic Damage of Reinforced Concrete Bridge Piers," by S.K. Kunnath, A. El-Bahy, A. Taylor and W. Stone, 9/2/97, (PB98-108814, A11, MF-A03).
- NCEER-97-0007 "Structural Details to Accommodate Seismic Movements of Highway Bridges and Retaining Walls," by R.A. Imbsen, R.A. Schamber, E. Thorkildsen, A. Kartoum, B.T. Martin, T.N. Rosser and J.M. Kulicki, 9/3/97, (PB98-108996, A09, MF-A02).
- NCEER-97-0008 "A Method for Earthquake Motion-Damage Relationships with Application to Reinforced Concrete Frames," by A. Singhal and A.S. Kiremidjian, 9/10/97, (PB98-108988, A13, MF-A03).
- NCEER-97-0009 "Seismic Analysis and Design of Bridge Abutments Considering Sliding and Rotation," by K. Fishman and R. Richards, Jr., 9/15/97, (PB98-108897, A06, MF-A02).
- NCEER-97-0010 "Proceedings of the FHWA/NCEER Workshop on the National Representation of Seismic Ground Motion for New and Existing Highway Facilities," edited by I.M. Friedland, M.S. Power and R.L. Mayes, 9/22/97, (PB98-128903, A21, MF-A04).
- NCEER-97-0011 "Seismic Analysis for Design or Retrofit of Gravity Bridge Abutments," by K.L. Fishman, R. Richards, Jr. and R.C. Divito, 10/2/97, (PB98-128937, A08, MF-A02).
- NCEER-97-0012 "Evaluation of Simplified Methods of Analysis for Yielding Structures," by P. Tsopelas, M.C. Constantinou, C.A. Kircher and A.S. Whittaker, 10/31/97, (PB98-128929, A10, MF-A03).
- NCEER-97-0013 "Seismic Design of Bridge Columns Based on Control and Repairability of Damage," by C-T. Cheng and J.B. Mander, 12/8/97, (PB98-144249, A11, MF-A03).
- NCEER-97-0014 "Seismic Resistance of Bridge Piers Based on Damage Avoidance Design," by J.B. Mander and C-T. Cheng, 12/10/97, (PB98-144223, A09, MF-A02).
- NCEER-97-0015 "Seismic Response of Nominally Symmetric Systems with Strength Uncertainty," by S. Balopoulou and M. Grigoriu, 12/23/97, (PB98-153422, A11, MF-A03).
- NCEER-97-0016 "Evaluation of Seismic Retrofit Methods for Reinforced Concrete Bridge Columns," by T.J. Wipf, F.W. Klaiber and F.M. Russo, 12/28/97, (PB98-144215, A12, MF-A03).
- NCEER-97-0017 "Seismic Fragility of Existing Conventional Reinforced Concrete Highway Bridges," by C.L. Mullen and A.S. Cakmak, 12/30/97, (PB98-153406, A08, MF-A02).
- NCEER-97-0018 "Loss Assessment of Memphis Buildings," edited by D.P. Abrams and M. Shinozuka, 12/31/97, (PB98-144231, A13, MF-A03).
- NCEER-97-0019 "Seismic Evaluation of Frames with Infill Walls Using Quasi-static Experiments," by K.M. Mosalam, R.N. White and P. Gergely, 12/31/97, (PB98-153455, A07, MF-A02).
- NCEER-97-0020 "Seismic Evaluation of Frames with Infill Walls Using Pseudo-dynamic Experiments," by K.M. Mosalam, R.N. White and P. Gergely, 12/31/97, (PB98-153430, A07, MF-A02).
- NCEER-97-0021 "Computational Strategies for Frames with Infill Walls: Discrete and Smeared Crack Analyses and Seismic Fragility," by K.M. Mosalam, R.N. White and P. Gergely, 12/31/97, (PB98-153414, A10, MF-A02).

- NCEER-97-0022 "Proceedings of the NCEER Workshop on Evaluation of Liquefaction Resistance of Soils," edited by T.L. Youd and I.M. Idriss, 12/31/97, (PB98-155617, A15, MF-A03).
- MCEER-98-0001 "Extraction of Nonlinear Hysteretic Properties of Seismically Isolated Bridges from Quick-Release Field Tests," by Q. Chen, B.M. Douglas, E.M. Maragakis and I.G. Buckle, 5/26/98, (PB99-118838, A06, MF-A01).
- MCEER-98-0002 "Methodologies for Evaluating the Importance of Highway Bridges," by A. Thomas, S. Eshenaur and J. Kulicki, 5/29/98, (PB99-118846, A10, MF-A02).
- MCEER-98-0003 "Capacity Design of Bridge Piers and the Analysis of Overstrength," by J.B. Mander, A. Dutta and P. Goel, 6/1/98, (PB99-118853, A09, MF-A02).
- MCEER-98-0004 "Evaluation of Bridge Damage Data from the Loma Prieta and Northridge, California Earthquakes," by N. Basoz and A. Kiremidjian, 6/2/98, (PB99-118861, A15, MF-A03).
- MCEER-98-0005 "Screening Guide for Rapid Assessment of Liquefaction Hazard at Highway Bridge Sites," by T. L. Youd, 6/16/98, (PB99-118879, A06, not available on microfiche).
- MCEER-98-0006 "Structural Steel and Steel/Concrete Interface Details for Bridges," by P. Ritchie, N. Kaulh and J. Kulicki, 7/13/98, (PB99-118945, A06, MF-A01).
- MCEER-98-0007 "Capacity Design and Fatigue Analysis of Confined Concrete Columns," by A. Dutta and J.B. Mander, 7/14/98, (PB99-118960, A14, MF-A03).
- MCEER-98-0008 "Proceedings of the Workshop on Performance Criteria for Telecommunication Services Under Earthquake Conditions," edited by A.J. Schiff, 7/15/98, (PB99-118952, A08, MF-A02).
- MCEER-98-0009 "Fatigue Analysis of Unconfined Concrete Columns," by J.B. Mander, A. Dutta and J.H. Kim, 9/12/98, (PB99-123655, A10, MF-A02).
- MCEER-98-0010 "Centrifuge Modeling of Cyclic Lateral Response of Pile-Cap Systems and Seat-Type Abutments in Dry Sands," by A.D. Gadre and R. Dobry, 10/2/98, (PB99-123606, A13, MF-A03).
- MCEER-98-0011 "IDARC-BRIDGE: A Computational Platform for Seismic Damage Assessment of Bridge Structures," by A.M. Reinhorn, V. Simeonov, G. Mylonakis and Y. Reichman, 10/2/98, (PB99-162919, A15, MF-A03).
- MCEER-98-0012 "Experimental Investigation of the Dynamic Response of Two Bridges Before and After Retrofitting with Elastomeric Bearings," by D.A. Wendichansky, S.S. Chen and J.B. Mander, 10/2/98, (PB99-162927, A15, MF-A03).
- MCEER-98-0013 "Design Procedures for Hinge Restrainers and Hinge Sear Width for Multiple-Frame Bridges," by R. Des Roches and G.L. Fenves, 11/3/98, (PB99-140477, A13, MF-A03).
- MCEER-98-0014 "Response Modification Factors for Seismically Isolated Bridges," by M.C. Constantinou and J.K. Quarshie, 11/3/98, (PB99-140485, A14, MF-A03).
- MCEER-98-0015 "Proceedings of the U.S.-Italy Workshop on Seismic Protective Systems for Bridges," edited by I.M. Friedland and M.C. Constantinou, 11/3/98, (PB2000-101711, A22, MF-A04).
- MCEER-98-0016 "Appropriate Seismic Reliability for Critical Equipment Systems: Recommendations Based on Regional Analysis of Financial and Life Loss," by K. Porter, C. Scawthorn, C. Taylor and N. Blais, 11/10/98, (PB99-157265, A08, MF-A02).
- MCEER-98-0017 "Proceedings of the U.S. Japan Joint Seminar on Civil Infrastructure Systems Research," edited by M. Shinozuka and A. Rose, 11/12/98, (PB99-156713, A16, MF-A03).
- MCEER-98-0018 "Modeling of Pile Footings and Drilled Shafts for Seismic Design," by I. PoLam, M. Kapuskar and D. Chaudhuri, 12/21/98, (PB99-157257, A09, MF-A02).

- MCEER-99-0001 "Seismic Evaluation of a Masonry Infilled Reinforced Concrete Frame by Pseudodynamic Testing," by S.G. Buonopane and R.N. White, 2/16/99, (PB99-162851, A09, MF-A02).
- MCEER-99-0002 "Response History Analysis of Structures with Seismic Isolation and Energy Dissipation Systems: Verification Examples for Program SAP2000," by J. Scheller and M.C. Constantinou, 2/22/99, (PB99-162869, A08, MF-A02).
- MCEER-99-0003 "Experimental Study on the Seismic Design and Retrofit of Bridge Columns Including Axial Load Effects," by A. Dutta, T. Kokorina and J.B. Mander, 2/22/99, (PB99-162877, A09, MF-A02).
- MCEER-99-0004 "Experimental Study of Bridge Elastomeric and Other Isolation and Energy Dissipation Systems with Emphasis on Uplift Prevention and High Velocity Near-source Seismic Excitation," by A. Kasalanati and M. C. Constantinou, 2/26/99, (PB99-162885, A12, MF-A03).
- MCEER-99-0005 "Truss Modeling of Reinforced Concrete Shear-flexure Behavior," by J.H. Kim and J.B. Mander, 3/8/99, (PB99-163693, A12, MF-A03).
- MCEER-99-0006 "Experimental Investigation and Computational Modeling of Seismic Response of a 1:4 Scale Model Steel Structure with a Load Balancing Supplemental Damping System," by G. Pekcan, J.B. Mander and S.S. Chen, 4/2/99, (PB99-162893, A11, MF-A03).
- MCEER-99-0007 "Effect of Vertical Ground Motions on the Structural Response of Highway Bridges," by M.R. Button, C.J. Cronin and R.L. Mayes, 4/10/99, (PB2000-101411, A10, MF-A03).
- MCEER-99-0008 "Seismic Reliability Assessment of Critical Facilities: A Handbook, Supporting Documentation, and Model Code Provisions," by G.S. Johnson, R.E. Sheppard, M.D. Quilici, S.J. Eder and C.R. Scawthorn, 4/12/99, (PB2000-101701, A18, MF-A04).
- MCEER-99-0009 "Impact Assessment of Selected MCEER Highway Project Research on the Seismic Design of Highway Structures," by C. Rojahn, R. Mayes, D.G. Anderson, J.H. Clark, D'Appolonia Engineering, S. Gloyd and R.V. Nutt, 4/14/99, (PB99-162901, A10, MF-A02).
- MCEER-99-0010 "Site Factors and Site Categories in Seismic Codes," by R. Dobry, R. Ramos and M.S. Power, 7/19/99, (PB2000-101705, A08, MF-A02).
- MCEER-99-0011 "Restrainer Design Procedures for Multi-Span Simply-Supported Bridges," by M.J. Randall, M. Saiidi, E. Maragakis and T. Isakovic, 7/20/99, (PB2000-101702, A10, MF-A02).
- MCEER-99-0012 "Property Modification Factors for Seismic Isolation Bearings," by M.C. Constantinou, P. Tsopelas, A. Kasalanati and E. Wolff, 7/20/99, (PB2000-103387, A11, MF-A03).
- MCEER-99-0013 "Critical Seismic Issues for Existing Steel Bridges," by P. Ritchie, N. Kauh and J. Kulicki, 7/20/99, (PB2000-101697, A09, MF-A02).
- MCEER-99-0014 "Nonstructural Damage Database," by A. Kao, T.T. Soong and A. Vender, 7/24/99, (PB2000-101407, A06, MF-A01).
- MCEER-99-0015 "Guide to Remedial Measures for Liquefaction Mitigation at Existing Highway Bridge Sites," by H.G. Cooke and J. K. Mitchell, 7/26/99, (PB2000-101703, A11, MF-A03).
- MCEER-99-0016 "Proceedings of the MCEER Workshop on Ground Motion Methodologies for the Eastern United States," edited by N. Abrahamson and A. Becker, 8/11/99, (PB2000-103385, A07, MF-A02).
- MCEER-99-0017 "Quindío, Colombia Earthquake of January 25, 1999: Reconnaissance Report," by A.P. Asfura and P.J. Flores, 10/4/99, (PB2000-106893, A06, MF-A01).
- MCEER-99-0018 "Hysteretic Models for Cyclic Behavior of Deteriorating Inelastic Structures," by M.V. Sivaselvan and A.M. Reinhorn, 11/5/99, (PB2000-103386, A08, MF-A02).

- MCEER-99-0019 "Proceedings of the 7<sup>th</sup> U.S.- Japan Workshop on Earthquake Resistant Design of Lifeline Facilities and Countermeasures Against Soil Liquefaction," edited by T.D. O'Rourke, J.P. Bardet and M. Hamada, 11/19/99, (PB2000-103354, A99, MF-A06).
- MCEER-99-0020 "Development of Measurement Capability for Micro-Vibration Evaluations with Application to Chip Fabrication Facilities," by G.C. Lee, Z. Liang, J.W. Song, J.D. Shen and W.C. Liu, 12/1/99, (PB2000-105993, A08, MF-A02).
- MCEER-99-0021 "Design and Retrofit Methodology for Building Structures with Supplemental Energy Dissipating Systems," by G. Pekcan, J.B. Mander and S.S. Chen, 12/31/99, (PB2000-105994, A11, MF-A03).
- MCEER-00-0001 "The Marmara, Turkey Earthquake of August 17, 1999: Reconnaissance Report," edited by C. Scawthorn; with major contributions by M. Bruneau, R. Eguchi, T. Holzer, G. Johnson, J. Mander, J. Mitchell, W. Mitchell, A. Papageorgiou, C. Scaethorn, and G. Webb, 3/23/00, (PB2000-106200, A11, MF-A03).
- MCEER-00-0002 "Proceedings of the MCEER Workshop for Seismic Hazard Mitigation of Health Care Facilities," edited by G.C. Lee, M. Ettouney, M. Grigoriu, J. Hauer and J. Nigg, 3/29/00, (PB2000-106892, A08, MF-A02).
- MCEER-00-0003 "The Chi-Chi, Taiwan Earthquake of September 21, 1999: Reconnaissance Report," edited by G.C. Lee and C.H. Loh, with major contributions by G.C. Lee, M. Bruneau, I.G. Buckle, S.E. Chang, P.J. Flores, T.D. O'Rourke, M. Shinozuka, T.T. Soong, C-H. Loh, K-C. Chang, Z-J. Chen, J-S. Hwang, M-L. Lin, G-Y. Liu, K-C. Tsai, G.C. Yao and C-L. Yen, 4/30/00, (PB2001-100980, A10, MF-A02).
- MCEER-00-0004 "Seismic Retrofit of End-Sway Frames of Steel Deck-Truss Bridges with a Supplemental Tendon System: Experimental and Analytical Investigation," by G. Pekcan, J.B. Mander and S.S. Chen, 7/1/00, (PB2001-100982, A10, MF-A02).
- MCEER-00-0005 "Sliding Fragility of Unrestrained Equipment in Critical Facilities," by W.H. Chong and T.T. Soong, 7/5/00, (PB2001-100983, A08, MF-A02).
- MCEER-00-0006 "Seismic Response of Reinforced Concrete Bridge Pier Walls in the Weak Direction," by N. Abo-Shadi, M. Saiidi and D. Sanders, 7/17/00, (PB2001-100981, A17, MF-A03).
- MCEER-00-0007 "Low-Cycle Fatigue Behavior of Longitudinal Reinforcement in Reinforced Concrete Bridge Columns," by J. Brown and S.K. Kunnath, 7/23/00, (PB2001-104392, A08, MF-A02).
- MCEER-00-0008 "Soil Structure Interaction of Bridges for Seismic Analysis," I. PoLam and H. Law, 9/25/00, (PB2001-105397, A08, MF-A02).
- MCEER-00-0009 "Proceedings of the First MCEER Workshop on Mitigation of Earthquake Disaster by Advanced Technologies (MEDAT-1), edited by M. Shinozuka, D.J. Inman and T.D. O'Rourke, 11/10/00, (PB2001-105399, A14, MF-A03).
- MCEER-00-0010 "Development and Evaluation of Simplified Procedures for Analysis and Design of Buildings with Passive Energy Dissipation Systems, Revision 01," by O.M. Ramirez, M.C. Constantinou, C.A. Kircher, A.S. Whittaker, M.W. Johnson, J.D. Gomez and C. Chrysostomou, 11/16/01, (PB2001-105523, A23, MF-A04).
- MCEER-00-0011 "Dynamic Soil-Foundation-Structure Interaction Analyses of Large Caissons," by C-Y. Chang, C-M. Mok, Z-L. Wang, R. Settgast, F. Waggoner, M.A. Ketchum, H.M. Gonnermann and C-C. Chin, 12/30/00, (PB2001-104373, A07, MF-A02).
- MCEER-00-0012 "Experimental Evaluation of Seismic Performance of Bridge Restrainers," by A.G. Vlassis, E.M. Maragakis and M. Saiid Saiidi, 12/30/00, (PB2001-104354, A09, MF-A02).
- MCEER-00-0013 "Effect of Spatial Variation of Ground Motion on Highway Structures," by M. Shinozuka, V. Saxena and G. Deodatis, 12/31/00, (PB2001-108755, A13, MF-A03).
- MCEER-00-0014 "A Risk-Based Methodology for Assessing the Seismic Performance of Highway Systems," by S.D. Werner, C.E. Taylor, J.E. Moore, II, J.S. Walton and S. Cho, 12/31/00, (PB2001-108756, A14, MF-A03).

- MCEER-01-0001 "Experimental Investigation of P-Delta Effects to Collapse During Earthquakes," by D. Vian and M. Bruneau, 6/25/01, (PB2002-100534, A17, MF-A03).
- MCEER-01-0002 "Proceedings of the Second MCEER Workshop on Mitigation of Earthquake Disaster by Advanced Technologies (MEDAT-2)," edited by M. Bruneau and D.J. Inman, 7/23/01, (PB2002-100434, A16, MF-A03).
- MCEER-01-0003 "Sensitivity Analysis of Dynamic Systems Subjected to Seismic Loads," by C. Roth and M. Grigoriu, 9/18/01, (PB2003-100884, A12, MF-A03).
- MCEER-01-0004 "Overcoming Obstacles to Implementing Earthquake Hazard Mitigation Policies: Stage 1 Report," by D.J. Alesch and W.J. Petak, 12/17/01, (PB2002-107949, A07, MF-A02).
- MCEER-01-0005 "Updating Real-Time Earthquake Loss Estimates: Methods, Problems and Insights," by C.E. Taylor, S.E. Chang and R.T. Eguchi, 12/17/01, (PB2002-107948, A05, MF-A01).
- MCEER-01-0006 "Experimental Investigation and Retrofit of Steel Pile Foundations and Pile Bents Under Cyclic Lateral Loadings," by A. Shama, J. Mander, B. Blabac and S. Chen, 12/31/01, (PB2002-107950, A13, MF-A03).
- MCEER-02-0001 "Assessment of Performance of Bolu Viaduct in the 1999 Duzce Earthquake in Turkey" by P.C. Roussis, M.C. Constantinou, M. Erdik, E. Durukal and M. Dicleli, 5/8/02, (PB2003-100883, A08, MF-A02).
- MCEER-02-0002 "Seismic Behavior of Rail Counterweight Systems of Elevators in Buildings," by M.P. Singh, Rildova and L.E. Suarez, 5/27/02. (PB2003-100882, A11, MF-A03).
- MCEER-02-0003 "Development of Analysis and Design Procedures for Spread Footings," by G. Mylonakis, G. Gazetas, S. Nikolaou and A. Chauncey, 10/02/02, (PB2004-101636, A13, MF-A03, CD-A13).
- MCEER-02-0004 "Bare-Earth Algorithms for Use with SAR and LIDAR Digital Elevation Models," by C.K. Huyck, R.T. Eguchi and B. Houshmand, 10/16/02, (PB2004-101637, A07, CD-A07).
- MCEER-02-0005 "Review of Energy Dissipation of Compression Members in Concentrically Braced Frames," by K.Lee and M. Bruneau, 10/18/02, (PB2004-101638, A10, CD-A10).
- MCEER-03-0001 "Experimental Investigation of Light-Gauge Steel Plate Shear Walls for the Seismic Retrofit of Buildings" by J. Berman and M. Bruneau, 5/2/03, (PB2004-101622, A10, MF-A03, CD-A10).
- MCEER-03-0002 "Statistical Analysis of Fragility Curves," by M. Shinozuka, M.Q. Feng, H. Kim, T. Uzawa and T. Ueda, 6/16/03, (PB2004-101849, A09, CD-A09).
- MCEER-03-0003 "Proceedings of the Eighth U.S.-Japan Workshop on Earthquake Resistant Design of Lifeline Facilities and Countermeasures Against Liquefaction," edited by M. Hamada, J.P. Bardet and T.D. O'Rourke, 6/30/03, (PB2004-104386, A99, CD-A99).
- MCEER-03-0004 "Proceedings of the PRC-US Workshop on Seismic Analysis and Design of Special Bridges," edited by L.C. Fan and G.C. Lee, 7/15/03, (PB2004-104387, A14, CD-A14).
- MCEER-03-0005 "Urban Disaster Recovery: A Framework and Simulation Model," by S.B. Miles and S.E. Chang, 7/25/03, (PB2004-104388, A07, CD-A07).
- MCEER-03-0006 "Behavior of Underground Piping Joints Due to Static and Dynamic Loading," by R.D. Meis, M. Maragakis and R. Siddharthan, 11/17/03, (PB2005-102194, A13, MF-A03, CD-A00).
- MCEER-03-0007 "Seismic Vulnerability of Timber Bridges and Timber Substructures," by A.A. Shama, J.B. Mander, I.M. Friedland and D.R. Allicock, 12/15/03.
- MCEER-04-0001 "Experimental Study of Seismic Isolation Systems with Emphasis on Secondary System Response and Verification of Accuracy of Dynamic Response History Analysis Methods," by E. Wolff and M. Constantinou, 1/16/04 (PB2005-102195, A99, MF-E08, CD-A00).


- MCEER-04-0002 “Tension, Compression and Cyclic Testing of Engineered Cementitious Composite Materials,” by K. Kesner and S.L. Billington, 3/1/04, (PB2005-102196, A08, CD-A08).
- MCEER-04-0003 “Cyclic Testing of Braces Laterally Restrained by Steel Studs to Enhance Performance During Earthquakes,” by O.C. Celik, J.W. Berman and M. Bruneau, 3/16/04, (PB2005-102197, A13, MF-A03, CD-A00).
- MCEER-04-0004 “Methodologies for Post Earthquake Building Damage Detection Using SAR and Optical Remote Sensing: Application to the August 17, 1999 Marmara, Turkey Earthquake,” by C.K. Huyck, B.J. Adams, S. Cho, R.T. Eguchi, B. Mansouri and B. Houshmand, 6/15/04, (PB2005-104888, A10, CD-A00).
- MCEER-04-0005 “Nonlinear Structural Analysis Towards Collapse Simulation: A Dynamical Systems Approach,” by M.V. Sivaselvan and A.M. Reinhorn, 6/16/04, (PB2005-104889, A11, MF-A03, CD-A00).
- MCEER-04-0006 “Proceedings of the Second PRC-US Workshop on Seismic Analysis and Design of Special Bridges,” edited by G.C. Lee and L.C. Fan, 6/25/04, (PB2005-104890, A16, CD-A00).
- MCEER-04-0007 “Seismic Vulnerability Evaluation of Axially Loaded Steel Built-up Laced Members,” by K. Lee and M. Bruneau, 6/30/04, (PB2005-104891, A16, CD-A00).
- MCEER-04-0008 “Evaluation of Accuracy of Simplified Methods of Analysis and Design of Buildings with Damping Systems for Near-Fault and for Soft-Soil Seismic Motions,” by E.A. Pavlou and M.C. Constantinou, 8/16/04, (PB2005-104892, A08, MF-A02, CD-A00).
- MCEER-04-0009 “Assessment of Geotechnical Issues in Acute Care Facilities in California,” by M. Lew, T.D. O’Rourke, R. Dobry and M. Koch, 9/15/04, (PB2005-104893, A08, CD-A00).
- MCEER-04-0010 “Scissor-Jack-Damper Energy Dissipation System,” by A.N. Sigaher-Boyle and M.C. Constantinou, 12/1/04 (PB2005-108221).
- MCEER-04-0011 “Seismic Retrofit of Bridge Steel Truss Piers Using a Controlled Rocking Approach,” by M. Pollino and M. Bruneau, 12/20/04 (PB2006-105795).
- MCEER-05-0001 “Experimental and Analytical Studies of Structures Seismically Isolated with an Uplift-Restraint Isolation System,” by P.C. Roussis and M.C. Constantinou, 1/10/05 (PB2005-108222).
- MCEER-05-0002 “A Versatile Experimentation Model for Study of Structures Near Collapse Applied to Seismic Evaluation of Irregular Structures,” by D. Kusumastuti, A.M. Reinhorn and A. Rutenberg, 3/31/05 (PB2006-101523).
- MCEER-05-0003 “Proceedings of the Third PRC-US Workshop on Seismic Analysis and Design of Special Bridges,” edited by L.C. Fan and G.C. Lee, 4/20/05, (PB2006-105796).
- MCEER-05-0004 “Approaches for the Seismic Retrofit of Braced Steel Bridge Piers and Proof-of-Concept Testing of an Eccentrically Braced Frame with Tubular Link,” by J.W. Berman and M. Bruneau, 4/21/05 (PB2006-101524).
- MCEER-05-0005 “Simulation of Strong Ground Motions for Seismic Fragility Evaluation of Nonstructural Components in Hospitals,” by A. Wanitkorkul and A. Filiatrault, 5/26/05 (PB2006-500027).
- MCEER-05-0006 “Seismic Safety in California Hospitals: Assessing an Attempt to Accelerate the Replacement or Seismic Retrofit of Older Hospital Facilities,” by D.J. Alesch, L.A. Arendt and W.J. Petak, 6/6/05 (PB2006-105794).
- MCEER-05-0007 “Development of Seismic Strengthening and Retrofit Strategies for Critical Facilities Using Engineered Cementitious Composite Materials,” by K. Kesner and S.L. Billington, 8/29/05 (PB2006-111701).
- MCEER-05-0008 “Experimental and Analytical Studies of Base Isolation Systems for Seismic Protection of Power Transformers,” by N. Murota, M.Q. Feng and G-Y. Liu, 9/30/05 (PB2006-111702).
- MCEER-05-0009 “3D-BASIS-ME-MB: Computer Program for Nonlinear Dynamic Analysis of Seismically Isolated Structures,” by P.C. Tsopelas, P.C. Roussis, M.C. Constantinou, R. Buchanan and A.M. Reinhorn, 10/3/05 (PB2006-111703).



- MCEER-05-0010 “Steel Plate Shear Walls for Seismic Design and Retrofit of Building Structures,” by D. Vian and M. Bruneau, 12/15/05 (PB2006-111704).
- MCEER-05-0011 “The Performance-Based Design Paradigm,” by M.J. Astrella and A. Whittaker, 12/15/05 (PB2006-111705).
- MCEER-06-0001 “Seismic Fragility of Suspended Ceiling Systems,” H. Badillo-Almaraz, A.S. Whittaker, A.M. Reinhorn and G.P. Cimellaro, 2/4/06 (PB2006-111706).
- MCEER-06-0002 “Multi-Dimensional Fragility of Structures,” by G.P. Cimellaro, A.M. Reinhorn and M. Bruneau, 3/1/06 (PB2007-106974, A09, MF-A02, CD A00).
- MCEER-06-0003 “Built-Up Shear Links as Energy Dissipators for Seismic Protection of Bridges,” by P. Dusicka, A.M. Itani and I.G. Buckle, 3/15/06 (PB2006-111708).
- MCEER-06-0004 “Analytical Investigation of the Structural Fuse Concept,” by R.E. Vargas and M. Bruneau, 3/16/06 (PB2006-111709).
- MCEER-06-0005 “Experimental Investigation of the Structural Fuse Concept,” by R.E. Vargas and M. Bruneau, 3/17/06 (PB2006-111710).
- MCEER-06-0006 “Further Development of Tubular Eccentrically Braced Frame Links for the Seismic Retrofit of Braced Steel Truss Bridge Piers,” by J.W. Berman and M. Bruneau, 3/27/06 (PB2007-105147).
- MCEER-06-0007 “REDARS Validation Report,” by S. Cho, C.K. Huyck, S. Ghosh and R.T. Eguchi, 8/8/06 (PB2007-106983).
- MCEER-06-0008 “Review of Current NDE Technologies for Post-Earthquake Assessment of Retrofitted Bridge Columns,” by J.W. Song, Z. Liang and G.C. Lee, 8/21/06 06 (PB2007-106984).
- MCEER-06-0009 “Liquefaction Remediation in Silty Soils Using Dynamic Compaction and Stone Columns,” by S. Thevanayagam, G.R. Martin, R. Nashed, T. Shenthan, T. Kanagalingam and N. Ecemis, 8/28/06 06 (PB2007-106985).
- MCEER-06-0010 “Conceptual Design and Experimental Investigation of Polymer Matrix Composite Infill Panels for Seismic Retrofitting,” by W. Jung, M. Chiewanichakorn and A.J. Aref, 9/21/06 (PB2007-106986).
- MCEER-06-0011 “A Study of the Coupled Horizontal-Vertical Behavior of Elastomeric and Lead-Rubber Seismic Isolation Bearings,” by G.P. Warn and A.S. Whittaker, 9/22/06 (PB2007-108679).
- MCEER-06-0012 “Proceedings of the Fourth PRC-US Workshop on Seismic Analysis and Design of Special Bridges: Advancing Bridge Technologies in Research, Design, Construction and Preservation,” Edited by L.C. Fan, G.C. Lee and L. Ziang, 10/12/06 (PB2007-109042).
- MCEER-06-0013 “Cyclic Response and Low Cycle Fatigue Characteristics of Plate Steels,” by P. Dusicka, A.M. Itani and I.G. Buckle, 11/1/06 06 (PB2007-106987).
- MCEER-06-0014 “Proceedings of the Second US-Taiwan Bridge Engineering Workshop,” edited by W.P. Yen, J. Shen, J-Y. Chen and M. Wang, 11/15/06 (PB2008-500041).
- MCEER-06-0015 “User Manual and Technical Documentation for the REDARS™ Import Wizard,” by S. Cho, S. Ghosh, C.K. Huyck and S.D. Werner, 11/30/06 (PB2007-114766).
- MCEER-06-0016 “Hazard Mitigation Strategy and Monitoring Technologies for Urban and Infrastructure Public Buildings: Proceedings of the China-US Workshops,” edited by X.Y. Zhou, A.L. Zhang, G.C. Lee and M. Tong, 12/12/06 (PB2008-500018).
- MCEER-07-0001 “Static and Kinetic Coefficients of Friction for Rigid Blocks,” by C. Kafali, S. Fathali, M. Grigoriu and A.S. Whittaker, 3/20/07 (PB2007-114767).
- MCEER-07-0002 “Hazard Mitigation Investment Decision Making: Organizational Response to Legislative Mandate,” by L.A. Arendt, D.J. Alesch and W.J. Petak, 4/9/07 (PB2007-114768).


- MCEER-07-0003 “Seismic Behavior of Bidirectional-Resistant Ductile End Diaphragms with Unbonded Braces in Straight or Skewed Steel Bridges,” by O. Celik and M. Bruneau, 4/11/07 (PB2008-105141).
- MCEER-07-0004 “Modeling Pile Behavior in Large Pile Groups Under Lateral Loading,” by A.M. Dodds and G.R. Martin, 4/16/07(PB2008-105142).
- MCEER-07-0005 “Experimental Investigation of Blast Performance of Seismically Resistant Concrete-Filled Steel Tube Bridge Piers,” by S. Fujikura, M. Bruneau and D. Lopez-Garcia, 4/20/07 (PB2008-105143).
- MCEER-07-0006 “Seismic Analysis of Conventional and Isolated Liquefied Natural Gas Tanks Using Mechanical Analogs,” by I.P. Christovasilis and A.S. Whittaker, 5/1/07.
- MCEER-07-0007 “Experimental Seismic Performance Evaluation of Isolation/Restraint Systems for Mechanical Equipment – Part 1: Heavy Equipment Study,” by S. Fathali and A. Filiatrault, 6/6/07 (PB2008-105144).
- MCEER-07-0008 “Seismic Vulnerability of Timber Bridges and Timber Substructures,” by A.A. Sharma, J.B. Mander, I.M. Friedland and D.R. Allicock, 6/7/07 (PB2008-105145).
- MCEER-07-0009 “Experimental and Analytical Study of the XY-Friction Pendulum (XY-FP) Bearing for Bridge Applications,” by C.C. Marin-Artieda, A.S. Whittaker and M.C. Constantinou, 6/7/07 (PB2008-105191).
- MCEER-07-0010 “Proceedings of the PRC-US Earthquake Engineering Forum for Young Researchers,” Edited by G.C. Lee and X.Z. Qi, 6/8/07.
- MCEER-07-0011 “Design Recommendations for Perforated Steel Plate Shear Walls,” by R. Purba and M. Bruneau, 6/18/07, (PB2008-105192).
- MCEER-07-0012 “Performance of Seismic Isolation Hardware Under Service and Seismic Loading,” by M.C. Constantinou, A.S. Whittaker, Y. Kalpakidis, D.M. Fenz and G.P. Warn, 8/27/07, (PB2008-105193).
- MCEER-07-0013 “Experimental Evaluation of the Seismic Performance of Hospital Piping Subassemblies,” by E.R. Goodwin, E. Maragakis and A.M. Itani, 9/4/07, (PB2008-105194).
- MCEER-07-0014 “A Simulation Model of Urban Disaster Recovery and Resilience: Implementation for the 1994 Northridge Earthquake,” by S. Miles and S.E. Chang, 9/7/07, (PB2008-106426).
- MCEER-07-0015 “Statistical and Mechanistic Fragility Analysis of Concrete Bridges,” by M. Shinozuka, S. Banerjee and S-H. Kim, 9/10/07, (PB2008-106427).
- MCEER-07-0016 “Three-Dimensional Modeling of Inelastic Buckling in Frame Structures,” by M. Schachter and AM. Reinhorn, 9/13/07, (PB2008-108125).
- MCEER-07-0017 “Modeling of Seismic Wave Scattering on Pile Groups and Caissons,” by I. Po Lam, H. Law and C.T. Yang, 9/17/07 (PB2008-108150).
- MCEER-07-0018 “Bridge Foundations: Modeling Large Pile Groups and Caissons for Seismic Design,” by I. Po Lam, H. Law and G.R. Martin (Coordinating Author), 12/1/07.
- MCEER-07-0019 “Principles and Performance of Roller Seismic Isolation Bearings for Highway Bridges,” by G.C. Lee, Y.C. Ou, Z. Liang, T.C. Niu and J. Song, 12/10/07.
- MCEER-07-0020 “Centrifuge Modeling of Permeability and Pinning Reinforcement Effects on Pile Response to Lateral Spreading,” by L.L. Gonzalez-Lagos, T. Abdoun and R. Dobry, 12/10/07.
- MCEER-07-0021 “Damage to the Highway System from the Pisco, Perú Earthquake of August 15, 2007,” by J.S. O’Connor, L. Mesa and M. Nykamp, 12/10/07, (PB2008-108126).
- MCEER-07-0022 “Experimental Seismic Performance Evaluation of Isolation/Restraint Systems for Mechanical Equipment – Part 2: Light Equipment Study,” by S. Fathali and A. Filiatrault, 12/13/07.

- MCEER-07-0023 “Fragility Considerations in Highway Bridge Design,” by M. Shinozuka, S. Banerjee and S.H. Kim, 12/14/07.
- MCEER-07-0024 “Performance Estimates for Seismically Isolated Bridges,” by G.P. Warn and A.S. Whittaker, 12/30/07.
- MCEER-08-0001 “Seismic Performance of Steel Girder Bridge Superstructures with Conventional Cross Frames,” by L.P. Carden, A.M. Itani and I.G. Buckle, 1/7/08.
- MCEER-08-0002 “Seismic Performance of Steel Girder Bridge Superstructures with Ductile End Cross Frames with Seismic Isolators,” by L.P. Carden, A.M. Itani and I.G. Buckle, 1/7/08.
- MCEER-08-0003 “Analytical and Experimental Investigation of a Controlled Rocking Approach for Seismic Protection of Bridge Steel Truss Piers,” by M. Pollino and M. Bruneau, 1/21/08.
- MCEER-08-0004 “Linking Lifeline Infrastructure Performance and Community Disaster Resilience: Models and Multi-Stakeholder Processes,” by S.E. Chang, C. Pasion, K. Tatebe and R. Ahmad, 3/3/08.
- MCEER-08-0005 “Modal Analysis of Generally Damped Linear Structures Subjected to Seismic Excitations,” by J. Song, Y-L. Chu, Z. Liang and G.C. Lee, 3/4/08.



**EARTHQUAKE ENGINEERING TO EXTREME EVENTS**

University at Buffalo, The State University of New York  
Red Jacket Quadrangle ▪ Buffalo, New York 14261  
Phone: (716) 645-3391 ▪ Fax: (716) 645-3399  
E-mail: [mceer@buffalo.edu](mailto:mceer@buffalo.edu) ▪ WWW Site <http://mceer.buffalo.edu>



University at Buffalo *The State University of New York*

ISSN 1520-295X